MONASH University

Role of Casein Kinase 1 of *Plasmodium falciparum* in parasite biology and as a target for novel anti-malarial drugs

Mitchell Batty

BSc Biotechnology

BSc Science (Hons.)

A thesis submitted for the degree of *Doctor of Philosophy* at

Monash University in 2018

Department of Microbiology

TABLE OF CONTENTS

Copyright notice

Abstract

Protein kinases (PKs) are paramount to maintaining essential cellular processes by phosphorylating protein substrates to regulate their activity. In recent years, much interest has been invested in exploiting PKs as therapeutic targets for diseases like cancer and neurological diseases where phosphorylation homeostasis is disrupted. Indeed, protein phosphorylation is also an essential process used by infectious agents such as the malaria parasite *P. falciparum*. However, unlike with model eukaryotic organism's such as humans and yeast, many processes regulated by *P. falciparum* PKs remain unclear.

During infection, *P. falciparum* exports an arsenal of virulence factors to manipulate its host red blood cell (RBC) and to modulate and evade immune responses to infection. The *P. falciparum* casein kinase 1 (PfCK1) appears on the RBC membrane during early developmental stages (ring and trophozoite) and is secreted to the extracellular medium. PfCK1 is an essential kinase and is the only identified member of the CK1 eukaryotic PK (ePK) family that constitutes a six-member family in humans and five in *S. cerevisiae*. Though CK1 has been extensively studied in these model organisms, the cellular processes regulated by PfCK1 still remain elusive. This thesis aimed at exploring the functions of PfCK1 in blood stage *P. falciparum* parasites using a combination of genetic, chemical and bioinformatic approaches.

We attempted to identify a mechanism that describes the secretion of PfCK1 and its appearance on the RBC membrane and suspected a mechanism involving multiple host proteins may be utilised. Indeed, we found that the host proteins GTPase-activating protein and VPS9 domain-containing protein 1 (GAPVD1) and sorting nexin 22 (SNX22), which have described functions in membrane trafficking in higher eukaryotes, consistently co-purify with PfCK1 suggesting the parasite utilises trafficking pathways previously thought to be inactive in RBCs. Further, we performed reciprocal immunoprecipitation experiments with GAPVD1 and identified parasite proteins suggestive of a

recycling pathway hitherto only described in higher eukaryotes to recycle membrane proteins. Thus, we have identified components of a trafficking pathway involving parasite proteins that act in concert with host proteins which we hypothesise coordinate the trafficking of PfCK1 during infection.

In this thesis, we demonstrated that PfCK1 localises to the parasite nucleus during late stage development and its import is sensitive to Ivermectin (IVM), a drug suspected of disrupting nuclear import machinery, indicating PfCK1 may contain a nuclear localisation signal (NLS). To identify the intrinsic nuclear functions of PfCK1, immunoprecipitation studies were performed on protein extracts from purified nuclei. The proteins recovered in a pilot experiment suggest that PfCK1 interacts with chromatin and we therefore attempted to identify regions of chromatin enriched in PfCK1-GFP by immunoprecipitation and sequencing of the associated DNA (ChIP-seq). Although the results from our first attempt are convoluted, we found that the recovered DNA fragments largely map to telomeric regions. What this means with respect to the functions of PfCK1 is yet to be established, however we have demonstrated the ability to obtain individual nucleosomes using the conditions optimised in this study for future work to build on.

Lastly, we explored PfCK1 as the lethal target of the ATP competitive inhibitor Purvalanol B as an early study suggested this compound preferentially binds to PfCK1 in *P. falciparum*. Using a predicted three-dimensional structure of PfCK1 we generated in this study, we made nine PfCK1 variants bearing single nonsynonymous mutations predicted to perturb Purvalanol B binding but not ATP. No difference in parasite sensitivity to Purvalanol B was observed for any PfCK1 mutant (compared to wild-type enzyme) which, in conjunction with our inability to select for drug resistant parasites suggests that PfCK1 is not the primary target of the anti-plasmodial activity of Purvalanol B, rather, Purvalanol B likely targets multiple proteins. Although our initial hypothesis was disproved, the tools we generated in this chapter may allow us to further explore PfCK1 as a drug target either through the modification

of existing compounds or the generation of new compounds by using our PfCK1 prediction model for rational drug design until a crystal structure can be produced.

Overall, this thesis has expanded on our understanding of PfCK1 biology in the asexual blood stages of *P. falciparum* parasites and has provided important avenues for further exploration of the precise cellular mechanisms that underpin PfCK1 function. An overall comprehensive understanding of PfCK1 function is paramount for the design of new therapeutics to reduce the burden of malaria.

Declaration

This thesis contains no material which has been accepted for the award of any other degree or diploma at any university or equivalent institution and that, to the best of my knowledge and belief, this thesis contains no material previously published or written by another person, except where due reference is made in the text of the thesis.

Acknowledgements

Firstly, I would like to acknowledge the traditional custodians of the land on which Monash University was built. I pay my respects to their elder's past, present and future. I would also like to thank the School of Biomedical Sciences at the Biomedicine Discovery Institute, Monash University for the financial assistance to partake in my doctorate studies over the three and a half years I received funding. This support was immensely helpful towards my studies.

Next, I would like to thank my supervisors and mentors, Associate Professor Jose Garcia-Bustos and Professor Christian Doerig for providing me with the opportunity to pursue my doctorate degree. Your time, patience, intellectual input, guidance and encouragement over these many years have provided me with a wealth of knowledge and the skills I require to become an independent researcher. For this, I cannot thank you enough. To Jose, your time and guidance during my impromptu drop-in meetings and for always helping me sort through issues and helping keep me on track have ensured that my time spent at Monash University were some of the best years of my life. I hope that I have made you proud over these years and it has been such a privilege to be mentored by you. To Christian, your enthusiasm towards understanding the malaria parasite has not gone un-noticed. Your continued excitement is contagious and always made for interesting discussions. I think it is safe to say that it has rubbed off on me and I am excited to continue research in this field and look forward to future projects that we may collaborate on some day.

I would like to extend my gratitude to my panel members Professor Hans Netter, Dr Sheena McGowan and Associate Professor David Piedrafita for their valuable discussions and guidance throughout my candidature and for helping to improve my skills as a researcher. I would also like to acknowledge my collaborators: Dr Matt Dixon and Professor Leanne Tilley from Bio21 Institute, Melbourne University

for their assistance with gametocyte immunofluorescence; Dr Brendan Russ and Professor Steven Turner for their assistance in developing ChIP-seq in our lab; Dr Ralf Schittenhelm for his help with mass spectrometry, Professor Johnathan Baell and Dr Nghi Nguyen for providing Purvalanol B and its derivatives for my studies and Dr Sheena McGowan for assisting with computational protein modelling.

I would like to extend my gratitude to friends and colleagues of the Department of Microbiology past and present, for making all of these years exciting and fun. It truly has been the most wonderful experience. To Dr Belinda Morahan, Dr Simona John Von Freyand, Dr Megan Bird and Dr Reza Haqshenas, I would like to thank you for your time devoted to teaching me lab techniques, for being wonderful friends and for the interesting discussions in and out of the lab. I wish to give a special thanks to my close friends Will, Rajini, Jack, Rhea, Vignesh and Maria for all of the in-lab shenanigans, culture room karaoke parties, coffee walks and always there to talk, vent frustrations and laugh. I am truly lucky to be graced with such wonderful people who are always so much fun to be around. I would also like to thank everyone else who has contributed to this study either directly or indirectly.

Last but not least, I would like to thank my family, particularly my parents Ken and Lorain for providing me with the education and support I needed to get to where I am today. To my wife Stephanie, words cannot express how grateful I am to have you by my side and for all of the love, support, encouragement and patience you have provided me over these many long years. Without you I never would have made it this far.

Dedications

To my darling wife Stephanie, in consideration of your continuous love, support and encouragement over the years.

List of figures and tables

Chapter 1

Chapter 2

Chapter 3

Chapter 4

Figure **Page**

Table **Page**

Chapter 5

Figure **Page**

Table **Page**

Supplementary figures and tables

Figure **Page**

Table

List of abbreviations

a.a	Amino acid
A. thaliana	*Arabidopsis thaliana*
A_{260nm}	Absorbance at 260nm
A_{280nm}	Absorbance at 280nm
ABC	Ammonium bicarbonate
ACN	Acetonitrile
ACT	artemisinin-Combination Therapy
ART	artemisinin
ATP	Adenosine triphosphate
AQ	Atovaquone
α	Alpha
β	Beta
bp	Base pairs
BLAST	Basic Local Alignment Search Tool
BSA	Bovine serum albumin
BSD	Blasticidin
CA	Carbonic anhydrase
ChIP-seq	Chromatin immunoprecipitation sequencing
CO_2	Carbon Dioxide
°C	Degree Celsius
Co-IP	Co-immunoprecipitation
CRT	Chloroquine resistance transporter
CQ	Chloroquine
δ	Delta
D. discoidium	*Dictyostelium discoideum*
Da	Dalton
ddH_2O	Double-distilled water
DHFR	Dihydrofolate reductase
DHPS	Dihydroptherate synthase
DMSO	Dimethyl sulphoxide
DNA	Deoxyribonucleic acid
DNase	Deoxyribonuclease
Dnmt1	Deoxyribonucleic acid methyltransferase 1
dNTP	Deoxyribonucleoside triphosphate

dsDNA	Double-stranded deoxyribonucleic acid
DTT	1,4-dithiothreitol
E. coli	*Escherichia coli*
EDTA	Ethylene diamine tetracetic acid
ePK	Eukaryotic protein kinase
ER	Endoplasmic Reticulum
F. solaris	*Fistulifera solaris*
γ	Gamma
G. lambila	*Giardia lambila*
GAPDH	Glyceraldehyde-6-phosphate dehydrogenase
GFP	Green fluorescent protein
GSK	Glycogen synthase kinase
GST	Glutathione-S-transferase
h	Hour
H3	Histone H3
H2A/H2B/2A.Z	Core histones H2B, H2B and variant H2A.Z
H3K36me3	Trimethylation at lysine 36 of Histone H3
H4	Histone H4
hDHFR	Human Dihydrofolate Reductase
HEPES	4-(2-hydroxyethyl)-piperazine-1-ethanesulphonic acid
Hs	*Homo sapiens*
IFA	Immunofluorescence
IP	Immunoprecipitation Assay
IPTG	Isopropyl-β-D-thiogalactopyranoside
IPTp	Intermittent preventative therapy for malaria in pregnancy
iRBC	Infected Red Blood Cell
kb	Kilobases (1,000 base pairs)
kDa	Kilodalton
KO	Knock-out
K13	Kelch-13 propeller domain
LB	Luria broth
M	Molar
MAPK	Mitogen-Activated Protein Kinase
Mb	Mega Bases (1,000,000 base pairs)
MCS	Multiple Cloning Site
MDR1	Multidrug resistance protein 1
mg	Milligram
$MgCl_2$	Magnesium Chloride

$MgSO_4$	Magnesium Sulphate
min	Minutes
ml	Millilitre
mM	Millimolar
mRNA	Messenger Ribonucleic Acid
MSP	Merozoite Surface Protein
MW	Molecular Weight
µ	Micro
µg	Microgram
µM	Micromolar
N_2	Nitrogen gas
NEB	New England Biolabs
ng	Nanogram
O_2	Oxygen
ORF	Open reading frame
P. falciparum	*Plasmodium falciparum*
PfCK1	*P. falciparum* Casein kinase 1
PfCK2	*P. falciparum* Casein kinase 2
PfEMP	*P. falciparum* Erythrocyte membrane protein
PAGE	Polyacrylamide gel electrophoresis
Pb	*Plasmodium berghei*
PBS	Phosphate buffered saline
PCR	Polymerase chain reaction
PEXEL	*Plasmodium* export element
PK	Protein kinase
PlasmoDB	*Plasmodium* Database
PMSF	Phenylmethylsulfonyl fluoride
pRBC	Parasite-infected red blood cell
PV	Parasitophorous Vacuole
PVM	Parasitophorous Vacuole Membrane
RBC	Red Blood Cell
RNA	Ribonucleic Acid
RNase	Ribonuclease
RPM	Revolutions per Minute
RPMI-1640 medium	Roswell Park Memorial Institute-1640 medium
RT	Room temperature
s	Second

SP	Sulphadoxine/pyrimethamine
S. cerevisiae	*Saccharomyces cerevisiae*
SDS	Sodium dodecyl sulphate
T. cruzi	*Trypanosoma cruzi*
TAE	Tris-acetate-EDTA
TBE	Tris-borate-EDTA
TBS	Tris buffered saline
TBST	Tris buffered saline with Tween®-20
TE buffer	Tris EDTA buffer
TEMED	N,N,N',N'-T etramethylethylenediamine
TK	Tyrosine kinase
TKL	Tyrosine Kinase Like-kinases
tRNA	Transfer Ribonucleic Acid
U	Unit
UTR	Untranslated Region
UV	Ultraviolet
V	Volts
Var	Variant antigen
v/v	Volume/Volume
w/v	Weight/Volume
WB	Western Blot
WHO	World Health Organisation
WT	Wild-type
X	Times
XA	Xanthurenic acid
3'UTR	Three prime untranslated region
5'UTR	Five prime untranslated region

Chapter 1

Introduction

1. Malaria

Malaria still remains a significant burden in countries where socioeconomic factors favour the distribution and severity of disease (Béguin et al., 2011). Malaria is caused by infection with unicellular protozoan parasites of the genus *Plasmodium* which invade and grow inside red blood cells (RBCs) (Engelbrecht and Coetzer, 2016). Five species of *Plasmodium* are capable of causing disease in humans: *Plasmodium malariae, Plasmodium ovale, Plasmodium knowlesi, Plasmodium vivax* and *Plasmodium falciparum* (Ribaut et al., 2008, Cox-Singh et al., 2008). Of the five species that are capable of infecting humans, *P. falciparum* is responsible for the greatest number of infections and the most lethal form of disease.

An estimated 260 million global cases of malaria were reported in 2000 with close to 900 thousand deaths, 86% of which occurred in children under the age of five (WHO, 2015). Between 2000 and 2015, however, these values have declined significantly with an estimated decrease in incidence rate of 41% and 62% for morbidity and mortality rate, respectively (WHO, 2016). This also includes a 16% decrease in the number of deaths in children under the age of five. These values represent a significant impact in the global effort to control and eradicate malaria amongst endemic countries; however more efforts are still necessary to ensure the continual implementation of effective treatments and intervention strategies. With the emergence of resistance to the frontline antimalarial Artemisinin (ART) (Miotto et al., 2013), in addition to poor accessibility to low quality and fragile health care, global malaria eradication targets are threatened (Ghansah et al., 2014, Alonso and Tanner, 2013). Phase 3 clinical trials of the RTS,S/AS01 malaria vaccine have recently been published (The RTS,S Clinical Trials Partnership, 2012) showing an efficacy that is lower than 40%. Thus, commercial availability of a

malaria vaccine is still far in the future, which suggests that insecticide-treated bed nets (ITNs), indoor residual spraying (IRS) and antimalarials will remain primary prevention and treatment methods in the foreseeable future. With the rise in drug resistance and the arsenal of effective antimalarial compounds decreasing, newer drugs are greatly needed.

1.1. *Plasmodium falciparum*

P. falciparum and other *Plasmodium* species are members of the phylum *Apicomplexa* as they contain a specialised assembly of structural and secretory elements collectively termed the apical complex (Katris et al., 2014) in addition to a large plastid-like organelle which contains a circular genome of ~35kb termed the apicoplast (Goodman and McFadden, 2014, Wilson et al., 1996). The apicoplast serves a specific biological purpose – the biosynthesis of macromolecules such as fatty acids, isoprenoid precursors and heme (Bowman et al., 2014); the apicoplast is thought to have originated through secondary endosymbiosis of algae by a common apicomplexan ancestor (Janouškovec et al., 2010). Apicomplexan obligate intracellular parasites that require a host to replicate.

1.2. Asexual development of *P. falciparum*

P. falciparum has a complex life cycle consisting of two phases: asexual development within the human host, and sexual development, which is initiated by the formation of gametocytes in the human host and continues within the mosquito vector. Infection of the human host begins with a blood meal from a female *Anopheles* mosquito, which releases sporozoites into the dermis (Yamauchi et al., 2007). Sporozoites then migrate to and infect the liver where they undergo schizogony over a period of approximately 6-12 days (Vaughan et al., 2012), producing thousands of merozoites which exit the liver and infect RBCs (Figure 1.1I), marking the beginning of a 48-hour erythrocytic asexual life cycle (Govindasamy et al., 2016, Tao et al., 2014). Invasion of the host cell is a complex process which involves the formation of invasion machinery through secretion of micronemes and rhoptry proteins (Tonkin et al., 2011, Besteiro et al., 2011). Once the invasion machinery is formed, a moving junction

(MJ) enables the parasite to penetrate the host erythrocyte forming a membrane-bound niche called the parasitophorous vacuole (PV) where the parasite remains throughout the course its asexual lifecycle. Once infection has been established in a RBC, merozoites mature through three morphologically distinct stages: ring, trophozoite and schizont stages (Figure 1.1II-IV) (Grüring et al., 2011), resulting in the release of 20-30 merozoites per parasite (Figure 1.1V) (Grüring et al., 2014) and the cycle propagates.

Asexual replication within the blood is responsible for the pathology of *Plasmodium* infection. The general symptoms of uncomplicated malaria including anaemia, nausea and fever. However, *P. falciparum* differs from other species of *Plasmodium* due to its ability to increase the cytoadhesive properties of infected RBCs (iRBCs), enabling mature trophozoite and schizont stage parasites to sequester in microvascular structures (Ochola et al., 2011, Grüring et al., 2011). Usually the microcirculatory beds of the spleen filter out altered RBCs allowing healthy cells to return to circulation (Safeukui et al., 2008), cytoadhesion prevents P. *falciparum* iRBCs from coming into contact with the spleen thereby avoiding clearance. Sequestration of these abnormally adherent cells within the microvasculature causes them to become blocked leading to severe complications associated with *P. falciparum* malaria such as multiple organ failure and cerebral malaria, ultimately resulting in coma and death (Ochola et al., 2011, Safeukui et al., 2008, Avril et al., 2012).

1.3. Sexual differentiation of *P. falciparum* (Gametocytogenesis)

To maintain an infection, *P. falciparum* parasites continuously invade and replicate within host RBCs. During asexual replication however, a subpopulation of schizonts produce merozoites which are committed to developing into sexual stage gametocytes (Eksi et al., 2012). The exact environmental triggers that cause *P. falciparum* parasites to switch from asexual to sexual development stills remains elusive, however high parasitaemia, endoplasmic reticulum (ER) and redox stress and RBC lysis have been proposed as gametocyte inducers (Duffy et al., 2016, Beri et al., 2017, Chaubey et al., 2014). This

suggests that parasites respond to multiple environmental stimuli relating to high levels of parasite biomass such as nutrient deprivation and haemolysis.

Once committed merozoites are released, they infect a RBC and form a committed ring that matures into a stage I gametocyte 24-30hrs later (Ikadai et al., 2013) and is morphologically similar to a trophozoite stage asexual parasite. Over the next 5-7 days immature sexual stage parasites subsequently develop through stages II – IV (SI-SIV), finally resulting in a mature stage V (SV) male or female gametocyte (Figure 1.1VI.). The duration of gametocytogenesis occurs over a period of 10-12 days and is essential for the transmission of parasites to the mosquito vector (Tibúrcio et al., 2015). Immature gametocytes (SII – SIV) share many characteristics to mature asexual stage parasites (trophozoites and schizonts), such as digestion of haemoglobin and sequestration in microvascular structures (Lamour et al., 2014, Eksi et al., 2012). Mature SV gametocytes re-enter circulation as quiescent parasites. During a blood meal, SV gametocytes are taken up by a mosquito where they are stimulated in the midgut to produce gametes (Figure 1.1Aii). Gametocyte formation is generally biased towards females (Tran et al., 2014); each male gametocyte develops into eight highly motile gametes through a process called exflagellation to compensate for this bias, triggered as a result of a sudden temperature change in the presence of xanthurenic acid, an activating factor in the mosquito midgut (Delves et al., 2013, Leba et al., 2015).

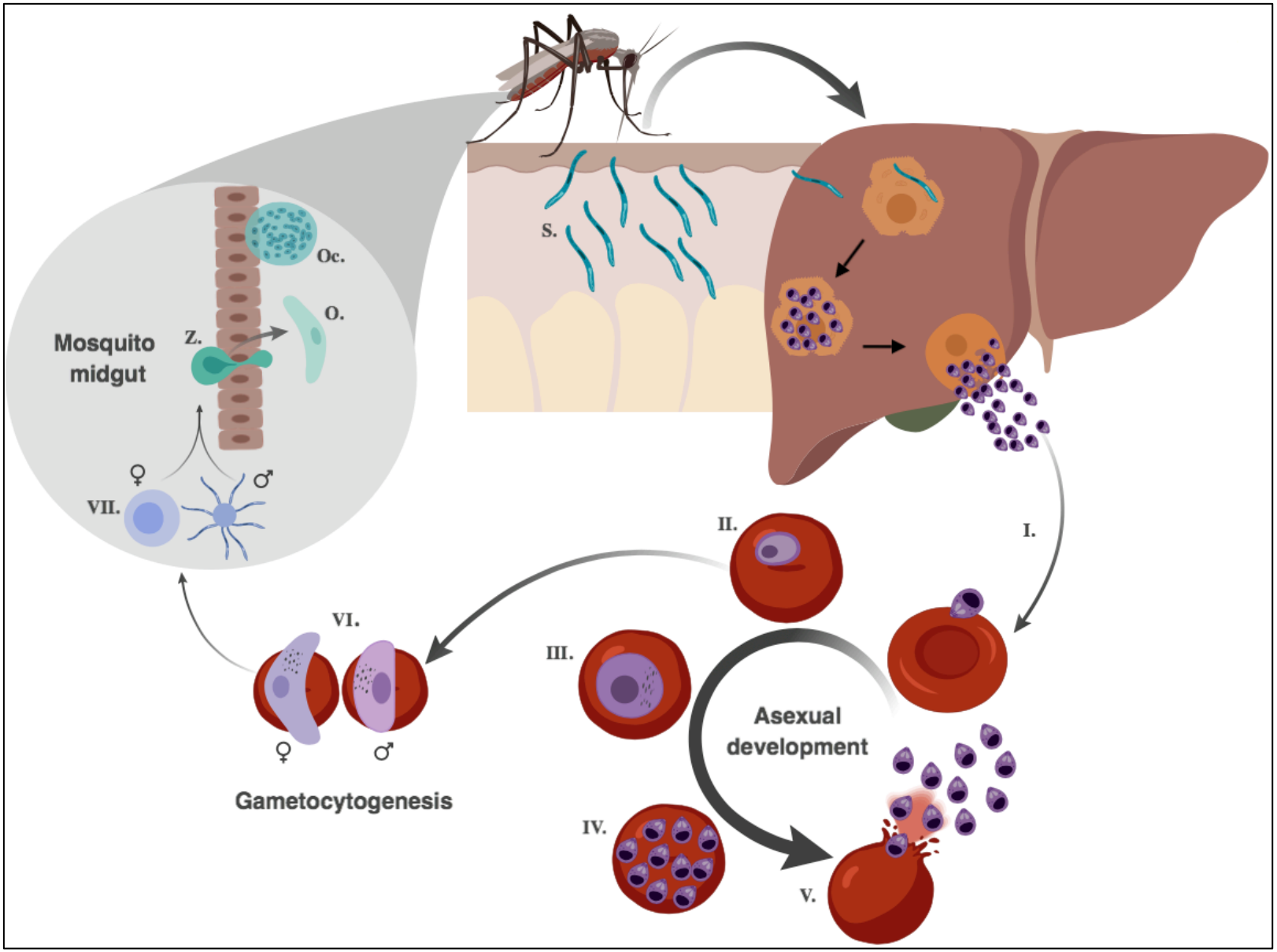
Mosquito midgut
Oc.
O.
Z.
VII.
♀
♂
S.
I.
II.
III.
IV.
V.
VI.
Asexual development
Gametocytogenesis

Figure 1.1. Lifecycle of P. falciparum. Following a blood meal by a female Anopheles mosquito, P. falciparum sporozoites (S) are released into the dermis and migrate to the blood, eventually finding the host's liver where they invade and undergo schizogony to produce thousands of merozoites. Merozoites are then released into the blood (I), infect an RBC and undergo blood stage asexual development through ring (II), trophozoite (III) and schizont (IV). Schizonts then rupture (V), releasing merozoites back into the blood stream where they invade RBCs and the life cycle continues. A small proportion of parasites commit to sexual differentiation and mature to become male and female gametocytes (VI) in the blood and are transmitted to the invertebrate during feeding. Within the mosquito, gametocytes are stimulated by environmental queues and differentiate into gametes (VII). Following this, further sexual differentiation takes place resulting in the formation of a zygote (Z) that transverses the mosquito midgut, developing into an ookinete (O) and finally an oocyst (Oc), producing sporozoites that migrate to the mosquito salivary glands. These events allow subsequent human infection.

1.4. Drug resistance

Treatment of malaria relies heavily on the use of antimalarial compounds, with several different drugs available. Currently, Artemisinin Combination Therapy (ACT) is the only recommended front-line treatment for *P. falciparum* malaria due to its efficacy in parasite clearance and transmission blocking (Phyo et al., 2012, Garner, 2013). However, a parasite phenotype associated with a prolonged rate of clearance in individuals treated with ACT has been observed in regions of Southeast Asia indicating the emergence of resistance to this front-line treatment (Beshir et al., 2013, Hunja et al., 2013, Phyo et al., 2012).

P. falciparum has become resistant to most of the available prophylactic and chemotherapeutic drugs including ART. Although very little is known about the mechanism of ART resistance, it is well established that mutations in the *P. falciparum* Kelch13 (K13) propeller domain are determinants of resistance (Tun et al., 2015, Thuy-Nhien et al., 2017). A delay in parasite clearance rate is hallmark of ART resistance, however it is a combination of resistance also to partner drugs that causes the greatest risk of treatment failures.

One of the more general drug resistance mechanisms is *Pf*MDR1 (multidrug resistance protein 1), a food vacuole (FV) membrane (FVM) transport protein which largely regulates parasite sensitivity to many antimalarials. For example, decreased sensitivity to the ACT partner drug amodiaquine (AQ) is linked to a widely prevalent N86Y mutation in *Pf*MDR1 (Veiga et al., 2016) which, in contrast, increases parasite susceptibility to the antimalarials dihydroartemisinin (DHA), lumefantrine (LMF) and mefloquine (MQ) (Wurtz et al., 2014).

Interestingly N86Y also decreases the sensitivity of parasites to chloroquine (CQ), perhaps one of the most well-known antimalarials. Although it is widely accepted that CQ resistance is largely mediated by a K76T mutation in the FVM protein *Pf*CRT1 (chloroquine resistance transporter) (Mayor et al., 2001, Lakshmanan et al., 2005), a large body of evidence suggests the involvement of both *Pf*CRT1 and *Pf*MDR1 (Eyase et al., 2013, Shrivastava et al., 2014). *Pf*MDR1 encodes a glycoprotein homolog,

and it is likely the N86Y mutation alters the protein's substrate specificity, thus reducing substrate uptake; whereas the 72-76 haplotype of CQ/AQ resistant *Pf*CRT1 encode a five amino acid change from wild-type CVMNK to either CVIET or SVMNT (Mvumbi et al., 2013, Oladipo et al., 2015). This haplotype is considered significant in terms of CQ and AQ resistance due to the pharmacological similarities between the two compounds and assuming a similar mechanism of resistance (Mvumbi et al., 2013). Although it is not exactly understood how *Pf*CRT1 and *Pf*MDR1 function together in a CQ resistance phenotype, it is most likely that the mutations in each individual protein (i.e. *Pf*MDR1 or *Pf*CRT1) result in an additive effect (Ruizendaal et al., 2017).

Resistance can also arise due to point mutations in more specific drug targets. For instance, double and triple point mutations in the dihydropterate synthase (DHPS) and dihydrofolate reductase (DHFR) genes confer resistance to the combination therapy sulfadoxine-pyrimethamine (SP) – a widely used treatment for intermittent preventative therapy for Malaria in pregnancy (IPTp) (Leke and Taylor, 2011). Several studies have identified combinations of mutations in DHFR and DHPS that are largely responsible for SP treatment failures; the DHFR triple mutant N51I/C59R/S108N and the DHPS double mutant A437G/K540E (Ruizendaal et al., 2017) are predominant mutations found in SP resistant isolates across Southeast Asia, South American and Africa (McCollum et al., 2007). A quadruple pyrimethamine resistant mutant (N51I/C59R/S108N/I164L), thought only to be present in Southeast Asia and South America has now emerged across Africa (McCollum et al., 2006) and will have a profound effect on future use of SP for IPTp. With this in mind, a recent study (Tarnchompoo et al., 2018) involving the design and use of a dual-pharmacophore inhibitor of PfDHFR shows great promise for use as an antimalarial therapy against parasites carry the PfDHFR quadruple mutations. Indeed, the compound BT3, which contains both rigid and flexible moieties, binds to wild type and mutant PfDHFR in a similar way which bypasses steric clashes with mutant residues of the active site that occurs with other antifolate inhibitors.

The widespread distribution of resistance to all common antimalarials represents a significant hindrance to current malaria eradication programs. Made worse by the threat of ACT resistance spreading to highly endemic regions like sub-Saharan Africa, the decline in usable antimalarials presents a strong need for new drugs. Understandably, however, the introduction of new compounds will not simply be the be-all-end-all solution. Strategies which combine drug-based therapies in coordination with the use of resistance markers for genotype surveying (for example N86Y, K76T and K13) may provide a more accurate way of administering new combination-therapies for treatment and may potentially aid in prolonging their use. Nevertheless, it is sensible to explore new drug targets which have a previously untapped mechanism of action in malaria treatment; compounds which inhibit essential parasite proteins that are not targeted by current antimalarials and therefore are unlikely to have any pre-existing resistance mechanisms associated with their inhibition. One class of promising targets which meet these criteria are protein kinases.

1.5. Protein phosphorylation

Advances in the sensitivity of mass spectrometry-based techniques have led to the elucidation of the phosphoproteome of various human cell lines (Lawrence et al., 2016, Sharma et al., 2014, Tsai et al., 2015). Protein phosphorylation by protein kinases (PKs) occurs on either serine (Ser), threonine (Thr) or tyrosine (Tyr) residues, with a greater tendency towards Ser and Thr phosphorylation. Within an individual cell it is estimated there are up to 700,000 phosphorylated sites, although the number of detectable phosphorylated sites vary between individual studies (Humphrey et al., 2013, Zhou et al., 2013, Sharma et al., 2014). When deregulated, phosphorylation contributes to a variety of disease pathologies including cancers (Fabbro et al., 2012), with PKs accounting to around 50% of the number of genes responsible for cancer formation (Fabbro et al., 2012). As such, PKs have become attractive drug candidates for the treatment of cancer (Katayama and Sen, 2010, Richter et al., 2014, Sánchez-Martínez et al., 2015) and other diseases like rheumatoid arthritis (Zou et al., 2016).

As with higher eukaryotes, phosphorylation contributes to complex signalling cascades in protozoan parasites such as *P. falciparum*. The complement of PK-encoding genes in the *P. falciparum* genome (the kinome) is smaller than that of higher eukaryotes, with 85 PKs accounting for approximately 1.5% of all genes, compared to more than 500 PKs accounting for around 1.7% of all genes in humans (Anamika et al., 2005, Doerig et al., 2008, Manning et al., 2002). However, the number of parasite proteins potentially phosphorylated accounts for close to 50% of its total proteome (Pease et al., 2013). Not surprisingly, a large proportion of these phosphoproteins vary greatly between the different stages of sexual and asexual development (Lasonder et al., 2012a, Pease et al., 2013). Although the *P. falciparum* kinome represents approximately the same proportion of the proteome as humans, the reduction in parasite PK number is likely a result of adopting a parasitic lifestyle (reviewed in (Talevich et al., 2012)).

Kinases are able to self-regulate their activity by a process known as autophosphorylation, which, as the name suggests, is the ability of the kinase to phosphorylate itself. This phenomenon has been observed for a number of PKs in yeast, humans and *P. falciparum* (Oligschlaeger et al., 2015, Beenstock et al., 2016, Peter et al., 2011, E. et al., 2016, Brandt and Bailey, 2013, Low et al., 2012) suggesting a conserved mechanism contributing to the regulation of kinase activity. As PKs are multi-functional enzymes, substrate specificity is important and autophosphorylation may contribute to tight control over this. Autophosphorylation can occur at many sites within a kinase on either a Ser, Thr or Tyr residue, changing the biochemical environment in the domain where the phosphorylation event occurred. The resulting conformational change exposes catalytic domains, opens binding pockets enabling substrate access, or closes other domains releasing bound substrates. Moreover, autophosphorylation may act to prime kinases to phosphorylate substrates at certain time points, for example, in cell division where timing needs to be tightly controlled. Although it is not fully understood how *P. falciparum* utilises phosphorylation processes to survive within its host, we can establish testable hypothesises derived from information of known homologues of other organisms with well understood mechanisms and pathways.

1.5.1. Protein kinases as potential drug targets

Many crucial processes such as cell cycle progression and invasion by pathogenic organisms are driven by the phosphorylation of target molecules by kinases. More than 500 PKs are encoded in the human genome which accounts for approximately 2% of all genes (Manning et al., 2002) and cluster in seven distinctive eukaryotic PK (ePK) groups: CK1, CMGC, TKL, AGC, CamK, STE and TyrK (Figure 1.2). The kinome of *P. falciparum* is significantly smaller, with 85 kinases identified through bioinformatic approaches and covering five of the seven ePK groups: CamK, AGC, CK1, CMGC and TKL or "TyrK like" kinases (Doerig et al., 2008). Absent from the kinase tree are the TK and STE families which, as outlined previously, may be the result of adapting to a parasitic lifestyle. Absent from the kinase tree are the TK and STE families which, as outlined previously, may be the result of adapting to a parasitic lifestyle. In addition, studies of the *P. vivax* proteome identified 49 PK orthologs which are transcribed during blood stage development (Bozdech et al., 2008), many of which are differentially transcribed during blood stage development compared to *P. falciparum*, highlighting important biological differences between the two parasites. A recent analysis of the proteome from *P. vivax* and *P. falciparum* sporozoites (Swearingen et al., 2017) also identified several PKs conserved between parasites.

P. falciparum also contains an expanded family of novel, apicomplexan-specific kinases called FIKK kinases, named due to a highly conserved Phe, Ile, Lys, Lys domain (Lin et al., 2017). These kinases may also present suitable drug targets given their uniqueness and absence from human cells. *P. falciparum* PKs which do not have orthologues to mammalian PKs (excluding FIKK kinases) and do not fall into any of the ePK groups are referred to as orphan protein kinases (OPKs). Of the 85 PK's predicted in *Plasmodium*, 36 are considered as likely essential to the asexual erythrocyte stage (Solyakov et al., 2011). It still remains unclear how many PKs are essential for sexual development in *P. falciparum*, although estimates in *P. berghei* indicate that approximately 12 PKs are required for *in vivo* parasite transmission to the mosquito vector and seven PKs are required for ookinete formation *in vitro* (Tewari et al., 2010).

PKs are prominent drug targets in human diseases such as cancer (Fabbro et al., 2012, Gherardi et al., 2012, Charrier et al., 2011, Katayama and Sen, 2010, Roskoski Jr, 2003, Tsai and Nussinov, 2013), with 39 small-molecule kinase inhibitors currently approved for use by U.S. Food and Drug Administration (FDA); recent literature places this number at 33 approved inhibitors (M., 2017), however for a complete summary see http://www.brimr.org/PKI/PKIs.htm. The rapidly advancing science of kinase inhibitor research highlights a strong interest in this field of therapeutics and the success of PK inhibition in humans lends hope that this is translatable to other diseases such as parasitic disease. For instance, 13,000 antimalarial hits were identified in a screen of more than 1,900,000 compounds from the GlaxoSmithKline's (GSK) inhibitors collection (Gamo et al., 2010), of which an astonishing 42% of the hit compounds with a known biochemical activity belong to a class of kinase inhibitors. This is promising and suggests that kinases represent suitable therapeutic targets in *P. falciparum*. Further, it is demonstrably possible to obtain compounds that exhibit high species-selective inhibition of parasite (over human) kinases (Fugel et al., 2013, Lucet et al., 2012, Gurnett et al., 2002).

The major focus of this thesis is to expand our understanding of the biology of casein kinase 1 (CK1) in *P. falciparum*. The following sections will review the current biology of CK1 in other eukaryotes and summarise our current knowledge of this enzyme in *P. falciparum*.

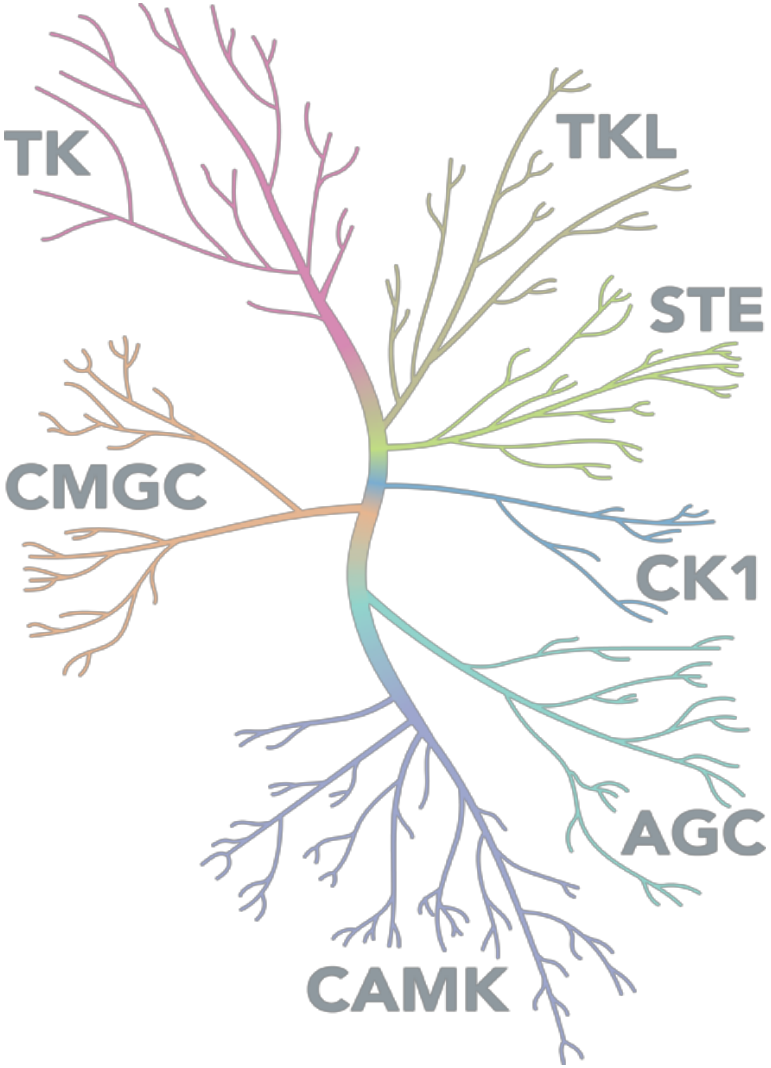
TK
TKL
STE
CMGC
CK1
AGC
CAMK

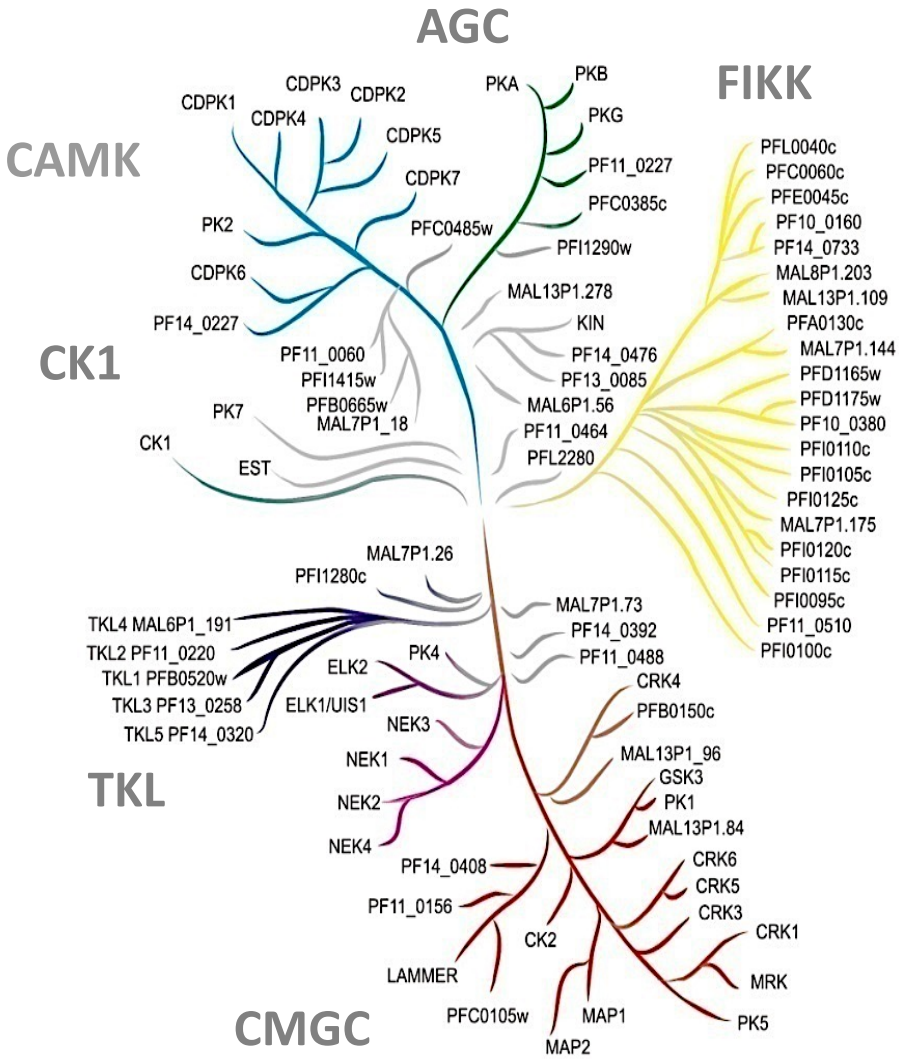
AGC
FIKK
CAMK
CK1
TKL
CMGC
CDPK1
CDPK4
CDPK3
CDPK2
CDPK5
CDPK7
PK2
CDPK6
PF14_0227
PF11_0060
PFI1415w
PFB0665w
MAL7P1_18
PK7
CK1
EST
PKA
PKB
PKG
PF11_0227
PFC0385c
PFC0485w
PFI1290w
MAL13P1.278
KIN
PF14_0476
PF13_0085
MAL6P1.56
PF11_0464
PFL2280
PFL0040c
PFC0060c
PFE0045c
PF10_0160
PF14_0733
MAL8P1.203
MAL13P1.109
PFA0130c
MAL7P1.144
PFD1165w
PFD1175w
PF10_0380
PFI0110c
PFI0105c
PFI0125c
MAL7P1.175
PFI0120c
PFI0115c
PFI0095c
PF11_0510
PFI0100c
MAL7P1.26
PFI1280c
TKL4 MAL6P1_191
TKL2 PF11_0220
TKL1 PFB0520w
TKL3 PF13_0258
TKL5 PF14_0320
ELK2
ELK1/UIS1
PK4
NEK3
NEK1
NEK2
NEK4
MAL7P1.73
PF14_0392
PF11_0488
CRK4
PFB0150c
MAL13P1_96
GSK3
PK1
MAL13P1.84
PF14_0408
PF11_0156
LAMMER
CK2
CRK6
CRK5
CRK3
CRK1
MRK
PK5
PFC0105w
MAP1
MAP2

Figure 1.2. Family tree of eukaryotic protein kinases (ePks). The family of eukaryotic protein kinases (left) cluster into seven distinctive groups: Tyrosine kinase (TK), Tyrosine kinase-like (TKL), Cyclin-dependant kinases, MAP kinases, GSK3 and CLKs (CMGC), PKs acting as MAPK regulators (STE), Calcium/calmodulin-dependant kinases (CamK) and Casein kinase 1 (CK1) families. Absent in the *P. falciparum* kinome (right) are the TK and STE kinase families but there is an expanded family of *apicomplexan*-specific FIKK kinases. Source; cellsignal.com (left tree) and Tewari et al. 2010 (right tree).

1.6. Casein kinase 1

This section will discuss the known biochemical functions of casein kinase 1 in eukaryotes and will address what is known about this enzyme in protozoan parasites.

1.6.1. Casein kinase 1 in higher eukaryotes

Casein Kinase 1 (CK1) genes form a distinct and small branch of the ePK tree (figure 1.2). CK1 is a pleotropic Ser/Thr PK first described by its activity on casein (reviewed in (Cheong and Virshup, 2011)) highlighting its preference for substrates containing acidic or pre-phosphorylated (primed) residues upstream of the CK1 phosphorylation site (Meggio et al., 1992, Flotow and Roach, 1991, Flotow et al., 1990). This led to the eventual identification of a CK1 phosphorylation consensus sequence of pS/pT X_{1-2} S/T, where pS/pT is a primed Ser or Thr residue, X denotes any amino acid and phosphorylation by CK1 occurs on the subsequent underlined Ser/Thr residue (Meggio et al., 1992). Additionally, clusters of acidic amino acids (Asp or Glu) upstream of a Ser or Thr may also provide the required "priming" signal for substrate phosphorylation by CK1 (Flotow and Roach, 1991). In mammals, CK1 exists as seven active isoforms: CK1α, CK1β (identified in bovine cells only), CK1δ, CK1ε, CK1γ_1, CK1γ_2 and CK1γ_3; the genes are expressed from different loci across five chromosomes (reviewed in (Cheong and Virshup, 2011)) and are all highly homologous in the kinase domain (Figure 1.3A). Importantly, the architecture of CK1 is conserved across all eukaryotes from humans to yeast and plants (Figure 1.3B and Figure 1.4).

CK1 activity is important for normal cellular function and is involved in many biological processes, including transcriptional regulation, circadian rhythm control and vesicular trafficking (see table 1.1 for a summary of CK1 substrates). Mutations in CK1 or inhibition of its kinase activity results in the dysregulation of biochemical pathways and can lead to the development of disease (Meng et al., 2010, Xu et al., 2005b, Foldynová-Trantírková et al., 2010) consistent with the importance of this kinase in normal cellular function. Yeast CK1 (Hrr25) phosphorylates Ede1 and promotes direct interaction

between Ede1-Hrr25 and initiation of clathrin-mediated endocytic sites for vesicular trafficking (Peng et al., 2015). In plants such as *Arabidopsis*, CK1 functions by phosphorylating cryptochrome 2, a conserved blue light sensor that regulates various cellular pathways such as response to light, stress responses and the circadian clock (Tan et al., 2013). In humans CK1α, δ and ε isoforms all regulate the β-catenin/Wnt signalling pathway through phosphorylation of various proteins leading to either the activation or degradation of β-catenin and subsequent transcriptional effects (Pablo et al., 2005, Rubinfeld et al., 2001, Amit et al., 2002). Additionally, CK1γ contributes to this signalling pathway through phosphorylation of proteins that interact with Axin, a key regulator in the formation of the β-Catenin destruction complex. Overexpression and dysregulation of CK1 can therefore affect transcriptional regulation and hence contribute to disease such as cancer (Richter et al., 2014). Furthermore, CK1α has been shown in murine and human erythrocytes to contribute to the regulatory mechanism of programmed cell death by modulating cytosolic calcium activity (Zelenak et al., 2012). This process is termed eryptosis and displays cellular phenotypes similar to typical apoptosis and enables cell turn-over.

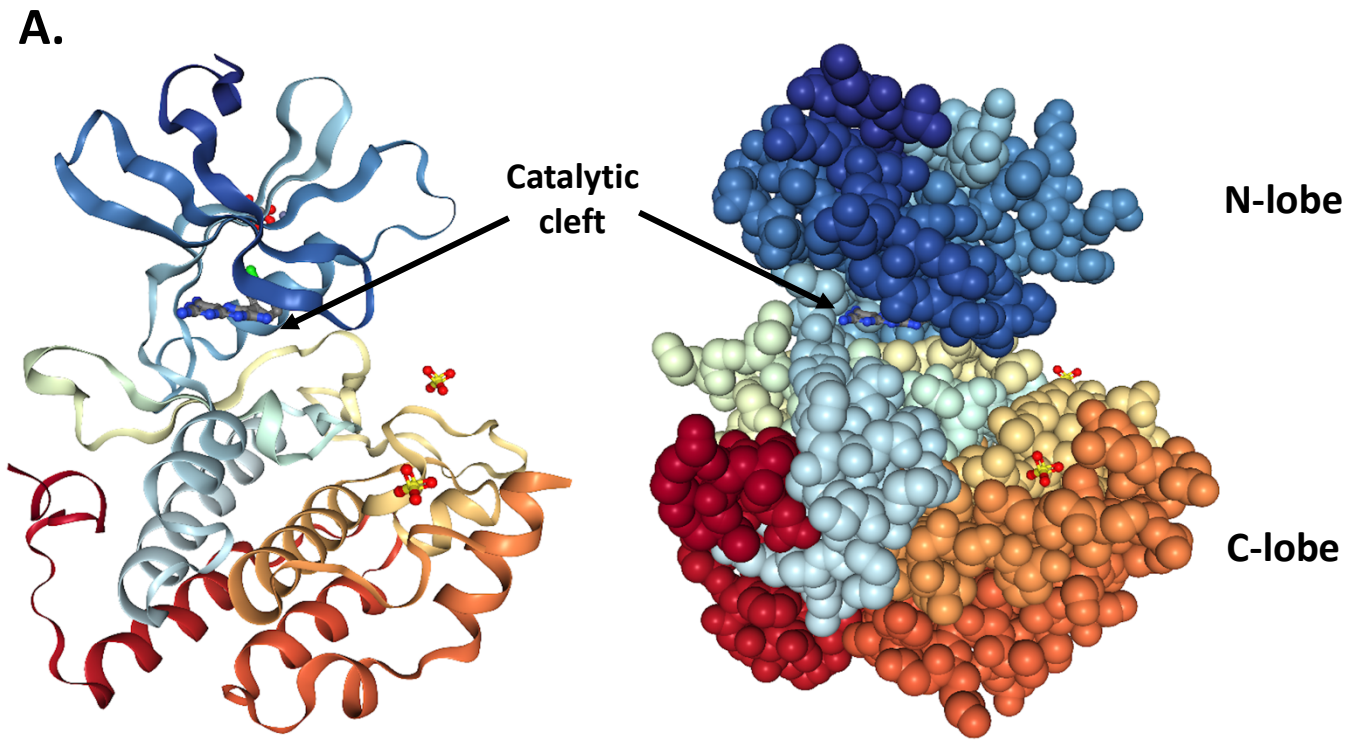
A.
Catalytic cleft
N-lobe
C-lobe

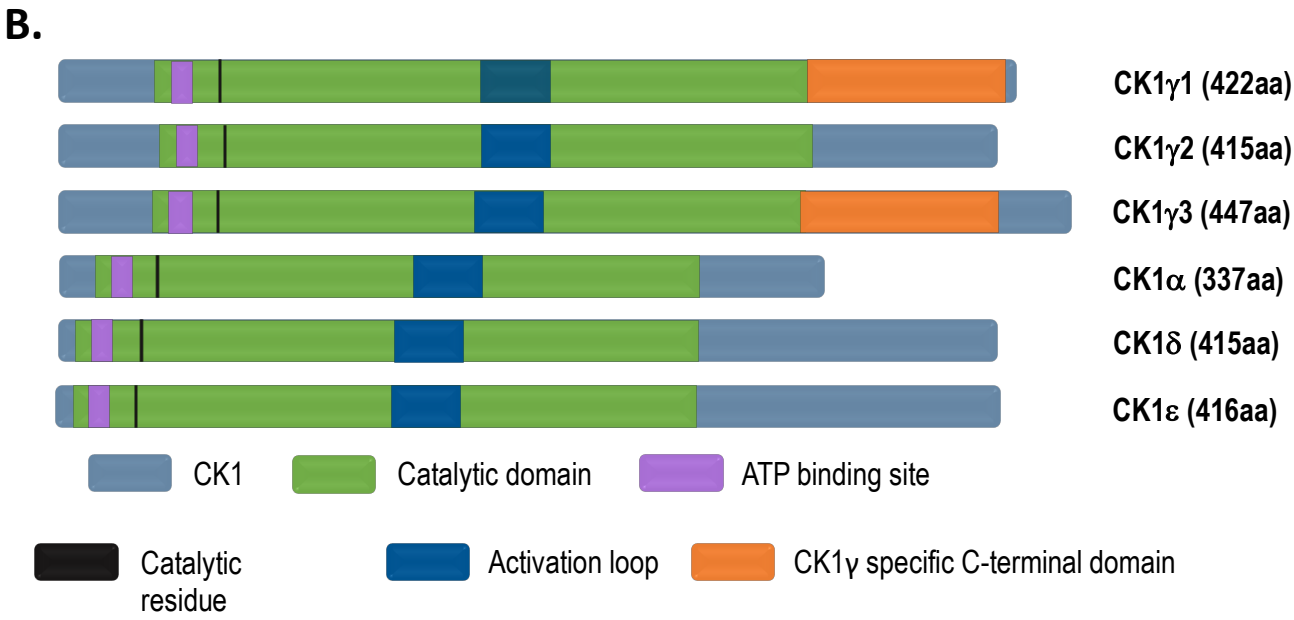
B.
CK1γ1 (422aa)
CK1γ2 (415aa)
CK1γ3 (447aa)
CK1α (337aa)
CK1δ (415aa)
CK1ε (416aa)
CK1
Catalytic domain
ATP binding site
Catalytic residue
Activation loop
CK1γ specific C-terminal domain

Figure 1.3. Three-dimensional structure of CK1 kinase domain. An example of the CK1 family represented by the kinase of domain of human CK1δ isoform (A) displayed as cartoon (left) and space-fill (right) models (PDB ID: 5IH5). Like all ePKs, CK1 has a bi-lobal fold characterised by a predominance of -sheets in the N-terminal lobe and an -helix-rich C-terminus, separated by a catalytic cleft (as distinguished by the ATP analogue Epiblastin A between the light and dark blue domains). The catalytic kinase domain of CK1 enzymes is highly conserved across all eukaryotes and constitutes an average of 67% of the total kinase structure. (B) Schematic representation of the domain architecture of human CK1 (blue). Overall architecture is preserved across isoforms; Catalytic domain (green): conserved PK kinase domain containing nucleotide binding domains and catalytic residues for the orientation of ATP and transfer of the gamma phosphate from ATP to a protein substrate. ATP binding site (purple): a glycine triad (GxGxxG) which encloses part of the ATP molecule. Catalytic residue (black): Asp amino acid thought to act as a base acceptor for hydrogen bonding with a hydroxyl group of a substrate. Activation loop (dark blue): the site of interaction with activity modulators. Phosphorylation of this domain is often required for the correct orientation of residues involved in the transfer of the gamma phosphate from ATP to a protein substrate. Shown in orange is an amino acid insertion unique to the CK1γ isoforms that likely regulates their specific cellular localisation and function.

1.6.2. Parasite CK1

Homologs of CK1 have been identified in parasites responsible for many major diseases in humans: *Leishmania*, *Toxoplasma* and *Plasmodium*, although functions of these kinases are not as well understood in parasites as they are in humans. Two isoforms have been isolated from *Toxoplasma gondii*: TgCK1α (38kDa) and TgCK1β (49kDa). Although very little is known of these two isoforms, TgCK1α has been shown to be present in the cytosol while the larger isoform is associated with the membrane (Donald et al., 2005). It is hypothesised that the cytosolic population may contribute to vesicular and membrane trafficking, while it is harder to make hypotheses about the membrane population (TgCK1β) as it lacks detectable kinase activity.

Leishmanial CK1 (LmCK1) activity has also been purified from crude promastigote extracts (the parasite stage which exists within a sand-fly vector) (Allocco et al., 2006). Two isoforms (LmCK1-1 and LmCK1-2) were identified, isoform 2 being the active enzyme. A secreted enzyme of *L. major* has also been shown to exhibit CK1 like activity, presumably the active isoform LmCK1-2, thought to potentially aid in parasite invasion by phosphorylating host proteins (Allocco et al., 2006). This is supported by a study that showed LmCK1 contributed to down regulating Type I interferon signalling and down regulating the host immune response to invasion (Liu et al., 2009).

1.6.3. Plasmodium falciparum CK1

P. falciparum CK1 (PfCK1) is a 36kDa orthologue of the mammalian CK1 kinases and shares greatest sequence homology with CK1δ (73%) based on bioinformatic algorithms. PfCK1 is known to be essential to the parasite asexual lifecycle as the genes are refractory to disruption although it is unknown whether one or both of the variants are biologically active.

Recently, the expression and localization of PfCK1 has been published for each stage of asexual parasite development, revealing two essentially separate populations (Dorin-Semblat, 2015). During the ring to early trophozoite phase, a large proportion of PfCK1 appears to be associated with the host erythrocyte membrane and could resemble an ectokinase (a PK with an extracellularly facing kinase

domain). A similar observation had been made in an earlier study that identified a membrane associated PK in *L. major* (Lester et al., 1990); although in this instance it was concluded the ectokinase did not belong to any of the established ePK groups. Progression to mature stages (late trophozoites and schizonts) shows PfCK1 becoming less associated with the membrane and more localised to the parasite itself, finally appearing in merozoites only. This membrane association is interesting because PfCK1 has no PEXEL (Plasmodium EXport ELement) motif or any form of recognisable export signal sequence. Instead it may become exported via another means, such as vesicular trafficking or post translational modification such as myristolation (Tillo et al., 2017), palmitoylation (Davidson et al., 2005) or glycosylphosphatidylinositol (GPI) anchoring (Zinecker et al., 2001). How PfCK1 then becomes associated with the erythrocyte membrane still remains unclear. In addition, PfCK1 activity has also been detected in the supernatant of parasite cultures indicating that this protein is also secreted during the asexual lifecycle, similarly to those of *Leishmania* and indeed it may play a role in phosphorylating host proteins on bystander cells.

1.6.4. PfCK1 in gametocytes

Unlike the localisation of PfCK1 in asexual stages of infection, nothing is known about PfCK1 presence or localisation in sexual stages. mRNA expression data from PlasmoDB (gene ID: PF3D7_1136500.2) identified by microarray shows no change in the level of expression of PfCK1 throughout maturation of gametocytes. It is also unknown whether these transcript levels translate to protein expression or if the transcripts are stored, with delayed translation (Mair et al., 2006b). An example of such genes are the mRNA transcripts of p25 and p28 (ookinete surface proteins required for transversal of the mosquito mid-gut (Tomas et al., 2001)) that bind to the Development of Zygote Inhibited (DOZI) and CAR-I/Trailer Hitch Homolog (CITH) protein complexes in female gametocytes (Mair et al., 2010). This mRNA/DOZI/CITH interaction yields translationally repressed transcripts that are transcribed upon fertilization of gametes within the mosquito to form a diploid zygote. Similarly, mRNA/DOZI repression of p25 and p28, as well as several other genes has been observed in *P. berghei* (Mair et al., 2006a)

indicating gene silencing is a conserved mechanism allowing the rapid onset of gene transcription and meiosis. Similar mechanisms of translational repression occur in humans and yeast (Coller and Parker, 2005, Chu and Rana, 2006).

Essentiality of PfCK1 has been confirmed in the asexual stages of infection (as previously described (Solyakov et al., 2011)). As a consequence, ΔPfCK1 parasite lines cannot be cultured *in vitro* and the essentiality of PfCK1 in sexual development cannot be explored by traditional "knockout" by gene disruption. This creates a gap in our understanding of if and how PfCK1 functions during blood stage sexual development and/or maturation within the mosquito. Replacing typical knockout methods with inducible "knockdown" systems to degrade and reduce transcript levels, thereby reducing the amount of translated protein, may provide a more suitable alternative to studying gene essentiality during sexual development. An excellent example of an inducible gene knockdown system is the G*lmS*-ribozyme system (Prommana et al., 2013). This system employs an inducible ribonuclease to self-cleave itself and the 3' poly-A tail from mRNA resulting in degradation of the transcript and subsequent loss of protein. Thus, these types of new molecular technologies coupled with traditional methods such as immunofluorescence imaging, immunopurification and mass spectrometry can help elucidate PfCK1 function during the sexual stages of development.

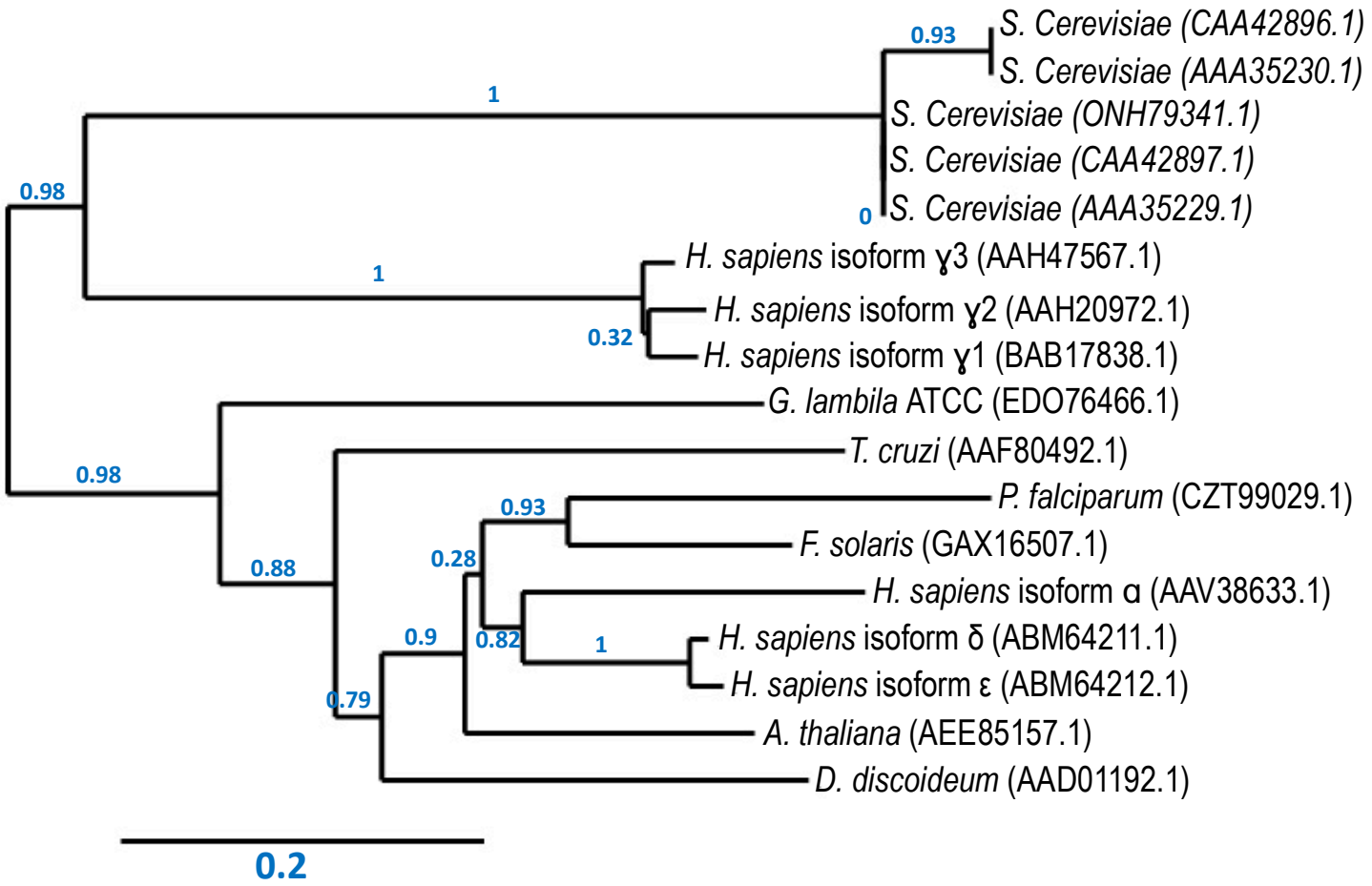

Figure 1.4. Phylogenetic tree of eukaryotic CK1 kinase domains. Members of the Casein kinase 1 (CK1) family are highly conserved amongst all eukaryotic cells. Despite large variation in the C-terminal domain, the catalytic kinase domain is highly conserved. Shown is a phylogenetic analysis of the kinase domain of CK1 isoforms from seven eukaryotic species. This tree was generated using the one-click phylogeny analysis (www.phylogeny.fr).

1.7. Localisation of PfCK1 to the RBC membrane

During the various stages of asexual development, *P. falciparum* exports a large number of proteins to remodel the host erythrocyte, and a number of these proteins are exported to the erythrocyte cell membrane. As mentioned previously, PfCK1 is one such protein exported to the erythrocyte membrane where it remains until the later part of the trophozoite stage. If PfCK1 is exposed to the extracellular environment, this specific localisation presents an opportunity for host immune pressure which raises two questions: What purpose does PfCK1 serve at the erythrocyte membrane? And how does it get there? To formulate hypotheses about how PfCK1 is trafficked to erythrocyte membranes and its function once there, this section will describe some of the known membrane trafficking mechanisms and the functions of proteins known to be associated with membranes.

1.7.1. The *Plasmodium* export element and membrane trafficking

During asexual development *P. falciparum* parasites extensively remodel the host RBC by exporting a repertoire of proteins to various RBC compartments. To do this, proteins must cross the parasite membrane and the PVM. The best characterised protein export pathway is the *Plasmodium* export element/Vacuolar transport signal (PEXEL/VTS) pathway (A et al., 2009) with more than 400 parasite proteins exported through this process (Sargeant et al., 2006). Proteins destined for secretion and which possess a PEXEL motif are processed in the endoplasmic reticulum (ER) by cleavage at the N-terminus by the aspartic acid protease plasmepsin V (Russo et al., 2010, Sleebs et al., 2014). Processed PEXEL proteins are then translocated across the PVM into the host cytoplasm via translocator machinery termed the *Plasmodium* translocon of exported proteins (PTEX) (Bullen et al., 2012). Importantly for exported proteins destined for the RBC membrane, for example the virulence factor *P. falciparum* erythrocyte membrane protein 1 (PfEMP1), they must first traffic to and associate with Maurer's clefts (MCs), parasite-derived membranous structures associated with the RBC cytoskeleton (Cornelia et al., 2008, Neline et al., 2003). How these proteins are then trafficked from the MCs to the

RBC plasma membrane still remains elusive, although some studies have suggested that vesicle trafficking may play a role in this process, as exemplified by the identification of resident MC proteins in parasite-derived vesicles (Mantel et al., 2013, Regev-Rudzki et al., 2013).

A number of parasite proteins are still exported into the host cytoplasm despite lacking a PEXEL sequence and are termed PNEPS (PEXEL-negative exported proteins) (Heiber et al., 2013). Interestingly, some PNEP parasite proteins such as the skeletal binding protein (PfSBP1) and membrane-associated histidine rich protein 1 (MAHRP1) exist as resident MC proteins, suggesting that a different mechanism enables proteins to transit to the MCs. For these two proteins, a transmembrane domain and the second half of the N-terminal domain are sufficient for export to MCs (Spycher et al., 2006, Theodora et al., 2009), whereas MAHRP2 requires the first 15 amino acids in addition to a histidine rich N-terminal domain (Esther et al., 2010). In the case of the ring-exported protein 1 (REX1), the first 10 amino acids plus a hydrophobic domain are sufficient for trafficking to MCs (A. et al., 2008); REX1 is exported as a soluble protein, indicating a possible mechanism for PNEPs to cross the PVM. Collectively this indicates that PNEP proteins may utilise a different type of signal motif sufficient for export.

PfCK1 does not contain any canonical or non-canonical PEXEL sequence (Schulze et al., 2015) and was not identified in an analysis of the predicted *P. falciparum* exported proteome based on the presence of the PEXEL motif (Sargeant et al., 2006) indicating this protein is a PNEP. Furthermore, the published interactome of MCs also failed to identify PfCK1 suggesting that it does not transit through MCs (Vincensini et al., 2005) and raising the question of how PfCK1 reaches the RBC membrane. Several other trafficking pathways exist in eukaryotes, which could serve as a possible protein export pathway in *P. falciparum* enabling membrane localisation and even secretion.

1.7.2. Vesicular trafficking

Extracellular vesicles (EVs) are key mediators of communication between cells, without the need for direct contact. EVs contain the cytosol of the cell of origin and can be categorised by size, content and origin (Marina Colombo et al., 2014). For example, microvesicles (MVs) are usually 0.1um – 1um in size and released by budding events at the plasma membrane, whereas EVs such as exosomes are typically smaller (30nm – 100nm) and derived from the exocytosis pathway (Di Vizio et al., 2009). Given that some EVs overlap in size, their origin of biogenesis is usually used to define them. Different cells secrete EVs which can trigger specific functions within a target cell. For example, it has been demonstrated that EVs of mouse mast cell origin contain mRNA which are transcribed into proteins upon fusion with human mast cells and content release into the cytoplasm (Valadi et al., 2007).

Vesicles are involved in transferring macromolecules to other cells and modulating downstream signalling events and also play a role in the maturation and differentiation of other cell types. For example, very little is known about the maturation process of RBCs and several theories have proposed the maturation and enucleation (expulsion of the nucleus) of erythroblasts – the metabolically active precursors to mature RBCs may be similar to cytokinesis (Skutelsky and Danon, 1970, Hebiguchi et al., 2008). An exquisite study in 2010 by Ganesan *et al* (Keerthivasan et al., 2010) demonstrated that inhibitors used to block these processes did not prevent enucleation events. It was further shown that endosomal trafficking was likely responsible for the enucleation process as supported by several lines of evidence: knockdown of clathrin inhibited enucleation; treatment of erythroblasts with vacuolin-1 (a molecule that induces vacuole formation) resulted in an increased number of enucleated cells and; treatment of cells with several inhibitors of the endosome pathway resulted in a decrease in the number of enucleated cells. This indicates that endosomal trafficking pathways are evident in RBC precursor cells and suggests the likelihood that remnants of these pathways may exist in mature RBCs.

Cell-cell communication by EVs has been confirmed in protozoan parasites like *P. falciparum* and *Leishmania*. A study in 2013 by Regev-Rudzki *et al* (Regev-Rudzki et al., 2013) examined the role of EVs in the transfer of macromolecules between *P. falciparum* parasites in culture. They showed that two parasite lines co-cultured together, each transfected with a different episome containing a drug resistance cassette to either blasticidin-S (CS2eBsd^{GFP}) or the anti-folate inhibitor WR99210 (3D7edhfr^{GFP}) and expressing GFP protein, were able to grow in the presence of both Bsd and WR99210. This was not observed when each parasite line was cultured separately in the presence of both inhibitors and transfer was independent of cell-cell contact. It was concluded that EV-like particles of ~70nm were responsible for the transfer of resistance between parasite populations. Similarly, a proteomic examination of the EV content of supernatants from schizont stage *P. falciparum* parasites identified a broad repertoire of host and parasite proteins (Mantel et al., 2013). It was shown that some activating factors for CD14+ primary blood monocytes (PBMCs) and CD19+ B cells were down-regulated when these cells were incubated with EVs from *P. falciparum* parasites. This indicates that one of the main functions of iRBC-derived EVs is to modulate immune responses during infection.

A similar study was performed for *Leishmania* parasites which also examined the proteomic content of EVs during the infection of macrophages (Silverman et al., 2010a). An astonishing 52% of the parasites secreted proteome are contained in EVs and are able to modulate immune system responses by inducing secretion of IL-8, a major neutrophil chemotactic factor (M. et al., 2011) but not tumour necrosis factor (TNF)-α. Comparable modulation of IL-10 secretion, but not TNF-α, has also been observed in *L. donovani* parasites (Silverman et al., 2010b). While the exact function of modulating such immune responses are beyond the scope of this thesis, it is noteworthy to comment on the broad immune responses that are affected by parasite-derived vesicles. It has also been shown that the proteomic content and abundance in *Leishmania* EVs is influenced by cellular stresses such as pH and temperature change highlighting a collection of potential virulence factors associated with specific environmental stimuli. It is interesting to consider the influence of environmental stress on the

proteomic content of EVs as they may play a role in parasite survival. In the same study by Regev-Rudzki *et al*, increasing levels of gametocytes were observed as the levels of asexual *P. falciparum* parasites was decreasing. Further, a 17-fold increase in the number of gametocytes was observed in 3D7edhfr^{GFP} and CS2eBsd^{GFP} co-cultures compared to culturing either parasite line separately, suggesting that drug selection may have prompted sexual commitment, possibly through cell-cell communication by EVs. This interesting observation suggests that environmental cues, for example drug pressure, result in the alteration of EV cargo which can elicit signalling responses in other parasitised cells when growth conditions are no longer favourable; a mechanism likely adapted to ensure parasite survival and disease transmission.

1.7.2.1. Rab GTPases

Although vesicular trafficking networks have been identified in *P. falciparum*, regulation of these networks is complex and not fully understood. Transcriptional and translational evidence suggests that *P. falciparum* expresses a family of proteins known to be involved in EV trafficking in higher eukaryotes, called Rab GTPases (Quevillon et al., 2003, Morse et al., 2016, Jambou et al., 1996, Spielmann and Beck, 2000, Wiesner et al., 2013). Rab GTPases are conserved members of the ras-related protein family of small GTPases and are involved in EV trafficking. In humans, approximately three quarters of the more than 60 Rab proteins are involved in vesicular related trafficking pathways [129], some better understood than others. Rab proteins are modified near the C-terminus by geranylgeranyl isoprenylation, which enables attachment to membranes (Gavriljuk et al., 2013, Li et al., 2014) and their activity is regulated by a guanine triphosphate/guanine diphosphate (GTP/GDP) switch which determines the “on/off” state of the enzyme; binding of GTP activates Rab proteins, whereas GDP binding results in an inactive confirmation. This on/off state and membrane attachment is tightly controlled by various regulatory proteins such as GTPase-activating proteins (GAPs), Rab geranylgeranyl transferases (RabGGTase), GDP disassociation inhibitors (GDIs) and guanine nucleotide exchange factors (GEFs) (Bos et al., Wu et al., 2010, Wu et al., 2011).

The *P. falciparum* genome encodes eleven Rab GTPases which represents a significant proportion of the prenylated proteome (prenylome) [124, 135]. All Rab genes are highly expressed throughout the parasite asexual cycle and, as with higher eukaryotes, contribute to various cellular functions, from maturation during mitosis to formation of invasion-related protein complexes (Agop-Nersesian et al., 2009, Agop-Nersesian et al., 2010, Morse et al., 2016) and in protein trafficking of the *cis- trans-* Golgi network (Hallée and Richard, 2015, Kaiser et al., 2016).

Rab5 is a defined marker of the endosomal system in many eukaryotes. In *L. donovani*, both LdRab5a and LdRab5b isoforms regulate different modes of endocytosis, either by fluid-phase (LdRab5a) or receptor-mediated (LdRab5b) processes (Rastogi et al., 2016). Importantly, null-mutants of both isoforms are non-viable, indicating these proteins are essential to parasite survival *in vitro*. Rab5 isoforms function in a similar way in *P. falciparum* by directing protein transport. *P. falciparum* Rab5 proteins exhibit interactions with haemoglobin, similar to the proposed function of LdRab5b in *L. donovani,* denoting distinct roles for these proteins in endosomal transport in protozoans. Immunofluorescence studies have shown that the *P. falciparum* PfRab5b isoform fails to co-localise with haemoglobin, whereas PfRab5a localises to haemoglobin containing compartments of the RBC (Ezougou et al., 2014). Immuno-transmission electron microscopy (immuno-TEM) also revealed that PfRab5a localises to small haemoglobin-containing vesicles (SHVs), and constitutively active PfRab5a mutants increase FV volume and aggregate volume of haemoglobin-containing vesicles (HVs) (Elliott et al., 2008). Together, these observations indicate a role for PfRab5a in directing haemoglobin uptake and transport.

PfRab5b is unique as it lacks the typical C-terminal isoprenylation site and instead contains an N-terminal myristoylation site (Ezougou et al., 2014) allowing membrane targeting of this GTPase. Fluorescence imaging has shown that PfRab5b is present in the parasite cytoplasm as well as the cytoplasmic face of the tubovesicular network (TVN), a tubule network region which extends into the iRBC cytoplasm from the PVM [143]. PfRab5b was also shown to complement the function of the rodent malaria parasite *P. berghei* Rab5b (PbRab5b), suggesting a conserved function in *Plasmodium*

parasites (Ebine et al., 2016); PfRab5b was also shown to complement the function of the rodent malaria parasite *P. berghei* Rab5b (PbRab5b) suggesting a conserved function in *Plasmodium* parasites (Ebine et al., 2016). Several *P. falciparum* virulence factors are directed to separate parasite compartments by interacting with PfRab5b. For example, the parasite invasion protein merozoite surface protein-1 (MSP1) is directed to the parasite food vacuole membrane (FVM), whereas PfCK1 is directed to the parasite plasma membrane (PPM) (Ezougou et al., 2014); it is unclear whether these structures are at the RBC membrane. Pull-down experiments have established PfCK1 as an interactor of PfRab5b (Rached et al., 2012) suggesting that these interactions may contribute to PfCK1 trafficking.

1.7.3. Post-translational modification

Post translational modification (PTM) of proteins is one way in which a cell can adapt to changing environmental conditions (Beltrao et al., 2013). The addition of lipids to proteins is a very common modification responsible for the trafficking and anchoring of proteins to biological membranes (Martin et al., 2012, Fujita and Kinoshita, 2012). Some proteins with ectokinase activity (proteins bound to the external side of plasma membranes that can phosphorylate extracellular proteins) are known to be anchored to membranes by lipid modifications. Likewise, exposure of PfCK1 on the erythrocyte membrane suggests that lipid modification may play a role this localisation.

1.7.3.1. Post-translational modification of CK1

Fatty acid modification of proteins, for instance palmitic acid, regulates their membrane association, protein stabilisation and protein-protein interactions (reviewed in (Aicart-Ramos et al., 2011)). Protein acyl transferases (PATs) are enzymes which contain a conserved Asp-His-His-Cys (DHHC) motif and catalyse the addition of palmitic acid onto proteins (Mitchell et al., 2010). These enzymes were first identified in *Saccharomyces cerevisiae* with two main enzymes having been described. The first is Akr1, which was identified as the PAT responsible

for the palmitoylation of yeast casein kinases YCK1p and YCK2p and their association with the plasma membrane (Politis et al., 2005). Deletion of Akr1 has been shown to dysregulate the localisation of the YCK proteins (Roth et al., 2002, Politis et al., 2005). A second PAT, which exists as a heterodimeric complex formed by Erf2 and Erf4, is responsible for the palmitoylation of Ras proteins (GTP-binding proteins) which occurs by a two-step process: Erf2 is first autopalmitoylated, thus acting as a palmitoyl-intermediate protein that is stabilised by Erf4 (Mitchell et al., 2012). The second and final step is the transfer of the palmitic acid moiety to the Ras protein (Mitchell et al., 2010). It was also shown by mutational analysis of the conserved DHHC motif that the catalytic activity of this domain is necessary for Erf2 autopalmitoylation and for the transfer of palmitic acid to protein substrates.

Although extensively studied in yeast, DHHC domain-containing enzymes are evolutionarily conserved across multiple eukaryotes including humans, mice, plants and parasitic protozoa (Merino et al., 2014, L. et al., 2016, Ohno et al., 2006, Li et al., 2016) and their dysregulation in humans has been linked to disease pathology like cancer (Sharma et al., 2017). Studies of CK1γ in humans, *Xenopus* and *Drosophila* show that a unique palmitoylation site at the C-terminal end (TKCCCFFKR) tethers this kinase to the membrane and couples it to the Wnt/β-catenin pathway by interacting with LDL-receptor related protein 5 and 6 (LRP5/6) (Davidson et al., 2005). Truncation of the C-terminal end of CK1γ abolishes membrane association and regulation of Wnt signalling.

Predicting protein palmitoylation sites can be difficult due to the promiscuity of the environment required for Cys-modification, and very few consensus sequences have been identified. A recent study examined the physiochemical properties that could potentially predict whether a protein is palmitoylated (Reddy et al., 2017). By utilising bioinformatic

approaches, it was suggested that enrichment of hydrophobic and basic residues, the amino acid sequence surrounding Cys residues and predicted cellular location all influence the propensity of a protein to be palmitoylated. While this provides a useful tool for predicting palmitoylation status, it is likely that additional modifications that influence a proteins biochemical environment (for example phosphorylation) may also play a role in determining palmitoylation sites. It has also been proposed that proteins can be palmitoylated in multiple regions of the same proteins. This is exemplified in the yeast CK1-homolog 2 (YCk2) which contains a tripartite palmitoylation site, i.e. several regions of the kinase domain and C-terminal domain are required for sufficient palmitoylation to direct membrane association (Roth et al., 2011). It was suggested that phosphorylation may also be required for recognition of YCk2 by Ark1.

Indeed, membrane localisation of PfCK1 during early stages of parasite development suggest that palmitoylation may contribute to cellular trafficking of this protein. An exquisite study by Jones *et al* 2012 (Jones et al., 2012) investigated the global palmitome in *P. falciparum* by using two independent chemical exchange strategies: metabolic labelling and click chemistry (MLCC), which labels parasites with a palmitic acid analogue allowing biotinylation through azide click chemistry (Martin et al., 2012), and acyl-biotin exchange (ABE), which requires a series of chemical cleavage and blocking steps to replace the thioester-linked palmitoyl group with a biotin moiety (Roth et al., 2006). The combined results from these two approaches identified over 400 predicted palmitoylated proteins. PfCK1 was identified in the initial sample enrichment, however it did not meet the strict threshold limits of a 5% false-discovery rate (FDR) and was therefore excluded in the final analysis. Nevertheless, this study reveals

the possibility that palmitoylation of PfCK1 may indeed contribute to its membrane trafficking, a hypothesis that is yet to be tested.

1.8. Nuclear localisation of CK1

Chromatin is a conserved eukaryotic structure which consists of nucleosomes separated by linker DNA; each nucleosome consists of 147bp of DNA wrapped around a histone octamer (Eustermann et al., 2018, Luger et al., 1997, White et al., 2001). The octameric core comprises two tetramers – the first consisting of two copies of the core histones H3 and H4 which is, foremost, inserted into the nucleosome, followed sequentially by the other tetramer consisting of two copies of histones H2A and H2B (reviewed in (Burgess and Zhang, 2013)). While the structure of chromatin is rather simple, modification of the histone core to regulate transcriptionally active (euchromatin) or repressive (heterochromatin) (Janssen et al., 2016) states is a complex process regulated by multiple histone modifying enzymes. In a transcriptionally silent state, heterochromatin is condensed and prevents the binding of transcription factors and RNA polymerases to promoter regions while conversely, euchromatin is open and relaxed which enables sufficient access to DNA for gene transcription.

Histones are extensively modified in their N-terminal tails by proteins called histone readers (recognise the histone marks), writers (catalyse histone modifications) and erasers (remove histone modifications) (reviwed in (Laia and Manel, 2015)). Collectively these groups of proteins regulate histone modifications such as acetylation (Xhemalce and Kouzarides, 2010), methylation (Schibler et al., 2016) and phosphorylation (Dastidar et al., 2013) and each modification consequently affects the transcriptional state of chromatin. For instance, lysine acetylation is a well-studied marker for transcriptional activation (Gajer et al., 2015, Yan et al., 2018) and is regulated by the opposing actions of histone acetyltransferases (HATs) and deacetylases (HDACs). In contrast, methylation of lysine or arginine residues – catalysed by histone methyltransferases (HMTs), can result in either transcriptional repression (Trojer et al., 2007) or activation (Lee et al., 2007).

In comparison to acetylation and methylation, the effects of Ser, Thr or Tyr phosphorylation on histone tails by PKs and their consequences on the transcriptional state of chromatin is less understood. It is suggested that phosphorylation of Ser1 of the core histones H4 (H4S1ph) and H2A (H2AS1ph) may have roles in chromatin condensation during the mitosis and in histone deposition during S-phase (Barber et al., 2004). This histone mark is evolutionarily conserved and has been identified in worm, fly and mammalian cells, consistent with its importance in maintaining chromatin structure.

Phosphorylation also affects histone methylation status. For example, H3 phosphorylation at Ser10 (H3S10ph) and Thr11 (H3T11ph) influence the dimethylation of Lys9 on H3 (H3K9me2) in mouse zygotes and the maintenance of 5-methyl cytosine (5mC) (Lan et al., 2017). The authors of this study showed that overexpression of mutants of H3 variants H3.1 and H3.2 (H3S10A/H3T11A) resulted in a decrease in H3K9me2 and 5mC and a concurrent increase in oxidised 5mC (5hmC), suggesting an important crosstalk between H3phos and H3K9me2 and subsequent protection of DNA from oxidation. The crosstalk between histone phosphorylation and methylation and its effects on the protection of DNA is further supported by a study which exquisitely showed that phosphorylation of the histone variant H2AX is upregulated in response to ionising radiation (Hausmann et al., 2018). In contrast to the cooperative effects observed for histone phosphorylation and H3K9me2, histone phosphorylation in HeLa cells by the kinase M6CK resulted in decreased levels of methylation in neighbouring Arg residues thereby influencing gene transcription (Krapivinsky et al., 2017). Collectively this shows the various functions of histone phosphorylation in regulating chromatin dynamics.

It is only in the last decade that histone phosphorylation in *P. falciparum* has really begun to be unravelled, with 14 phosphorylation sites having been identified (Dastidar et al., 2013). Similar to the crosstalk between histone phosphorylation and methylation, many of the histone phosphosites identified in *P. falciparum* were found to be adjacent to acetylated lysine residues suggesting a

possible interplay between modifications and subsequent transcriptional activity. In yeast, phosphorylation of H3S10 by the Snf1 kinase provides a binding site for the HAT Gcn5 which subsequently acetylates Lys14 to enhance the transcription of INO1 (Lo et al., 2001). In mouse JB6 cells it has been shown that inhibition of HDACs promotes H3S28ph by the MAP kinase ERK2 which, consequentially, facilitates H3L9ac (Zhong et al., 2003) and this may have an impact on chromatin remodelling and transcription.

Thus, the recognition of phosphorylated histones by reader proteins is an important regulatory mechanism of transcriptional activity. In many model organisms the 14-3-3 protein recognises H3S10ph (Macdonald et al., 2005, Winter et al., 2008) and binds to HDACs to sequester them in the cytoplasm, thereby inhibiting the deacetylation of histones and transcriptional silencing (Grozinger and Schreiber, 2000). The *P. falciparum* 14-3-3 homologue (Pf14-3-3I) recognises H3S28ph and H3S10ph but exhibits a preference towards H3S28ph, irrespective of neighbouring modifications (Dastidar et al., 2013). Although the functional consequences of these interactions still remain to be established it could be that H3S28ph binding by Pf14-3-3 allows subsequent interactions to be formed with chromatin regulating enzymes such as HDACs or HATs, thereby providing a mechanism of transcriptional regulation similar to those observed in other cells.

Histones H2A, H2A variant, H3 and H4, as well as the catalytic subunit of Casein kinase 2 (PfCK2α) were recovered in PfCK1 immunoprecipitates (Dorin-Semblat et al., 2015). PfCK2 is a substrate of PfCK1, but it remains unclear whether H4 or any other histones are PfCK1 substrates *in vitro*. Interestingly, PfCK2 has been shown to phosphorylate various chromatin structural and regulatory elements including histones, the DNA/RNA binding proteins (Alba) and nucleosome assembly proteins (Naps) thus functioning in chromatin assembly (Dastidar et al., 2012). To be deposited into nucleosomes histones must be trafficked into the nucleus, a process which requires the formation of an import complex with the nucleosome assembly protein-1 (Nap1). Naps are conserved in all higher eukaryotes (Park and Luger, 2006, Ito et al., 1996, Okuwaki et al., 2010) and are responsible for binding

and depositing histones H2A and H2B (Aguilar-Gurrieri et al., 2016, Son et al., 2015). Nap1 also binds to the importin proteins karyopherin α/β which are required for the nuclear import of proteins, thus establishing a nucleocytoplasmic shuttling system (Mosammaparast et al., 2002). In addition to co-purifying with histone proteins, PfCK1 interacts with and phosphorylates NapL, a Nap1 homologue in *P. falciparum,* suggesting a possible role in regulating chromatin structure. However, the nuclear localisation of PfCK1 has not been validated and its function in the nucleus has not been examined.

Some early studies have identified nuclear functions for CK1 in various eukaryotes. CK1 has been implicated in the DNA-damage response in *Drosophila melanogaster* and the yeast *S. cerevisiae* (Santos et al., 1996, Ho et al., 1997). *D. melanogaster* CK1 (DMCK1) has also been implicated in regulating the circadian clock (Lam et al., 2015) by phosphorylating the transcriptional activator CLK to regulate its clearance from the promoter region of PER (transcriptional repressor). DMCK1 also phosphorylates and destabilizes PER in the nucleus and coordinates the nuclear entry of PER from the cytoplasm. In mammalian cells, CK1 isoforms have also been identified as nuclear kinases. For instance, CK1δ localises to the nucleus; however, it is not thought to contribute to gene transcription, but rather it localises to spindle poles in mitotic cells and may contribute to chromosomal segregation (Milne et al., 2001). Interestingly, CK1δ nuclear localization is not regulated by its C-terminal domain; instead, kinase activity is required, as shown by fluorescence imaging of wild-type and kinase dead (KD) CK1δ constructs. It could be that nuclear localisation may be the result of CK1δ complex formation with proteins that shuttle between the cytoplasm and nucleus, supported by an accumulation of CK1δ in nuclei following treatment with the nuclear export inhibitor Leptomycin B (Milne et al., 2001). During embryo development, mouse oocytes require nuclear CK1α for correct chromosomal segregation. Inhibition of CK1 activity results in polar body extrusion, pro-M1 arrest and failure of chromosomes to align at the spindle equator (chromosomal congression) (Wang et al., 2013). Immunofluorescence staining also showed that CK1α co-localises to condensed chromosomes during oocyte maturation, consistent with histone phosphorylation associated with chromatin

condensation (reviewed in (Rossetto et al., 2012)) which suggests a possible role for CK1 proteins in histone phosphorylation and maintenance of heterochromatin.

1.9. Purvalanol B kills *P. falciparum in vitro*

Purvalanol B is a 2,6,9-trisubstituted ATP-competitive analogue and a potent inhibitor of cyclin dependent kinases (CDKs) in many eukaryotes including humans (as low as 6nM on purified CDK, Ruetz et al., 2003). The high cell-free potency of Purvalanol B notwithstanding, the compound is inactive in cell-based assays, thought to be due to the presence of a free carboxylate group at the 6-anilino end of the purine backbone that prevents passive diffusion across biological membranes (Villerbu et al., 2002). Crystallographic studies of kinases with docked Purvalanol B show that this carboxyl moiety is not directly involved in interactions with target proteins (Figure 1.5), but it instead extends outwards from the binding domain (Gray et al., 1998, Holton et al., 2003). This compound orientation enables chemical modification of the carboxyl group to provide a useful tool for biochemical studies, without disrupting interactions between compound and target protein, and to modulate compound potency. Analogues of Purvalanol B are being tested for their usefulness in the field of cancer biology to target CDKs. Fluorescent dansyl moieties have been synthetically coupled to the 6-anilino carboxyl to make compound uptake easier to detect. The target CDKs are intracellular proteins and neutralising the free carboxylate charge would increase the compounds cell-membrane permeability, allowing passive diffusion and access to intracellular targets. For example, Purvalanol B modified with fluorescent dansyl moieties (VMY-1-101 and VMY-1-103) have been tested on breast cancer cell lines for their CDK inhibitory activities (Yenugonda et al., 2011, Ringer et al., 2010). Cells treated with both Purvalanol B derivatives were killed at concentrations less than 10μM and the number of cells entering the S-phase of mitosis was decreased compared with unmodified Purvalanol B.

Several PK inhibitors with antimalarial activity, for example imidazopyridazines, are currently being explored as possible therapeutics (Crowther et al., 2016, Hallyburton et al., 2017, Green et al., 2016).

However, as with any repurposed compound, the possibility of finding a selective mode of action that minimises effects on the host must be considered. Purvalanol B displayed low micromolar antimalarial activity against *P. falciparum* parasites in [^{3}H]-hypoxanthine incorporation assays with a reported IC_{50} of 7μM (Harmse et al., 2001), contrary to its lack of potency against mammalian cells, indicating this cell-impermeable compound may have unique pharmacological properties in malaria that could be exploited. Indeed, Purvalanol B is a known inhibitor of mammalian CDKs which belong to the CMGC PK family and also make up a significant proportion of the *P. falciparum* kinome (Figure 1.2). Interestingly, CDKs are not the targets of Purvalanol B in *P. falciparum* and other parasitic protozoa, as described in a previous study by Knockaert *et al*. which explored the intracellular targets of purine inhibitors (Knockaert et al., 2000). Inhibitors including Purvalanol B were immobilised on agarose beads (in the case of Purvalanol B this was by coupling the carboxyl group to the agarose) and incubated with protein lysates from various organisms to detect target proteins by microsequencing. Cell extracts of *P. falciparum* were analysed, resulting in the identification of four protein bands able to interact with the compound; PfCK1 was the only detectable selective target. Methylation of a secondary amine at the N6 position, key for kinase inhibition, abrogated compound binding to PfCK1, indicating that the interaction is specific. CK1 was also identified as a Purvalanol B target in other parasitic protozoa such as *Toxoplasma, Leishmania* and *Trypanosoma* (Knockaert et al., 2000).

Purvalanol B can inhibit purified PfCK1 with an IC_{50} of 100nM (Karine Le Roch, unpublished PhD thesis), suggesting that PfCK1 is a sensitive target. A significant proportion of PfCK1 is associated with the RBC membrane during early stages of parasite development (see section 1.4.3); therefore, the simplest mode of action hypothesis would be that Purvalanol B may be killing *Plasmodium* through inhibition of surface exposed PfCK1, which would be a unique mode of antimalarial action. However, intake through parasite-induced permeation pathways and inhibition of intracellular PfCK1 or other kinases cannot be excluded at this stage. To date there have been no attempts to assess the involvement of PfCK1 in the antiplasmodial activity of Purvalanol B. If the hypothesis of an extracellularly-located CK1 as the lethal target of Purvalanol is confirmed, we would have identified a valid antimalarial target

accessible from the external medium, which simplifies significantly the pharmacological requirements for a drug and avoids resistance mechanisms based on efflux systems. Furthermore, by utilising Purvalanol B as a chemical tool, one could study a variety of biological questions relating to PfCK1 function during different stages of the lifecycle. We can approach this by analysing the effects of Purvalanol B at different stages of the parasite lifecycle, coupled with quantitative whole-cell phosphoproteomics (Lasonder et al., 2012, Solyakov et al., 2011, Leykauf et al., 2010) to identify phosphorylation targets of PfCK1.

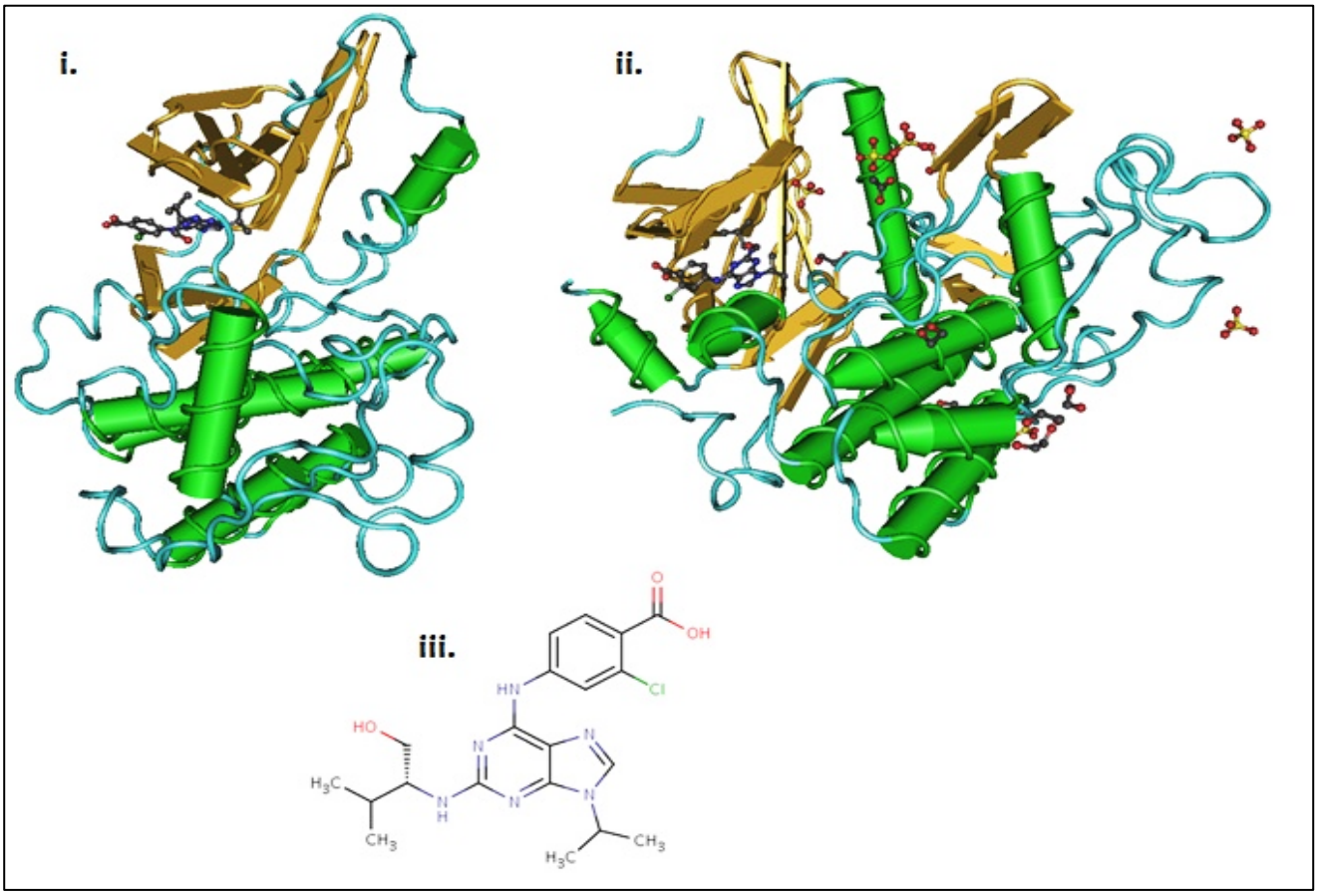

Figure 1.5. Binding orientation of Purvalanol B. Solved diffraction crystal structures of i) *P. falciparum* protein kinase 5 (Pfpk5: PDB ID 1V0P) and ii) Serine-Arginine rich protein specific kinase 2 (Srpk2: PDB ID; 2X7G). The molecular structure of Purvalanol B is shown as iii.

1.10. Specific aims of this thesis

The dysregulation of protein phosphorylation by PKs has led to the exploitation of PKs as therapeutic targets. As a result, more than 30 PK inhibitors have been approved by the Food and Drug Administration (FDA) for use in human diseases such as cancer (M., 2017). PKs also control protein phosphorylation in malaria parasites but are not the lethal targets of any approved antimalarials, thus making them appropriate targets for pharmacological intervention as there is little chance of pre-existing resistance mechanisms associated with their inhibition. However, several gaps exist in our current understanding of how many fundamental biological processes are controlled by malaria PKs, therefore restricting the possible avenues for drug interference.

The work in this PhD thesis aims at expanding our current understanding of how PfCK1, the sole member of the CK1 PK family in *P. falciparum*, contributes to the virulence of *P. falciparum* during asexual replication within its RBC host. To determine the roles for PfCK1 during asexual development, we performed experiments to address the following aims:

1. Identify the cellular mechanisms that modulate the secretion of PfCK1 and its trafficking to the RBC membrane at distinct times of asexual development

2. Determine the functions of PfCK1 within the parasite's nucleus and possible contributions to chromatin dynamics and transcriptional activity

3. Investigate the contribution of PfCK1 in the Purvalanol B mechanism of antiplasmodial activity

Chapter 2

Materials & Methods

2.1. *P. falciparum* cell culture

2.1.1. Preparation of cell culture media

Incomplete Roswell Park Memorial Institute (RPMI) media 1640-HEPES (Gibco) was prepared by adding hypoxanthine (Sigma) and gentamycin (Pfizer) to an aqueous solution of RPMI 1640 to final concentrations of 50mg/ml and 10mg/L respectively. The pH was adjusted to 6.74 and sterilised by filtration through a 0.2μm pore-size filter (Merk) prior to storage at 4°C. Complete RPMI 1640 was made by supplementing 500ml of incomplete RPMI 1640 with 15ml of 7.5% w/v sodium bicarbonate (Sigma) (0.22% w/v final concentration) and 12.5 ml of 20% w/v Albumax II (lipid rich bovine serum albumin) (Gibco) to a final concentration of 0.5% w/v and stored at room temperature.

2.1.2. Preparation of human RBCs for cell culture

O+ blood was supplied by the Australia Red Cross Service as red blood cell concentrate, harvested from healthy volunteers and stored in anticoagulant CDPA and stored at 4°C. Packed red blood cells (RBCs) were prepared fresh each week by centrifuging RBCs at room temperature for 10min at 650 x g, after which the supernatant containing the anticoagulant was removed by aspiration. Packed RBCs were washed in 40ml of complete RPMI 1640 and resuspended in equal volumes of complete RPMI 1640 and stored at 4°C for a maximum of one week.

2.1.3. Plasmodium falciparum cell culture

P. falciparum 3D7 parasites (Table 2.9) were cultured in T25 or T75 tissue culture flasks (Sarstedt) in O^+ red blood cells at 4% haematocrit in complete RPMI 1640 media. Cultures were gassed with 1% O_2, 5% CO_2 and 94% N_2 (1s/ml of culture) and kept at 37°C. Where required, cells were cultured under drug selection with either 5nM WR99210 or 5.4μM Blasticidin S-HCl (Table 2.9). To estimate lifecycle stage and parasitaemia, 2μl of parasite culture was prepared as a thin blood smear on a glass slide, air dried for 30sec and fixed for 10sec in 100% methanol (Chem-Supply) prior to being stained for 5min in a 10% v/v aqueous Giemsa solution (Merk). Blood smears were examined by light microscopy at 100x objective magnification. To calculate parasitaemia, the number of infected cells were counted as a percentage of the total number of RBCs present across three fields of view.

2.1.4. Cryopreservation of parasites

Approximately 9-10ml of parasite culture (at ≥5% parasitaemia ring stage) were harvested by centrifugation for 5min at 650 x g followed by complete removal of media by aspiration. The parasite pellet was resuspended in 2x pellet-volumes of freezing solution at room temperature (Table 2.1), gently mixed and approximately 1ml was transferred to a Nunc™ cryopreservation tube (Thermo Fisher) and stored at -80°C as a parasite stabilite.

2.1.5. Thawing cryopreserved parasite stabilites

Parasites stabilities (see above) were thawed at 37°C. The thawed culture was transferred to a 50ml centrifuge tube (Corning) and 200μl of thawing solution 1 (Table 2.1) was added drop-wise while swirling. Immediately thereafter, 10ml each of thawing solution 2 and thawing solution 3 (Table 2.1) were slowly added while swirling to tube and centrifuged for 5min at 650 x g. Pellets were washed with 20ml of incomplete RPMI 1640 and then resuspended in 10ml of complete RPMI 1640, supplemented with 400μl of packed RBCs to achieve a cell concentration of 4% haematocrit. For transgenic parasites, the required concentration of drug was added one day post-thawing.

2.1.6. Enrichment of ring-stage parasites by sorbitol synchronisation

Parasite cultures were synchronised by selecting Ring stage parasites from a 30ml culture at ≥5% parasitaemia. Cells were pelleted at 650 x g for 5 minutes at room temperature, resuspended in 15ml 5% D-sorbitol solution (Table 2.1) and incubated for 15 minutes at 37°C to lyse RBCs harbouring mature stages parasites. Following incubation, surviving cells were centrifuged at 650 x g for 5min and washed once with 30ml of incomplete RPMI 1640, then centrifuged again. Finally, the pellet (containing uninfected RBCs and ring-infected RBCs) was resuspended in 30ml of complete RPMI 1640. To more stringently synchronise cells, sorbitol synchronisation was repeated 4-6hrs later.

2.1.7. Generation of parasite lysates

2.1.7.1. Magnet-purification of late stage parasites

To purify asexual parasites from blood cultures, mature stage parasites (trophozoites and schizonts) were centrifuged and resuspended in 5ml of complete RPMI 1640 medium. Cultures were loaded onto a VarioMACS^{TM} CS magnetic column (Miltenyl Biotec), able to retain cells containing the paramagnetic haemozoin crystals resulting from haemoglobin digestion inside mature parasites. Before loading the parasties, the column was pre-equilibrated with 1x column volume of incomplete RPMI 1640 and 2x column volumes of complete RPMI 1640 and then placed in a VarioMACS^{TM} Separator (Miltenyl Biotec). The loaded 5 ml of culture were allowed to flow through the column at a rate of approximately 1.5ml/min. Retained cells were washed with 5x column volumes of complete RPMI 1640 and eluted by removing the column from the magnetic separator and gently flushing with 25ml of complete RPMI 1640. Purified cells were centrifuged and resuspended in fresh complete RPMI 1640 for quantification.

2.1.7.2. Purification of *P. falciparum* parasites by saponin lysis

Incubation of cells with saponin results in the lysis of uninfected and infected RBCs, leaving parasites intact (comprising the parasite membrane and parasitophorous vacuole membrane) for downstream protein extraction. Proteins were extracted from saponin pellets of high parasitaemia, magnet purified parasite cultures. Late stage parasites (trophozoite or schizont) were magnet-purified and centrifuged at 700 x g for 5min. The supernatant was removed, and pellets were gently resuspended in ice cold 0.08% w/v saponin solution (Table 2.1) and mixed by inversion 5-6 times. Following centrifugation at 1500 x g for 5min at 4°C, this process was repeated until supernatants were clear of visible haemoglobin contamination (dark red colouring of supernatant). Saponin-purified parasites were centrifuged, and the pellet washed with 3x 1ml of ice cold 1X PBS and processed for downstream application.

2.1.8. Induction of sexual stage parasite development (gametocytogenesis)

Wild-type 3D7 parasites or parasites expressing endogenous PfCK1-GFP were induced in cell culture by nutrient deprivation to undergo gametocytogenesis. Cells were grown in 30ml flasks to a parasitaemia of 8-10% ring stages, sorbitol synchronised and incubated overnight at 37°C (day -2). The following day (day -1), trophozoite-stage parasites were fed with fresh RPMI 1640 and split as a 1:3 dilution into a 30ml culture (10ml culture added to 20ml of fresh RPMI 1640 at 4% haematocrit) and incubated overnight at 37°C to induce sexual stage commitment. On day 0, sexually committed ring stage parasites were fed with fresh RPMI 1640 supplemented with N-acetyl glucosamine (GluNAc, Table 2.1) (Sigma) at a final concentration of 68mM to remove remaining late stage asexual parasites. Cultures were fed daily with RPMI 1640 supplemented with 68mM GluNAc and parasites harvested at days 4, 6, 8 and 10 for immunofluorescence imaging of gametocytes.

2.1.9. *In vitro* parasite growth inhibition assays

The susceptibility of wild-type 3D7 and multidrug resistant Dd2 clonal parasite lines to inhibitors was determined by a modified SYBR Green fluorescence-based DNA quantification method (Dery et al., 2015), used as an indicator for parasite growth. Parasites were adjusted to a final parasitaemia of 0.25% in 2% haematocrit and dispensed in a 96 well plate (Corning). A two-fold drug dilution series (50μM – 0.0008μM) was then prepared by adding 1.5μl of the stock inhibitor (prepared at a concentration of 10mM in DMSO) to the first well containing 300μl of parasite culture, thoroughly mixed and 150μl was transferred to the next well (containing 150μl of parasite culture). This was repeated for the remaining drug dilution points. A set of controls were prepared for each assay by adding 1.5μl of DMSO to 300μl of cells (DMSO growth control) and 1.5μl each of chloroquine and artemisinin (from10mM stocks) to 300μl of cells as a negative growth control. All dilution points were then split into triplicates of 50μl, the plates were gassed as per section 2.1.3 and incubated for 72hr at 37°C. Following incubation, plates were frozen at -80°C and thawed at room temperature for 4hrs to facilitate cell lysis. DNA was quantified as a proxy for parasite numbers, by incubating lysates with 1X SYBR Gold buffer (Table 2.1) for 2hrs at room temperature in the dark with gentle agitation. Fluorescence was measured on a Tecan M200 plate reader using an excitation wavelength of 495nm and emission wavelength of 537nm, with gain set to 80. IC_{50} values (concentration of compound required to inhibit parasite growth by 50%) are the averages of three experiments that were calculated from nonlinear regression analysis of dose-response inhibition using GraphPad Prism software (version 7).

2.1.10. *In vitro* selection of drug resistant parasites

Selection of parasites resistant to Purvalanol B was carried out using single-step selection. Clonal wild-type 3D7 and multidrug resistant Dd2 parasites were initially cultured in 30ml of complete RPMI 1640 at 5% haematocrit to a parasitaemia of 5%. Parasites were split into 4x 10ml flasks, each containing $2x10^8$ iRBCs at 5% haematocrit. Parasites were cultured continuously in complete media containing 180µM (3D7) or 230µM (Dd2) Purvalanol B (equivalent to 10x the IC_{50} for 3D7 and Dd2 clonal lines) daily for the first seven days and then once every two days. Cultures were split at a 1:3 ratio once per week and maintained for three months. Any resistant parasites obtained within this time will then be sub-cultured in inhibitor-free media for one week and then cultured in media containing inhibitor to test for resistance stability.

2.1.11. Preparation of plasmids for parasite transfection

To transfect *P. falciparum* parasites, a minimum of 100ug plasmid DNA is recommended (Crabb and Gilson, 2007). Per transfection, 150-200ug of plasmid DNA (Table 2.8) was harvested from *E. coli* cells (section 2.3.6.1) and precipitated from solution by addition of 1/10 volume of 3M sodium acetate pH 5.2 and two volumes of 100% ethanol (Thermo Fisher). Samples were briefly mixed by inversion and centrifuged at 16,000 x g for 30min at 4°C. The DNA pellet was washed with 1ml of 70% v/v ethanol in a sterile biosafety cabinet, centrifuged at room temperature. The ethanol was removed, and DNA pellets allowed to air dry for approximately 10min and then resuspended in 30µl of warm TE buffer (Table 2.4) prior to electroporation. The plasmids used for parasite transfection (Table 2.8) contained the hDHFR cassette which enables selection with the inhibitor WR99210.

2.1.12. Transfection of *P. falciparum*

P. falciparum cultures were tightly synchronised using the sorbitol method (section 2.1.6) and transfections were carried out when cultures reached 5-8% ring-stage parasitaemia. Cultures were centrifuged at 650 x g for 5min at room temperature and the supernatants discarded. Pellets were

gently resuspended in 370µl of warm Cytomix solution (Table 2.1) plus 30µl of plasmid in TE buffer (from above) and transferred to a 0.2cm electroporation cuvette (Cell Projects). Transfections were carried out at 0.31kV, 950uF and resistance set to infinite using a Gene Pulser Xcell™ (Bio-rad). The time constant for each electroporation was between 8-10 msec. Immediately following electroporation, the parasites were resuspended in 2ml of complete RPMI and transferred to a T25 culture flask containing 8ml of complete RPMI 1640, adjusted to 4% haematocrit, gassed and incubated at 37°C. Approximately 2hrs post-transfection, media was replaced with 9.5ml of fresh complete RPMI and cultures returned to 37°C. The following day, WR99210 was added at a concentration of 2.5nM to commence selection of successfully transfected parasites. Cultures were fed daily for the first seven days post-transfection, then every two days until parasites were detected by Giemsa staining. Transfected parasites were cryopreserved once a parasitaemia of 3-5% ring stages was obtained.

2.2. Bioinformatic analysis

2.2.1. Multiple sequence alignment and phylogenetic analysis

Protein sequences were obtained from UniProt (http://Uniprot.org) and PlasmoDB (http://www.plasmoDB.org). Protein multiple sequence alignments were performed using the open access software MUSCLE, available from the EMBL server (http://www.ebi.ac.uk). Phylogenetic analysis was performed by importing a protein sequence into the analysis package implemented at http. www.phylogeny.fr.

2.2.2. Protein Structural Fold and Function Assignment (FFAS) analysis

Multiple sequence alignments were submitted via the open access software found at http://www.ffas.stanfordburnham.org and protein Fold and Function Assignment (FFAS) was performed using the default parametres, generating a file containing secondary structure information.

2.2.3. Homology modelling

The three-dimensional predicted protein structure of PfCK1 was generated using the modelling software Chimera (University of California, San Francisco). The software imported the PfCK1 protein sequence from Uniprot and implemented its own BLASTP analysis. We selected one BLASTP hit with a solved X-ray structure of ≤3Å resolution was and imported its structure using the software. A 3-D structure of PfCK1 was then predicted and modelled onto the imported homologous X-ray structure.

2.2.4. Prediction of subcellular localisation

Prediction of protein cellular localisation was performed using the Euk-mPLoc, Plant-PLoc and Hum-PLoc software available through the Cell-PLoc package (http://www.csbio.sjtu.edu.cn). As positive controls, the peptide sequences of seven human proteins with published cellular localisations were obtained from Uniprot and included in the prediction analysis.

2.3. Recombinant DNA techniques

2.3.1. Polymerase chain reaction (PCR)

The primers used in this study were designed using Serial Cloner 2-6-1 software, based on the genomic DNA sequence of PfCK1 available from PlasmoDB (http://www.plasmodb.org). Oligonucleotide primers were ordered from Sigma-Aldrich (Australia) as 100µM stocks in TE buffer and stored at -20°C. All primers used in this study are listed in Table 2.2. For the amplification of *P. falciparum* DNA fragments for cloning a polymerase with proofreading activity was used (Phusion polymerase, Finnzyme), while for diagnostic PCR Taq DNA polymerase (Roche) was used.

2.3.1.1. General PCR reaction composition

Reagent	Final concentration	Vol. per reaction (ul)
5X buffer (Phusion) or 10X buffer (Taq)	1X	10 or 5
10mM dNTPs	200µM	1
10µM Oligonucleotide Primer (Fwd)	1µM	1
10µM Oligonucleotide Primer (Rev)	1µM	1
Phusion/Taq polymerase		0.2
Plasmid DNA	150ng	Variable
ddH_2O	-	Variable
Total volume		*50*

2.3.1.2. PCR thermocycler conditions

PCR conditions used for *P. falciparum* DNA amplification and cloning were performed using the optimised primer annealing and extension times below.

Standard PCR conditions:		
Initial denaturation	98°C	2min
32 cycles consisting of		
Denaturation	98°C	30sec
Annealing	55°C	30sec
Extension	72°C	1min
Final extension	72°C	7min

2.3.2. Site-directed mutagenesis

Mutagenesis of PfCK1 was performed using the QuikChange® site-directed mutagenesis protocol (Strata Gene). Primers used in this study (Table 2.2) were ordered from Sigma-Aldrich (Australia) as above and designed using Serial Cloner 2-6-1 and Reverse Complement software (http://www.bioinformatics.org). Each forward primer contained an alteration in DNA sequence corresponding to a desired non-synonymous amino acid mutation, flanked 5' and 3' by unaltered DNA sequence according to the manufacturers protocol. The DNA sequence for each reverse primer was generated as a reverse complement of the forward primer sequence. Reactions were prepared as shown in section 2.2.2.1 using *Pfu* Turbo DNA polymerase (New England Biolabs) and PCR reactions performed using conditions optimised as in the QuikChange® site-directed mutagenesis protocol (section 2.2.2.2). Following PCR amplification, methylated parental plasmid containing wild-type PfCK1 was digested using the *DpnI* restriction endonuclease (New England Biolabs) and the resulting mixture (containing only non-methylated mutant plasmid) was used to transform competent *E. coli* by heat shock (see section 2.3.4).

2.3.2.1. Mutagenesis PCR reaction composition

Reagent	Final used	Vol. per reaction (ul)
10X *Pfu* Turbo buffer	1X	5
10mM dNTPs	200µM	1
Oligonucleotide Primer Fwd	125ng	Variable
Oligonucleotide Primer Rev	125ng	Variable
Pfu Turbo DNA polymerase (2.5U/ul)	2.5U	1
Plasmid DNA	50ng	Variable
ddH_2O	-	Variable
Total volume		*50*

2.3.2.2. Site-directed mutagenesis PCR conditions

Conditions were used according to the QuikChange® site-directed mutagenesis protocol for single amino acid changes and an extension time based on 1min/kb of plasmid length.

Initial denaturation	95°C	30sec
16 cycles consisting of		
Denaturation	95°C	30sec
Annealing	55°C	1min
Extension	68°C	6min

2.3.3. Agarose gel electrophoresis

To separate by size and to purify DNA fragments, agarose gel electrophoresis was used. Agarose was used at concentrations of 1% – 3% w/v prepared in 1X TAE buffer (Table 2.4) and dissolved by microwave heating. SYBR Green DNA intercalating dye (Life Technologies) was added to the dissolved agarose at a final concentration of 1X. DNA samples were prepared by addition of 5X DNA loading dye (Qiagen) to a final concentration of 1X and loaded into an agarose gel. As a marker to estimate the size of DNA fragments, 5-10µl of Hyperladder 1kb (Bioline) was used. Gels were run at 100V for 1hr in TAE buffer and visualised by exposure to UV light using a ChemiDoc™ XRS+ (Biorad) and image processed using Image Lab software (Biorad).

2.3.4. Quantification of DNA

DNA concentration was determined by measuring absorbance at 260nm by UV spectrophotometry. Approximately 1-1.5µl of DNA sample was loaded onto a Nanodrop spectrophotometer (Thermo Fisher) and the absorbance measured at 260nm and 280nm to determine purity of the sample. A maximum A_{260}/A_{280} ratio of 1.8 gave an indication of a high purity of DNA with little protein contamination.

2.4. Molecular cloning techniques

2.4.1. Isolation of plasmid DNA

2.4.1.1. Isolation of plasmid DNA from *E. coli* cells

Miniprep reactions were performed to isolate small quantities of plasmid DNA from *E. coli* cells. Positive clones containing plasmid with the correct sequence were grown as 10ml cultures in LB medium (Table 2.4) overnight at 37°C with continuous shaking at 200rpm. The following day, cells were pelleted, and plasmid DNA was harvested using a high pure plasmid isolation miniprep kit (Sigma -Aldrich) according to the manufacturer's instructions. DNA was eluted in 30µl of TE buffer and quantified in a Nanodrop instrument. For experiments requiring larger quantities of plasmid DNA, Maxiprep kits (Qiagen) were used to harvest plasmid from 500ml of overnight *E. coli* culture according to the manufacturer's instructions and collected in 2ml of TE buffer.

2.4.1.2. Recovery of DNA from agarose gels

Samples were separated by agarose gel electrophoresis at 100V for 1hr and DNA bands of the desired size were excised using a scalpel blade under ultraviolet (UV) light. DNA was extracted from excised gel fragments using QIAquick gel extraction kit (Qiagen) according to the manufacturer's protocol. Samples were eluted into 50µl of TE buffer and recovered DNA was quantified using the Nanodrop absorbance method.

2.4.1.3. Recovery of DNA from solutions

After restriction enzyme digestion, total DNA requiring downstream processing was recovered from solution using a QIAquick PCR purification kit (Qiagen) according to the manufacturer's instructions. Samples were eluted into 50µl of TE buffer and DNA quantified in a Nanodrop instrument.

2.4.2. Restriction endonuclease digestion of DNA

DNA fragments or plasmid were digested with specific restriction endonucleases (Table 2.3). Samples were incubated at 37°C for 2hrs with enzyme using the appropriate buffers, according to the manufacturer's instructions (New England Biolabs). Reactions were quenched by the addition of 5X loading dye to a final concentration of 1X. For screening of plasmids, samples were analysed by agarose gel electrophoresis and visualised as per section 2.3.3. For samples used in sub cloning, reactions were quenched by heat inactivation at temperatures recommended by the manufacturer and bands separated and visualised by agarose gel electrophoresis. DNA fragments of the correct size were excised from the gel using a scalpel blade, transferred to a microfuge tube and purified according to section 2.4.1.2 for further processing.

2.4.3. Alkaline phosphatase treatment and ligation of DNA fragments

After the purification of digested plasmid from agarose gels, samples were dephosphorylated with Antarctic phosphatase (New England Biolabs) to prevent recircularization. Alkaline phosphatase buffer (5X) and 1U of Antarctic phosphatase were added to the DNA samples and incubated at 37°C for 20min. Reactions were quenched by heat inactivation and DNA purified from solution according to section 2.4.1.3 and quantified as described in 2.3.4. Purified dephosphorylated plasmid DNA was mixed with DNA fragments corresponding of the size expected for the desired cDNA insert, at a vector to insert ratio of 1:3 in a 50µl reaction volume containing 5X rapid ligation buffer and 1µl of T4 Rapid DNA ligase (5U/µl, Thermo Fisher), according to the manufacturer's instructions. Samples were incubated at room temperature for 15min prior to transformation into chemically competent *E. coli* cells (section 2.4.4). A control ligation reaction containing only plasmid (no insert) was prepared in parallel to assess the level of background transformation resulting from recircularized plasmids.

2.4.4. Transformation of heat-shock competent *E. coli*

A 200µl aliquot of chemically competent DH5α *E. coli* cells, kept stored at -80°C, was thawed on ice and incubated with 100ng of purified plasmid or 50µl of ligation mixture (section 2.4.3) on ice for 30min. Cell mixtures were heat shocked at 42°C for 45s followed by incubation on ice for a further 2min. Sterile LB media (350µl, Table 2.4) was added to the cells in a microfuge tube and incubated with rotation at 37°C for 1hr. Cells were centrifuged at 2500 x g and pellets resuspended in 500µl of sterile LB media, followed by plating 20µl of the cell suspension onto LB agar plates supplemented with 100ug/ml Ampicillin, which were than incubated overnight at 37°C.

2.4.5. Screening for recombinant plasmids

Screening of transformed *E. coli* cells for the correct plasmid insert was performed by colony PCR. Randomly selecting colonies from the transformation plates were collected using a sterile micropipette tip and cross-patched onto fresh LB agar plates supplemented with 100µg/ml Ampicillin. The same tip was then briefly dipped into a PCR tube containing a standard PCR mixture (section 2.3.1.1). Plates were incubated overnight at 37°C and colony PCR was performed using the conditions outlined in section 2.3.1.2, with primers described in Table 2.2. PCR amplifications were analysed by agarose gel electrophoresis. Plasmids were isolated from positive *E. coli* clones using the GenElute^{TM} HP miniprep kit (Sigma-Aldrich) and collected in 30µl of TE buffer (Table 2.4). Purified plasmids were digested with appropriate restriction endonucleases and run on an agarose gel for analysis. Inserts in several plasmids containing DNA fragments of the correct size were also analysed by DNA sequencing to ensure no mutations had been inadvertently introduced.

2.4.6. Nucleotide sequencing analysis

Plasmids containing the correct insert size were analysed by sequencing after linear PCR amplification. DNA sequencing reactions were prepared as for standard PCR using Applied Biosystems PRISM BigDye Terminator mix in place of Taq DNA polymerase. Standard PCR conditions were used, containing either a forward or reverse primer designed to anneal to regions of the plasmid flanking the DNA insert (Table 2.2). Following 32 rounds of PCR amplification, DNA amplicons were ethanol precipitated (section 2.1.11) and pellets air dried and submitted for analysis. All DNA sequencing analysis was performed by the Micromon Genomics, Biotechnology and Diagnostics service at Monash University and samples were processed using an Applied Biosystems 3730s Genetic Analyser. DNA electrophorograms were provided by Micromon and sequences viewed using Contig Express software (Vector NTI).

2.4.7. Codon optimisation and gene synthesis

Nuclear localisation mutant PfCK1 DNA sequences were codon-optimised based on codon usage data presented in (Yadav and Swati, 2012). Codon-optimised PfCK1 was synthesised as a gBlocks® gene fragments from Integrated DNA technologies (IDT). Fragments were digested and ligated into the pGLUX vector (Table 2.8) using the *XhoI* and *KpnI* restriction sites, to be used for subsequent bacterial transformation.

2.5. Biochemical techniques

2.5.1. Sodium dodecyl sulphate polyacrylamide gel electrophoresis (SDS-PAGE)

For general separation of protein samples for Coomassie staining and Western blotting, SDS-PAGE gels were hand-cast using the mini-PROTEAN® gel casting system (Biorad). The resolving gel (12%) and stacking gel (4%) was prepared according to the manufacturer's instructions (see Table 2.5). Samples were boiled in 2X reducing sample buffer (Biorad) at 98°C, sonicated briefly, loaded into the wells and run at 165V for 1hr in SDS-PAGE running buffer (Table 2.5). For analysis of samples by mass

spectrometry, Bolt® 4-12% Bis-Tris gradient gels (Life Technologies) were used and run on a Bolt® gel electrophoresis system using 1X MOPS running buffer (Life Technologies). After electrophoresis, gels were stained for 1hr in Coomassie Blue staining solution and destained in destaining solution (Table 2.5) until bands became visible.

2.5.2. Protein quantification

To determine protein concentration in solutions, 200µl of Quick Start™ Bradford protein assay reagent (Biorad) was added to 5µl of protein sample in a 96 well plate (in triplicate) as per the manufacturer's instructions. Samples were incubated for a minimum of 10min in the dark and absorbance measured at 595nm using an M200 plate reader (Tecan). Protein concentrations of each sample were determined by interpolation into a standard curve generated using dilutions of a BSA protein standard (1mg/ml – 0.25mg/ml) prepared in the same plate, parallel to the samples.

2.5.3. Western blot analysis

Protein samples resolved on a hand-cast 12% polyacrylamide gel (BioRad) were transferred onto nitrocellulose membranes (GE Healthcare) for 1hr at 100V in cold transfer buffer (Table 2.5) on ice. The membrane was blocked for either 1hr or overnight in a 4% w/v solution of skim milk (Diploma) in TBST buffer (Table 2.5) at room temperature with gentle agitation. The membrane was briefly rinsed with TBST and incubated with primary antibody diluted in 3% bovine serum albumin (BSA)/TBST (Table 2.5) for 1hr at RT with gentle agitation. Membranes were washed 3x with TBST for 10min at room temperature with stringent agitation (150rpm) then incubated with horse radish peroxidase (HRP)-conjugated anti-rabbit secondary antibody (Monash Antibody Technologies Facility) diluted 1:5000 in 4% w/v skim milk/TBST for 1hr at room temperature. Membranes were washed with 3x TBST for 10min and then incubated with ECL Prime Western Blotting Detection Reagent (GE Healthcare). The bound antibodies were detected by chemiluminescence on a ChemiDoc™ XRS+ system and the image processes using Image Lab™ software (Bio-Rad).

2.5.4. Purification of recombinant proteins from *E. coli*

The 976bp coding sequence of PfCK1 was ligated into the bacterial expression plasmid pGEX-4T3 between the *Bam*HI and *Not*I restriction sites. Plasmids containing the PfCK1 insert were transformed into chemically competent BL21 Gold *E. coli* (as per section 2.3.3) and cells were grown overnight at 37°C on Ampicillin selective LB agar plates. A 10ml starter culture was prepared by inoculating Ampicillin selective LB media with a single bacterial colony and incubated overnight at 37°C. The following day, 100ml of selective LB media was inoculated with 1/10 volume of starter culture and grown at 37°C with shaking to an optical density (OD_{600}) of 0.5-0.6, cooled to 20°C and protein expression induced by addition of 100mM isopropyl-β–D-thiogalactopyranoside (IPTG). Cultures were incubated further for 18hrs at 20°C with gentle agitation. Proceeding the induction step, cells were harvested by centrifugation, resuspended in 10ml of ice-cold lysis buffer (Table 2.4) per 1g of pellet, briefly mixed and homogenised by sonication on ice using 3x30sec pulses with a 30sec rest in between. Supernatants were clarified by centrifugation at 15, 000 x g for 20min at 4°C using an SS34 rotor and an Evolution High Speed centrifuge (Sorvall) followed by incubation for 2hrs at 4°C with 2ml of pre-washed Glutathione sepharose beads (GE Healthcare) under rotation. Beads were washed with 3x 5ml of wash buffer (Table 2.4) and protein eluted by incubating with 1ml of elution buffer (Table 2.4) for 5min under constant rotation at room temperature. Sample purity of was analysed by sodium dodecyl sulphate polyacrylamide gel electrophoresis and purified proteins identified by Western blot. Protein quantity was analysed by the Bradford method (see 2.5.2).

2.5.5. Cellular fractionation and protein extraction

Late stage parasites were magnet-purified and allowed to recover for 1hr at 37°C, then pelleted at 700 x g for 5min and washed once with 1ml PBS. Parasite pellets were resuspended in 1ml of cold 0.08% w/v saponin buffer supplemented with protease inhibitor cocktail (Table 2.1), mixed briefly by inversion 5-6 times and centrifuged at 1500 x g for 2min at 4°C. Supernatants were removed, and pellets resuspended in 5ml of cold 0.08% w/v saponin, mixed and centrifuged. This process was

repeated until the red colour of haemoglobin was no longer visible. Saponin pellets containing parasites liberated from host RBCs were washed with 3x 2ml of ice-cold PBS and resuspended in 200µl of ice-cold cell lysis buffer supplemented with protease inhibitor cocktail (Table 2.5). Samples were incubated on ice for 15min followed by a further 5min incubation with the non-ionic detergent IGEPAL (0.65% v/v final concentration). Nuclei were harvested by centrifuging lysates at 10,000 x g for 10min at 4°C. The supernatant (parasite cytoplasm) was retained for later analysis. Pellets which contain the purified nuclei were washed 3x with 800µl of cell lysis buffer (from above) and nuclei were lysed in 200µl of a high salt extraction buffer (Table 2.5) for 30min at 4°C with rotation, centrifuged at 10,000 x g for 10min and supernatant retained (soluble nuclear fraction). Cellular fractions were either processed for immunoprecipitation for mass spectrometry or boiled in 2X reducing sample buffer for 5min at 98°C and analysed by Western blot.

2.5.6. Protein Immunoprecipitation

2.5.6.1. Immunoprecipitation using GFP Trap®

Immunoprecipitation reactions were carried out according to the manufacturer's (Chromotek) instructions. Lysates were prepared from parasites expressing PfCK1-GFP from the endogenous locus by harvesting $1x10^8$ iRBCs, which were centrifuged and washed once in 1X PBS before being resuspended in cold lysis buffer (Table 2.5). Wild-type 3D7 parasites were used as a negative control. Samples were incubated at 4°C for 30min on a rotator wheel and clarified by centrifugation at 20,000 x g for 10min at 4°C. Approximately 50µl of unconjugated agarose beads were pre-equilibrated with TBSE buffer and incubated with lysates for 1hr at 4°C to pre-adsorb samples. Supernatants were then incubated with 30µl of pre-equilibrated GFP-Trap agarose beads for 2hrs at 4°C. Beads were pelleted at 2500 x g, 4°C for 2min and washed with 3x 1ml of high salt wash buffer followed by 2x 1ml of TBSE (Table 2.5) before being eluted.

Beads were boiled in 60µl of 2X reducing sample buffer for 10min at 98°C to disassociate immunocomplexes. Subsequently, proteins were run for 5min on a 4-12% Bis-tris gradient Bolt® polyacrylamide gel, stained for 2hrs with Instant Blue™ (Expedion) and de-stained overnight in milliQ water. Following this, the entire gel fragment containing protein was excised from the gel for mass spectrometric analysis.

2.5.6.2. Immunoprecipitation using cognate antibodies

Magnet-purified trophozoite stage parasites were resuspended in 500µl of cold lysis buffer (Table 2.5), incubated for 30 min at 4°C on a rotator wheel and clarified by centrifugation at 20, 000 x g for 10min at 4°C. Precipitation of protein complexes from cell lysates was performed by incubating the clarified supernatants overnight at 4°C under rotation with rabbit anti-Gapex-5 (4ug/ml) antibodies bound to Protein A agarose. Agarose beads were centrifuged at 2500 x g for 2min at 4°C, washed 3x with 1ml of wash buffer (Table 2.5) and 2x with 1ml TBSE.

Protein complexes were eluted from the beads by firstly incubating them for 10min at 50°C with 50µl of 2X non-reducing sample buffer, the supernatant was collected by centrifugation and 100mM DTT were added (elution 1). Beads were resuspended in 50µl of 2X reducing sample buffer and incubated for 10min at 50°C (elution 2). Both elution fractions were pooled and boiled for 5min at 98°C, run on a 4-12% Bis-tris gradient Bolt® polyacrylamide gel (Thermo Fisher), stained and de-stained as per section 2.2.1. and the entire protein-containing gel fragment excised for analysis by mass spectrometry.

2.5.6.3. Immunoprecipitation of nuclear PfCK1-GFP

Soluble nuclear proteins were prepared by high salt extraction of purified nuclei as described in section 2.5.5 diluted 3-fold in TBSE buffer (Table 2.5) and incubated with 30µl of pre-washed GFP Trap® agarose beads for 2hrs at 4°C. Beads were centrifuged at 2500 x g for 2min at 4°C and washed with 3x 1ml of wash buffer (Table 2.5) before proteins were eluted by boiling for 5min at 98°C in 50µl

of 2x reducing sample buffer, run into a 4-12% w/v SDS-PAGE gel and submitted for analysis by mass spectrometry.

2.5.6.4. Chromatin Immunoprecipitation and sequencing (ChIP-Seq)

Late stage wild-type 3D7 parasites, and parasites expressing PfCK1-GFP from the endogenous locus were magnet-purified from 5% parasitaemia cultures and left to recover for 1hr at 37°C. Parasite macromolecules were crosslinked by centrifuging magnet purified parasites at 650 x g, resuspending pellets in 1% v/v formaldehyde solution (Table 2.6) and incubated for 10min at 37°C with rotation. Crosslinking was stopped by addition of 2.5M glycine to a final concentration of 125mM and incubation for a further 10min at 37°C. Nuclei were purified as per section 2.6.4 (high salt extraction step omitted), washed extensively with 5x 1ml of wash buffer (Table 2.5), and stored at -80°C.

Nuclei were resuspended in 300µl of SDS sonication buffer (Table 2.6) and chromatin fragmented by sonicating samples in an ice-ethanol bath for 5sec (70% amplitude), followed immediately by a 15sec rest using a thin probed ultrasonic processor (Cole Parmer). The procedure was repeated for a total of 6min, samples were clarified by centrifugation at 20, 000 x g for 10min at 4°C, and supernatants diluted 10-fold in dilution buffer (Table 2.6). Chromatin was recovered by indirect-immunoprecipitation with 30µl of washed GFP Trap® beads overnight at 4°C and beads were washed with 1ml each of high salt wash buffer, low salt buffer and lithium chloride (LiCl) buffer (Table 2.6), and twice with 1ml of TE buffer (Table 2.6). Chromatin complexes were eluted in 2x 300µl of elution buffer (Table 2.6) for 2hr at 70°C then subsequently incubated at 65°C overnight to reverse crosslinking. Following this, 2.5ul of 20mg/ml Proteinase K (Promega) was added to samples and incubated for 2hrs at 45°C, then DNA was recovered by phenol:chloroform:isoamyl alcohol (25:24:1 v/v) (Thermo Fisher) extraction followed by ethanol precipitation. DNA was resuspended in filtered MilliQ water and quantified on a Qubit3 Fluorometer (Thermo Fisher). Library preparation and sequencing was prepared externally at The University of Melbourne, Microbiology and Immunology

department and sequenced on an Illumina MiSeq Desktop sequencer using the MiSeq kit (Illumina) with a paired-end 150bp run.

2.5.6.5. Purification of PfCK1-GFP from *P. falciparum* culture supernatants

Ring stage parasites were synchronised by two consecutive rounds of 5% sorbitol treatment, approximately 6hr apart. The following day, trophozoite stage parasites were centrifuged at 650 x g and the supernatant discarded as it contains BSA (from the complete RPMI) which hinders downstream processing. Cells were washed three times with 10ml PBS and resuspended in 10ml of RPMI incomplete medium, incubated at 37°C for 5hr, centrifuged and the supernatant was retained. Cells were resuspended in complete media and returned to 37°C. Harvested supernatants were concentrated on Amicon Ultra-15 30kDa centrifugation filters (Merk) to a volume of 500µl (20X concentrate) and incubated with 20µl of pre-washed GFP Trap® agarose for 1hr at 4°C. Beads were washed with 3x 1ml of wash buffer (Table 2.5) and subsequent experiments performed using protein bound to beads.

2.5.7. In-gel tryptic digestion and preparation for mass spectrometry analysis

Gel fragments were cut into approximately small pieces using a scalpel blade, placed into a 1.5ml microfuge tube. Gel pieces were washed with 10x gel volume of 100mM ammonium bicarbonate (ABC)/50% acetonitrile (ACN) under gentle agitation for 20min and supernatant discarded and repeated twice more. Once the gel pieces had been destained, samples were incubated with 100µl of 100mM ABC and 5mM dithiothreitol (DTT) and incubated for 30min at 65°C to reduce disulphide bonds. Post reduction, samples were cooled to RT and alkylated by addition of 200mM chloroacetamide (CAA) to a final concentration of 13mM and incubated at room temperature in the dark for 20min to block Cys residues. Gel pieces were dehydrated by washing with 1ml 50% ACN and 50mM ABC for 10min with gentle agitation at RT and repeated twice with 10x gel volume of 100% ACN. Remaining ACN was evaporated and gel pieces rehydrated in 1x gel volume of pre-chilled 100mM

ABC/5% ACN. Sequencing grade Trypsin (Promega) at a concentration of 12.5ng/µl was added and samples were incubated on ice for 30min. A further 0.5x gel volume of Trypsin solution was added and incubated for an additional 2hrs on ice, then transferred to a 37°C incubator and incubated for 15hrs. Reactions were quenched quickly by the addition of 0.5x gel volumes of 50% ACN/5% formic acid (FA) and vortexing. The supernatant was collected (no centrifugation necessary) and transferred to a fresh Eppendorf Lo-Bind tube (Eppendorf) and the gel pieces were washed twice by centrifugation in 1.5x gel volumes of 50% ACN/5% FA. Supernatants containing extracted peptides were pooled together, snap frozen at -80°C and dried to completion in a speed-vac system. Dried peptides were resuspended in 20µl of 2% ACN/0.1% FA, sonicated for 10min in a sonication bath at room temperature on maximum setting and transferred to LCMS certified vials (Thermo Fisher). Mass spectrometric analysis was carried out by our collaborator Dr. Ralf Schittenhelm from the Monash University Proteomics Platform.

2.5.8. Isolation of microvesicles (MVs) by ultrafiltration

Microvesicles (MVs) were isolated from the conditioned media of trophozoite-stage cultures. Ring stage parasites from a wild-type 3D7 strain, and from a strain expressing PfCK1-GFP, were grown in a T75 flask containing 30ml of complete RPMI 1640 at 4% haematocrit to a parasitaemia of 5% and synchronised by two consecutive rounds of 5% w/v sorbitol treatment, approximately 6hrs apart. Cultures were left at room temperature for 3hr then placed at 37°C to delay the parasites life cycle. The following day, trophozoite stage cultures were centrifuged at 650 x g, supernatants removed (see section 2.5.6.5), and cells washed with 2 x 30ml PBS. Cells were resuspended in 30ml of incomplete RPMI and incubated at 37°C for 6hr. Supernatants were removed (conditioned media) and stored at 4°C until required. To isolate MVs, conditioned media was separated into MV enriched and MV depleted fractions using Amicon Ultra-5 100kDa high molecular weight (MW) cut-off centrifuge filters (Merk), a process previously described to separate MVs from media (Kornilov et al., 2018). Fractions were washed with 3x filter volumes of cold PBS and concentrated 40X by centrifugation at 2500 x g

for 1hr at 4°C. Samples were analysed by Western blot for the presence of MVs and PfCK1 using anti-Stomatin (1:500) (Santa Cruz) and anti-GFP (1:1000) (MATF) antibodies, respectively.

2.5.9. Protein kinase activity assay

Protein kinase activity was assayed using [γ-^{32}P] ATP as substrate ds. Assays were prepared in 30µl reactions as described below.

Reagent	Final used	Vol. per reaction (ul)
Test proteins (1mg/ml)	5µg	5
α-casein (5mg/ml)	5µg	1
10X kinase buffer	1X	3
Adenosine Triphosphate (1mM)	10µM	0.3
[γ-^{32}P] ATP (10uCi/ul)	5µCi	0.5
ddH_2O	-	20.2
Total reaction volume		*30*

Reactions were carried out at 30°C for 30min, after which they were stopped by addition of 5X reducing sample buffer and boiling at 98°C for 10min. Samples were run on a 4-12% gradient SDS-PAGE gel at 165V for 1hr, stained for 1hr in Coomassie Blue staining buffer (Table 2.5) and destained for 2hr in destaining buffer (Table 2.5). Gels were sealed in cellophane membranes and air dried overnight in a laminar flow hood. SDS_PAGE gels were exposed to a BAS Storage Phosphor Screen (GE Healthcare) and visualised on a Typhoon Trio Imager (GE Healthcare) to detect phosphorylated substrate protein by phosphorescence.

2.5.10. Chemical inhibition of nuclear import

To chemically inhibit the import of proteins into the parasite nucleus, late stage asexual wild-type 3D7 and PfCK1-GFP expressing parasites were magnet-purified and recovered for 1hr at 37°C. Cells were split into 2x 10ml flasks and incubated with either 50µM Ivermectin (Panchal et al., 2014) (Sigma Aldrich) (prepared from a 10mM stock in DMSO) or an equivalent volume of DMSO and incubated for 2hr at 37°C. Thin blood smears (section 2.1.3) and immunofluorescence assays (see section 2.7.2) were performed on 0hr and 2hr post-treatment using 2µl and 50µl parasite culture respectively. The remaining cell culture was centrifuged at 650 x g, supernatant removed, and parasite cytoplasm and nuclei prepared as in section 2.6.4. Cell fractions were normalised for cell number and loaded on an SDS-PAGE gel, to be analysed by Western blot using antibody markers (Table 2.7) for each cell fraction (kindly provided by Leanne Tiley and Mike Duffy).

2.6. Fluorescence microscopy

2.6.1. Live cell imaging

Ring stage wild-type 3D7 cultures (2-3% parasitaemia) were used for live microscopy to try determine the cellular localisation of Purvalanol B. Cells were incubated with 10x the IC_{50} of fluorescent Purvalanol B analogues MIPS-0010419 (dansylated Purvalanol B) or MIPS-0010325 (dansylated methyl Purvalanol B) for 4hrs at 37°C. Approximately 2µl of cell suspension were spotted onto a glass microscope slide, prepared as a thin smear and immediately visualised by fluorescence microscopy using the UV excitation channel on an Olympus BX51 microscope (100X magnification).

2.6.2. Immunofluorescence assay (IFA) for protein localisation

The required amounts of wild-type 3D7 cells or parasites expressing PfCK1 tagged with GFP were collected by centrifugation at 700 x g for 3min and washed with 1ml of 1X PBS. Cells were again pelleted and gently resuspended in 1X PBS. 30µl of cell suspension was deposited on a glass microscope coverslip coated with 0.1mg/ml *Phaseolus vulgaris* Erythroagglutinin (PHA-E) (Sigma-

Aldrich) and incubated at 37°C for 20min. Unbound cells were washed off the coverslip with 1X PBS and bound cells were fixed with 4% paraformaldehyde (PFA)/0.008% glutaraldehyde (GA) in PBS for 15min at RT. Samples were washed with 3x 1ml of 1X PBS and permeabilised for 10min at RT with 0.1% w/v saponin/PBS. Washed cells were then blocked for 1hr at RT with 5% normal goat serum (NGS) in PBS and incubated with 30µl of primary antibody for 2hrs at RT (Table 2.7). Samples were washed with 3x 1ml of 1X PBS and then incubated for 1hr in the dark with 30µl of goat anti-rabbit or anti-mouse secondary antibodies (Life Technologies) diluted 1:500 in 1% BSA/PBS. Following secondary antibody labelling and washing, cells were counter stained with 30µl of 2ug/ml 4', 6-diamidino-2-phenylindole, di-hydrochloride (DAPI) (Roche) to stain the nucleus, mounted on a glass slide with VectaShield® (Vecta Laboratories) to prevent photo bleaching and sealed with clear liquid nail polish for imaging. Fluorescence was detected on an upright Olympus BX51 microscope containing an episcopic illuminator to detect DAPI, fluorescein isothiocyanate (FITC) and tetramethylrhodamine (TRITC) fluorescence and images were processed using Fiji software (modified version of ImageJ version 2.0.0).

2.7. Tables of biologicals, chemicals and reagents, plasmids and parasite lines used and generated in this study

Table 2.1 – Tissue culture buffers and reagents

Reagent	Composition	Company
Roswell Park Memorial Institute (RPMI) media 1640 (incomplete)	1.62% w/v RPMI 1640/HEPES powder, 0.005% w/v Hypoxanthine & 0.001% Gentamycin sulphate dissolved in ddH_2O, pH adjusted to 6.74 and sterilised through a 0.22µm filter	Baxter, Sigma-Aldrich, Gibco, Pfizer, Millipore
Roswell Park Memorial Institute (RPMI) media 1640 (complete)	500ml of incomplete RPMI 1640 supplemented with 0.22% sodium bicarbonate and 0.5% Albumax II (lipid rich Bovine serum albumin)	Sigma-Aldrich, Gibco
1x phosphate buffered saline (PBS)	1 tablet dissolved in ddH_2O. Sterilised by autoclave	(Oxoid)
5% w/v d-sorbitol	25g of D-Sorbitol dissolved in 500ml of 1X phosphate buffered saline. Filter sterilised using a 0.22µm filter	Sigma-Aldrich, Millipore
0.08% saponin	0.16g saponin dissolved in 200ml of 1X PBS. Sterilised through 0.22µm filter.	MP Biomedicals
5mg/ml Blasticidin	10mg Blasticin S-HCl dissolved in 2ml of ddH_2O. Sterilised by 0.22µm filtration	InvivoGen
20um WR99210	78.94mg WR99210 powder dissolved in 10ml DMSO to make 20mM stock and stored at -20°C long term. Prepared as a 20uM working stock by 1:1000 dilution in incomplete RPMI 1640 and sterilised through a 0.22µm filter.	Jacobus Pharmaceuticals
Cytomix	20mM KCl, 0.15mM $CaCl_2$. 2mM EGTA, 5mM $MgCL_2$, 10mM K_2HPO_4/KH_2PO_4 (pH 7.6), 25mM HEPES (pH 7.6). pH adjusted to 7.6 and made to 100ml with ddH_2O. Sterilised through 0.22µm filter	Sigma-Aldrich
Freezing solution	28% v/v glycerol, 3% w/v D-sorbitol, 0.65% w/v NaCl dissolved in ddH_2O to 50ml. Sterilised through 0.22µm filter and stored at 4°C.	Sigma-Aldrich
Thawing solutions	*Thawing solution 1:* 11.3g NaCl dissolved in 100ml PBS (12% w/v) *Thawing solution 2:* 0.9g NaCl dissolved in 100ml PBS (1.6% w/v) *Thawing solution 3:* 0.2g NaCl & 0.2g D-glucose dissolved in 100ml (0.9% w/v NaCl, 0.2% w/v glucose)	Sigma-Aldrich, (Oxoid)
255mm N-Aceyl glucosamine	5.64g N-actylglucosamine dissolved in 100ml. Sterilised by 0.22µm filter	Sigma-Aldrich
1x SYBR gold buffer	20mM Tris-HCl (pH 7.5), 5mM EDTA (pH 8.0), 0.008% w/v saponin, 0.08% v/v Triton-X100, 1µl SYBR Gold (10,000 X concentrate)	Life Technologies

Table 2.2 – Oligonucleotide primers used in this study. Restriction endonuclease sites are underlined and shown in bold are codons changes for site-directed mutagenesis.

Primer	Forward sequence	Reverse sequence
Primers for site-directed mutagenes		
PfCK1_L15M	GAAAAAAA**ATG**GGGAGTGGTTCCTTTGGTG	CACCAAAGGAACCACTCCC**CAT**TTTTTTTC
PfCK1_L15W	GAAAAAAA**TGG**GGGAGTGGTTCCTTTGGTG	CACCAAAGGAACCACTCCC**CCA**TTTTTTTC
PfCK1_A36W	GATGGAAGAATTT**TGG**GTAAAATTAGAATC	GATTCTAATTTTAC**CCA**AAATTCTTCCATC
PfCK1_M80K	AGAAGGGGATTTTACTATC**AAA**GTTCTTG	CAAGAAC**TTT**GATAGTAAAATCCCCTTCT
PfCK1_M80W	AGAAGGGGATTTTACTATC**TGG**GTTCTTG	CAAGAAC**CCA**GATAGTAAAATCCCCTTCT
PfCK1_S88A	AGGCCCA**GCG**CTTGAAGATTTATTTACC	GGTAAATAAATCTTCAAG**CGC**TGGGCCT
PfCK1_S88L	CTTGATTTATTAGGCCCA**CTG**CTTGAAG	CTTCAAG**CAG**TGGGCCTAATAAATCAAG
PfCK1_D91H	CCCATCCCTTGAA**CAT**TTATTTACCTTATG	CATAAGGTAAATAA**ATG**TTCAAGGGATGGG
PfCK1_D91N	CCCATCCCTTGAA**AAC**TTATTTACCTTATG	CATAAGGTAAATAA**GTT**TTCAAGGGATGGG
PfCK1_L135K	CCAGATAACTTT**AAA**ATAGGACGAGGGAAA	TTTCCCTCGTCCTAT**TTT**AAAGTTATCTGG
PfCK1_I148K	AAAGTTACCTTAATACATATT**AAA**GATTTTGG	CCAAAATC**TTT**AATATGTATTAAGGTAACTTT
Primers for sub-cloning		
PfCK1_XhoI	CCGCTCGAGATGGAAATTAGAGTGGCAAATAAATATG	-
PfCK1_KpnI	-	CGGGGTACCTTAATTTTGCTTTACTCTTCCTTCTTGA
DNA sequencing primers		
pGEX-4T3	GGGCTGGCAAGCCACGTTTGGTGG	CCGGGAGCTGCATGTGTCAGCGC
pGLUX	TAATAAATACACGCAGTC	CCATTAACATCACCATC

Table 2.3. Restriction endonucleases used in this study. Cleavage point indicated by ^

Restriction endonuclease	Restriction site	Plasmid used	Buffer	Company
BamHI-HF	G^GATCC	pGEX-4T3	CutSmart® buffer	New England Biolabs
NotI-HF	GC^GGCCGC	pGEX-4T3	CutSmart® buffer	New England Biolabs
XhoI	C^TCGAG	pGLUX	CutSmart® buffer	New England Biolabs
KpnI-HF	GGTAC^C	pGLUX	CutSmart® buffer	New England Biolabs

Table 2.4 – Composition of buffers for molecular analysis.

Reagent	Composition	Company
1x Tris-Acetate-EDTA (TAE) buffer	40mM Tris Acetate, 1mM EDTA (pH 8.0) dissolved in ddH_2O	
Luria Bertani (LB) media	1% w/v NaCl, 1% w/v Tryptone, 0.5% yeast extract dissolved in ddH_2O and sterilised by autoclave.	
Luria Bertani (LB) agar	1% w/v NaCl, 1% w/v Tryptone, 0.5% yeast extract, 1.5% w/v agar dissolved in ddH_2O and sterilised by autoclave.	
Tris-EDTA (TE) buffer	10mM Tris-HCl (pH 7.5), 1mM EDTA (pH 8.0)	
100mg/ml Ampicillin	200mg Ampicillin dissolved in 2ml of ddH_2O. Used at 100ug/ml	Amresco
Lysis buffer	25mM Tris-HCl, pH 7.5, 250mM NaCl, 5% v/v glycerol, 2mM dithiothreitol (DTT), 0.1% v/v Triton-X100 and 1X Protease inhibitor cocktail dissolved in 50ml ddH_2O	Roche
Wash buffer	25mM Tris-HCl, pH 7.5, 250mM NaCl, 5% v/v glycerol, 1mM dithiothreitol (DTT) and 1X Protease inhibitor cocktail dissolved in 50ml ddH_2O	Roche
Elution buffer	50mM Tris-HCl, pH 7.5, 250mM NaCl, 5% v/v glycerol, 10mM reduced glutathione, 5mM dithiothreitol (DTT) dissolved in 10ml ddH_2O	Roche, Invitrogen
5x DNA Loading dye	-	Qiagen
SYBR Green II nucleic acid dye	10,000 X concentrate – dilute to 1X before use	Life Technologies

Table 2.5 – Reagents for biochemical analysis.

Reagent	Composition	Company
Cell lysis buffer	10mM Tris-HCl (pH 7.5), 150mM NaCl, 0.5mM EDTA, 0.5%-1% v/v IGEPAL, 10mM NaF, 10mM β-glycerophosphate, 0.1mM Na_3VO_4, 1mM PMSF, 1X protease inhibitor cocktail dissolved in ddH_2O. Sterilised through a 0.22µm filter	Millipore, Roche, Sigma-Aldrich
Wash buffer	10mM Tris-HCl (pH 7.5), 150mM NaCl, 0.5mM EDTA, 10mM NaF, 10mM β-glycerophosphate, 0.1mM Na_3VO_4, 1mM PMSF, 1X protease inhibitor cocktail dissolved in ddH_2O. Sterilised through a 0.22µm filter	Millipore, Roche, Sigma-Aldrich
Stringent wash buffer	10mM Tris-HCl (pH 7.5), 500mM NaCl, 0.5mM EDTA, 1% v/v IGEPAL, 10mM NaF, 10mM β-glycerophosphate, 0.1mM Na_3VO_4, 1mM PMSF, 1X protease inhibitor cocktail dissolved in ddH_2O. Sterilised through a 0.22µm filter	Roche
Tris buffered saline-EDTA (TBSE)	10mM Tris-HCl (pH 7.5), 150mM NaCl, 0.5mM EDTA, dissolved in ddH_2O. Sterilised through a 0.22µm filter	Millipore, Roche,
High salt extraction buffer	20mM HEPES (pH 7.8), 800mM KCl, 1mM EDTA (pH 8.0), 1mM DTT, 10mM NaF, 10mM β-glycerophosphate, 0.1mM Na_3VO_4, 1mM PMSF, 1X protease inhibitor cocktail dissolved in ddH_2O	

12% v/v resolving buffer	375mM Tris-HCl (pH 8.8), 12% v/v Bis-acrylamide, 0.1% w/v SDS, 0.05% w/v APS, 0.0005% v/v TEMED dissolved in ddH_2O	Biorad, Amresco
4% v/v stacking buffer	126mM Tris-HCl (pH 6.8), 12% v/v Bis-acrylamide, 0.1% w/v SDS, 0.05% w/v APS, 0.001% v/v TEMED dissolved in ddH_2O	Biorad, Amresco
1x SDS_PAGE running buffer	0.3% w/v Tris base, 1.4% w/v glycine, 0.1% w/v SDS dissolved in ddH_2O, pH adjusted to 8.3	
Tris buffered saline, tween-20 (TBST)	10mM Tris-HCl (pH 8.0), 150mM NaCl, 1% v/v Tween-20 dissolved in ddH_2O	
Coomassie blue stain	0.1%w/v Coomassie Blue R250, 25% v/v methanol, 7% v/v glacial acetic acid dissolved in ddH_2O	
Coomassie blue destain	10% v/v glacial acetic acid, 40% v/v methanol dissolved in ddH_2O	
Western blot blocking agent	4% w/v skim milk powder dissolved in TBST	
Western blot transfer buffer		
Antibody dilution buffer (western blot)	3% w/v bovine serum albumin dissolved in TBST	Sigma-Aldrich
Antibody dilution buffer (immunofluorescence)	1% w/v bovine serum albumin dissolved in PBS	Sigma-Aldrich
Normal goat serum	5% v/v normal goat serum diluted in PBS	Life Technologies
4x reducing laemmli buffer	62.5mM Tris-HCl (pH 6.8), 10% v/v glycerol, 1% lithium dodecyl sulphate (LDS), 0.005% w/v bromophenol blue, 355mM 2-mercaptoethanol	Biorad
4x non-reducing laemmli buffer	62.5mM Tris-HCl (pH 6.8), 10% v/v glycerol, 1% lithium dodecyl sulphate (LDS), 0.005% w/v bromophenol blue	Biorad

Table 2.6 – Reagents used for Chromatin Immunoprecipitation & sequencing (ChIP-Seq)

Reagent	Composition
1% Formaldehyde solution	37% v/v formaldehyde solution diluted to 1% in PBS
2.5M glycine	18.8g of glycone dissolved in 100ml of ddH_2O
High salt wash buffer	20mM Tris-HCl (pH 8.0), 0.1% w/v SDS, 1% v/v Triton-X100, 2mM EDTA, 500mM NaCl dissolved in ddH_2O
Low salt wash buffer	20mM Tris-HCl (pH 8.0), 0.1% w/v SDS, 1% v/v Triton-X100, 2mM EDTA (pH 8.0), 150mM NaCl dissolved in ddH_2O
LiCl wash buffer	10mM Tris-HCl (pH 8.0), 1mM EDTA (pH 8.0), 250mM LiCl, 1% v/v IGEPAL, 1% v/v deoxycolate dissolved in ddH_2O
SDS sonication buffer	50mM Tris-HCl (pH 8.0), 10mM EDTA (pH 8.0), 1% w/v SDS dissolved in ddH_2O
SDS dilution buffer	16.7mM Tris-HCl (pH 8.0), 150mM NaCl, 1.2mM EDTA (pH 8.0), 1.1% v/v Triton-X100, 0.01% w/v SDS dissolved in ddH_2O
Elution buffer	1% w/v SDS, 100mM $NaHCO_3$ dissolved in ddH_2O (prepared fresh)

Table 2.7 – Antibodies used in this study.

Antibody	Species	Stock conc.	Working dilution	Supplier	Purpose
Primary antibodies					
Anti-GFP	Rabbit	1mg/ml	1:500 – 1:1000	Thermo Fisher	Detection of GFP tagged protein for either IFA (1:500) or Western blot (1:1000)
Anti-GFP	Mouse	1mg/ml	1:500	Monash Antibody Technologies Facility (MATF)	Detection of GFP tagged protein for co-stain IFA (1:500)
GAPEX5	Rabbit	0.2mg/ml	2-4ug/ml	Abcam	Detection of human protein Gapex-5 for IFA, IP & Western blot
SNX22	Rabbit	0.4mg/ml	4-8ug/ml	Abcam	Detection of human protein Sorting nexin 22 for IFA and Western blot
PfS16	Rabbit	-	1:1000	Dr. Matt Dixon/Prof. Leanne Tilley	Gametocyte specific marker
Histone H2A.Z	Rabbit	-	1:4000	Dr. Mike Duffy	Marker for parasite nucleus
GAPDH	Rabbit	-	1:10,000	Prof. Leanne Tiley	Marker for parasite cytoplasm
Stomatin	Mouse		1:1000	Santa Cruz Biotech.	Detection of isolated microvesicles
Secondary antibodies					
Anti-rabbit IgG-HRP	Goat		1:4000	Life Technologies	Analysis of Western blots probed with rabbit antibodies
Anti-rabbit IgG Alexa Fluor 488	Goat	2mg/ml	1:500	Life Technologies	Analysis of IFA by detecting samples probed with rabbit antibody
Anti-mouse IgG Alexa Fluor 488	Goat	2mg/ml	1:500	Life Technologies	Analysis of IFA by detecting samples probed with mouse antibody
Anti-rabbit IgG Alexa Fluor 568	Goat	2mg/ml	1:500	Life Technologies	Analysis of IFA by detecting samples probed with rabbit antibody

Table 2.8 – Plasmids generated in this study for expression of recombinant protein in *E. coli* and the transfection of *P. falciparum* parasites.

Plasmid	Description	Source
Bacterial expression		
pGEX-4T3	Transformation vector for inducible protein expression in *E. coli.* Tags protein with GST at C-terminus. Amp^R	Prof Ross Coppel
pGEX-4T3-PfCK1	Plasmid for expression of recombinant PfCK1-GST	This study
pGEX-4T3-PfCK1^{A36W}	Plasmid for expression of PfCK1 A36W-GST	This study
pGEX-4T3-PfCK1^{M80K}	Plasmid for expression of PfCK1 M80K-GST	This study
pGEX-4T3-PfCK1^{M80W}	Plasmid for expression of PfCK1 M80W-GST	This study
pGEX-4T3-PfCK1^{S88A}	Plasmid for expression of PfCK1 S88A-GST	This study
pGEX-4T3-PfCK1^{S88L}	Plasmid for expression of PfCK1 S88L-GST	This study
pGEX-4T3-PfCK1^{D91H}	Plasmid for expression of PfCK1 D91H-GST	This study
pGEX-4T3-PfCK1^{D91N}	Plasmid for expression of PfCK1 D91N-GST	This study
pGEX-4T3-PfCK1^{L135K}	Plasmid for expression of PfCK1 L135K-GST	This study
pGEX-4T3-PfCK1^{I148K}	Plasmid for expression of PfCK1 I148K-GST	This study
P. falciparum expression		
pGLUX	Transfection vector for the episomal expression of proteins in *P. falciparum*. Tags proteins with GFP at C-terminus. $HDHFR^R$	Prof Ross Coppel
pGLUX-PfCK1	Transfection vector used for episomal expression of PfCK1.	This study
pGLUX-PfCK1^{A36W}	Transfection vector used for episomal expression of PfCK1 A36W.	This study
pGLUX-PfCK1^{M80K}	Transfection vector used for episomal expression of PfCK1 M80K. $hDHFR^R$	This study
pGLUX-PfCK1^{M80W}	Transfection vector used for episomal expression of PfCK1 M80W. $hDHFR^R$	This study
pGLUX-PfCK1^{S88A}	Transfection vector used for episomal expression of PfCK1 S88A. $hDHFR^R$	This study
pGLUX-PfCK1^{S88L}	Transfection vector used for episomal expression of PfCK1 S88L. $hDHFR^R$	This study
pGLUX-PfCK1^{D91H}	Transfection vector used for episomal expression of PfCK1 D91H. $hDHFR^R$	This study
pGLUX-PfCK1^{D91N}	Transfection vector used for episomal expression of PfCK1 D91N. $hDHFR^R$	This study
pGLUX-PfCK1^{L135K}	Transfection vector used for episomal expression of PfCK1 L135K. $hDHFR^R$	This study
pGLUX-PfCK1^{I148K}	Transfection vector used for episomal expression of PfCK1 I148K. $hDHFR^R$	This study
pGLUX-PfCK1^{KKDK}	Transfection vector used for episomal expression of PfCK1 nuclear localisation mutant KKDK. $hDHFR^R$	This study
pGLUX-PfCK1^{KKYR}	Transfection vector used for episomal expression of PfCK1 nuclear localisation mutant KKYR. $hDHFR^R$	This study

Table 2.9. Parasite lines used and generated in this study

Parasite line	Description	Drug selection	Source
3D7	Parental line of all transgenic parasite lines generated in this study	-	
DD2	Multidrug resistant parasite line	-	
3D7 PfCK1-GFP	Parasite line expressing PfCK1-GFP from the endogenous locus	2.5ug/ml Blasticidin	Dr Dominique Dorin-Semblat/Prof. Christian Doerig
pGlux-PfCK1	3D7 parasites transfected with pGlux, expresses wild-type PfCK1-GFP	5nM WR99210	This study
pGlux-PfCK1^{A36W}	3D7 parasites transfected with pGlux, expresses A36W mutated PfCK1	5nM WR99210	This study
pGlux-PFCK1^{M80K}	3D7 parasites transfected with pGlux, expresses M80K mutated PfCK1	5nM WR99210	This study
pGlux-PfCK1^{M80W}	3D7 parasites transfected with pGlux, expresses M80WW mutated PfCK1	5nM WR99210	This study
pGlux-PfCK1^{S88A}	3D7 parasites transfected with pGlux, expresses S88A mutated PfCK1	5nM WR99210	This study
pGlux-PfCK1^{S88L}	3D7 parasites transfected with pGlux, expresses S88L mutated PfCK1	5nM WR99210	This study
pGlux-PfCK1^{D91H}	3D7 parasites transfected with pGlux, expresses D91H mutated PfCK1	5nM WR99210	This study
pGlux-PfCK1^{D91N}	3D7 parasites transfected with pGlux, expresses D91N mutated PfCK1	5nM WR99210	This study
pGlux-PfCK1^{L135K}	3D7 parasites transfected with pGlux, expresses L135K mutated PfCK1	5nM WR99210	This study
pGlux-PfCK1^{I148K}	3D7 parasites transfected with pGlux, expresses I148K mutated PfCK1	5nM WR99210	This study

Chapter 3

Trafficking and secretion of PfCK1 during *P. falciparum* asexual development.

3.1. Introduction

Post-translational modifications (PTMs) are essential biochemical switches that regulate protein interactions and many cellular functions. Dysregulation of this essential modification contributes to the establishment of diseases such as cancer. A PTM of major importance is protein phosphorylation, a dynamic process regulated by protein kinases (PKs) and protein phosphatases (PPs), with over 500 PKs and more than 200 PPs identified in the human kinome and phosphatome respectively (Manning et al., 2002, Sacco et al., 2012); multiple protein kinases and some phosphatases are being extensively studied as therapeutic targets. In *P. falciparum* the number of kinases and phosphatases is smaller, with 86 annotated kinases and close to 30 phosphatases (Solyakov et al., 2011, Wilkes and Doerig, 2008, Talevich et al., 2012). Of the 86 *P. falciparum* PKs identified, 36 are essential for the asexual blood stages (Solyakov et al., 2011) – the stages of development responsible for disease pathology and the target of most current antimalarials. In view of the success in targeting PKs in diseases like cancer (Dauch et al., 2016, Diaz et al., 2012), *P. falciparum* PKs are viewed as potential targets for drugs with novel modes of action and therefore free of pre-existing resistance mechanisms (Reviewed in (Lucet et al., 2012)).

Casein kinase 1 (CK1) is a highly conserved eukaryotic PK with seven isoforms identified in mammalian cells, some of which also exist as multiple splice variants (Fu et al., 2001). Isoforms of CK1 are responsible for phosphorylating a large number of substrates across various cellular compartments, contributing to multiple biochemical processes such as Wnt/β-catenin signalling, cell cycle regulation and apoptosis (reviewed in (Schittek and Sinnberg, 2014)). CK1 is present as a single isozyme *P. falciparum* and it is one of the 36 essential PKs identified in this parasite (Solyakov et al., 2011). Recent work has identified the cellular distribution and possible processes that involve PfCK1 (Dorin-Semblat, 2015). A significant fraction of PfCK1 can be observed on the infected red blood cell (iRBC) plasma membrane during the ring and early trophozoites stages, with a proportion of PfCK1 also secreted to the extracellular medium during trophozoite stages [10].

Interestingly, PfCK1 does not contain canonical or non-canonical PEXEL sequence motifs (Schulze et al., 2015), meaning it is probably not subject to proteolytic processing in the endoplasmic reticulum (ER) and subsequently translocated across the parasitophorous vacuole membrane (PVM) to the host cytoplasm via the PTEX transposon ((Hiss et al., 2008, Elsworth et al., 2016) and reviewed in (C. et al.)). Furthermore, there appears to be no interaction of PfCK1 with Maurer's clefts either. These are parasite-derived membranous structures associated with the RBC cytoskeleton able to transport parasite proteins to the RBC membrane (Vincensini et al., 2005). This indicates that trafficking and secretion of PfCK1 may occur via a hitherto undescribed mechanism. We hypothesised that, nevertheless, trafficking of PfCK1 to the host cell plasma membrane probably involves interactions with host proteins. In order to identify such host proteins, we used affinity purification and mass spectrometry to analyse co-precipitates obtained from transgenic parasites expressing PfCK1-GFP from the endogenous locus and verified candidate interactors by reciprocal co-immunoprecipitation.

This allowed us to show that PfCK1 does indeed interact with host cell proteins known to be involved in endosomal protein trafficking and phosphatidylinositol-3-phosphate (PtdIns3) signalling pathways.

3.2. Results

3.2.1. PfCK1 interacts with host proteins involved in trafficking pathways

We wanted to examine the possible involvement of host proteins in the trafficking of PfCK1 to the host RBC membrane. To test this, we used immunoprecipitation and mass spectrometry to investigate the human protein composition of PfCK1 co-precipitates obtained from unfractionated parasite culture lysates, containing RBC cytoplasm, as described in section 2.5.6.1. This method had been successfully used previously to document the parasite interactome of PfCK1, using purified parasites as the starting material (Dorin-Semblat et al., 2015). Briefly, whole blood lysates were prepared from a 3D7 parasite line expressing PfCK1-GFP from its endogenous locus and harvested at ring, trophozoite and schizont stages. Lysates were immunoprecipitated using GFP Trap® beads, and peptides were generated by in-gel tryptic digestion and analysed by mass spectrometry. A 3D7 wild-type parasite line, expressing its native untagged PfCK1, was used as a negative control.

Proteins obtained from a single immunoprecipitation experiment were ranked from highest to lowest enrichment on GFP Trap® beads by the number of unique peptides detected, and only proteins displaying $\geq$3-fold difference between PfCK1-GFP and wild-type samples were selected. These proteins are shown in Table 3.1. PfCK1 and GFP were detected in the PfCK1-GFP samples, while absent in immunoprecipitates obtained from wild-type parasites, as expected. A large subset of proteins associated with the RBC cytoskeletal network were

identified as enriched in PfCK1-GFP samples: α– and β– spectrin, Ankyrin, Band 3, protein 4.1 and stomatin. More peptides were recovered in ring and trophozoite samples than from later stages, consistent with the RBC-membrane localisation of PfCK1 during the former stages. However, for a majority of these proteins, more than three unique peptides were obtained also in wild-type samples, suggesting that some of these interactions may be non-specific. By contrast, four other host proteins: GTPase-activating protein-VPS9 domain-containing protein 1 (GAPVD1), sorting nexin 22 (SNX22), casein kinase 1 alpha (CK1α) and 14-3-3 protein epsilon were found only in PfCK1-GFP samples, indicating they are possible specific interactors. Given the membrane association and secretion of PfCK1 during trophozoite stages, further experiments were performed using RBCs infected with trophozoite stage parasites.

Table 3.1. Human proteins identified by MS peak counting in immunoprecipitates obtained using GFP Trap® beads. Numbers in each column represent the quantity of unique peptides identified for each protein.

Protein name	3D7-GFP			Wild-type 3D7		
	Ring	Trophozoite	Schizont	Ring	Trophozoite	Schizont
P. falciparum Casein kinase 1	34	13	87	-	-	-
Green fluorescent protein	31	13	66	-	-	-
GTPase-activating protein and VPS9 domain-containing protein 1 (GAPVD1)	49	29	69	-	-	-
Sorting nexin-22 (SNX22)	11	5	18	-	-	-
Casein kinase 1, isoform alpha (CK1α)	5	3	13	-	-	-
14-3-3 protein epsilon (YWHAE)	2	2	4	-	-	-
Spectrin alpha chain, erythrocytic (SPTA1)	26	72	-	9	4	-
Spectrin beta chain, erythrocytic (SPTB1)	20	65	-	-	5	-
Ankyrin-1 (ANK1)	8	43	-	5	-	-
Protein 4.1 (EPB41)	8	18	-	5	-	-
Band 3 anion transport protein	-	52	41	-	7	9
Erythrocyte band 7 (Stomatin)	-	12	-	-	-	-

Highlighted in orange is parasite CK1 and GFP, illustrating the selectivity of the GFP Trap® beads

We further optimised our immunoprecipitations by testing several wash buffer conditions, gradually increasing the concentration of NaCl and IGEPAL detergent (500mM – 1M NaCl and 1%-2% v/v IGEPAL from 150mM NaCl and 0.5% v/v IGEPAL) in an attempt to remove the weaker interactors from the precipitates. A single precipitation reaction was performed on trophozoite stage parasites using the same conditions outlined above but incorporating the new wash conditions. The resulting set of proteins is displayed in table 3.2, where they were ranked and selected as in Table 3.1. PfCK1 and GFP were again prominent in PfCK1-GFP samples as expected. In contrast to the previous experiment however, proteins associated with the RBC cytoskeleton were not detected under these washing condtions, indicating that they belonged among the weaker interactors in the first immunoprecipitates (Table 3.1). Interestingly, GAPVD1, SNX22 and CK1α were again identified under all three wash conditions (shown in blue, table 3.2), further supporting the likelihood that they are specific interactors of PfCK1 *in vitro*. All subsequent experiments were performed using wash conditions containing 0.5M NaCl and 1% IGEPAL detergent.

Table 3.2. Human proteins identified by MS peak counting after stringent washing of precipitates on GFP Trap® beads. Wash conditions are outlined under each parasite line and numbers in each column represent the number of unique peptides identified for each protein.

Protein name	3D7-GFP			Wild-type 3D7		
	0.5M salt 1% TX-100	0.5M salt 2% TX-100	1.5M salt 2.5% TX-100	0.5M salt 1% TX-100	0.5M salt 2% TX-100	1.5M salt 2.5% TX-100
P. falciparum Casein kinase 1 (PfCK1)	43	55	52	-	-	-
Green fluorescent protein (GFP)	33	33	35	-	-	-
GTPase-activating protein and VPS9 domain-containing protein 1 (GAPVD1)	118	129	119	-	3	6
Sorting nexin-22 (SNX22)	24	27	25	-	-	-
Casein kinase 1, isoform alpha (CK1α)	20	18	29	-	-	-
Elongation factor 1-gamma (EF1G)	14	14	14	1	-	-
Serpin B6 (SPB6)	20	15	24	-	-	-
14-3-3 protein gamma (YWAG)	8	9	7	-	1	1
Ribonucleotide-diphosphate reductase, large subunit (RIR1)	8	7	5	1	1	-
Clathrin heavy chain 1 (CLH1)	19	12	10	-	-	3

Highlighted in orange are PfCK1 and GFP to illustrate the selectivity of the GFP Trap® beads; blue indicates host proteins consistently identified in the PfCK1-GFP immunoprecipitates.

To determine whether the identified host proteins GAPVD1, SNX22 and CK1α are indeed interactors of PfCK1, three independent immunoprecipitation experiments were performed using the optimised conditions outlined above. The raw spectral data from PfCK1-GFP and wild-type PfCK1 experiments were subjected to principal component analysis (PCA) by the Monash Proteomics facility and subsequent statistical analysis was performed in MaxQuant. The results are presented as a volcano plot in Figure 3.1B. The plot compares the -Log (p-value) derived from a student's t-test for statistically significant differences, against the Log_2 fold-difference in abundance between PfCK1-GFP and wild-type samples (see section 2.5.7). Error-corrected p-values are used to define the false discovery rate (FDR) and the hyperbolic curve that separates probable false-positives from high probability interactors. A good separation between PfCK1-GFP and wild-type samples was observed in the principal component analysis (Figure 3.1A) and PfCK1 was identified in precipitates obtained from PfCK1-GFP samples but not from wild-type-derived samples, as expected. Both GAPVD1 and SNX22 were identified as high probability interactors in our samples. Additional host proteins whose presence in PfCK1-GFP co-precipitates was considered possibly significant (-log p-value $\geq$1.3) but did not meet the stringent cut off limits of the FDR included 14-3-3 proteins and chaperones involved in protein folding (see supplementary table 3.3.1 for a full list of identified proteins).

We further examined our MaxQuant data for peptides containing phosphorylated Ser(+80) or Thr(+80) residues mapping to host proteins identified in PfCK1-GFP precipitates - indicating possible host substrates of PfCK1. In all three PfCK1-GFP samples, but not wild-type negative control samples, phosphopeptides were identified which matched various regions of GAPVD1 (Table 3.3). Two of the eight phosphopeptides identified (containing pS903 and pS1104) were

identified in all three PfCK1-GFP samples. A cluster of acidic amino acids is located upstream of pS1104 (underlined), typically present in CK1 phosphorylation motifs; the classical CK1 recognition motif is *pS/pT* $X_{1\text{-}2}$ *S/T* where pS/pT denotes a "primed" phosphorylated Ser/Thr residue, X is any amino acid and CK1 phosphorylation occurs on the next Ser/Thr residue (underlined). A cluster of acidic amino acid residues upstream of CK1 phosphosites can also be enough to prime CK1 phosphorylation (Victor et al., 1999). The S972 phosphosite, although only identified in a single experiment, contains a cluster of acidic amino acids, consistent with a putative CK1 phosphorylation motif. Neither of these phosphopeptides map to the Vps9 domain (which acts as a guanine nucleotide exchange factor) or the Ras-GTPase activating protein (Ras-GAP) domain, suggesting that the identified phosphosites probably do not regulate catalysis but likely function in regulating other processes, such as adaptor protein interactions.

A.

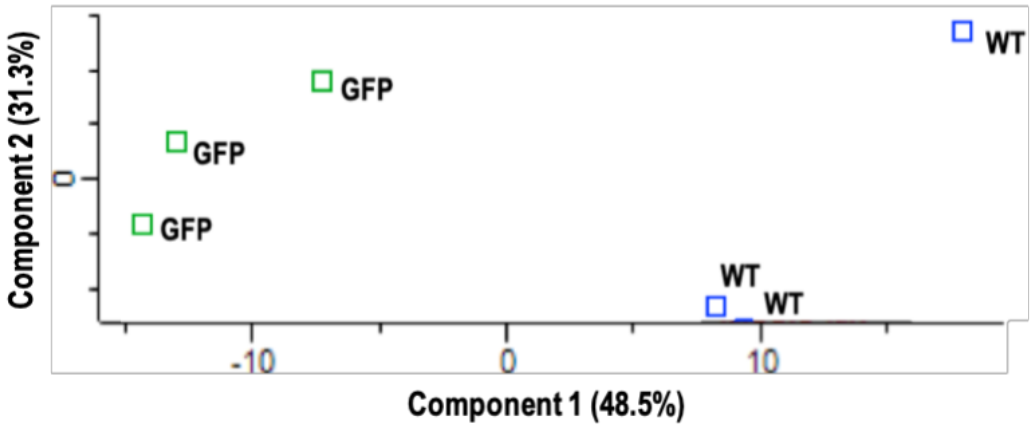
WT
GFP
GFP
GFP
WT
WT
Component 2 (31.3%)
0
-10
0
10
Component 1 (48.5%)

B.

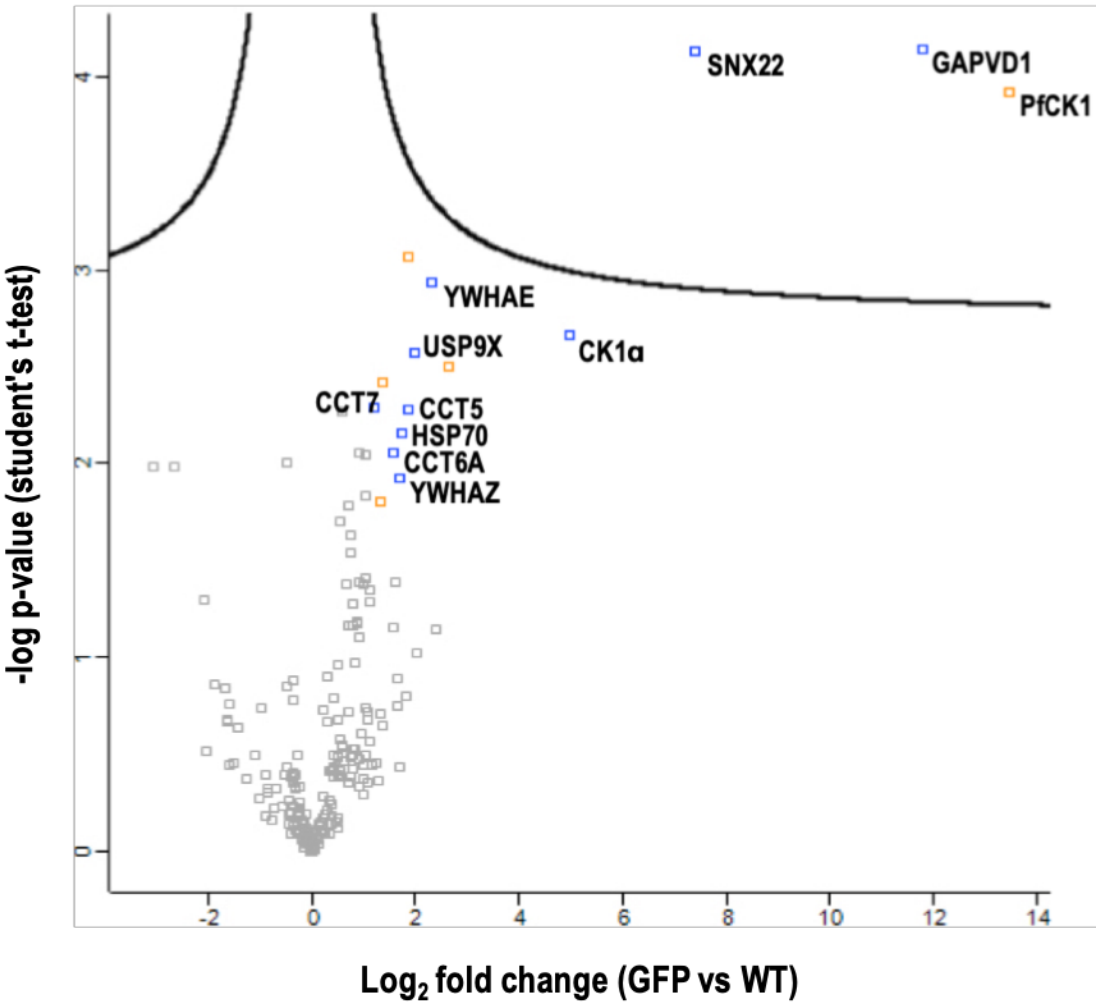
SNX22
GAPVD1
PfCK1
YWHAE
USP9X
CK1α
CCT7
CCT5
HSP70
CCT6A
YWHAZ
-log p-value (student's t-test)
0
1
2
3
4
-2
0
2
4
6
8
10
12
14
Log2 fold change (GFP vs WT)

Figure 3.1. Label-free quantitative analysis of human interactors of PfCK1. (A) Principal component analysis (PCA) of triplicate immunoprecipitation experiments obtained from PfCK1-GFP and wild-type lysates using GFP Trap® beads. Component 1 (x-axis) accounts for the variation between sample conditions whilst component 2 (y-axis) accounts for the remaining variability within samples of the same condition. (B) Volcano plot representing the logarithmic ratio of LFQ values between PfCK1-GFP/WT samples, plotted against the negative logarithm of p-values obtained from Student's t-test of triplicate experiments (FDR = 0.1). A hyperbolic curve separates high-probability interactors (above the curve) from background. Parasite proteins are coloured orange and host proteins blue. Proteins that could still be possible interactors of PfCK1 are annotated below the curve.

Table 3.3. Number of GAPVD1 phosphopeptides obtained from PfCK1-GFP precipitations. Bold and red indicates the identified phosphosites and underlined are possible consensus sequence for CK1 phosphorylation.

Phosphosite	GFP 1	GFP 2	GFP 3	Peptide
T391	-	2	1	RAVE**T**PPLSSVNLLEGLSRT
Y461	-	2	-	KSSSLEMTP**Y**NTPQLSPATTPANKKN
S903	2	2	4	RSR**S**SDIVSSVRR
S904	-	2	3	RS**S**DIVSSVRR
S915	-	1	-	RRPM**S**DPSWNRR
S972	-	1	-	K<u>DDP</u>**S**PRLSAQAQVAEDILDKY
S999	2	4	-	KRTSP**S**DGAMANYESTEVMGDGESAHDSPRD
S1104	2	4	1	RDEALQNISA<u>DDLPD</u>**S**ASQAAHPQDSAFSYRD

3.2.2. Validation of PfCK1 interactions with GAPVD1 and SNX22

We experimentally tested the association of PfCK1 with GAPVD1 (UniProt ID: Q14C86) and SNX22 (UniProt ID: Q96L94), in light of their various roles in protein trafficking and their high abundance and specific presence in PfCK1-GFP immunoprecipitates.

3.2.2.1. Western blot analysis

For these two proteins, we performed Western blot analysis of immunoprecipitates obtained with GFP Trap beads, probing each blot with cognate antibodies. In both cases, presence of the target protein was confirmed in precipitates obtained from parasite samples expressing GFP-tagged PfCK1, but not in samples expressing the wild-type kinase (Figure 3.2). We observed multiple bands in blots probed with anti-GAPVD1 antibody, at higher and lower molecular weight than expected. The former likely indicate multiple phosphorylation sites, consistent with our identification of several phosphopeptides, while the latter are likely a result of GAPVD1proteolysis. The predicted molecular weight of native GAPVD1 is approximately 165kDa and is indicated by the arrow in Figure 3.2.

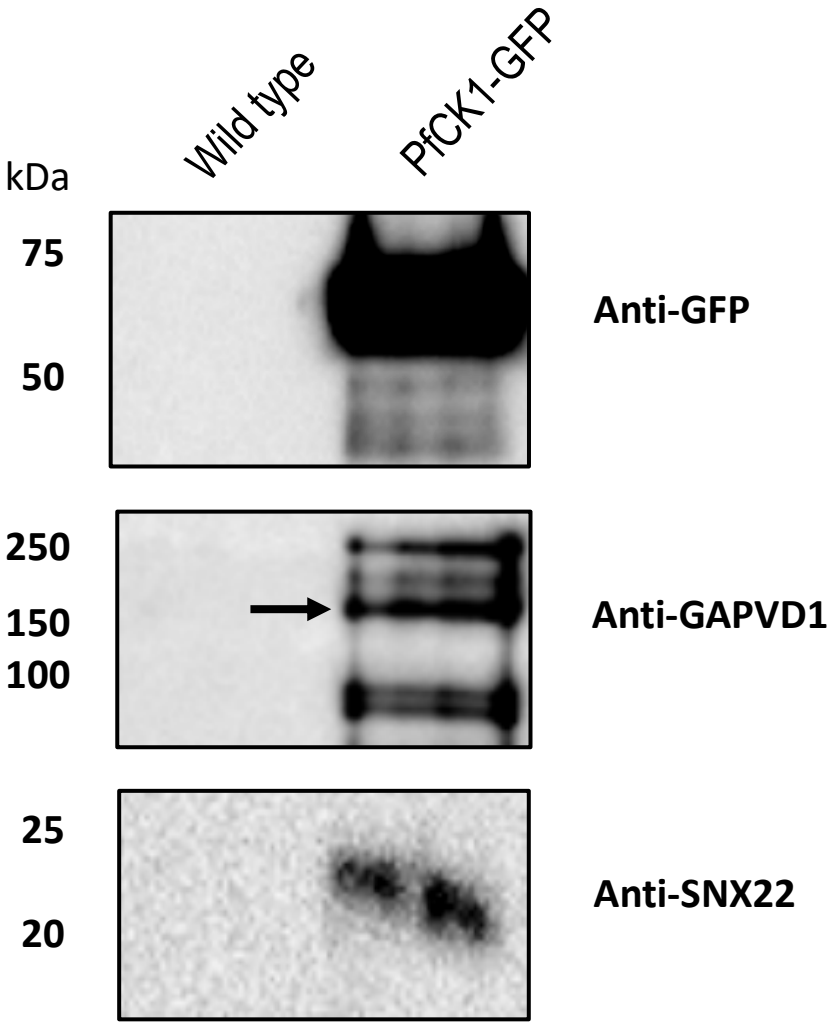

Figure 3.2. Interaction between PfCK1-GFP and human proteins GAPVD1 and SNX22. Immunoprecipitation experiments were performed on whole blood culture extracts from transgenic parasites expressing PfCK1-GFP from the endogenous locus and wild-type 3D7 parasites using GFP Trap® beads. Blots were probed with rabbit antibodies against GFP, GAPVD1 and SNX22. Arrow indicates the estimated size of GAPVD1.

3.2.2.2. Immunofluorescence localisation of GAPVD1 and SNX22 in RBCs

The major function of GAPVD1 in various human cell types centres around the control of a major glucose transporter (GLUT4), accomplished by promoting its cycling between the cytosol and plasma membrane (Lodhi et al., 2007). Members of the sorting nexin family of proteins contain a Phox homology (PX) domain, which modulates interactions of cargo proteins with membranes enriched in phosphatidylinositol 3-phosphate (PdtIns3P). To date, the cellular distribution of GAPVD1 and SNX22 has not been documented in RBCs and in this work, we have sought to determine the cellular location of the two human proteins in this system by immunofluorescence. Cells were fixed according to methods described in section 2.6.2 and were incubated with 8ug/mL of rabbit anti-SNX22 or 2ug/mL rabbit anti-GAPVD1 commercial antibodies, and subsequently labelled with anti-rabbit Alexa Fluor-488 and -568 conjugated secondary antibodies, respectively. RBCs labelled with anti-GAPVD1 antibody and the Alexa 488 secondary (top panel, Figure 3.3) showed a diffuse distribution of fluorescence over the whole RBC membrane, which may represent remnants of a protein trafficking complement. The distribution of SNX22 was less uniform over the RBC membrane and it had a punctate appearance (bottom panel, Figure 3.3), possibly because these are regions enriched in PdtIns3P and consequently endosomes, as reported for similar sorting nexins (Lenoir et al., 2018).

We next performed co-localisation experiments to determine whether the distribution of PfCK1 overlapped with that of GAPVD1. Parasites expressing PfCK1-GFP were prepared as above and co-stained with mouse-anti GFP and rabbit anti-GAPVD1. As a negative control, wild-type 3D7 parasites were used. As previously described (Dorin-Semblat et al., 2015), PfCK1 displayed a strong signal associated with the RBC membrane, with some cytoplasmic

staining also observed (Figure 3.4). This signal was not present in wild-type parasites. Interestingly, GAPVD1 showed a largely punctate cytoplasmic distribution, with some membrane staining suggesting the presence of endosomes and consistent with a membrane receptor trafficking role. No significant co-localisation was observed between GAPVD1 and PfCK1-GFP by immunofluorescence.

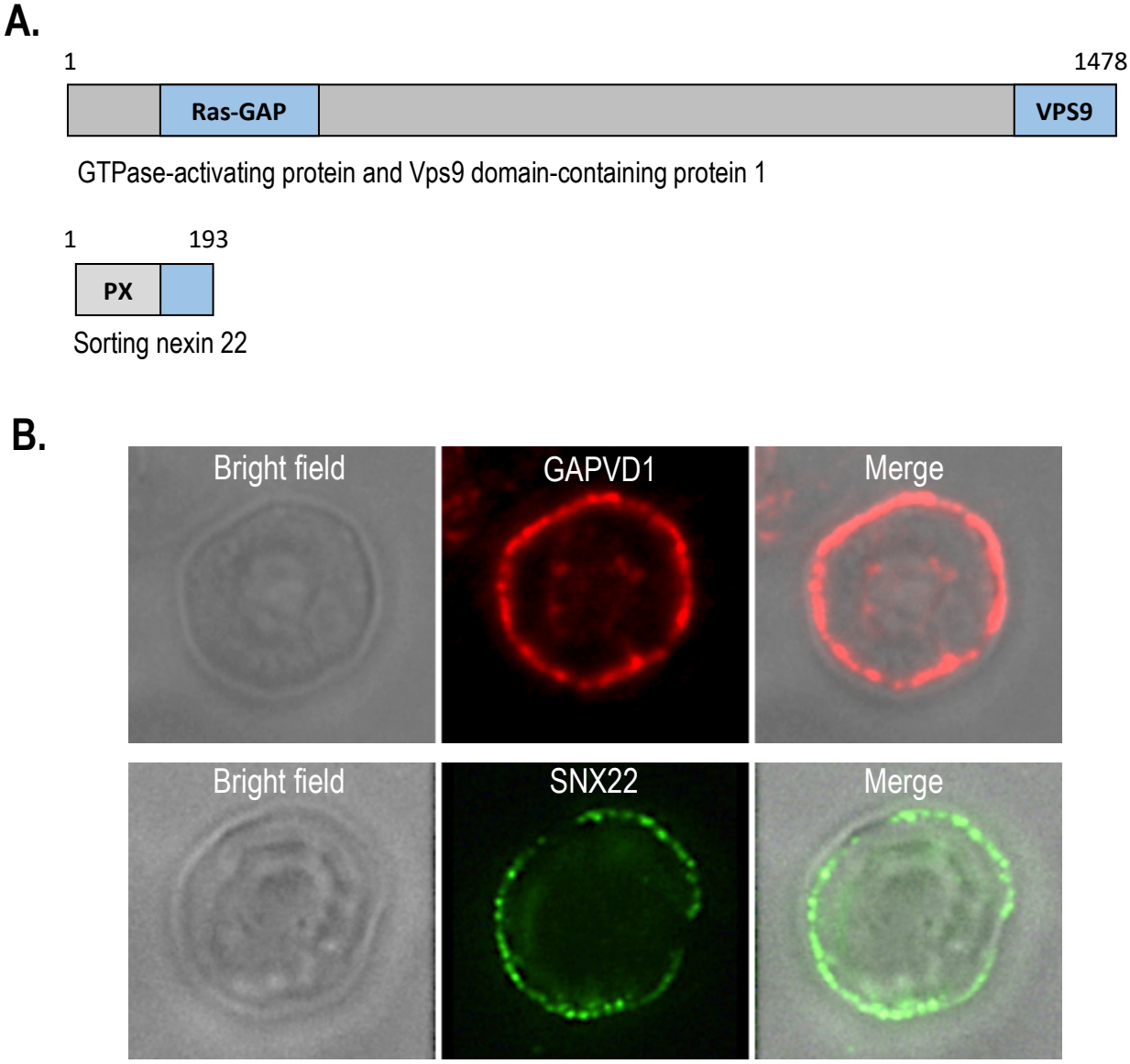

Figure 3.3. Localisation of human proteins GAPVD1 and SNX22 in uRBCs. (A) Schematic diagram of the domain organisation of GAPVD1 and SNX22 with each functional domain denoted; GTPase activating protein (Ras-GAP), Guanine nucleotide exchange factor (VPS9) and Phox homology domain (PX). (B) Immunofluorescence localisation of GAPVD1 and SNX22 in paraformaldehyde fixed uninfected RBCs.

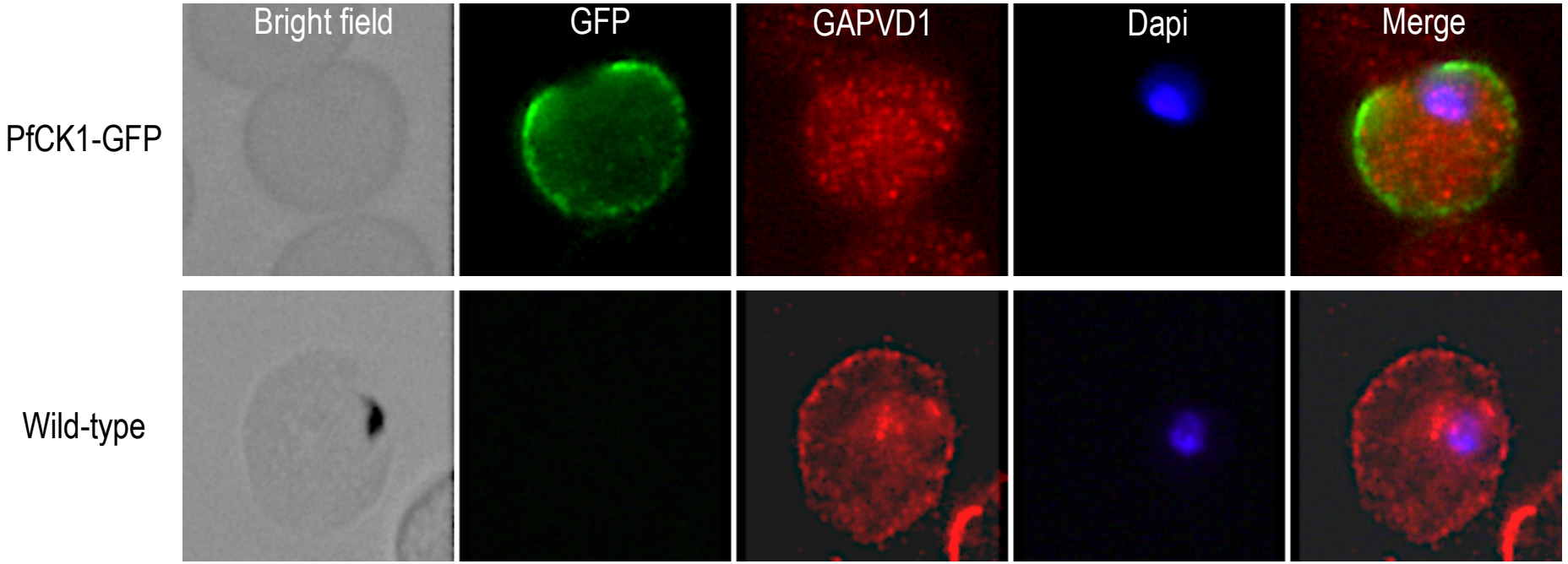

Figure 3.4. Co-localisation of PfCK1 and GAPVD1 in iRBCs. 3D7 parasites expressing PfCK1 tagged at the C-terminus with GFP were examined by immunofluorescence using a mouse antibody against GFP and a rabbit antibody against GAPVD1. Cells were co-labelled with Alexa Fluor conjugated secondary antibodies 488 and 568 respectively. DAPI was used to stain the nucleus and wild-type 3D7 parasites were used as a negative control for GFP.

3.2.3. PfCK1 localisation in gametocytes

In the context of PfCK1 trafficking and localisation, we were interested to investigate the cellular localisation of this enzyme in sexually committed parasites. PfCK1 is essential for vegetative growth of blood-stage parasites and it is also detectable in gametocyte protein extracts (Dorin-Semblat et al., 2015), however to date the cellular distribution of the enzyme in these sexually-committed cells has not been documented. To address this, the expression pattern of PfCK1 during gametocytogenesis was investigated by immunofluorescence analysis of parasites expressing PfCK1-GFP from the endogenous locus, as detected with a rabbit anti-GFP antibody (see section 2.6.2). Wild-type 3D7 parasites were again used as a negative control. Stage III-V gametocytes were generated and successfully imaged (Figure 3.5) and in contrast to PfCK1 staining in both parasite and host compartments observed in asexual blood stage parasites [105], gametocytes showed a strong diffuse staining restricted to the parasite cytoplasm. No GFP signal was observed in wild-type parasites (Figures 3.5B, D and F).

A. *Pf*CK1-GFP Stage III gametocyte

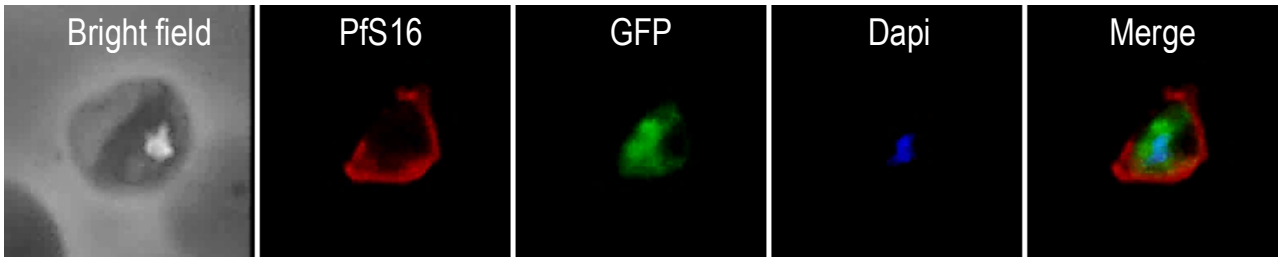

B. Wild-type Stage III gametocyte

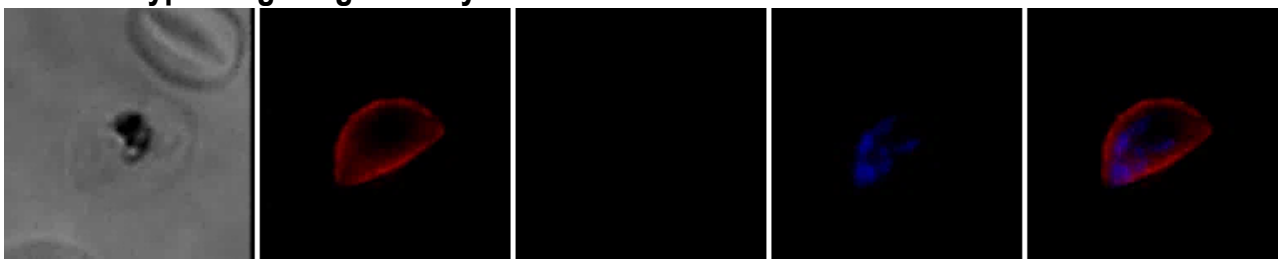

C. *Pf*CK1-GFP Stage IV gametocyte

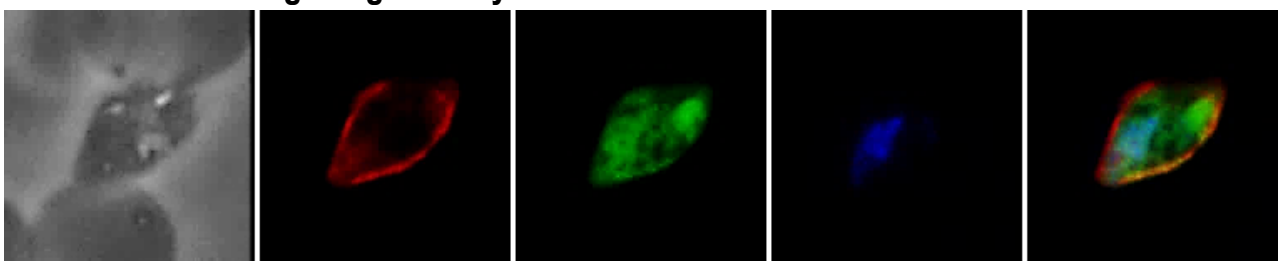

D. Wild-type Stage IV gametocyte

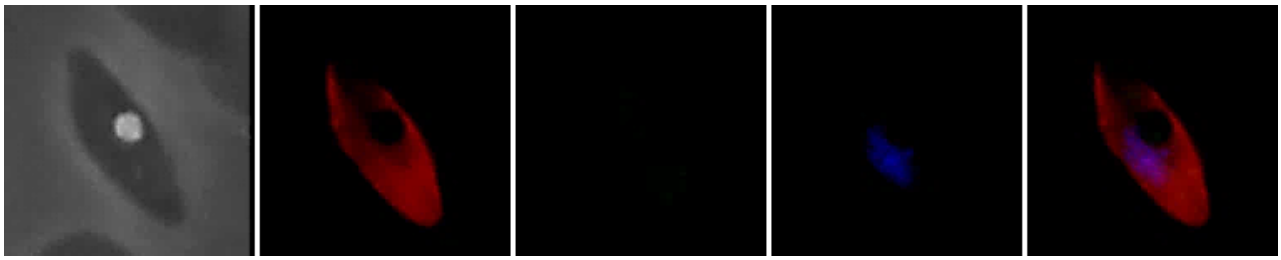

E. *Pf*CK1-GFP Stage V gametocyte

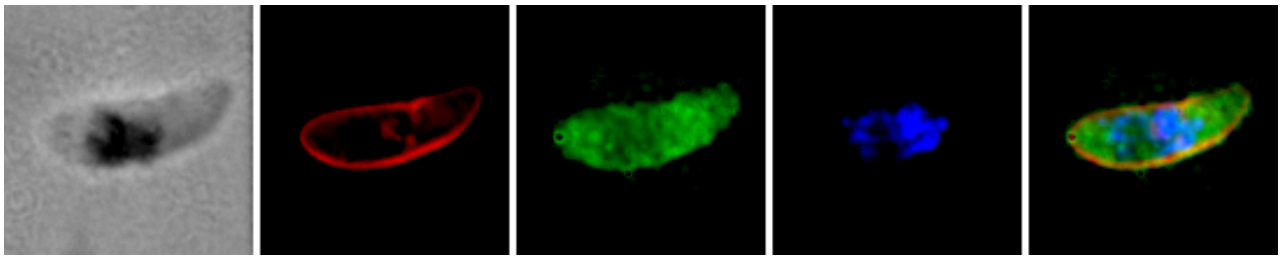

F. Wild-type Stage V gametocyte

Figure 3.5. Immunofluorescence assay of PfCK1 localisation during gametocytogenesis. Gametocytes from wild-type parasite cultures or transgenic parasite lines expressing PfCK1-GFP were examined by immunofluorescence, using an anti-GFP primary antibody and an Alexa Fluor 488-conjugated secondary anti-rabbit antibody. Parasites were also labelled with a primary antibody against the gametocyte marker Pfs16 and co-labelled with an Alexa Fluor 568-conjugated secondary antibody. DAPI was used to stain nuclei. Merged images represent the overlay of GFP, Pfs16 and DAPI signals.

3.2.4. PfCK1 co-precipitates with GAVPD1 and SNX22 in reciprocal immunoprecipitations

To further test the reproducibility of the interactions between GAPVD1 and PfCK1 in infected cells we analysed the presence of PfCK1 in immunoprecipitates obtained using an antibody against GAPVD1. Anti-GAPVD1 antibody was pre-incubated with Protein A agarose beads and then incubated with lysates prepared from $2x10^8$ magnetically-enriched wild-type parasites (see section 2.5.6.2). Following precipitation and washing of the beads (as in 2.5.6.1), eluted samples were briefly run into a 4-12% gradient polyacrylamide gel, samples were excised and subjected to in-gel digestion, mass spectrometry and MaxQuant analysis (as described above for the GFP Trap® IP experiments). The results from independent triplicate experiments are displayed as a volcano plot (Figure 3.6B).

Good separation between iRBCs and uRBCs was observed in the PCA (Figure 3.6A) and PfCK1 was detected in the subset of 36 parasite proteins identified as high probability GAPVD1 interactors based on the threshold limits of the volcano plot (supplementary table 3.3.3). This provided independent confirmation that PfCK1 forms a protein complex with GAPVD1. We matched all 36 parasite proteins to pathways described in the "Metabolic Pathways of Malaria Parasites" (http://mpmp.huji.ac.il; performed using the May 2018 version) and found that protein trafficking and export is one of the most represented functional groups in the immunoprecipitate (Figure 3.6C).

A.

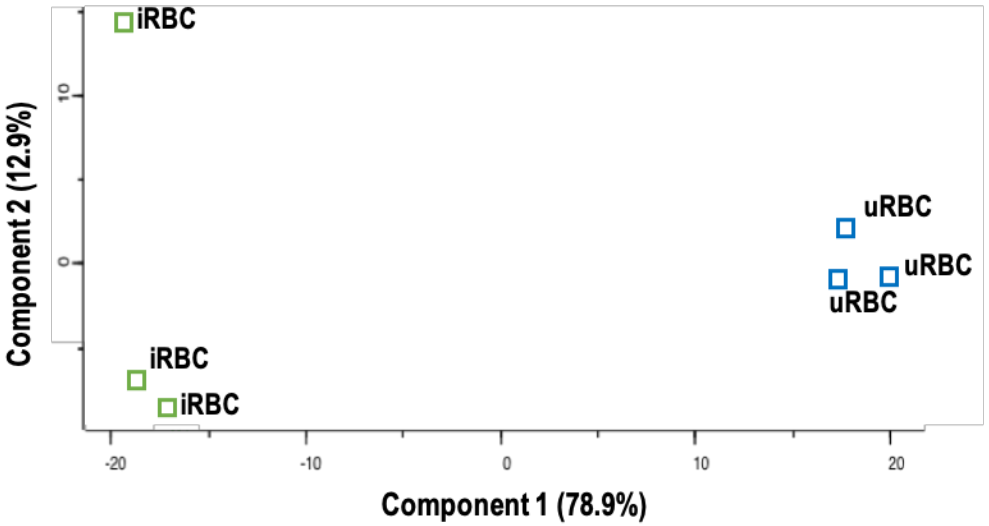
iRBC
uRBC
uRBC
uRBC
iRBC
iRBC
Component 2 (12.9%)
Component 1 (78.9%)

B.

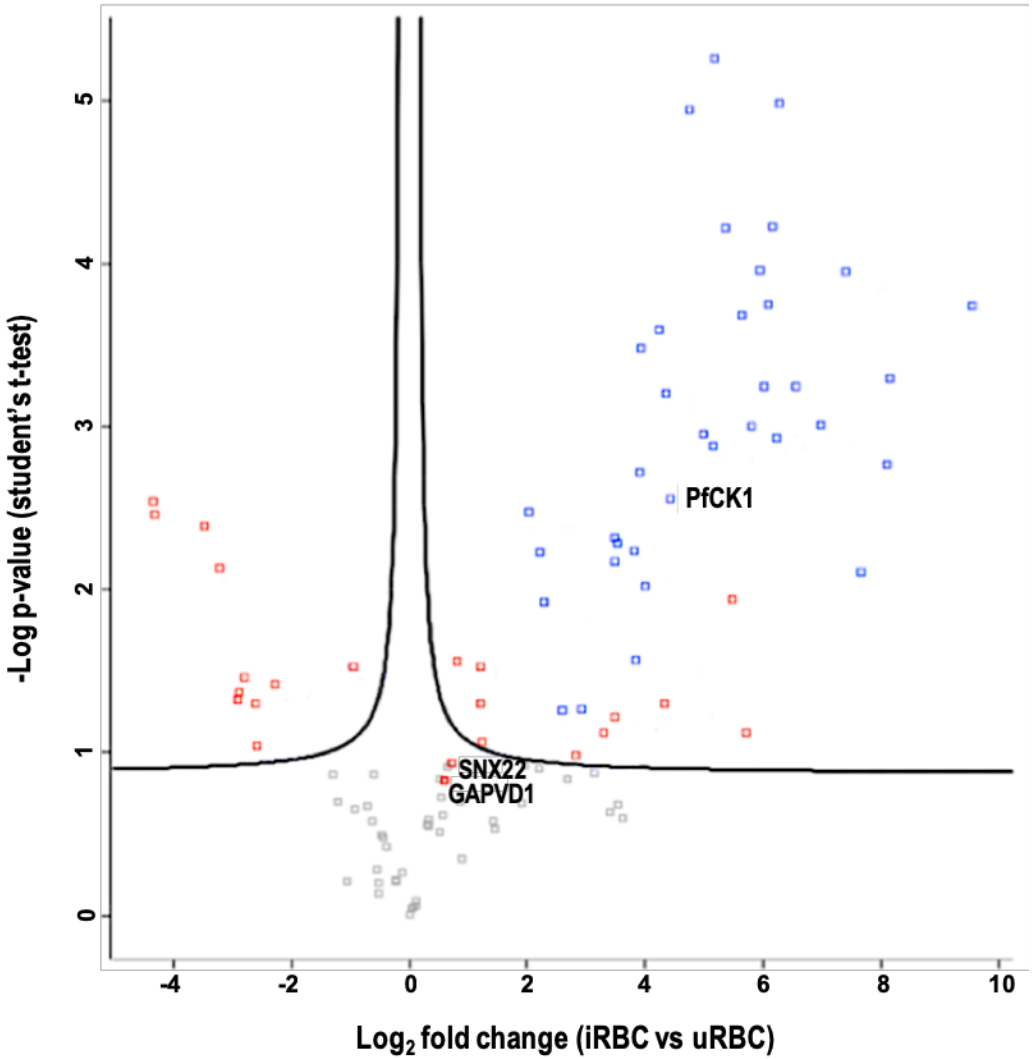
PfCK1
SNX22
GAPVD1
-Log p-value (student's t-test)
Log2 fold change (iRBC vs uRBC)

C.

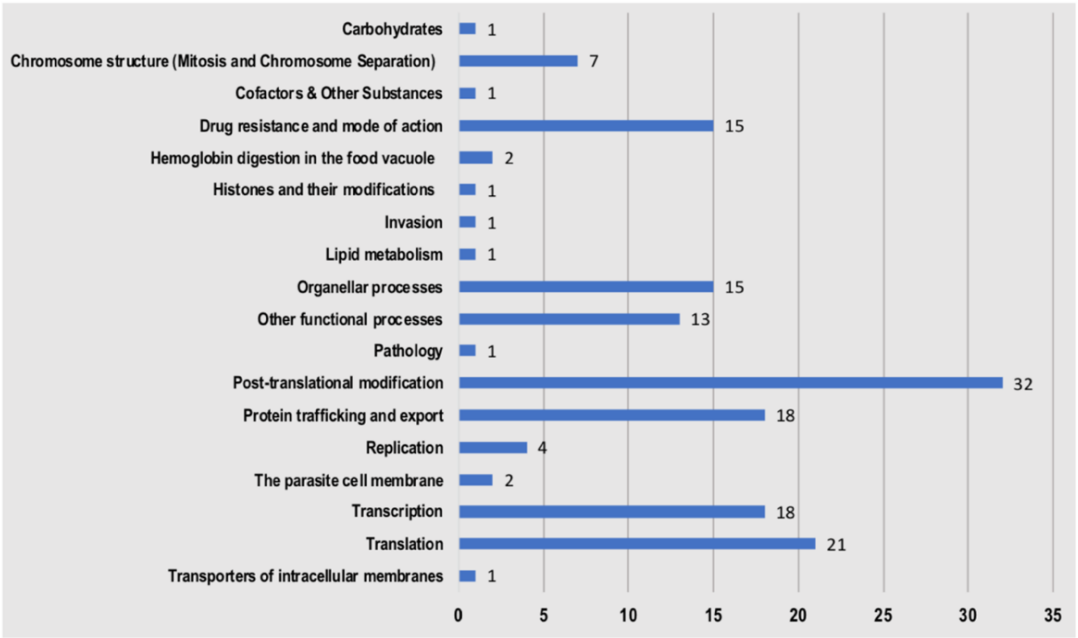
Carbohydrates 1
Chromosome structure (Mitosis and Chromosome Separation) 7
Cofactors & Other Substances 1
Drug resistance and mode of action 15
Hemoglobin digestion in the food vacuole 2
Histones and their modifications 1
Invasion 1
Lipid metabolism 1
Organellar processes 15
Other functional processes 13
Pathology 1
Post-translational modification 32
Protein trafficking and export 18
Replication 4
The parasite cell membrane 2
Transcription 18
Translation 21
Transporters of intracellular membranes 1

Figure 3.6. Label free quantitative analysis of parasite interactors of GAPVD1. (A) Principal component analysis (PCA) of triplicate immunoprecipitation experiments obtained from iRBC and uRBC lysates using using anti_GAPVD1 antibody. (B) Volcano plot representing the logarithmic ratio of LFQ values between uRBS/iRBCs incubated with GAPDV1 antibody which are plotted against the negative logarithmic p-values obtained from student's t-test of triplicate experiments (FDR = 0.1). A hyperbolic curve separates high-probability interactors (above the curve) from background. Parasite proteins are coloured blue and host proteins red. Host proteins GAPVD1 and SNX22 are also annotated. (C) Parasite proteins identified as high-probability interactors of GAPVD1 distributed across the various metabolic pathways of the malaria parasite. The histogram represents the number of parasite proteins mapped to each pathway described in the Metabolic Pathways of Malaria Parasites website (http://mpmp.huji.ac.il//).

3.2.5. PfCK1 is secreted into the extracellular medium as a soluble protein

PfCK1 is secreted into the extracellular medium during trophozoite stages, yet, the mechanism which directs PfCK1 from the parasite to the RBC plasma membrane remains unclear. The identification of two human interactors of PfCK1, GAPVD1 and SNX22, suggests that vesicle trafficking may contribute to this process, given the known cellular roles of the two human proteins. If so, PfCK1 could be secreted either as soluble protein or as cargo inside extracellular vesicles (EVs), as described for other parasite macromolecules (Mantel et al., 2013). To investigate these possibilities, the supernatant from synchronised trophozoite stage cultures (hereon referred to as conditioned media) was analysed by ultrafiltration (Figure 3.7A). This method utilises 100kDa cut-off centrifuge filters to remove EVs from supernatants, resulting in EV-enriched (retentate) and EV-depleted (filtrate) fractions. This technique has been previously used for the depletion of EVs from foetal bovine serum (Kornilov et al., 2018).

Firstly, to test whether PfCK1 is secreted in amounts detectable using the small sample volumes of this method, media conditioned for 6hrs with trophozoite stage cultures (5% parasitaemia) was harvested, concentrated 40X using a 30kDa centrifugation filter and analysed by Western blot to confirm the presence of PfCK1. Blots showed a strong signal at 62kDa in the PfCK1-GFP sample when probed with rabbit anti-GFP antibody, meaning that we have enough sensitivity under the conditions described above (Figure 3.6B.). No signal was observed in conditioned media from wild-type 3D7 samples.

Using the parameters outlined above, conditioned media was harvested from a 30mL trophozoite culture expressing PfCK1-GFP and wild-type 3D7 as a negative control for GFP. Medium was centrifuged at 2500 x g for 1hr at 4°C in 100kDa cut-off filters to separate supernatants into an EV-enriched fraction (retentate) and a soluble protein enriched fraction (filtrate). The retentate was then washed with 3 filter volumes (approximately 15ml each) of PBS. Each fraction was concentrated 40X using a 30kDa-cutoff centrifuge filter and analysed by Western blot, using a rabbit anti-GFP antibody to identify PfCK1. As a marker for EVs, blots were probed with anti-human Band 7 (stomatin) antibody, as this protein is known to be present in both human- and parasite-derived EVs (Mantel et al., 2013). Conditioned media from wild-type 3D7 parasites was used as a negative control.

Blots probed with anti-Band 7 antibody showed a signal at approximately 34kDa in size associated only with the 40X retentate fractions, signifying that EVs were enriched in this fraction as expected, both in samples from wild-type and PfCK1-GFP expressing parasites (Figure 3.6C). Blots probed with anti-GFP antibody showed a strong signal at approximately 62kDa, corresponding to the correct size of PfCK1-GFP, in the 40X filtrate from PfCK1-GFP samples only, indicating that at least a major portion of PfCK1 is not secreted in EVs, but rather as a soluble protein or protein complex.

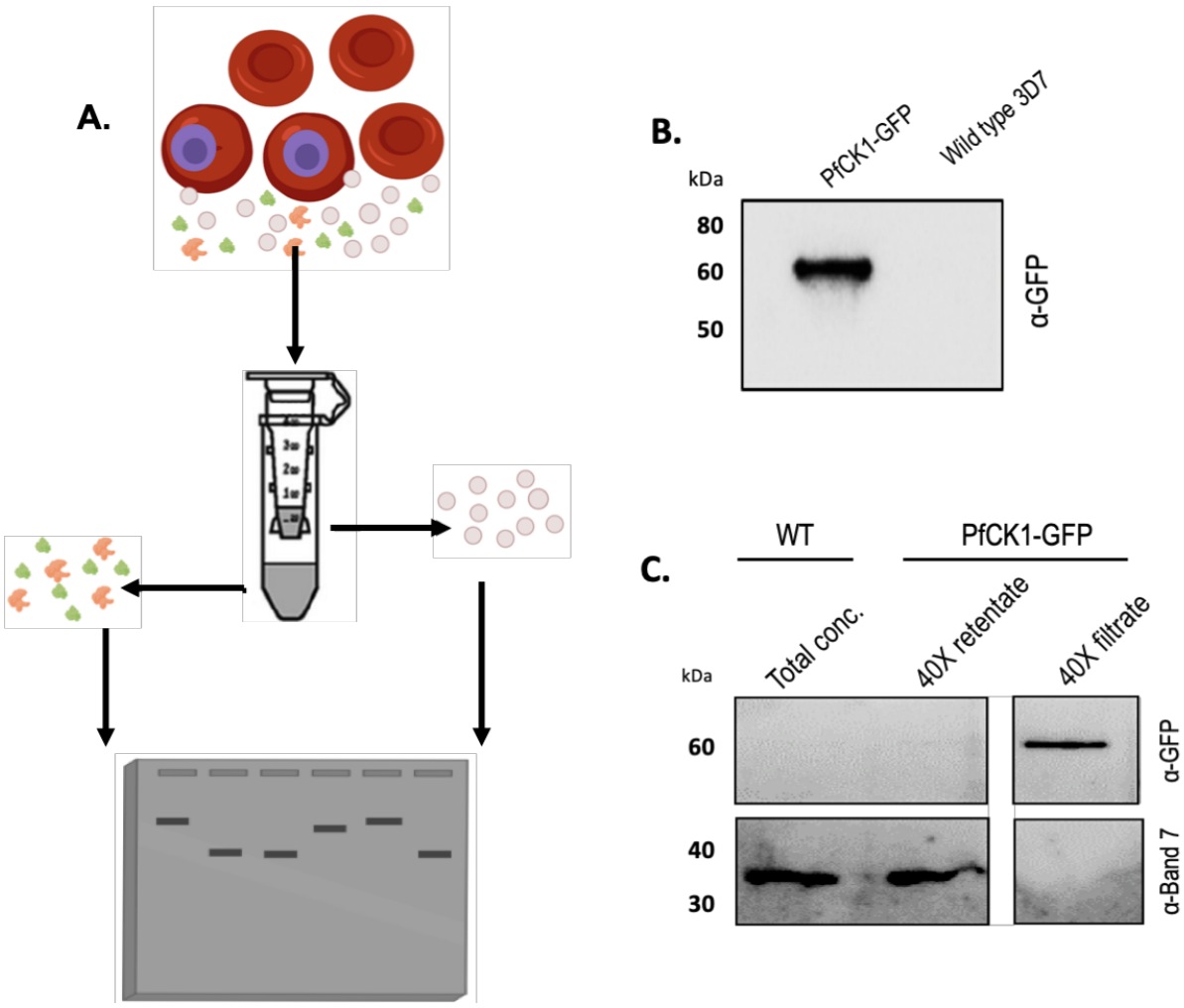

Figure 3.7. Fractionation of culture supernatants by ultrafiltration and analysis of PfCK1 in the extracellular vesicle (EV) and soluble protein-containing fractions. (A) Schematic diagram of the ultrafiltration process for the separation of EVs from soluble protein. Small red circles represent EVs and soluble proteins are shown in green and orange. (B) Immunoprecipitation of PfCK1 from supernatants of synchronised trophozoite cultures using GFP Trap® beads. Supernatants from trophozoite stage wild-type 3D7 were used as a negative control. (C) Enrichment of EV containing fractions from supernatants of synchronised trophozoites expressing PfCK1-GFP from the endogenous locus. 40X retentate: EV enriched fraction concentrated 40X less than original input volume; 40X filtrate: Soluble protein containing fraction concentrated to a volume 40X less than original input. Samples were analysed by Western blot and probed with GFP antibody to detect PfCK1-GFP and Band 7 as a marker for EVs. Wild-type 3D7 culture supernatants were concentrated 40X using a 30kDa filter as a total concentrate (Total conc.) and used as a negative control for GFP.

3.3. Discussion

3.3.5.1. PfCK1 co-precipitates with host proteins involved in endosomal trafficking pathways

PfCK1 associates with host RBC membranes during early stages of infection (ring and early trophozoite), with a fraction of the enzyme also being secreted into the extracellular supernatant during trophozoite stages (Dorin-Semblat et al., 2015). To date, the cellular mechanisms which underpin these processes have not been investigated and could provide new targets for chemotherapeutic intervention. We report here that mass spectrometry consistently detected the association of host proteins GAPVD1 and SNX22 with PfCK1-GFP, even after stringent washing of immunoprecipitates (see Results section above), which strongly indicates that PfCK1 is associated with intracellular vesicle trafficking pathways, either as a cargo or maybe as a regulator.

GAPVD1 (also known as Gapex-5) regulates various cellular events by interacting with a multitude of effector proteins. It is described its involvement in epidermal growth factor receptor (EGFR) trafficking in HeLa cells (Su et al., 2007) and GLUT4 glucose transporter trafficking in adipocytes. The evolutionarily conserved Vps9 domain of GAPVD1 (Figure 3.3A) (K. et al.) functions as a guanine nucleotide exchange factor (GEF) for the Ras-related GTP-binding protein Rab31, thus activating this signalling protein and enabling basal levels of intracellular GLUT4 to be maintained. GAPVD1 also forms a complex with the multidomain effector molecule CIP4, which is trafficked to the plasma membrane following activation of its effector molecule TC10 after insulin stimulation. Recruitment of the CIP4/GAPVD1 complex to the plasma membrane relieves GEF activity on Rab31 thus enabling GLUT4 translocate to the plasma membrane (Lodhi et al., 2007).

Interestingly, we observed a cytoplasmic distribution of GAPVD1 in RBCs infected with *P. falciparum* parasites expressing PfCK1-GFP (Figure 3.4), rather than the membrane association observed in uRBCs. In contrast, RBCs infected with wild-type parasites appear to have both membrane and cytoplasmic presence of GAPVD1. This could indicate that the GFP moiety is affecting the localisation of PfCK1-GFP/GAPVD1 complexes, but we need to discard first the possibility that the difference in GAPVD1 distribution is due to a difference in parasite age, as in the experiments illustrated in Fig. 3.4 wild-type-infected iRBCs appear to contain trophozoites already, whereas PfCK1-GFP expressing parasites are usually at ring stages. We are currently performing a time-course immunofluorescence assay to investigate GAPVD1 and PfCK1 co-localisation during parasite maturation.

Trafficking of GAPVD1 to the plasma membrane by activated TC10 in mammalian cells has been shown to recruit and activate Rab5, which enables the regulation of PtdIns synthesis and turnover by coordinating two distinct PtdIns3-kinases (PI3K) (Lodhi et al., 2008). Although the interplay between the GAPVD1 trafficking pathways and PtdIns3 signalling is not fully understood, it has been shown that some proteins possess both a GAP domain and binding motifs for phosphoinosinositol-3-phosphate (PtdIns3). That makes them suitable binding partners for GAPVD1, which contains a GEF domain but not PtdIns binding domains, creating a complex able to integrate G-protein and PtdIns3 signalling in the control of vesicular trafficking (Zheng et al., 2001).

Sorting nexins (SNXs) are evolutionarily conserved adapter proteins which anchor cargo proteins to membranes enriched in PtdIns3, thanks to their Phox homology (PX) domain (Figure 3.3A). We consistently identified a member of this family (SNX22) in complex with

GAPVD1 and PfCK1, suggesting a possible interaction between these two host proteins (Figure 3.1). Whilst there are no known functions described for SNX22, other members of this family are better understood. For instance, SNX3 is a well-studied sorting nexin known to function in directing retromer-mediated vesicle transport to the TGN, a conserved trafficking pathway first identified in yeast which guides the retrieval, sorting, recycling and retrograde transport of membrane receptors (Feng et al., 2017).

Recently, it was found that the *P. falciparum* genome encodes several members of the retrograde transport system – vacuolar protein sorting proteins Vps26, Vps29 and Vps35, thereby indicating that *P. falciparum* parasites utilise trafficking pathways similar to those of higher eukaryotes (Krai et al., 2014). The retromer complex co-localises with PfRab7 in punctate structures within close proximity to the Golgi apparatus, consistent with the known association of retromers with endosomes in other organisms (Burda et al., 2002, Belenkaya et al., 2008, Bujny et al., 2007).

Importantly, *P. falciparum* does not encode any members of the SNX family, considered key players in retromer sorting. Our data suggest that during infection *P. falciparum* parasites recruit host SNX proteins (in this case SNX22) to recognise membrane areas enriched in PtdIns3, thereby anchoring complexes containing parasite proteins to parasite endosomes. Interestingly, SNX proteins have been implicated in the retromer-dependent secretion of several proteins, including those in the wingless/Wnt pathway in *Drosophila* and iron receptors in yeast (Zhang et al., 2011, Strochlic et al., 2007). Further to this, the endosomal trafficking pathway protein GARP (Golgi-associated retrograde protein) has also been linked to protein secretion through the anterograde route (protein transport to the plasma membrane) (Hirata et al., 2015), suggesting a possible role of SNX family members in protein secretion.

In our reciprocal GAPVD1 precipitation data set (Figure 3.5, supplementary tables 3.3.2 and supplementary 3.3.3), we identified as a high probability interactor PfVps51 – a predicted parasite protein thought to be involved in GARP transport. In eukaryotes, GARP is a protein complex formed by Vps51, Vps52, Vps53 and Vps54 (Liewen et al., 2005, Pahari et al., 2014, Luo et al., 2011), and knock-outs of either of these proteins has been demonstrated to severely disrupt anterograde endoplasmic reticulum (ER) protein transport in Hek293 cells (Hirata et al., 2015). Vps51 regulates endosome fusion with the TGN via interactions with SNARE proteins and all these elements are also present in *Leishmania, Toxoplasma* and *Plasmodium* (Ayong et al., 2011, Canton and Kima, 2012, J. et al., 2013), indicating that this pathway is conserved in multiple Protist pathogenic to humans.

Phosphorylation within the PX domain of SNX3 abolishes PtdIns binding, thus resulting in cytosolic localisation and demonstrates the modulation of SNX function by PKs (Lenoir et al., 2018). The interplay between SNX proteins, GAPVD1 and PKs has been demonstrated in studies which identified unique protein-protein interactions in bait-prey affinity purification experiments (Huttlin et al., 2017, Hein et al., 2015). The mammalian CK1 isoform CK1ε was found to pull-down GAPVD1 and also SNX24 (which clusters with SNX22 in phylogenetic trees (reviewed in (Worby and Dixon, 2002))), further supporting a role for PKs in regulating protein function and interactions along various protein trafficking pathways.

Consistent with this, we identified PfCK1 as a high-probability interactor in immunoprecipitates obtained from iRBC lysates incubated with human anti-GAPVD1 antibodies (Figure 3.5), unlike in uRBC controls. We describe here the first evidence for the presence of GAPVD1 and SNX22-dependent protein trafficking pathways in human RBCs. Furthermore, our co-precipitation data suggests that both GAPVD1 and SNX22 function in a

complex, providing evidence of interplay between pathways. Their exact functions in RBCs still remain unknown; we are performing AP-MS experiments to identify human interactors of GAPVD1, to gain a further insight into its possible roles in such enucleated cells. It would be of interest to perform similar experiments with SNX22 as well. The presence of human CK1α in the complexes suggests a possible regulation of GAPVD1/SNX22 pathways by CKs. Indeed, the identification of PfCK1 in this complex also suggests that during infection, *P. falciparum* parasites commandeer the remanent endosomal trafficking machinery in RBCs, repurposing its components for trafficking parasite proteins to membranes and possibly also to the external medium.

3.3.5.2. PfCK1 is secreted as a soluble protein

Proteins and other molecules secreted from cells inside extracellular vesicles (EVs), or exosomes, have the ability to elicit physiological effects on other cells. It is well known that the immune system can be engaged in response to proteins secreted in EVs, thereby enabling cell proliferation in response to a specific antigen (Qazi et al., 2009, Admyre et al., 2007). Importantly, the secretion of molecules in EVs by parasites during infection may be crucial to their survival by conditioning their surrounding environment, possibly allowing immune evasion (Twu et al., 2013, Buck et al., 2014, Silverman et al., 2010b).

The human pathogen *Leishmania* is an excellent example of an organism which manipulates its environment by secreting approximately 52% of its proteome in exosomes (Silverman et al., 2010a). A proteomic analysis of exosomes obtained from *Leishmania spp.* identified more than 300 proteins and demonstrated that this type of protein secretion is influenced by various environmental cues, like pH and temperature. Among the proteins listed as secreted vesicle cargo was a casein kinase-like enzyme which displays homology to mammalian CK1

isoforms, indicating that *Leishmanial* CK1 is secreted in exosomes. Furthermore, an analysis of *L. donovani* exosomes demonstrated that the cargo contained within these vesicles elicited a predominantly immunosuppressive response (Silverman et al., 2010b), consistent with the understanding that parasites manipulate their host environment for survival.

Comparative studies appear to demonstrate similar phenomena in *Plasmodium* parasites, as mice infected with *P. berghei* carry heightened EV populations in their blood, able to induce a pro-inflammatory response. Similar observations have been made in *P. falciparum*. EVs obtained from the supernatants of *P. falciparum* cultures contain various macromolecules, including DNA competent to transfer genetic information between parasite populations, while the protein content appears to elicit immune-modulatory responses (Regev-Rudzki et al., 2013). It was also shown that a decline in the number of asexual stage parasites coincided with an increase in gametocytes, suggesting that EVs may provide extracellular signals for sexual differentiation. The influence of environmental factors on the macromolecular content of EVs, described in *Leishmania*, may also hold true for *P. falciparum*, where unfavourable growth conditions provide stimuli for sexual differentiation, although the involvement of secreted proteins has not yet been investigated. An analysis of *P. falciparum* EVs identified a significant number of proteins which may play a role in immune modulation and pre-conditioning of surrounding RBCs for invasion (Mantel et al., 2013). Unlike in *Leishmania*, however, PfCK1 was not identified in the protein set. It is worth noting that this study analysed supernatants from schizont stage parasite cultures, as EV secretion peaks at this stage of asexual development. However, PfCK1 secretion occurs predominantly during trophozoite stages (Dorin-Semblat et al., 2015) and it is therefore possible that PfCK1 may have been missed in this analysis. Nevertheless, our data shows that at least a large fraction of PfCK1 is secreted as soluble protein (Figure 3.6), readily detectable in samples depleted of

vesicles as corroborated by the absence of the EV marker stomatin. In *L. major,* secreted CK1 (LmCK1) phosphorylates mammalian type-1 interferon receptors (IFNAR1) to modulate immune system activity (Liu et al., 2009). It is tempting to speculate a similar role for PfCK1 in immune modulation during malaria infection and we have started a collaboration with Meredeth O'Keeffe at Monash University to test this hypothesis.

3.3.5.3. PfCK1 protein is expressed during gametocytogenesis

Transcriptomic analysis of gametocyte stages I-V shows steady-state transcription of PfCK1 (see PF3D7_1136500 at http://PlasmoDB.org and (Young et al., 2005)). PfCK1 is also expressed in male and female gametocytes, as described in a global proteomic analysis of male and female gametocytes (Miao et al., 2017). In our analysis of the cellular distribution of PfCK1 during gametocytogenesis (Figure 3.7) PfCK1 is restricted to the parasite cytoplasm across all of the mid to late gametocyte stages we examined (SIII to SV) which is in contrast to PfCK1 distribution in asexual stages. It remains to be determined whether this is also the case for SI and SII gametocytes. Whereas SIII and SIV appear to have diffuse PfCK1 staining, SV gametocytes display a more punctate pattern (Figure 3.7E), suggestive of distinct stage-specific PfCK1 packaging and function during sexual differentiation. This would be in line with the multiple roles of PfCK1 suggested in asexual blood stages and observed in CKs from other eukaryotic organisms.

It is well documented that *Plasmodium* gametocytes store mRNA transcripts, in a translationally repressed state, for rapid protein expression during the sexual stages in the mosquito vector (Lasonder et al., 2016, Zhang et al., 2013, Mair et al., 2006b). In *P. berghei*, a rodent model for human malaria, approximately 50% of the maternal gametocyte

transcriptome associates with the DDX6-class RNA helicase DOZI (Development of Zygotes Inhibited), forming a complex which is required for mRNA stabilisation and translational repression (Mair et al., 2006b, Guerreiro et al., 2014). Interestingly, PbDOZI-null mutants develop normally during sexual and asexual blood stages but fail to develop fertilised female gametes (zygotes). Immunofluorescence imaging reveals that these DOZI-mRNA complexes form punctate structures in the parasite cytoplasm, similar to the PfCK1 distribution we observed in SV gametocytes. In line with the presumed function of PfCK1 in transcriptional and translational pathways during asexual development, it is tantalising to hypothesise a possible role for PfCK1 in translational repression. Although this would require extensive testing, PKs have been implicated in the translational repression of transcripts, as illustrated by the calcium-dependent protein kinase CDPK1 (Sebastian et al., 2012).

During the sexual phase of the parasite cycle, SV gametocytes enter the mosquito vector following a blood meal on the mammalian host, undergo fertilisation in the gut and develop into zygotes, with rapid translation of stored mRNA transcripts. The zygote matures into an ookinete after two consecutive rounds of meiosis (reviewed in (Guttery et al., 2015)). Protein phosphorylation plays a crucial role in ookinete development, demonstrating the essential role of PKs during this process (Tewari et al., 2010, Reininger et al., 2005, Reininger et al., 2009). However, the entire complex nature of sexual development within the mosquito is still not well understood and is likely to involve multiple kinases. CK1 is known to play essential roles during meiosis in yeast and other eukaryotes, largely in kinetochore assembly and in regulating chromosome segregation (Wang et al., 2013, Sakuno and Watanabe, 2015, Petronczki et al., 2006). Transcripts for CK1 have been detected in *P. falciparum* sporozoites and various sexual stages of *P. berghei,* suggesting a possible role for PfCK1 during late sexual developmental (Hall et al., 2005, Le Roch et al., 2004). One way we are considering to test the

essentiality of PfCK1 during these stages is to implement the GlmS ribozyme system (Prommana et al., 2013) to selectively knockdown gene expression of PfCK1 and examine the progression of parasite sexual development. Since PfCK1 is expressed in the gametocyte stages examined in this chapter, we could presume the same is true for early gametocyte stages also. If true, the most logical stage of parasite development to induce PfCK1 knock-down would be either stage I or stage II gametocytes as this would enable gametocyte maturation to be tracked. If successful, this method could be applied to other essential PKs, thus expanding the repertoire of possible transmission blocking drug targets in *P. falciparum*.

Chapter 4

Nuclear PfCK1 pool

4.1. Introduction

The best understood pathway for the import of proteins into the nucleus involves the recognition of a signal sequence by the karyopherin import complex. Independent studies have examined the interaction between karyopherin-α and peptides containing a classical nuclear localisation signal sequence (cNLS), revealing the minimally required amino acids motif and the biochemical environment necessary for signal recognition by the import machinery (Conti and Kuriyan, 2000, Fontes et al., 2003). A cNLS consensus is loosely defined as *K(K/R)X(K/R)* where a lysine is required at position P1, followed by a basic residue at positions P2 and P4, separated by any amino acid, *X* (reviewed in (Lange et al., 2007)). A comprehensive set of studies in yeast (Stark et al., 2006, Huh et al., 2003, Benson et al., 2005) determined the frequency of cNLS sequences and nuclear localisation of proteins and found that 28.6% of the 5850 genes predicted to encode proteins included a monopartite (single) cNLS consensus sequence. Furthermore, it was confirmed that 30.9% of 1515 nuclear-localised proteins contained a monopartite cNLS, whilst a further 25.8% contained a bipartite sequence. The remaining 43% may use other mechanisms independent of the karyopherin import pathway to enter the nucleus. Indeed, the cNLS frequency suggests that numerous proteins may localise the nucleus at some point in other eukaryotes and is the most utilised mechanism of nuclear import.

Casein kinase 1 (CK1) enzymes contribute to the regulation of multiple cellular processes and several isoforms have been identified in the eukaryotic nucleus. For example, in mammalian cells, CK1α regulates the cellular localisation of the transcription factor NFAT (nuclear factor of activated T cells) by phosphorylating its SRR-1 regulatory domain in the nucleus to promote cytoplasmic translocation

(Okamura et al., 2004, Okamura et al., 2000). Another isoform able to localise to the nucleus, CK1δ, produces two very different effects on the circadian rhythm protein PER2. Phosphorylation of S659 within the FASP domain promotes PER2 stabilisation and transcriptional repression of PER2-regulated genes, while phosphorylation at S478 in the β-TrCP site results in PER2 destabilisation and de-repression (Eng et al., 2017). The long-chain splice variant of CK1α (CK1α-L) contains a KRKR motif within a 28-amino acid insertion which has been demonstrated to be a functional cNLS (Fu et al., 2001). Also, in yeast, CK1 homolog Hrr25 forms a nuclear complex with the transcription factor Swi6 to regulate G_1-phase specific transcription of cyclins and S-phase proteins in response to DNA damage (Ho et al., 1997). The interactome of CK1 in isolated human malaria *P. falciparum* parasites has recently been described, and it included several parasite proteins involved in nuclear processes such as transcription, splicing and chromatin assembly (Dorin-Semblat et al., 2015). Among the proposed interactors were histones H2A, H2A.Z, H3 and H4, core components of the nucleosome that constitutes the basic organisational unit of chromatin (Kensche et al., 2016), and the catalytic subunit of *P. falciparum* casein kinase 2 (PfCK2α) suggesting a role for PfCK1 in in the parasite nucleus. To date, however, the involvement of PfCK1 in nuclear-related processes has not been directly investigated. This chapter focuses on (i) confirming that PfCK1 is indeed a nuclear kinase by combining bioinformatic, chemical and molecular methods to establish cellular localisation and investigate protein import mechanisms, and (ii), attempting to identify the function(s) of PfCK1 in the parasite nucleus by proteomic as well as chromatin immunoprecipitation and sequencing (ChIP-seq)-based methods.

4.2. Results

4.2.1. PfCK1 is a predicted nuclear kinase

We first wanted to determine if PfCK1 is predicted to localise to the nucleus. To do this, two bioinformatic web-servers: Euk-mPLoc and Hum-mPLoc (available from www.csbio.sjtu.edu.cn) were used (Chou and Shen, 2008) and seven human proteins with known cellular distributions were included as controls to validation the software. Table 4.1 shows the human proteins with known localisation were accurately predicted by both Euk-mPLoc and Hum-mPLoc servers. PfCK1 was predicted to have a bi-compartmental distribution between the cytoplasm and nucleus, similar to the human homolog CK1δ.

4.2.2. PfCK1 is detected in the parasite nucleus

We next validated the predicted bi-compartmental distribution of PfCK1 by fractionating parasites into cytoplasmic and nuclear compartments (Figure 4.1A) and analysing the proportion of the kinase between the two compartments by immunoblot methods. Parasites expressing PfCK1-GFP, as well as negative control wild-type 3D7 parasites, were separated from uRBC using VarioMACs magnetic columns (see section 2.1.7.1). Next, parasites were purified away from host RBCs by saponin treatment (see section 2.1.7.2) and their nuclei were obtained as per section 2.5.5. Soluble nuclear proteins were extracted in a high salt buffer. Each sample was normalised to the protein content extractable from $1x10^8$ cells (for both, parasite cytoplasm and nucleus) and analysed by Western blot using an anti-GFP antibody (section 2.5.3). The membrane was also probed with antibodies against known markers of cellular compartments to test the purity of each fraction, namely: PfGAPDH for the parasite cytoplasm and H2A.Z for the nuclear fraction.

As indicated by a strong signal of approximately 15kDa corresponding to the parasite histone variant PfH2A.Z, nuclei were successfully purified from both PfCK1-GFP and wild-type cells (Figure 4.1A). The absence of PfGAPDH signal from nuclear preparations indicates the lack of detectable contamination with parasite cytoplasm. Blots probed with anti-GFP to detect the presence of PfCK1 show a strong

signal at 62kDa in both the cytoplasmic and nuclear fractions, consistent with the predicted localisation shown in table 4.1 and confirming the presence of PfCK1 in the parasite nucleus. Densitometry was performed on the PfCK1 band from cytoplasmic and nuclear fractions to determine PfCK1 distribution. Percentages were calculated by dividing the intensity of PfCK1 in each fraction by the sum of PfCK1 intensities in all fractions. Proportions were calculated from triplicate Western blots prepared from independent samples. Figure 4.1C shows that approximately equal amounts of PfCK1 are distributed between the cytoplasm (48$\pm$5%) and nucleus (52$\pm$5%), indicating a truly bi-compartmental distribution of this parasite kinase.

Table 4.1. Prediction of protein nuclear localisation using the Cell-PLoc web servers.

Protein name	Organism	Subcellular localisation	Predicted localisation		References
			Euk-mPLoc	Hum-mPLoc	
Spectrin, α−chain	*H. sapiens*	Cytoplasm (cytoskeleton), cytoplasm (cell cortex)	Cytoskeleton	Cytoskeleton	Patel-Hett, Wang et al. 2011, Machnicka, Grochowalska et al. 2012, Fletcher, Elbediwy et al. 2015
Carbonic anhydrase 1	*H. sapiens*	Cytoplasm	Cytoplasm	Cytoplasm	Temperini, Innocenti et al. 2007, Beyza Öztürk Sarıkaya, Gülçin et al. 2010
Creatine kinase, S-type	*H. sapiens*	Mitochondrion, inner membrane	Cytoplasm, mitochondrion	Cytoplasm, extracellular, mitochondrion	Schlattner, Gehring et al. 2004, Chen, Zhao et al. 2011, Wallimann, Tokarska-Schlattner et al. 2011
Succinate dehydrogenase, subunit B	*H. sapiens*	Mitochondrion, inner membrane	Mitochondrion	Extracellular, mitochondrion	Gill, Benn et al. 2010, Alston, Davison et al. 2012, Gill 2012
Histone H4	*H. sapiens*	Nucleus, chromosome	Nucleus	Nucleus	Sharma, So et al. 2010, Tardat, Brustel et al. 2010, Allahverdi, Yang et al. 2011
Aurora kinase B	*H. sapiens*	Nucleus, chromosome, centromere, cytoskeleton spindle, midbody	Centrosome, nucleus	Centrosome, nucleus	Cho, Shimazu et al. 2012, Diaz, Golbourn et al. 2012, Sgourdou, Mishra-Gorur et al. 2017
Casein kinase 1δ	*H. sapiens*	Cytoplasm, nucleus, centrosome, Perinuclear region, cell membrane, spindle, golgi apparatus	Cytoplasm, nucleus	Cytoplasm, nucleus	Milne, Looby et al. 2001, Cruciat 2014, Zemp, Wandrey et al. 2014, Greer, Gao et al. 2017
Casein kinase 1	*P. falciparum*	Cytoplasm, nucleus	Cytoplasm, nucleus	Cytoplasm, nucleus	-

Web servers are available at www.csbio.sjtu.edu.cn/bioinf/Cell-PLoc

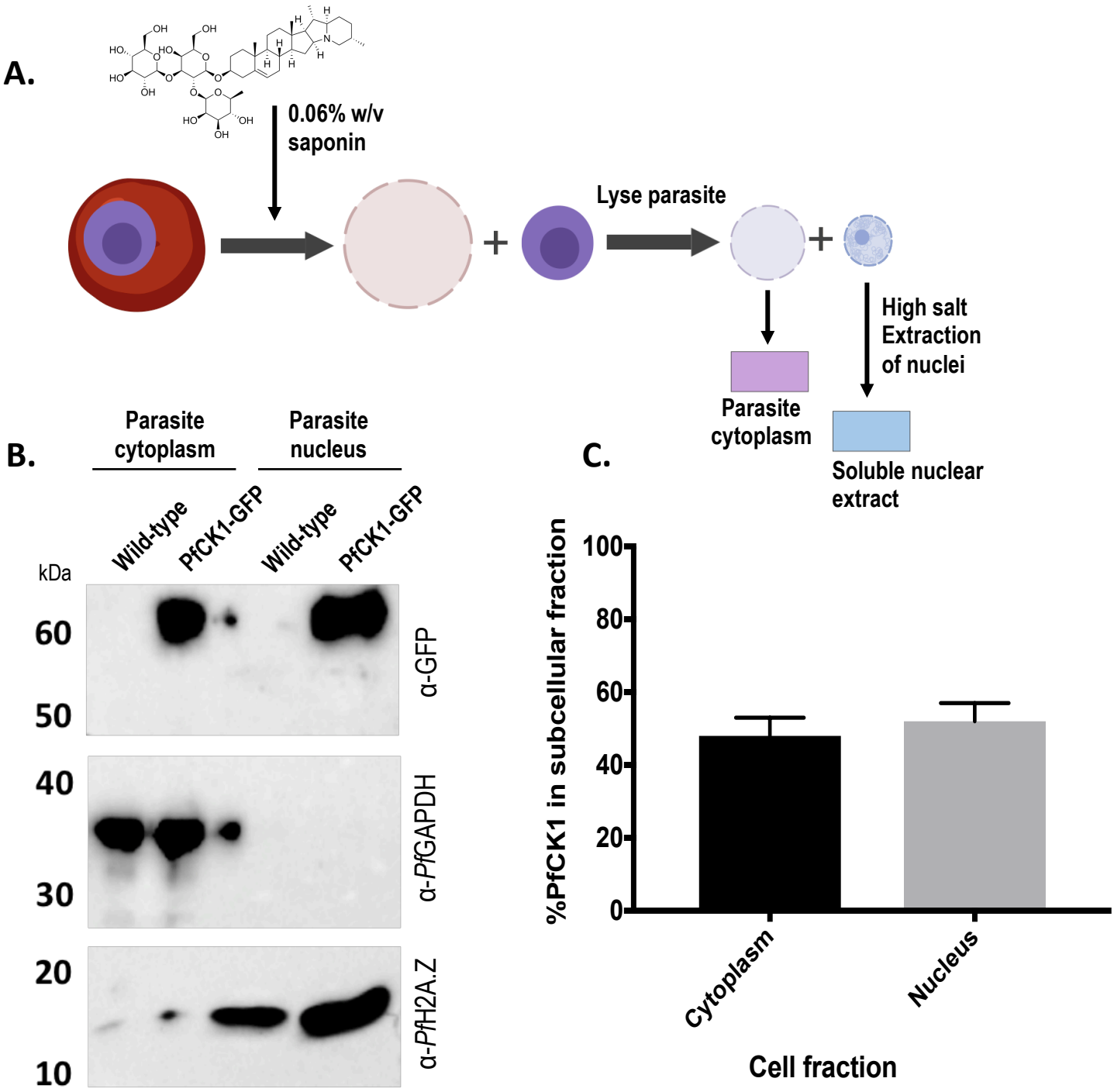
A.
0.06% w/v
saponin
Lyse parasite
High salt
Extraction
of nuclei
Parasite
cytoplasm
Soluble nuclear
extract
B.
Parasite
cytoplasm
Parasite
nucleus
Wild-type
PfCK1-GFP
Wild-type
PfCK1-GFP
kDa
60
50
40
30
20
10
α-GFP
α-PfGAPDH
α-PfH2A.Z
C.
%PfCK1 in subcellular fraction
100
80
60
40
20
0
Cytoplasm
Nucleus
Cell fraction

Figure 4.1. Western blot analysis of PfCK1-GFP subcellular distribution. (A) Schematic representation of the subcellular fractionation process. Red circle: RBC; purple oval: parasite; dotted red circle: saponin permeabilised RBC; dotted purple oval: lysed parasite; blue circle: nucleus. (B) Subcellular fractions prepared from magnet purified late stage parasites expressing PfCK1-GFP from the endogenous locus, and from wild-type parasites used as a negative control. Samples were probed with anti-GFP antibody (1:1000) to detect PfCK1 in each fraction. Samples were probed with anti-PfGAPDH (1:10,000) and anti-PfH2A.Z (1:4000) antibodies as markers for the parasite cytoplasm and parasite nucleus, respectively. (C) Percent distribution of PfCK1 in each subcellular fraction. Percentages were calculated on the assumption that the sum of the cytoplasm and nuclear fractions equalled the total amount of PfCK1 present in purified parasites. Error bars represent the mean $\pm$ standard error of the mean (SEM) of triplicate experiments.

4.2.3. PfCK1 contains classical nuclear localisation signal (cNLS) sequences

The identification of equally distributed PfCK1 in the nucleus and cytoplasm suggests that PfCK1 possesses an NLS. A major mechanism of nuclear import is the recognition of cargo proteins by the karyopherin importin complex, mediated through interactions with an NLS sequence. We sought to identify if indeed PfCK1 contains such an amino acid sequence.

PfCK1 was aligned against two human CK1 isoforms, CK1δ and the long variant CK1α, considering their known presence and function in the nucleus of mammalian cells. The human CK1α isoform contains a known functional cNLS sequence in a 28 amino acid insertion (blue box, figure 4.2) (Fu et al., 2001) which is absent from both CK1δ and PfCK1. Closer inspection of the amino acid sequence of PfCK1 reveals that two clusters of basic residues that could constitute cNLS sequences are present in separate domains of the kinase (figure 4.2) – *KKYR* (green box) and *KKDK* (orange box). The absence of any additional upstream clusters of basic amino acids, characteristic of bi-partite NLS sequences (Lange et al., 2007), indicate that *KKYR* and *KKDK* would be monopartite cNLS's. Similar clusters of amino acids are present in both human CK1 proteins. Next, we examined the position of the candidate cNLS sequences within the 3D structure of the enzyme, using a modified version of a three-dimensional homology model of PfCK1 we had previously generated (see chapter 5 for full structure). Both cNLS sequences are solvent exposed in the model (Figure 4.3), consistent with their being accessible for a possible recognition by the karyopherin complex.

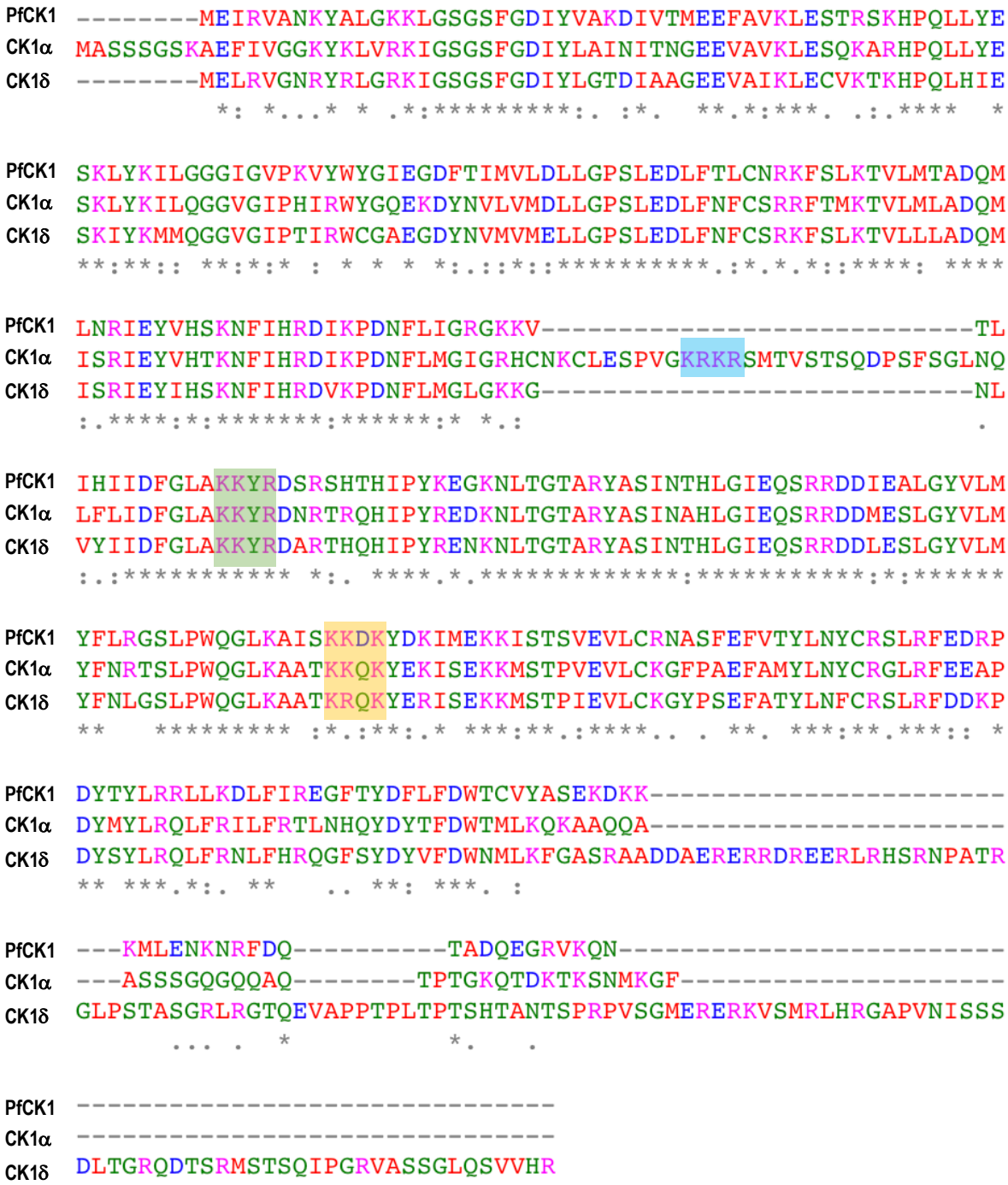

Figure 4.2. Analysis of nuclear localisation sequences in CK1 homologues. Multiple sequence analysis was performed in MUSCLE using sequences of human isoforms CK1α, CK1δ and P. falciparum CK1. The blue box highlights a confirmed NLS sequence in CK1α between residues 160-163 of the long variant and the green box represents putative NLS sequences present in all three kinases between residues 154-157 and 224-227.

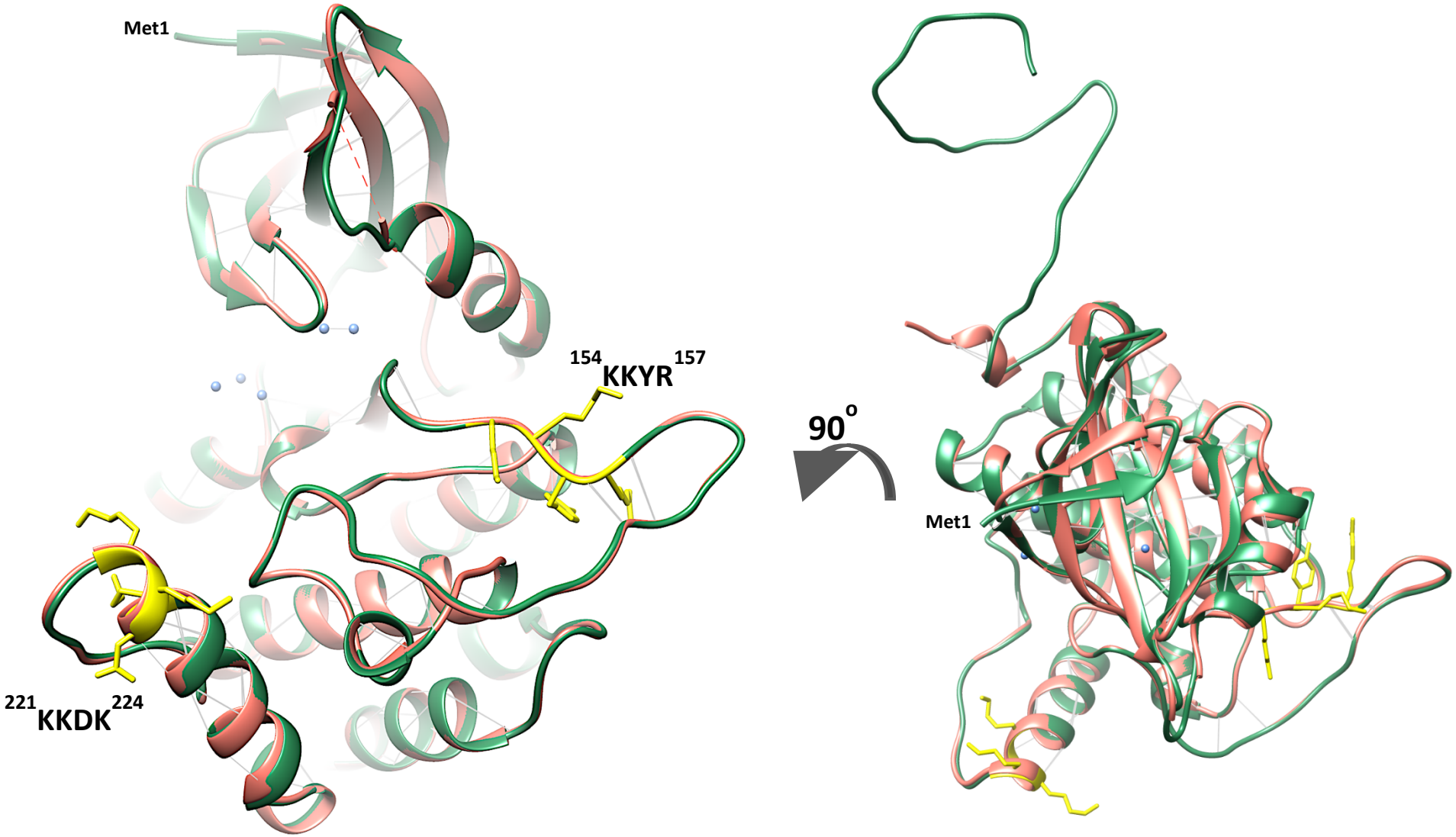
Met1
154 KKYR 157
221 KKDK 224
90°
Met1

Figure 4.3. PfCK1 structure depicting candidate cNLS sequences. A three-dimensional predicted structure of PfCK1 (green) superimposed to an X-ray structure of the human CK1δ (red) isoform depicting the candidate cNLS sequences (yellow). The structure has been modified to show a faded (left) and top-down (right) view to emphasise the solvent-facing orientation of amino acids which constitute the candidate PfCK1 cNLS sequences KKDK and KKYR (see chapter 5 for full PfCK1 structure, analysis and discussion).

4.2.4. PfCK1 nuclear import is sensitive to treatment with Ivermectin (IVM)

Since the nuclear import of proteins with an NLS sequence is controlled by interactions with karyopherins, inhibiting the formation of this complex with small molecule should reduce nuclear protein import. Ivermectin (IVN) has been described to be able to inhibit the karyopherin complex (Panchal et al., 2014)), although the more widely accepted biological effects of avermectins in general is to block GABA and glutamate-gated neural ion channels (Zufall et al., 1989, Duce and Scott, 1985). Mixed late stage parasites expressing PfCK1-GFP from the cognate chromosomal locus, and wild-type parasites as control, were magnet purified and incubated with either 50μM IVM () or the DMSO vehicle for 2hrs, prior to fractionation into subcellular compartments as per 4.2.2. Prior to fractionation, Giemsa stains were prepared from thin blood smears of cultures 2hrs after treatment, and 2μl of parasites were fixed for subsequent immunofluorescence imaging.

Giemsa staining showed that parasites treated with DMSO progressed normally through the lifecycle during the incubation period, whilst parasites treated with 50uM IVM had faint and discontinuous staining of nuclear material, suggesting that IVM treatment is affecting nuclear structure (Figure 4.4A). Western blots probed with anti-GFP antibody showed bi-compartmental distribution of PfCK1-GFP (Figure 4.4B), consistent with our previous fractionation experiment. However, we observed a significant disappearance of cytoplasmic PfCK1 in some of our experiments and suspected that partial parasite lysis might be occurring. We tested that possibility by retaining and analysing the cytoplasmic content of RBCs following saponin permeabilisation and found that, indeed, the RBC cytoplasm fraction in DMSO-treated samples contained a novel protein band corresponding to PfCK1-GFP. We therefore assumed that the sum of PfCK1 from the RBC and parasite cytoplasmic fractions was equivalent to the total cytoplasmic population of PfCK1, equating to approximately 43% of total PfCK1 as determined by densitometry (Figure 4.4C), whilst nuclear PfCK1 was more abundant at around 57% of total PfCK1. In contrast, parasites treated with 50μM IVM showed a reversal of PfCK1 distribution, with the larger pool observed in the cytoplasmic factions (approximately 57%) and a concomitant decrease of nuclear PfCK1 to around 43% of the total. These results seem to show the expected effect

of a nuclear transport inhibitor, although we did not test if the differences were statistically significant. No signal was detected for wild-type parasites as expected.

Results obtained by IFA in PfCK1-GFP expressing parasites labelled with an anti-GFP antibody agreed with the cell fractionation results. Cells incubated with DMSO displayed a bi-compartmental localisation between the cytoplasm and nucleus, but the PfCK1-GFP signal appears more restricted to the cytoplasm in cells incubated with 50μM IVM (Figure 4.5). As expected, no signal was observed in wild-type parasites stained with anti-GFP antibody.

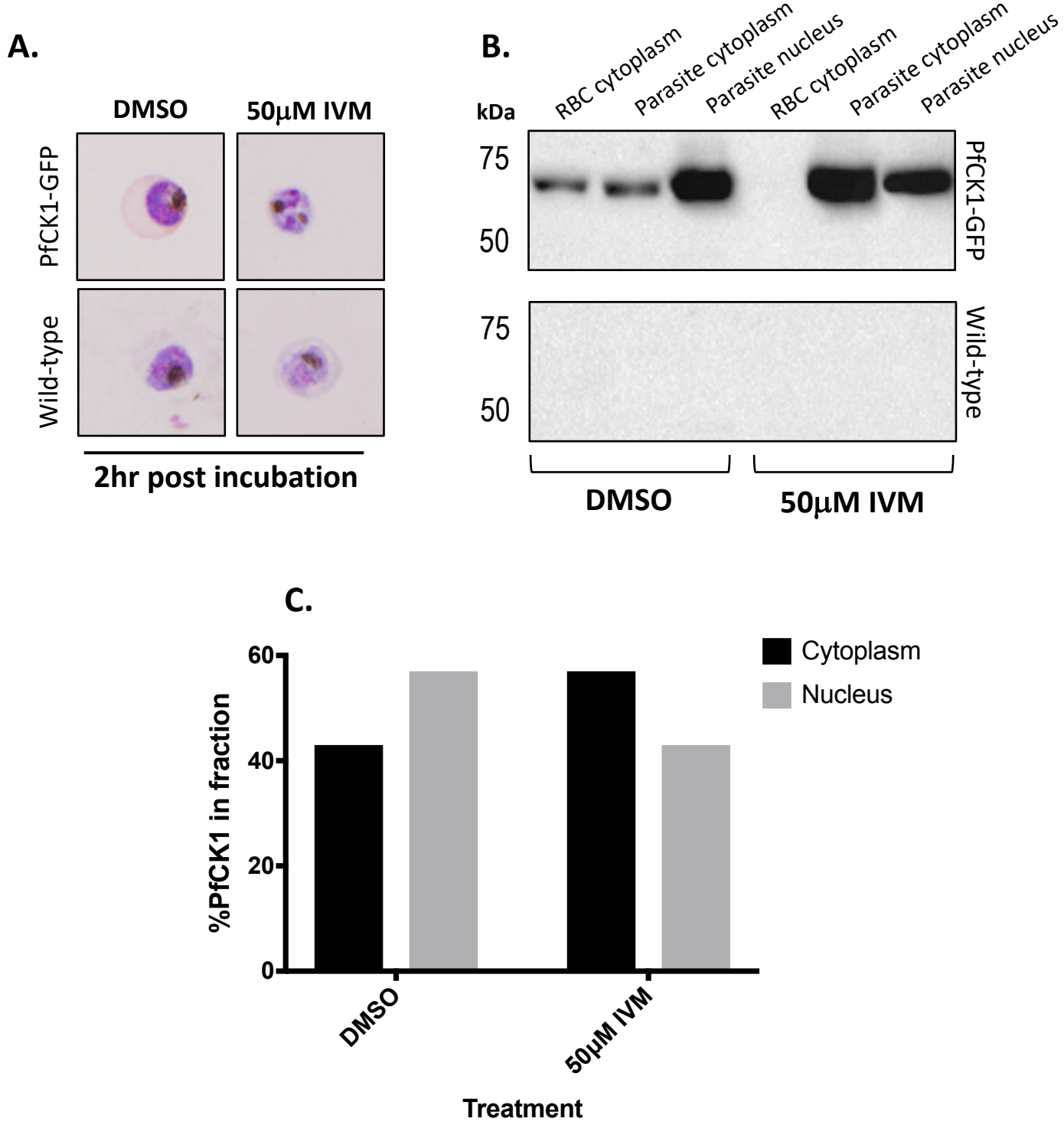

Figure 4.4. Chemical inhibition of PfCK1 nuclear import. (A) Giemsa stained blood smears of PfCK1-GFP expressing (top) or wild-type (bottom) parasites 2hrs post treatment with 50μM IVM or vehicle control. (B) Western blot analysis of PfCK1-GFP subcellular distribution after treatment with 50μM IVM or vehicle control. Blots were probed with anti-GFP antibody and wild-type parasites were used as a negative GFP control. (C) Quantification of PfCK1-GFP subcellular distribution by densitometry after treatment with 50μM IVM or vector only. Histogram

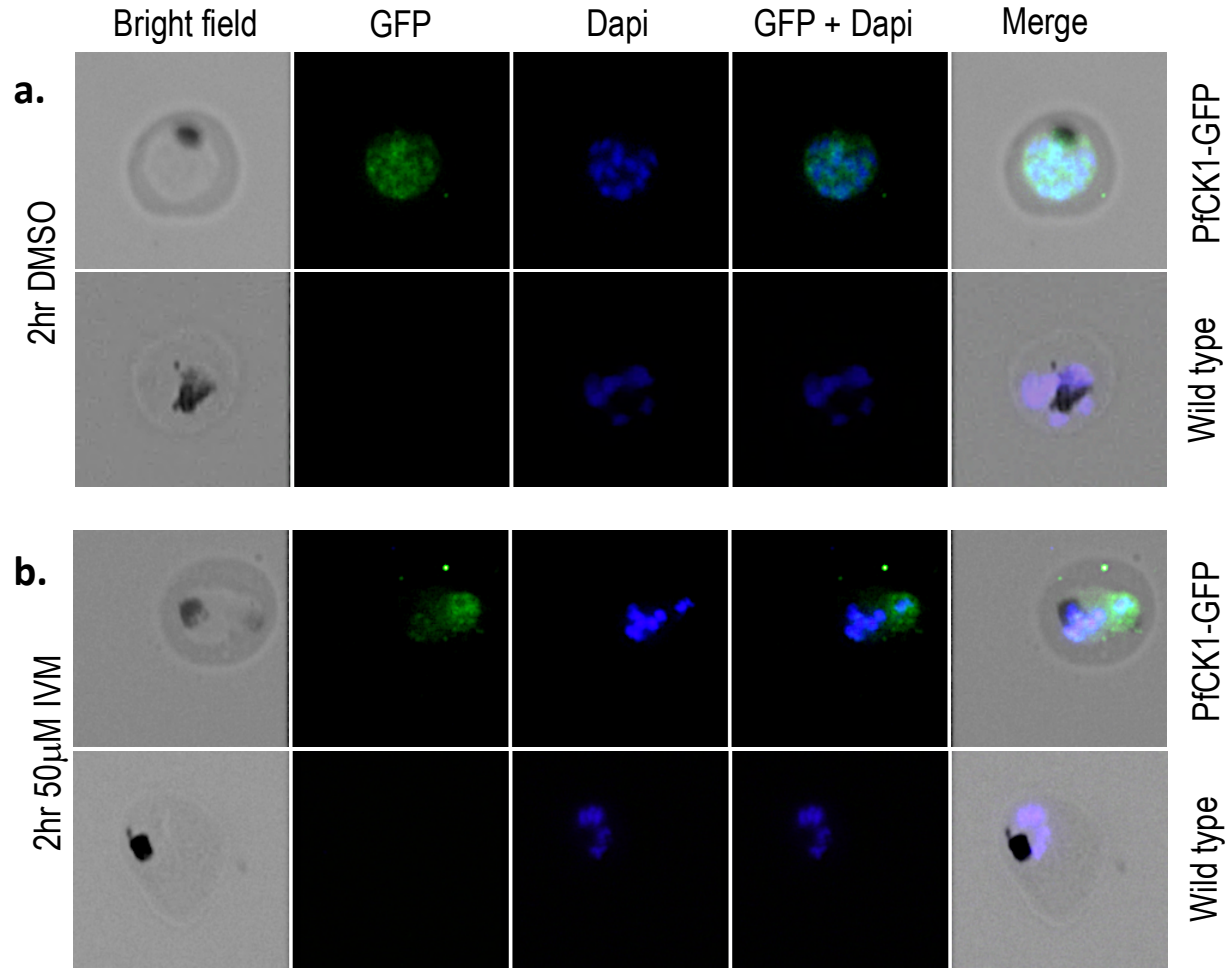

Figure 4.5. Effect of Ivermectin treatment on the localisation of PfCK1-GFP. Magnet-purified late stage parasites were recovered at 37°C for 1hr prior to incubation with drug for 2hr. Upper panel in each block are cells expressing PfCK1-GFP from the cognate locus and bottom panel in each are wild-type control cells. **(a)** DMSO treated control parasites after 2hr incubation and **(b)** parasites following a 2hr incubation with 50µM Ivermectin (IVM).

4.2.5. PfCK1 immunoprecipitates chromatin-related proteins from parasite nuclei

To gain insight into the possible nuclear-associated functions of PfCK1, and in view of published data suggesting interaction pPfCK1 with chromatin components (Dorin-Semblat), we performed a pilot interactomics study to analyse the protein content of immunoprecipitates obtained from nuclei of transgenic parasites expressing PfCK1-GFP from the cognate chromosomal locus. Wild-type 3D7 parasites were used as a negative control. Proteins were precipitated from the nuclei of approximately $2x10^8$ magnet-purified late stage parasites using GFP Trap® agarose beads (see section 2.5.5.3), eluted from the beads and run for 5mins into a 4-12% SDS polyacrylamide gel and stained as per section 2.5.1. Sections of the gel containing protein were excised, subject to in-gel tryptic digest and the digested peptides were analysed by mass spectrometry. The data from three IP experiments were analysed by MaxQuant and the results displayed as a volcano plot (Figure 4.6).

PfCK1 was identified in the immunoprecipitates as expected, although it was not tagged as a high probability interactor based on the FDR threshold (black hyperbolic curve, Figure 4.6B). The distribution of experimental replicates indicates some overlap between the PfCK1-GFP and wild-type datasets, as shown by Principal Component Analysis of our samples (Figure 4.6A). Although no proteins met the stringent threshold limits for significance of the volcano plot, several nuclear proteins identified in the pilot experiment are listed in table 4.2. Included in this list are the core histone proteins H2A, H2B and H3, as well as the catalytic subunit of casein kinase 2 PfCK2α, which is known to be involved in chromatin assembly in *P. falciparum* (Dastidar et al., 2012). Although this work requires further experimental verification, this pilot data set suggests a role for PfCK1 in chromatin dynamics.

A.

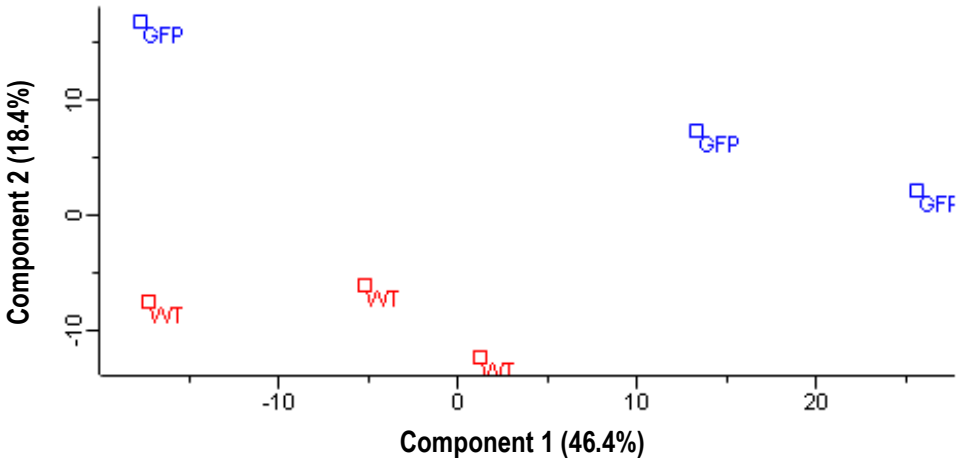
GFP
GFP
GFF
WT
WT
WT
Component 2 (18.4%)
Component 1 (46.4%)
10
0
-10
-10
0
10
20

B.

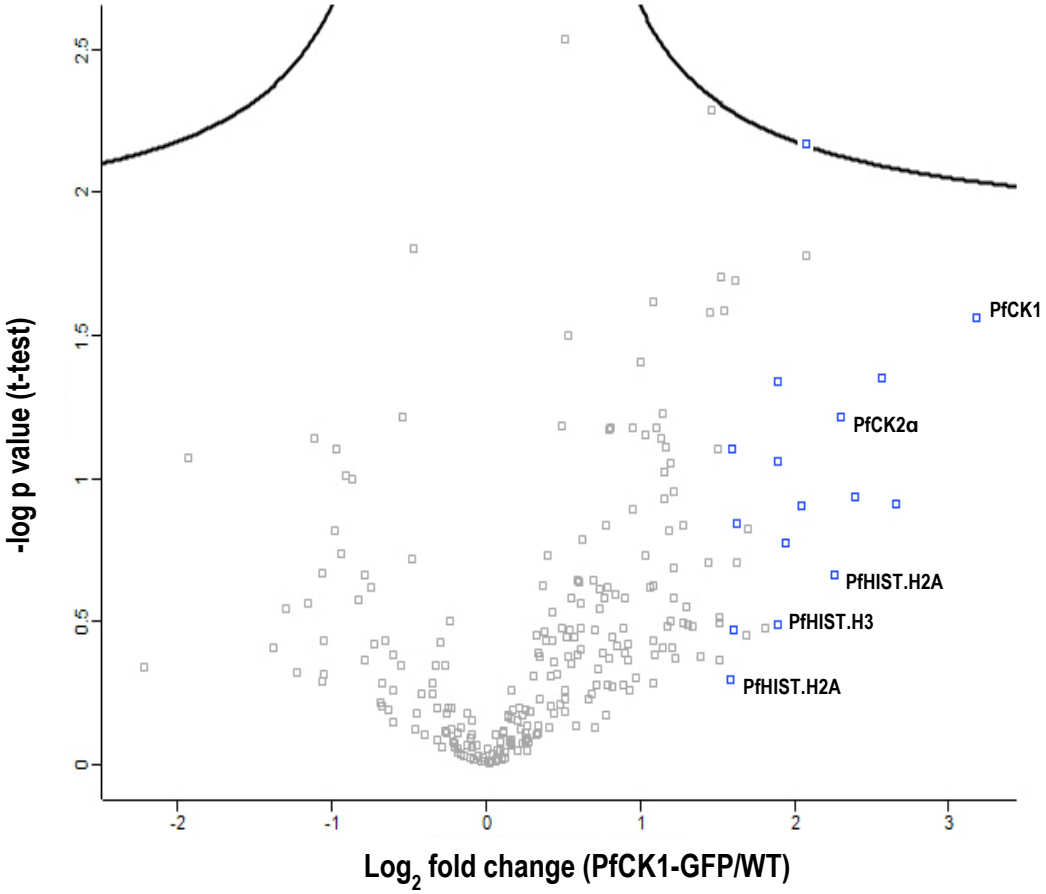
PfCK1
PfCK2α
PfHIST.H2A
PfHIST.H3
PfHIST.H2A
-log p value (t-test)
Log2 fold change (PfCK1-GFP/WT)
2.5
2
1.5
1
0.5
0
-2
-1
0
1
2
3

Figure 4.6. Label free quantitative analysis of PfCK1 interacting protein from purified nuclei. (B) Volcano plot representing the logarithmic fold change between PfCK1-GFP and wild type samples plotted against the negative logarithmic p values obtained from triplicate experiments (FDR threshold = 1%). Interacting proteins are separated from background by a parabolic curve. Blue squares represent interesting parasite proteins obtained from analysis of total protein content in this pilot precipitation experiment.

Table 4.2. *P. falciparum* proteins co-purifying with PfCK1 in nuclear protein extracts.

Protein description	-Log (p-value)	Fold difference (GFP vs. WT)	UniProt ID
Rhoptry-associated protein 1	2.16	4.2	Q8ILZ1
Casein kinase I	**1.56**	**9.1**	**Q8IHZ9**
Thioredoxin-related protein (putative)	1.34	5.9	Q8IDH5
Rhoptry-associated protein 2	1.34	3.7	Q8I484
Casein kinase II, subunit alpha	1.21	4.9	Q8IIR9
Eukaryotic translation initiation factor 3 subunit M	1.12	3.03	Q8I1Q5
High molecular weight rhoptry protein 2	1.06	3.7	C0H571
DNA primase small subunit	0.94	5.2	Q7KQM1
Proliferating cell nuclear antigen	0.91	6.3	P61074
Uncharacterised protein (nucleus)	0.91	4.1	Q8IIC0
Fibrillarin (putative)	0.78	3.9	Q8IM23
Glideosome-associated protein 50	0.7	3.1	Q8I2X3
Histone H2A	0.66	4.8	C6KT18
Histone H3	0.49	3.7	C6KSV0
Histone H2B	0.47	3.03	Q8IIV1
Eukaryotic translation initiation factor 3 subunit D	0.45	3.2	Q8IJW4

Proteins with ≥3-fold difference between GFP-trap pull-down samples obtained from PfCK1-GFP-expressing and wild-type parasites. Proteins are ranked in order from highest to lowest by -log (p-value)

4.2.6. PfCK1 interacts with DNA-containing structures

Identification of chromatin-associated proteins in PfCK1-GFP immunoprecipitates from purified nuclei led to experiments aiming to investigate a possible role of PfCK1 in chromatin organisation. We performed Chromatin Immunoprecipitation and Sequencing (ChIP-seq) experiments, in which nuclear content was sheared by sonication to fragment chromatin into individual nucleosomes, which were subsequently purified by immunoprecipitation to recover and sequence the associated DNA (Figure 4.7A).

This process first required optimisation of shearing time to yield adequate quantities of nucleosomes containing DNA fragments in a size range of 300-800bps for library construction, while maintaining epitope structure and protein-protein interactions for immunoprecipitation. Nuclei were purified from late stage wild-type 3D7 parasites (see section 2.5.5.4) and pulsed with ultrasound waves at 5sec intervals with a 15sec rest in between pulses on ice for a total of 6, 7 and 8mins. DNA was recovered from nucleosomes (omitting the immunoprecipitation steps) as per section 2.5.6.4 and analysed by gel electrophoresis (Figure 4.7B). All three sonication conditions yielded DNA fragments in the size range of approximately 250-600bp. Therefore, we selected the shortest time (6mins) for subsequent ChIP-seq experiments, in order to preserve the epitope structure and protein-protein interactions for immunoprecipitation. Next, we obtained nucleosomes from parasites expressing PfCK1 tagged with GFP at the C-terminus using the sonication conditions optimised above. As a negative control, nucleosomes were prepared from wild-type 3D7 parasites. Samples were incubated overnight with 30ul of GFP Trap® agarose to immunoprecipitate PfCK1-nucleosome complexes, extensively washed and DNA recovered as above, resulting in a total of 2.8ng (0.28ng/µl) of DNA recovered from PfCK1-GFP samples for library construction and sequencing. No DNA was detected in wild-type samples using the same quantification methods (section 2.5.6.4). Samples were ligated with universal adapters and amplified by PCR to yield final concentrations of ~5.6ng/µl for PfCK1-GFP samples and ~1.7ng/µl for wild type samples respectively. Analysis of DNA fragment sizes at Micromon using a *Fragment*

Analyzer^{TM} (Figure 4.8) shows a distribution similar to estimates made in Figure 4.7, with average sizes of 424bp (PfCK1-GFP) and 397bp (wild-type).

Following construction of our DNA libraries and sequencing, we visually inspected our data and found that the recovered sequences mapped to various broad regions of the genome (Figure 4.9A). Closer inspection of individual chromosomes showed an enrichment of sequences present at sub-telomeric regions, more noticeable in chromosome 2 (Figure 4.9B and C). DNA read numbers appeared to peak within coding sequences, rather than at the intergenic regions expected for effectors of transcriptional activation or repression.

DNA recovered from wild-type precipitates revealed a genomic distribution surprisingly similar to those in the PfCK1-GFP samples. To double check if our control sample really came from an untagged 3D7 culture, the GFP gene sequence was mapped in the sequencing reads obtained from PfCK1-GFP and wild-type immunoprecipitates. A total of 3000 reads were detected in the PfCK1-GFP sample, whilst only 16 were obtained from wild-type samples (data not shown) indicating a low level of GFP contamination.

Although it is difficult to reach conclusions from one ChIP-seq experiment, the study does demonstrate that fixation and shearing conditions have been adequately optimised, and the preliminary results agree with the proteomic data in pointing to a PfCK1 function in chromatin-related cellular processes.

A.

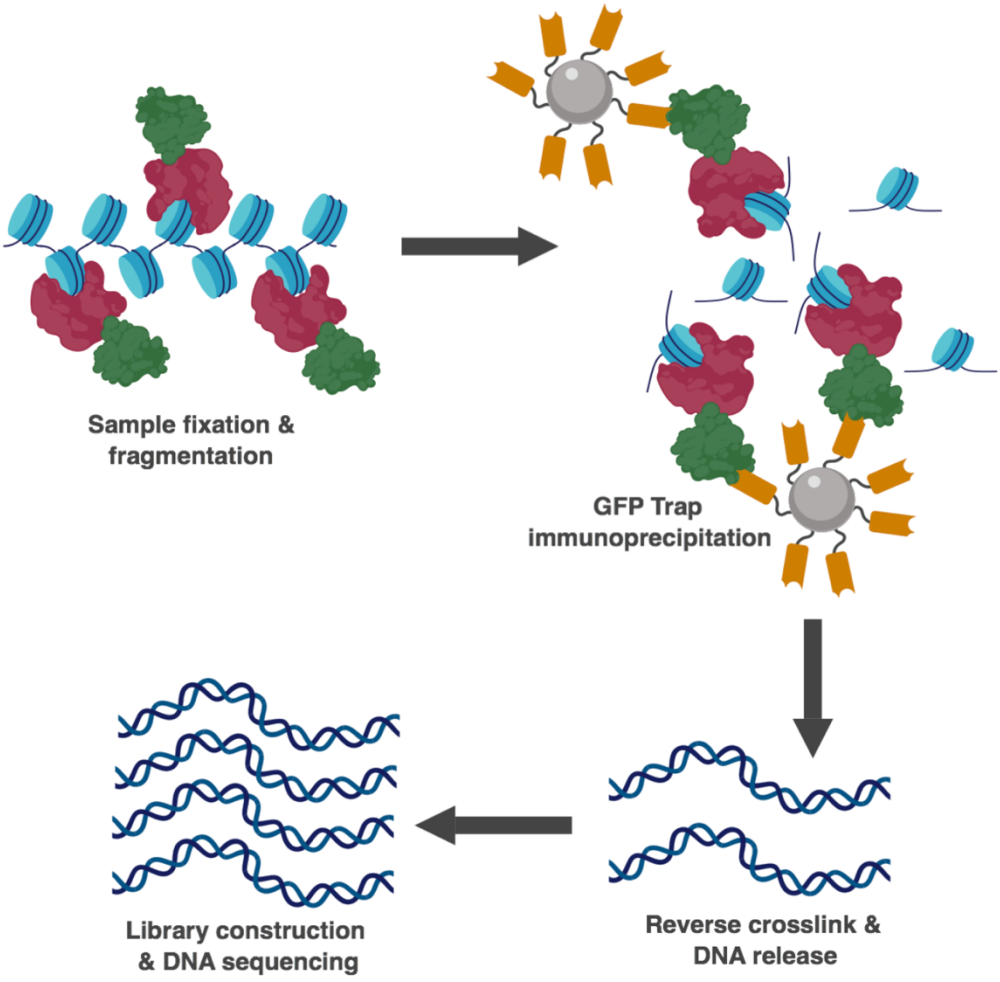
Sample fixation &
fragmentation
GFP Trap
immunoprecipitation
Reverse crosslink &
DNA release
Library construction
& DNA sequencing

B.

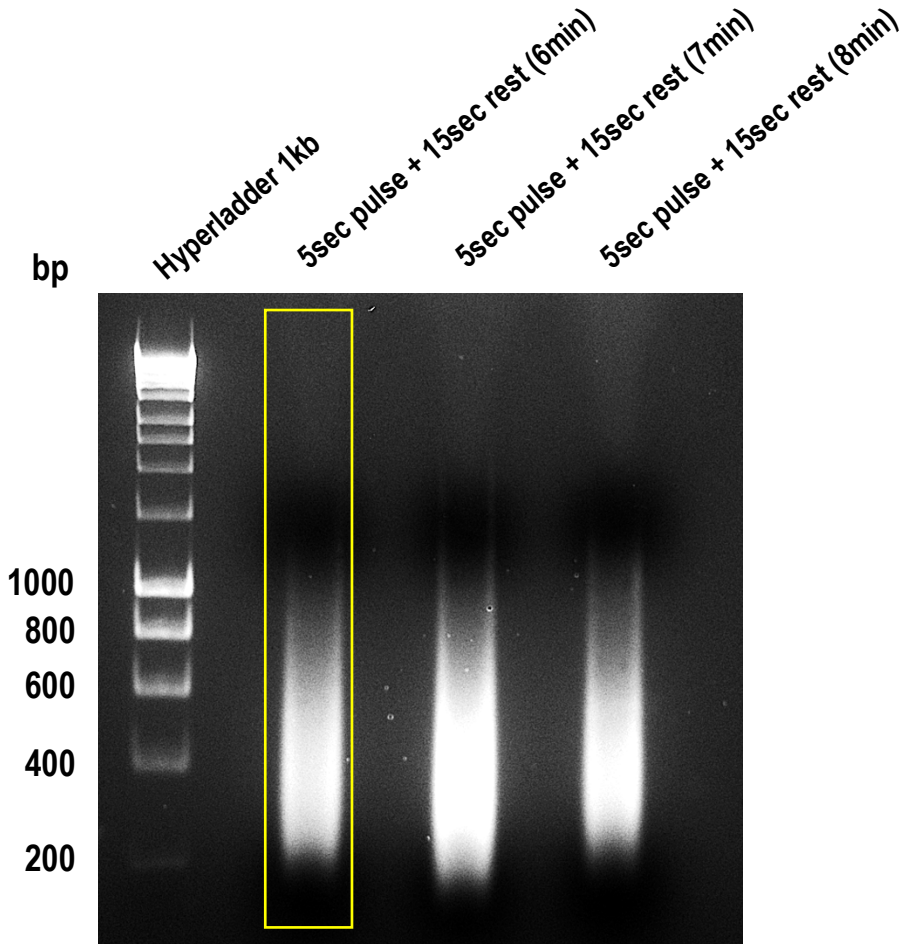
bp
Hyperladder 1kb
5sec pulse + 15sec rest (6min)
5sec pulse + 15sec rest (7min)
5sec pulse + 15sec rest (8min)
1000
800
600
400
200

Figure 4.7. Optimised DNA shearing conditions for ChIP-seq. (A) Diagram representing the chromatin immunoprecipitation and sequencing (ChIP-seq) process for pull-down samples of PfCK1-GFP (red and green respectively) bound to chromatin (blue). (B) Optimised DNA shearing conditions established for nuclei of magnet-purified wild type 3D7 parasites and analysed by electrophoresis on a 2% agarose gel. Shearing conditions selected for subsequent experiments are highlighted by the yellow box.

A.

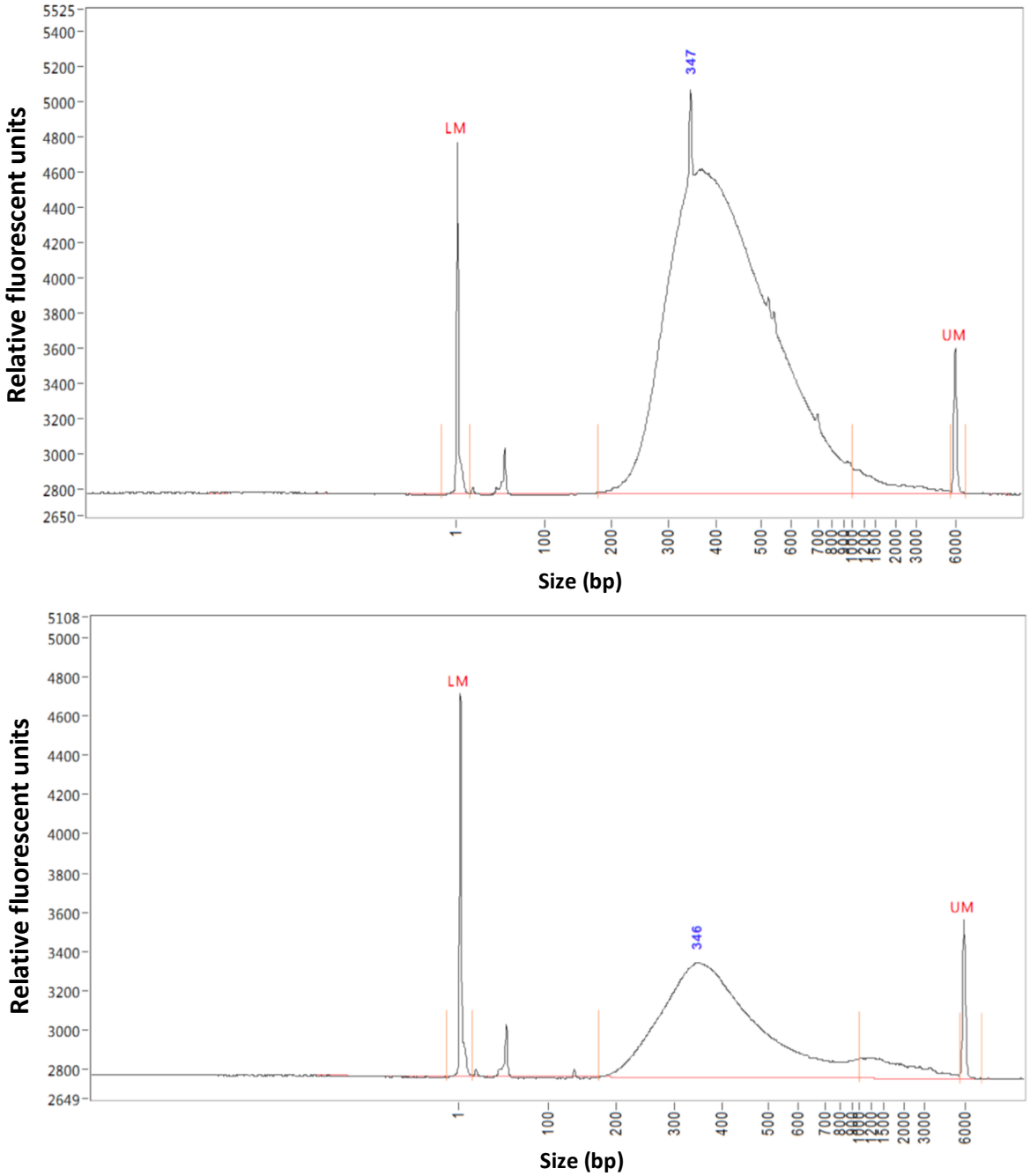

B.

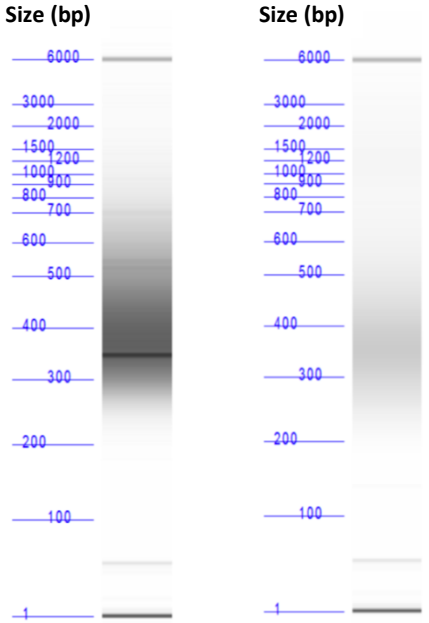

	GFP	WT
Size range (bp)	179-1013	176-1007
Average size (bp)	424	397
Concentration (ng/µl)	5.64	1.69

Figure 4.8. Bioanalyzer chase of DNA fragments obtained from PfCK1 chromatin immunoprecipitation. (A) Schematic showing DNA band size (bp) distribution and quantity (relative fluorescent units) for PfCK1-GFP (top) and wild-type (bottom) samples. Peaks at 346 and 347 represent an artefact. *LM*: lower marker, *UM*: upper marker. (B) Lane profile of DNA obtained from PfCK1-GFP (left) and wild-type (right) ChIP experiments and analysed by capillary gel electrophoresis in a *Fragment Analyzer™*. To the left of each lane is a DNA ladder to indicate fragment size (bp). Table insert summarises the DNA fragment profile for each sample.

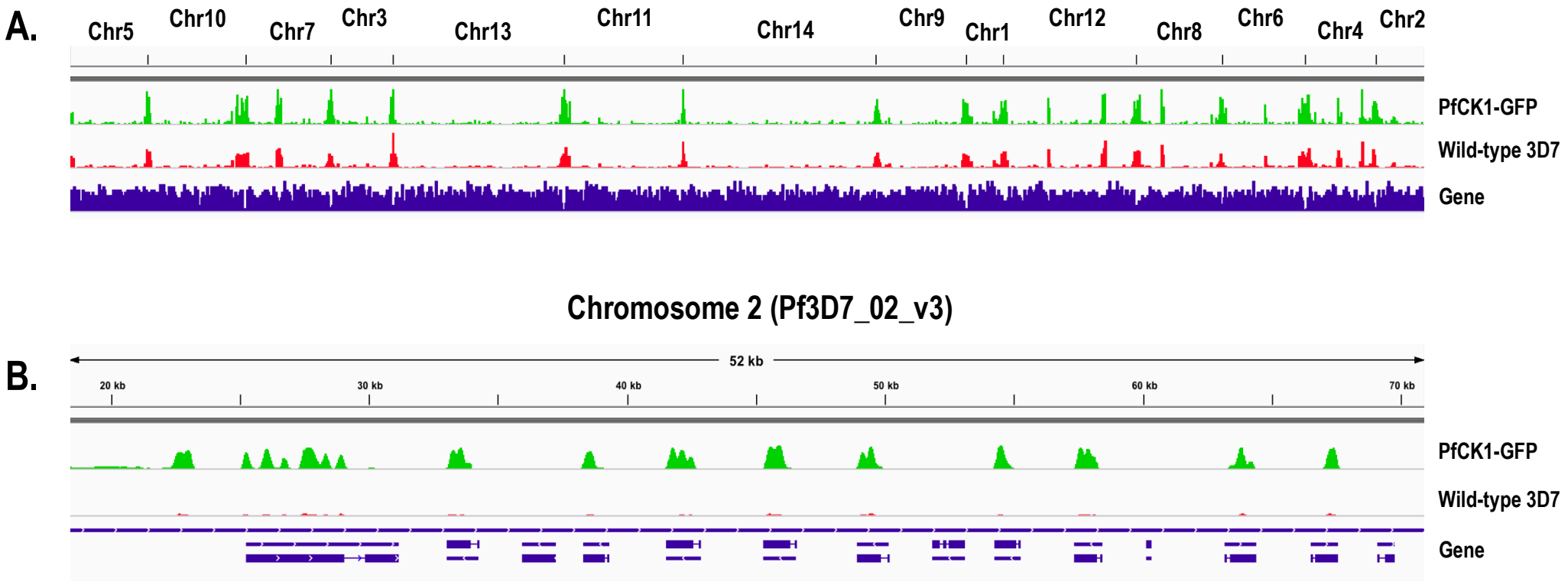

Figure 4.9. DNA sequencing and chromosomal mapping of PfCK1-chromatin immunoprecipitates. (A) Genome wide distribution of DNA fragments obtained from formaldehyde fixed nucleosomes co-immunoprecipitated with PfCK1-GFP (green) and wild-type 3D7 (red) parasites using GFP Trap agarose beads. DNA sequencing reads are mapped to all 14 chromosomes of the *P. falciparum* genome (version 9.0 used) and the distribution of genes is shown in blue. (B) Close-up view of a sub-telomeric region of chromosome 2 with each individual peak representing a single nucleosome. Coding regions are shown in blue beneath each mapped nucleosome.

4.3. Discussion

4.3.1. A PfCK1 population is located in the parasite nucleus

In this chapter we investigated PfCK1 as a possible nuclear localised PK and show that indeed PfCK1 exists as a population in both the parasite cytoplasm and nucleus (Figure 4.1), indicating PfCK1 has a bi-compartmental distribution. The main nuclear import mechanism for proteins involves interactions of the nuclear import receptors importin-α and -β with a nuclear localisation signal sequence (NLS) in the cargo protein (Depping et al., 2008, Chaston et al., 2017, Conti and Kuriyan, 2000). We have identified two clusters of basic amino acids which may function as NLS sequences in PfCK1 (Figure 4.2). Moreover, these cNLS sequences appear to be solvent exposed, as required for adequate sequence recognition by the karyopherin complex.

These motifs are also present in the two human CK1 isoforms we used in our sequence alignments (CK1α and CK1β). Interestingly, these CK1 isoforms exhibit two seemingly different nuclear import mechanisms. CK1δ does not require an NLS sequence for nuclear import, but rather kinase activity within the N-terminal domain is required (Milne et al., 2001). This phosphorylation-dependent mechanism of nuclear localisation is also used by yeast hexokinase Hxk2 (Fernandez-Garcia et al., 2012) and STAT3 dimers (Vogt et al., 2011).

In contrast, the long-variant of CK1α contains a KRKR cluster in a 28-amino acid insert which has been demonstrated through mutagenesis studies to act as a functional NLS sequence (Fu et al., 2001). CK1α isoforms lacking this 28-amino acid insertion are predominantly, but not fully, cytoplasmic, suggesting that residual nuclear localisation may be mediated by other NLS sequences, perhaps aided by phosphorylation, which is known to play a role in the recognition of NLS sequences in transport substrates by importins (Patrick et al., 2018, Yan et al., 2007, Grindheim et al., 2014).

It still remains unknown whether PfCK1 nuclear import requires a functional cNLS, kinase activity or both. We are approaching this question by mutating the putative NLS sequences in the PfCK1 gene. Several criteria are used to determine whether a candidate NLS sequence is a true signal sequence.

Firstly, disruption of nuclear localisation by mutagenesis is initially attempted, typically by mutating the first two basic residues to establish whether nuclear import is impaired (reviewed in (Lange et al., 2007)). For this purpose, we have generated three gene fragments (IDT gBlocks® gene fragments) containing a codon optimised nucleotide sequence of PfCK1 (based on codon usage in *P. falciparum* (Yadav and Swati, 2012)) and cloned them into the expression vector pGlux; one containing a KKDK mutant, another containing a KKYR mutant and a third containing mutations in both NLS's, in case the two sequences are functionally redundant. In each case, the first two Lys residues have been mutated to Ala. Parasites will be transfected next with each construct, to allow expression of GFP tagged PfCK1 NLS mutants in a wild-type background that enables IFA and Western blot analysis of subcellular distribution.

In addition to affecting nuclear import by mutating NLS sequences, chemical methods are also used to investigate nuclear protein transport. Although there are several nuclear export inhibitors (Soung et al., 2017, Jang et al., 2003), very few import inhibitors are available (Hintersteiner et al., 2010). A relatively recent study by Panchal *et al* investigated the use of Ivermectin (a drug used to treat scabies and some helminth infections (Palmeirim et al., 2018, Romani et al., 2015)) to study the nuclear import of proteins in *P. falciparum* (Panchal et al., 2014). It was suspected that IVM inhibited the formation of the karyopherin-cargo complex, thus disrupting protein localisation. We attempted similar experiments in *P. falciparum* to approach the nuclear import of PfCK1 by Western blot (Figure 4.4) and IFA (Figure 4.5), using experimental conditions similar to those reported in the study above. Our data suggest that nuclear import of PfCK1 is affected by IVM, however additional experimental repeats are necessary to establish statistical significance. Moreover, under the treatment conditions used in our study several small, condensed trophozoites were observed by IFA analysis (supplementary figure 4.1). Similarly, Panchal *et al* observed small, dense parasites which were described as arrested trophozoites. However, this morphology also resembles a death phenotype, which suggests that the drug used at these concentrations may be killing parasites during treatment. Therefore, it is difficult

to conclude at this stage whether the disruption of PfCK1 nuclear shuttling is a result of inhibiting the import pathway or more trivially due to parasite death. Nevertheless, we consider it is warranted to try optimising IVM treatment as a tool for exploring the nuclear import and function of PKs in *P. falciparum*.

4.3.2. PfCK1 may participate in chromatin dynamics

"Omics"-based approaches provide a vast quantity of information regarding possible functions of a protein of interest. In our pilot PfCK1-GFP immunoprecipitation experiment we identified several nuclear proteins by mass spectrometry that are candidates to interact functionally with PfCK1. In other eukaryotes, CK1 enzymes contribute to various biochemical processes within the nucleus. In the model organisms *S. cerevisiae* and *D. melanogaster* for example, CK1 functions in the cellular response to DNA damage. In *D. melanogaster*, CK1 undergoes significant transport into the nucleus of embryos following stimulation with γ-radiation (Santos et al., 1996), suggesting that DmCK1 may play a role in repairing DNA during embryogenesis. In yeast, the CK1 homolog Hrr25 interacts with and phosphorylates the transcription factor Swi6, required in complexes with other proteins to enable the specific transcription of G_1 cyclins and S-phase genes (Ho et al., 1997). In these cases, CK1 functions by phosphorylating nuclear effector proteins which in turn regulate DNA replication and transcription. Chromatin structure is also regulated by this kinase family. In mice, CK1δ/ε isoforms phosphorylate Ser146 in the N-terminal domain of the DNA methyltransferase-1 (Dnmt1) (Sugiyama et al., 2010), reducing its affinity for DNA compared to its unphosphorylated state (Sugiyama et al., 2010). Furthermore, phosphorylation is more prominent when Dnmt1 is bound to DNA. Methylated DNA correlates with gene silencing (reviewed in (Jones, 2012)) and crosstalk with histone methylation has also been observed, in that histone methylation can result in the recruitment of DNA methyltransferases, which subsequently modify DNA near the phosphorylated histones (Dhayalan et al., 2010, Zhao et al., 2009). Therefore, CK1 enzymes can act as transcriptional regulators and chromatin re-modellers, by interacting with and modifying effector molecules bound to DNA.

Although our pilot experiment requires confirmation, histones H2A, H2B and H3 and the catalytic α-subunit of PfCK2 were recovered in precipitates with PfCK1 and they are possible functional interactors (table 4.2), implicating PfCK1 in the chromatin assembly pathway, as already suggested by data in a global PfCK1 interactome study (Dorin-Semblat et al., 2015). Histones form the core component of nucleosomes, the basic unit of chromatin (Chen et al., 2016), and multiple histone modifications influence the transcriptional state of the cell (Casadio et al., 2013, Hyland et al., 2005, Xu et al., 2005a). For example, histone H2A is phosphorylated at Tyr57 by the Ser/Thr kinase CK2 (Basnet et al., 2014). It was shown that mutation of H2ATyr57 and consequent inhibition of CK2 action impairs transcriptional elongation. It also causes a loss of ubiquitination and H3K4me3 and H3K79me3 histone marks associated with transcriptional activation, indicating that CK2 functions in gene transcription. Histone H4 is also phosphorylated by CK2 as a response mechanism to DNA damage in *S. cerevisiae* (Cheung et al., 2005). These pathways are consistent with the observed biochemical activity of PfCK2 in *P. falciparum* as a Tyr kinase (Ruiz-Carrillo et al., 2018) able to phosphorylate several proteins involved in chromatin dynamics (Dastidar et al., 2012), suggesting a similar role for PfCK2 in *P. falciparum*. Since the catalytic PfCK2α subunit was identified as an interacting protein in our dataset and it is known to be a phosphosubstrate of PfCK1 (Dorin-Semblat et al., 2015), a logical conclusion would be that PfCK1 is involved in chromatin assembly, possibly by regulating the activity of chromatin-interacting proteins. Future experiments will include kinase assays to determine whether histone proteins themselves are *in vitro* substrates of PfCK1, as this would support a role for the kinase in chromatin and/or transcriptional-related functions.

We performed indirect ChIP-seq experiments by immunoprecipitating PfCK1-GFP from the nuclei of formaldehyde fixed cells (Figure 4.7), in an attempt to observe possible PfCK1-DNA interactions and to establish functions for PfCK1 in chromatin dynamics. Although it was difficult to interpret results from wild-type control precipitates that displayed a distribution of DNA fragments similar to our PfCK1-GFP samples, we did observe that DNA fragments obtained from immunoprecipitated

nucleosomes are distributed across the whole genome (Figure 4.9A). An enrichment of immunoprecipitated nucleosomes was observed at the telomeric regions of each chromosome, with stronger peaks identified in Chromosome 2 from PfCK1-GFP samples (Figure 4.9B); these regions encode genes of the *var* family such as PfEMP1 and other virulence factors such as Rifins and Stevor. Since *P. falciparum* expresses only one of 60 *var* genes at a time to maintain a continuous infection (Jiang et al., 2013), PfCK1 could be involved in this process. H3K36me3 methylation by histone methyltransferase PfSET2 is found at *var* genes (Ukaegbu et al., 2014, Jiang et al., 2013), and interactions between PfSET2 and RNA polymerase II are regulated by phosphorylation of the polymerase C-terminal domain (CTD) (Ukaegbu et al., 2014, Fuchs et al., 2012) and reviewed in (Saldi et al., 2016)). Thus, it is tempting to assign a function to PfCK1 in this process. The identification of individual nucleosomes associated with gene coding regions (Figure 4.9B) provides some support to this hypothesis. This would be distinct from reported functions of CK1 in regulating transcription factors, which generally do not involve interactions with protein-coding sequences in DNA (Walton et al., 2009, Eng et al., 2017, Okamura et al., 2004).

Phosphorylation of the RNA polymerase II CTD has been shown to regulate different transcriptional processes, such as 3' mRNA capping and splicing (Davidson et al., 2014, Martinez-Rucobo et al., 2015), as well as transcriptional pausing when hyperphosphorylated at Ser5 (Nojima et al., 2015). As transcription elongation resumes, Ser5 phosphorylation is gradually removed and Ser2 phosphorylation increases (Nojima et al., 2015), indicating that this phosphosite acts as a transcriptional activation signal. The RNA polymerase II CTD is conserved in *P. falciparum*, with high homology to higher eukaryotes ((Kishore et al., 2009) and reviewed in (Ukaegbu and Deitsch, 2015)), but some marked differences in CTD phosphorylation and the recruitment of associated transcriptional machinery has been observed between *P. falciparum* and mammalian cells (Kizer et al., 2005, Ukaegbu et al., 2014). This suggests the existence of mechanisms for transcriptional processing unique to the parasite, opening up possibilities for a role of PfCK1 I them (Dorin-Semblat et al., 2015). Ongoing work is optimising the ChIP-seq protocol to improve its performance in our

system and confirm the possible involvement of PfCK1 in functions regarding transcriptional processing and chromatin maintenance in *P. falciparum*.

To conclude, we have shown that PfCK1 is a kinase with a newly established nuclear localisation in *P. falciparum*. Initial experiments hint to an import mechanism that is sensitive to the effects of the proposed nuclear import inhibitor, IVM, though further work is required to verify the observed effects are due to inhibition of PfCK1 import, and not an effect on nuclear structure. Further, we have identified a list of candidate interacting proteins that co-precipitate with PfCK1 in protein extracts obtained from purified nuclei. Their confirmation would strongly suggest a role for this kinase in regulating chromatin structure. Combined with data from ChIP-seq experiments, we are building a strong case for parasite kinases as regulators of essential processes in the nucleus, their role in orchestrating virulence in *P. falciparum* and their importance as targets for pharmacological intervention.

Chapter 5

Investigating the contribution of PfCK1 to the mechanism of action of Purvalanol B

5.1. Introduction

The arsenal of effective antimalarials currently being used to treat malaria is decreasing due to drug resistance, thus new antimalarials are greatly needed. The *P. falciparum* genome encodes 86 protein kinases (PKs), of which 65 belong to the protein kinase families defined in higher eukaryotes. Approximately 42% of the 86 PKs are considered likely essential for asexual development (Solyakov et al., 2011) which makes them sensible targets for new antimalarials. Parasite PKs are not currently targeted by any known antimicrobial compounds; therefore, it is unlikely that any pre-existing drug resistance mechanisms associated with the inhibition of PKs will be present. Furthermore, PKs are being successfully exploited as drug targets for human diseases such as cancer and inflammatory disorders (Tigno-Aranjuez et al., 2014, Mavrou et al., 2014), with 37 kinase inhibitors currently approved by the FDA (Santos et al., 2016).

Purvalanol B, a 2,6,9-trisubstituted purine compound, is a potent inhibitor of human cyclin-dependent kinases (CDKs). Initially explored as a compound for use in treating cancer, this compound inhibits CDKs at nanomolar concentrations in cell-free assays (Yenugonda et al., 2011) but fails to inhibit cell growth, with a reported IC_{50} of >100μM. This is likely due to the carboxyl group at the 6-anilino substitution, which when ionised would make Purvalanol B more cell impermeable and thus prevent it from reaching efficacious intracellular

concentrations (Villerbu et al., 2002). Protein crystallography studies have shown that the 6-anilino carboxyl group is not involved in interactions between Purvalanol B and the ATP binding pocket of a target kinase (Holton et al., 2003). This means that the group can be chemically modified, for example by adding a fluorophore or a different functional group, potentially altering the membrane permeability of the compound. Moreover, crystallographic information suggests that modification of the carboxyl group will not disrupt interactions between Purvalanol B and a target protein, making this group a useful handle to study the effects of the parent compound on cell biology.

The first use of modifications of the carboxyl group in Purvalanol B is reported in an early study by Knockaert *et al* (2000), who used the 6-anilino carboxyl group to immobilise the compound on agarose beads. These beads were then incubated with soluble cell lysates to capture the intracellular targets of Purvalanol B in various cell types, including the parasitic protozoa *P. falciparum, Toxoplasma gondii and Leishmania mexicana* (Knockaert et al., 2000). Interestingly, the most common target found to bind to Purvalanol B beads in these parasites was casein kinase 1 (CK1), not the CDKs observed in mammalian cells. Furthermore, Purvalanol-CK1 interactions were demonstrated to be rather specific, since CK1 binding was absent in samples incubated with a methylated Purvalanol B analogue which does not bind PKs (Knockaert et al., 2000), suggesting that CK1 is a biologically relevant target of this compound. It has also been shown that Purvalanol B kills *P. falciparum* parasites at low micromolar concentrations in a growth inhibition assay (Harmse et al., 2001) and directly inhibits purified PfCK1 protein (Le Roch, unpublished). The cellular localisation of the essential parasite kinase PfCK1 during the asexual blood stages has recently been established (Dorin-Semblat, 2015) revealing that a significant population of the enzyme is associated with RBC membranes during ring and trophozoite stages, suggesting the possibility that the cell-

impermeable Purvalanol B may inhibit *P. falciparum* through an extracellular mechanism of action, possibly through inhibition of RBC membrane-associated PfCK1. The implications of these observations are significant, since an antimalarial agent able to kill parasites without the need to enter cells would have greatly reduced toxicity linked to host protein inhibition, and it would not be subject to drug resistance mechanisms dependent on efflux pumps.

In this study, we have used genetic and biochemical methods to explore whether Purvalanol B kills parasites through and extracellular mechanism of action, and to determine whether PfCK1 is the most sensitive target of Purvalanol B in *P. falciparum*.

5.2. Results

5.2.1. *P. falciparum* parasites are sensitive to Purvalanol B and its analogues

As a first step to investigating the involvement PfCK1 in the anti-malarial activity of Purvalanol B, we wanted to measure the concentration of Purvalanol B and analogues required to inhibit parasite growth by 50% (IC_{50}), for use in subsequent experiments. Parasites were incubated with 2-fold dilutions of MIPS-0008408 (Purvalanol B), MIPS-0010345 (methyl Purvalanol B) or their fluorescent analogues MIPS-0010325 (dansylated Purvalanol B) and MIPS-0010419 (dansylated methyl Purvalanol B) for 72hrs. Samples were freeze-thawed and DNA content at that time was measured with the intercalating dye SYBR Gold, as a proxy for parasite numbers.

The two dansylated derivatives were synthesised to allow comparisons of inhibitor concentration inside and outside cells by fluorescence microscopy. The set of Purvalanol B compounds used in this study displayed a wide range of inhibitory activities against *P. falciparum* (Figure 5.1). Unexpectedly, MIPS-0010345, which does not inhibit PKs in biochemical assays (Knockaert et al., 2000), displayed an IC_{50} value of 12.7uM, comparable to the inhibitory levels obtained with the parent compound MIPS-0008408 (IC_{50} = 18.3uM). Dansylation of both Purvalanol B (MIPS-0010419) and methyl Purvalanol B (MIPS-0010325) resulted in improved inhibitory potency against parasites (IC_{50}; 2.3uM and 4.4uM respectively). IC_{50} values obtained with the dansyl derivatives evidenced comparable inhibitory potency between methylated and non-methylated compounds, consistent with observations made with the non-dansylated inhibitors. At face value, this indicated that Purvalanol B might be killing *P. falciparum* parasites through a kinase-independent mechanism, whilst dansylation increased antimalarial activity, possibly through an increase in

hydrophobicity, since although MIPS-0010419 retains a carboxylate net negative charge at physiological pH, ClogP (logarithm of calculated octanol/water partition coefficient) increased by at least one unit upon dansylation. It is unclear at present if increased hydrophobicity affects target(s) engagement, cell permeability or both.

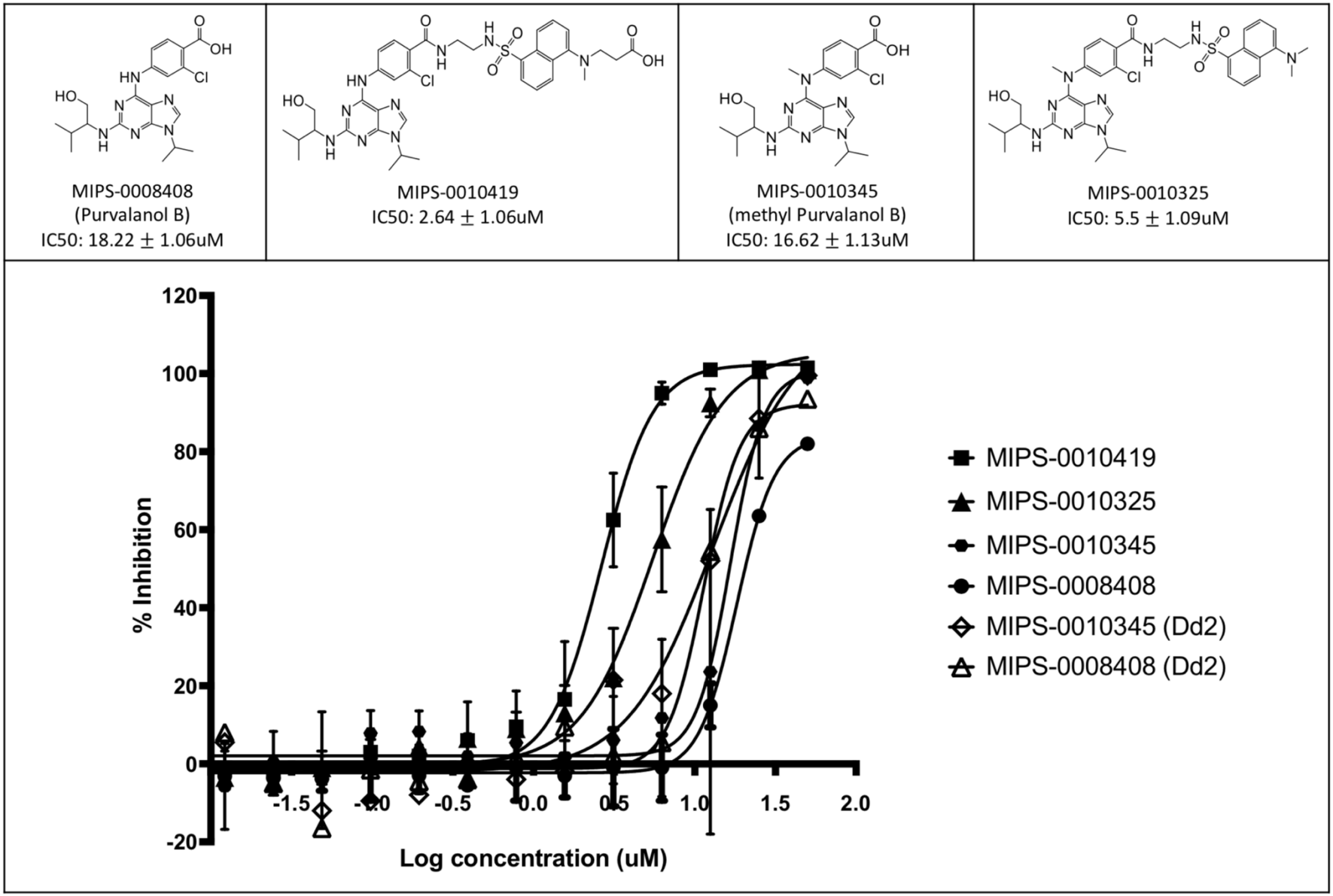
MIPS-0008408
(Purvalanol B)
IC50: 18.22 ± 1.06uM
MIPS-0010419
IC50: 2.64 ± 1.06uM
MIPS-0010345
(methyl Purvalanol B)
IC50: 16.62 ± 1.13uM
MIPS-0010325
IC50: 5.5 ± 1.09uM
% Inhibition
Log concentration (uM)
MIPS-0010419
MIPS-0010325
MIPS-0010345
MIPS-0008408
MIPS-0010345 (Dd2)
MIPS-0008408 (Dd2)

Figure 5.1. Dose-response inhibition curves of Purvalanol B and its analogues. Asynchronous wild-type cultures (200ul) were plated in 96 well format at a parasitaemia of 0.25% and haematocrit of 2% and incubated in the presence of two-fold serial dilutions of MIPS-0008408, MIPS-0010419, MIPS-0010345 or MIPS-0010325 for a 72hr period. Each point on the curve represents a single drug dilution and denotes the % inhibition of parasite growth relative to a DMSO control, displaying the mean ± SD of triplicate samples. Dose-response curves and IC50 values were obtained with Graphpad Prism 7 using non-linear regression. The structure of each inhibitor tested is represented above.

5.2.2. Purvalanol B is not cell impermeable in parasite-infected cells

Since Purvalanol B is described to be cell impermeable (Ringer et al., 2010), fluorescence microscopy was used to determine if early blood stage parasite cultures incubated with dansylated Purvalanol B (MIPS-0010419) displayed fluorescence predominantly outside RBCs, as expected. Or even if there was a visible accumulation of inhibitor on a putative target at the iRBC membrane.

Ring stage parasites were incubated with 10x the IC_{50} concentration of MIPS-0010419 (23uM final concentration) for 4hrs and mounted onto a glass slide as a thin blood smear (see Chapter 2.6.1). A strong signal was observed within the intracellular parasite and not inside RBCs or on the iRBC membrane (Top panel, Figure 5.2), indicating that dansylated Purvalanol B enters infected cells. This was unforeseen, since MIPS-0010419 contains a free carboxyl group attached to the 6-anilino dansyl substitution (Figure 5.1), ostensibly mimicking the impermeable properties of the parental Purvalanol B compound. The absence of detectable fluorescence in the surrounding uRBCs indicates that compound accumulation is specific to parasitised cells.

Next, we performed a similar cellular imaging of ring stage parasites treated with the dansylated analogue of methyl Purvalanol B (MIPS-0010325), to examine whether compound accumulation is related to kinase inhibition. Since methylation of Purvalanol B purportedly abolishes interactions with its target protein kinases (Knockaert et al., 2000), less compound should be observed inside parasites if sensitive members of this enzyme class are involved in its accumulation. Cells were incubated with MIPS-0010325 using the experimental conditions described above. We detected a fluorescence signal in the parasite of iRBCs (bottom panel, Figure 5.2), similar to what was observed with the non-methylated dansyl derivative

MIPS-0010419. Collectively, the selective accumulation of both dansylated Purvalanol B analogues in iRBCs indicates that compound import is due to a parasite-induced permeability mechanism and probably not to interactions with protein kinases.

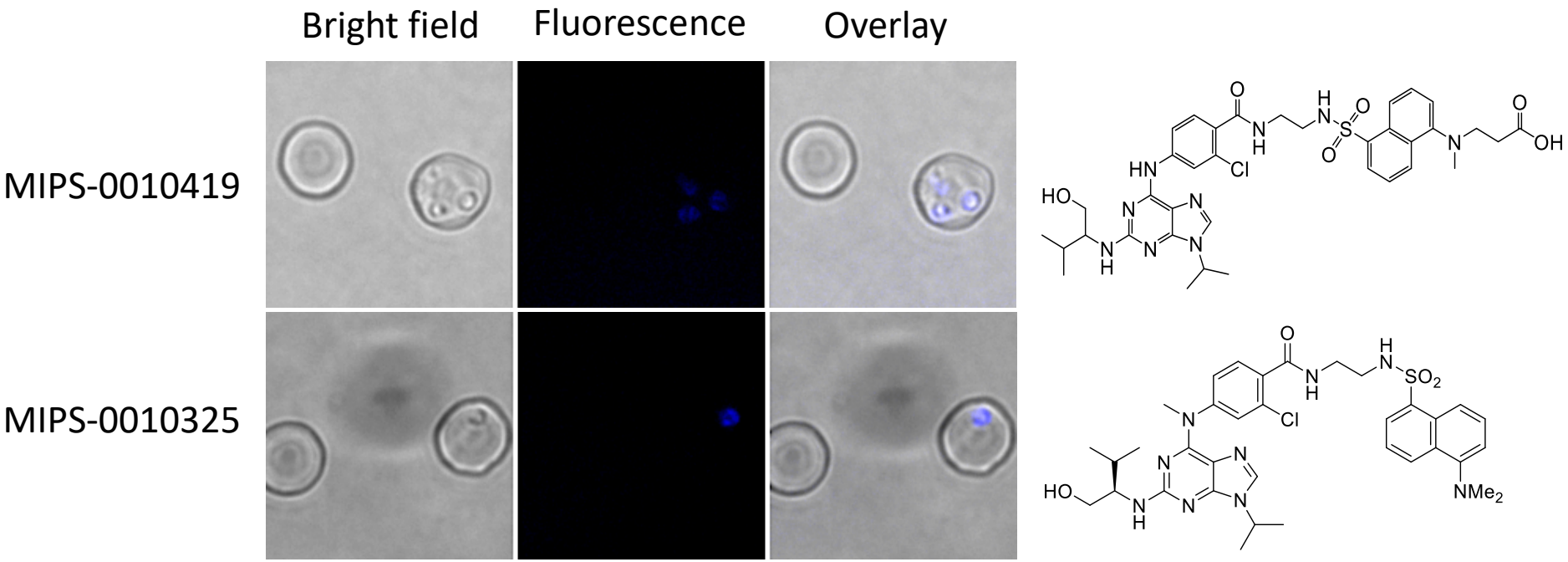

Figure 5.2. Imaging of Purvalanol B cellular localisation. Wild-type 3D7 parasite cultures were incubated with either MIPS-0010419 (top) or MIPS-0010325 (bottom) at 10x IC_{50} concentrations for 4hrs. Thin blood smears on glass slides were prepared and cells imaged using an Olympus BX51 microscope to visualise compound localisation.

5.2.3. Purvalanol B does not select for resistant *P. falciparum* parasites *in vitro*

We performed single-step selection experiment for spontaneous drug resistant parasites, in an attempt to identify the most sensitive intracellular target of Purvalanol B in *P. falciparum*. Successfully used previously to identify the intracellular targets of a number of antimalarial inhibitors (our group's unpublished observations and those reviewed in (Nzila and Mwai, 2010)), this method involves the continuous culturing of parasites in the presence of inhibitor at a concentration that inhibits at least 90% of the growth of sensitive parasites. If a resistant cell line emerges, the genome of the resistant parasites is then analysed by whole genome DNA sequencing to identify any mutations linked to drug resistance.

We cultured $2x10^8$ wild type 3D7 clonal parasites in the presence of inhibitor at 10x the IC_{50}. In parallel, we also selected for resistance in the multidrug resistant line Dd2, as it is suggested that some parasite lines exhibiting multidrug resistance can develop resistance to additional compounds at a faster rate and be more prone to genetic mutation than common laboratory drug-sensitive cell lines (Nzila and Mwai, 2010, Rathod et al., 1997). Using this method, our group had successfully obtained resistant mutants to another kinase inhibitor within approximate three months of continuous selection pressure (Morahan, personal communication). It was for this operatonal reason above that both 3D7 and Dd2 cultures were maintained under Purvalanol B pressure for three months. Following our attempts however, neither parasite line gave rise to a resistant population. The unsuccessful selection attempt of parasites with significant resistance and the absence of potency differences between the parent drug and its theoretically inactive derivative, strongly suggest that Purvalanol B has multiple targets in *P. falciparum*.

5.2.4. Homology modelling & site-directed mutagenesis of PfCK1

5.2.4.1. Bioinformatic analysis

PfCK1 is one of the most overrepresented parasite proteins among binders of immobilised Purvalanol B in a published pull-down assay (Knockaert et al., 2000), indicating a possible role for this essential kinase in the lethal activity of this compound against *P. falciparum*. The aim of this section's work was to investigate if and how PfCK1 contributes to the antiplasmodial activity of Purvalanol B. To this end, we aimed to replace amino acids in the PfCK1 ATP-binding domain with non-synonymous substitutions that could abrogate Purvalanol B binding while maintaining sufficient affinity for ATP, thus resulting in an active yet hopefully Purvalanol B-resistant kinase. This process is hindered, however, by the absence of a solved X-ray structure for PfCK1. To overcome this issue, we performed bioinformatic analysis to identify the closest homolog of parasite CK1 with a solved 3D structure in the ATP-bound conformation, which was then used to generate a three-dimensional homology model for PfCK1.

The kinase domain of PfCK1 closer resembles those of several human CK1 isoforms more than other model eukaryotes (Chapter 1, Figure 1.4) so the protein sequences of PfCK1 and the six human orthologues were obtained from PlasmoDB (PF3D7_1136500) and the UniProt database, to be analysed by CLUSTAL Omega and Phylogeny (www.phylogeny.fr). All human CK1 orthologues aligned to PfCK1 with a high degree of similarity (Figure 5.3A), consistent with conservation of this kinase family across eukaryotes. The gamma isoforms vary from other CK1 isoforms by a large amino acid insertion in the N-terminus, whereas CK1δ and CK1ε contain a longer C-terminal domain, likely a result of adaption to specific signalling pathways. Phylogenetic analysis of the kinase domains (Figure 5.3B) evidenced the similarity of the CK1γ isoforms which cluster together on the same branch (bootstrap = 1), whereas CK1δ and CK1ε cluster together separately (bootstrap = 0.97). In contrast, CK1α represents a separate

group that stems from the common ancestor of CK1δ and CK1ε. Similarly, PfCK1 is placed in its own distinct group and appears to stem from the common ancestor of the CK1δ, ε and α isoforms (a compelling bootstrap value of 1), indicating that PfCK1 is related to these latter isoforms. We next performed a BLASTP analysis to identify which of the human orthologues would best represent the structure of PfCK1. As expected, several human CK1 sequences aligned significantly with PfCK1 (the top five hits are shown in Table 5.1), but the highest score was obtained for CK1δ (E score of $2e^{-160}$, 69% identity), which was selected for homology modelling.

Fold and Function Assignment (FFAS) analysis was performed for PfCK1 and CK1δ to gain a better understanding of secondary structure formation. Figure 5.4 depicts an N-terminal catalytic region rich in beta-sheets, whilst the C-terminal domain has abundant alpha-helices in both species, consistent with the bi-lobal shape characteristics of PKs. Based on these observations and the analysis performed above, we selected CK1δ as a scaffold to build a reasonably predictive structure of PfCK1 by homology modelling.

A.

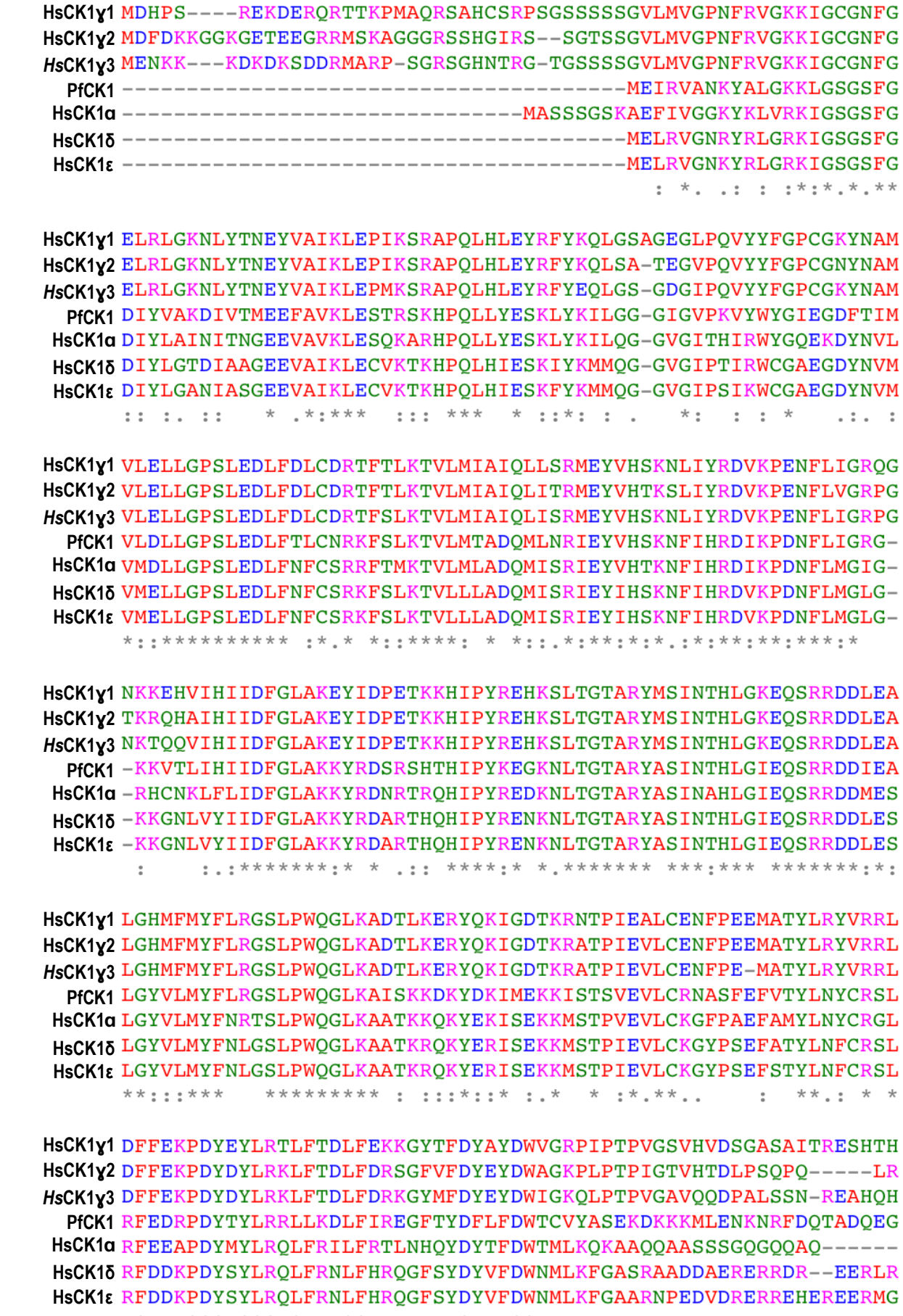
HsCK1γ1 MDHPS----REKDERQRTTKPMAQRSAHCSRPSGSSSSSGVLMVGPNFRVGKKIGCGNFG
HsCK1γ2 MDFDKKGGKGETEEGRRMSKAGGGRSSHGIRS--SGTSSGVLMVGPNFRVGKKIGCGNFG
HsCK1γ3 MENKK---KDKDKSDDRMARP-SGRSGHNTRG-TGSSSSGVLMVGPNFRVGKKIGCGNFG
PfCK1 ----------MEIRVANKYALGKKLGSGSFG
HsCK1α ----------MASSSGSKAEFIVGGKYKLVRKIGSGSFG
HsCK1δ ----------MELRVGNRYRLGRKIGSGSFG
HsCK1ε ----------MELRVGNKYRLGRKIGSGSFG
HsCK1γ1 ELRLGKNLYTNEYVAIKLEPIKSRAPQLHLEYRFYKQLGSAGEGLPQVYYFGPCGKYNAM
HsCK1γ2 ELRLGKNLYTNEYVAIKLEPIKSRAPQLHLEYRFYKQLSA-TEGVPQVYYFGPCGNYNAM
HsCK1γ3 ELRLGKNLYTNEYVAIKLEPMKSRAPQLHLEYRFYEQLGS-GDGIPQVYYFGPCGKYNAM
PfCK1 DIYVAKDIVTMEEFAVKLESTRSKHPQLLYESKLYKILGG-GIGVPKVYWYGIEGDFTIM
HsCK1α DIYLAINITNGEEVAVKLESQKARHPQLLYESKLYKILQG-GVGITHIRWYGQEKDYNVL
HsCK1δ DIYLGTDIAAGEEVAIKLECVKTKHPQLHIESKIYKMMQG-GVGIPTIRWCGAEGDYNVM
HsCK1ε DIYLGANIASGEEVAIKLECVKTKHPQLHIESKFYKMMQG-GVGIPSIKWCGAEGDYNVM
HsCK1γ1 VLELLGPSLEDLFDLCDRTFTLKTVLMIAIQLLSRMEYVHSKNLIYRDVKPENFLIGRQG
HsCK1γ2 VLELLGPSLEDLFDLCDRTFTLKTVLMIAIQLITRMEYVHTKSLIYRDVKPENFLVGRPG
HsCK1γ3 VLELLGPSLEDLFDLCDRTFSLKTVLMIAIQLISRMEYVHSKNLIYRDVKPENFLIGRPG
PfCK1 VLDLLGPSLEDLFTLCNRKFSLKTVLMTADQMLNRIEYVHSKNFIHRDIKPDNFLIGRG-
HsCK1α VMDLLGPSLEDLFNFCSRRFTMKTVLMLADQMISRIEYVHTKNFIHRDIKPDNFLMGIG-
HsCK1δ VMELLGPSLEDLFNFCSRKFSLKTVLLLADQMISRIEYIHSKNFIHRDVKPDNFLMGLG-
HsCK1ε VMELLGPSLEDLFNFCSRKFSLKTVLLLADQMISRIEYIHSKNFIHRDVKPDNFLMGLG-
HsCK1γ1 NKKEHVIHIIDFGLAKEYIDPETKKHIPYREHKSLTGTARYMSINTHLGKEQSRRDDLEA
HsCK1γ2 TKRQHAIHIIDFGLAKEYIDPETKKHIPYREHKSLTGTARYMSINTHLGKEQSRRDDLEA
HsCK1γ3 NKTQQVIHIIDFGLAKEYIDPETKKHIPYREHKSLTGTARYMSINTHLGKEQSRRDDLEA
PfCK1 -KKVTLIHIIDFGLAKKYRDSRSHTHIPYKEGKNLTGTARYASINTHLGIEQSRRDDIEA
HsCK1α -RHCNKLFLIDFGLAKKYRDNRTRQHIPYREDKNLTGTARYASINAHLGIEQSRRDDMES
HsCK1δ -KKGNLVYIIDFGLAKKYRDARTHQHIPYRENKNLTGTARYASINTHLGIEQSRRDDLES
HsCK1ε -KKGNLVYIIDFGLAKKYRDARTHQHIPYRENKNLTGTARYASINTHLGIEQSRRDDLES
HsCK1γ1 LGHMFMYFLRGSLPWQGLKADTLKERYQKIGDTKRNTPIEALCENFPEEMATYLRYVRRL
HsCK1γ2 LGHMFMYFLRGSLPWQGLKADTLKERYQKIGDTKRATPIEVLCENFPEEMATYLRYVRRL
HsCK1γ3 LGHMFMYFLRGSLPWQGLKADTLKERYQKIGDTKRATPIEVLCENFPE-MATYLRYVRRL
PfCK1 LGYVLMYFLRGSLPWQGLKAISKKDKYDKIMEKKISTSVEVLCRNASFEFVTYLNYCRSL
HsCK1α LGYVLMYFNRTSLPWQGLKAATKKQKYEKISEKKMSTPVEVLCKGFPAEFAMYLNYCRGL
HsCK1δ LGYVLMYFNLGSLPWQGLKAATKRQKYERISEKKMSTPIEVLCKGYPSEFATYLNFCRSL
HsCK1ε LGYVLMYFNLGSLPWQGLKAATKRQKYERISEKKMSTPIEVLCKGYPSEFSTYLNFCRSL
HsCK1γ1 DFFEKPDYEYLRTLFTDLFEKKGYTFDYAYDWVGRPIPTPVGSVHVDSGASAITRESHTH
HsCK1γ2 DFFEKPDYDYLRKLFTDLFDRSGFVFDYEYDWAGKPLPTPIGTVHTDLPSQPQ-----LR
HsCK1γ3 DFFEKPDYDYLRKLFTDLFDRKGYMFDYEYDWIGKQLPTPVGAVQQDPALSSN-REAHQH
PfCK1 RFEDRPDYTYLRRLLKDLFIREGFTYDFLFDWTCVYASEKDKKKMLENKNRFDQTADQEG
HsCK1α RFEEAPDYMYLRQLFRILFRTLNHQYDYTFDWTMLKQKAAQQAASSSGQGQQAQ------
HsCK1δ RFDDKPDYSYLRQLFRNLFHRQGFSYDYVFDWNMLKFGASRAADDAERERRDR--EERLR
HsCK1ε RFDDKPDYSYLRQLFRNLFHRQGFSYDYVFDWNMLKFGAARNPEDVDRERREHEREERMG
N-terminal domain
C-terminal domain

```
HsCK1ɣ  ---RDRPSQQQPLRNQSLRTVT---A--EHYDVNN-------------------------
HsCK1ɣ  ---DKTQPH---SKNQALNSTN---G--ELNADDPTAGHSNAPITAPAEVEVADETK---
HsCK1ɣ  ---RDKMQQ---SKNQVVSSTN---G--ELNTDDPTAGRSNAPITAPTEVEVMDETNCQK
PfCK1   RDQRNN-----------------------------------------------------
HsCK1α  ----------TPTGKQTDKSKSNMKGF-------------------------------
HsCK1δ  -HSRNPATRGLPSTA-----SGRLRGTQEVAPPTPLTPTSHTANTSPRPVSGME------
HsCK1ε  -QLRGSATRALPPGPPTGATANRLRSAAEPVASTPASRIQPAGNTSPRAISRVD------

HsCK1ɣ  -SAIWH-----RGRGT-----------------------------------------
HsCK1ɣ  -----CCCFFKRRKRKSLQRHK-----------------------------------
HsCK1ɣ  VLNMWCCCFFKRRKRKTIQRHK-----------------------------------
PfCK1   -----------------------------------------------------------
HsCK1α  -----------------------------------------------------------
HsCK1δ  -----------RERKVSMRLHRGAPVNISSSDLTGRQDTSRMSTSQNSIPFEHHGK
HsCK1ε  -----------RERKVSMRLHRGAPANVSSSDLTGRQEVSRIPASQTSVPFDHLGK
```

C-terminal domain

B.

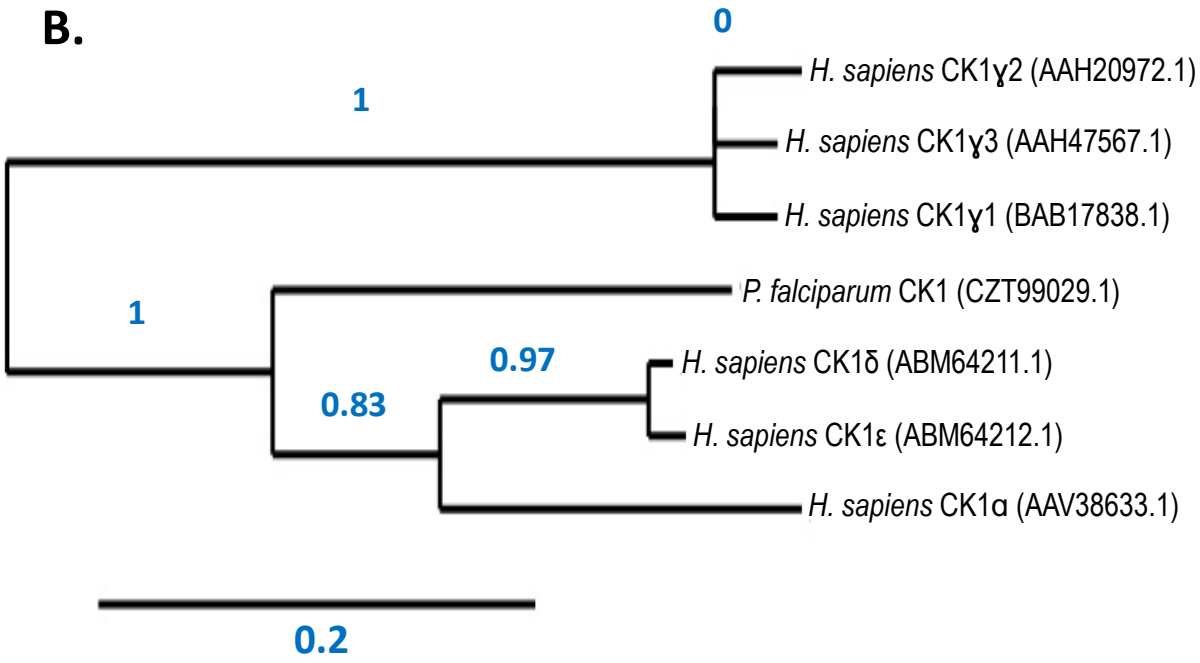

Figure 5.3. Phylogenetic analysis of Casein kinase 1. (A) The analysis involved seven amino acid sequences. The alignment was generated using the kinase domain of the six *Homo sapiens* CK1 isoforms and the single *P. falciparum* CK1. Code for amino acids; [*] = identical amino acids, [:] = conserved amino acid substitutions. (B) Phylogenetic tree generated from the sequences above. The evolutionary history was inferred using the Neighbour-joining method. Bootstrap values are inferred from 1000 replicates and represents the evolutionary history of the analysed taxa. The denoted percentage is associated with the taxa clustered in the bootstrap test and is shown next to each cluster. Analyses was performed using phylogeny.fr.

Table 5.1. Summary of BLASTP best human hits from searches with *P. falciparum* CK1 sequence. Proteins are ranked by their E value corresponding to the number of hits expected to be observed for each human protein by chance.

Human CK1	Max score	Total score	Identity	E value	Accession
Casein kinase 1, isoform delta isoform 1	456	456	69%	2e-160	NP_001884.2
Chain A, Crystal structure of Apo CK1δ	451	451	69%	2e-160	3UYS_A
Casein kinase 1 isoform epsilon	455	455	69%	6e-160	NP_001885.1
Casein kinase 1 isoform alpha, isoform 2	426	426	62%	1e-149	NP_001883.4
Casein kinase 1, alpha 1, isoform CRA_h	426	426	62%	1e-149	EAW61775.1

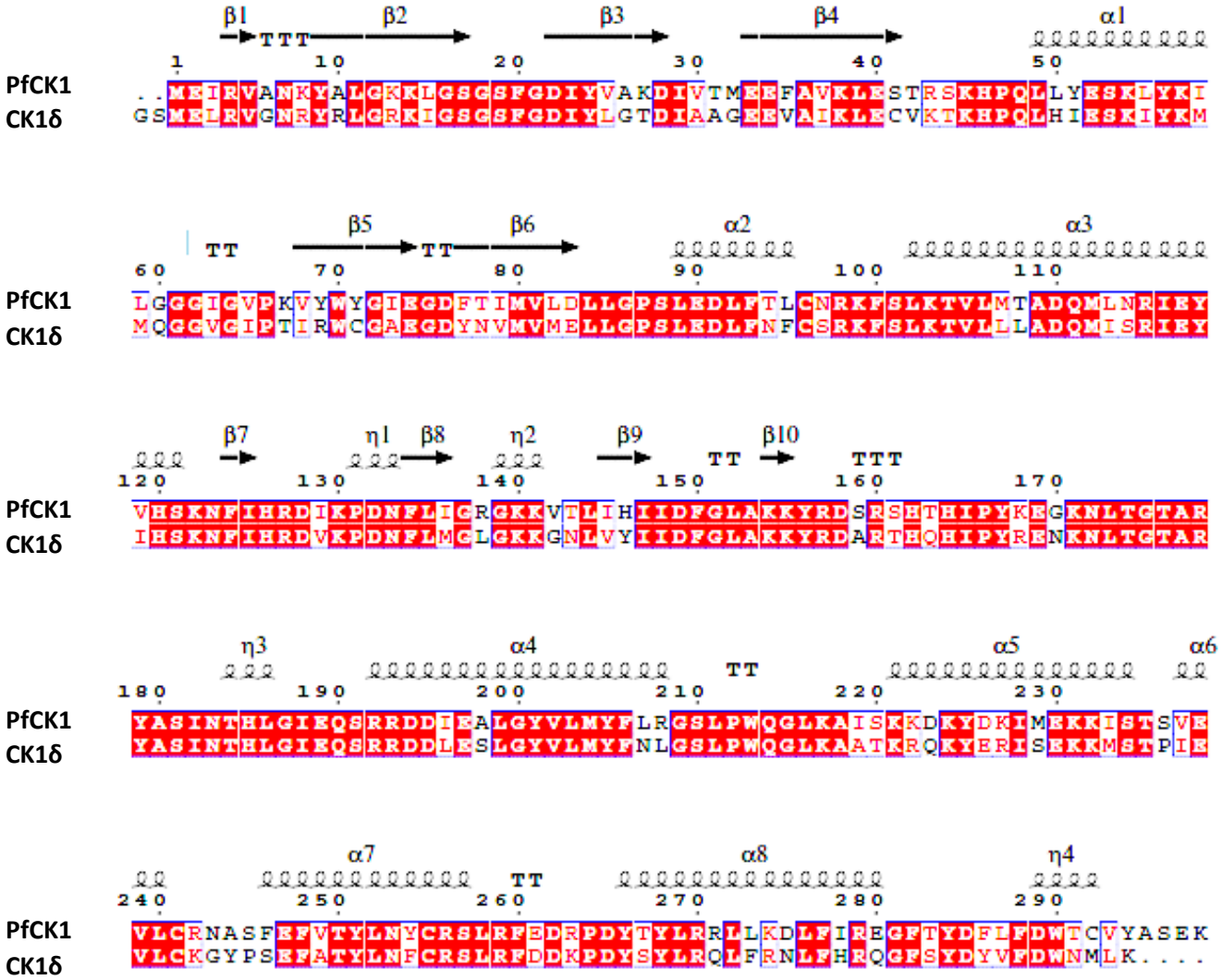

Figure 5.4. Fold and function assignment (FFAS) of human CK1d aligned with PfCK1. Human (UniProt ID; P48730) and PfCK1 (UniProt ID; Q8IHZ9) protein FASTA sequences for were obtained from the UniProt data base and aligned using Clustal Omega. Alignment files were imported to EsPript3 to display secondary structure information. Red boxes denote identical amino acids between both human and parasite CK1, red lettering signifies conserved amino acid families and black lettering represents non-conserved amino acid residues. Secondary structure information for human CK1δ is also provided which highlights regions of alpha helical and beta sheet formation.

5.2.4.2. Homology modelling of PfCK1

To construct a homology model of PfCK1 we started by locating a suitable 3D structure of CK1δ. The protein data bank (PDB) contains an X-ray structure of human CK1δ at 2.07Å resolution co-crystallised with an ATP competitive ligand pf4800567 (magenta, Figure 5.5) (PDB ID: 4HNF). Since the aim of generating a homology model was to select residues that would perturb the binding of ATP analogues when mutated, we accepted the synthetic ligand in the 4HNF structure as a proxy for the natural one, selecting targets for mutation among amino acid residues located within a 1.5 Å distance of ligand atoms. Using the modelling software Chimera (University of California, San Francisco), we imported the PfCK1 amino acid sequence and performed and internal BLASTP analysis against proteins within the PDB to retrieve the 4HNF structure, which was then selected and imported into the programme to generate a three-dimensional structure of PfCK1 (Green structure, Figure 5.5).

As expected, the predicted PfCK1 structure displayed a bi-lobal fold which is characteristic of the PK superfamily, with an N-terminal lobe consisting mostly of beta-sheets and a single prominent alpha-helix (αC), and a C-terminal lobe predominantly alpha-helical. A normalized Discrete Optimized Protein Energy (zDOPE) statistical score of -0.58 indicated that our model contained a reasonable three-dimensional structure and a GA341 model score of 1.00 indicated a >95% probability of PfCK1 really having the fold shown in Figure 5.5. Highlighted in purple, several structurally conserved catalytic subdomains are indicated in this model, including the phosphate binding loop (GXGXXG) and the DFG and HRDXXXXN domains. Key amino acid residues Lys38 and Glu52 (cyan) which are involved in ATP orientation were also present in the modelled structure. The remaining regions of PfCK1, which are structurally

dissimilar to CK1δ, are in the C-terminal tail – the domain which largely distinguishes CK1 family members and which exhibits isoform specific functions.

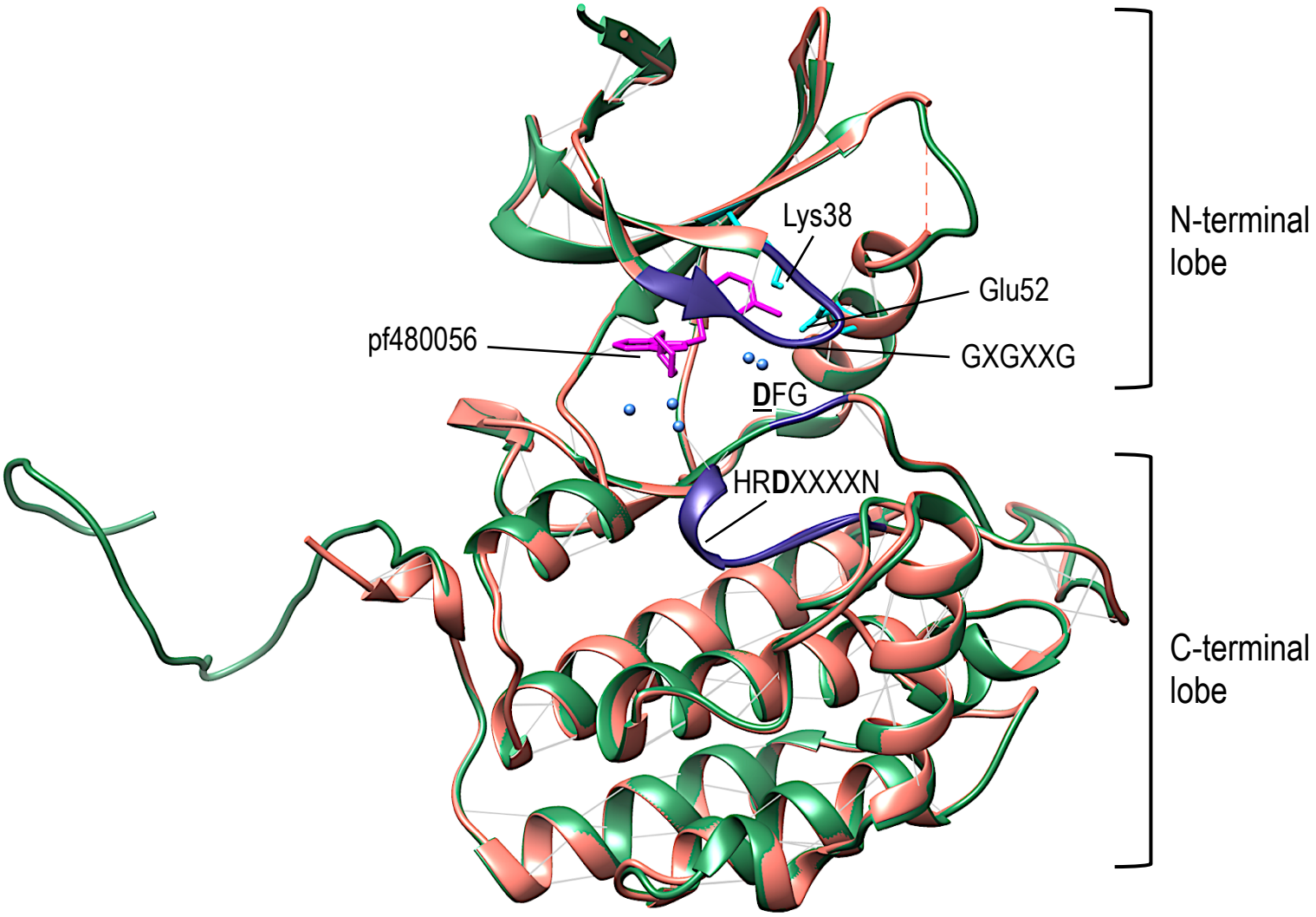

Figure 5.5. Homology modelling of *P. falciparum* CK1. A) The solved structure of human CK1δ (light red), was used as a scaffold to predict a protein structure for PfCK1 (green). Hydrogen bonds are depicted as grey and water molecules in blue. The structure of CK1 consists of a beta sheet rich N-terminal lobe and an alpha helix rich C-terminal lobe which is characteristic of the eukaryotic protein kinase superfamily. Annotated are key kinase domains GXGXXG, DFG and HRDxxxN (purple), and residues Lys38 and Glu52 (cyan) involved in ATP orientation. Shown in magenta is the inhibitor pf480056 and the blue spheres located around the inhibitor are water molecules. Model was generated using Chimera (University of California, San Fransico).

5.2.4.3. Site-directed mutagenesis

The structure of CK1δ we selected for homology modelling provided structural information about the orientation of amino acids surrounding pf480056 (magenta, Figures 5.5 & 5.6) and enabled us to select amino acids in the kinase domain of PfCK1 that we predicted may perturb the binding of Purvalanol B while retaining sufficient affinity for ATP. This latter point is relevant because a total lack of kinase function would not provide any drug resistance to the cell. Seven residues were selected (shown in yellow, Figure 5.6) within approximately 1.5Å of pf480056 and a total of eleven conservative and non-conservative substitutions were chosen to be introduced by mutagenesis, to increase the chances of generating a resistant but functional enzyme.

A 969 bp DNA fragment corresponding to the coding sequence of PfCK1 (omitting the stop codon) was cloned into the pGEX-4T3 bacterial expression vector (Figure 5.7A) between the *BamH1* and *NotI* restriction sites for subsequent recombinant protein expression. The resulting pGEX-4T3-PfCK1 construct (Figure 5.7B) was subject to 16 cycles of polymerase chain reaction (PCR) (Chapter 2, section 2.3.2) using the primers presented in Table 2.2 (Chapter 2, section 2.7) to introduce each desired mutation (Figure 5.6). Parental methylated plasmid was digested with the *DpnI* restriction endonuclease and the remaining non-methylated plasmids containing the desired mutations were transfected into DH5α *E. coli* (see section 2.4.4). DNA sequencing confirmed that A36W, M80K, M80W, S88A, S88L, D91H, D91N, L135K and I148K mutations were successfully introduced into pGEX-4T3-PfCK1 without any additional, undesired mutations.

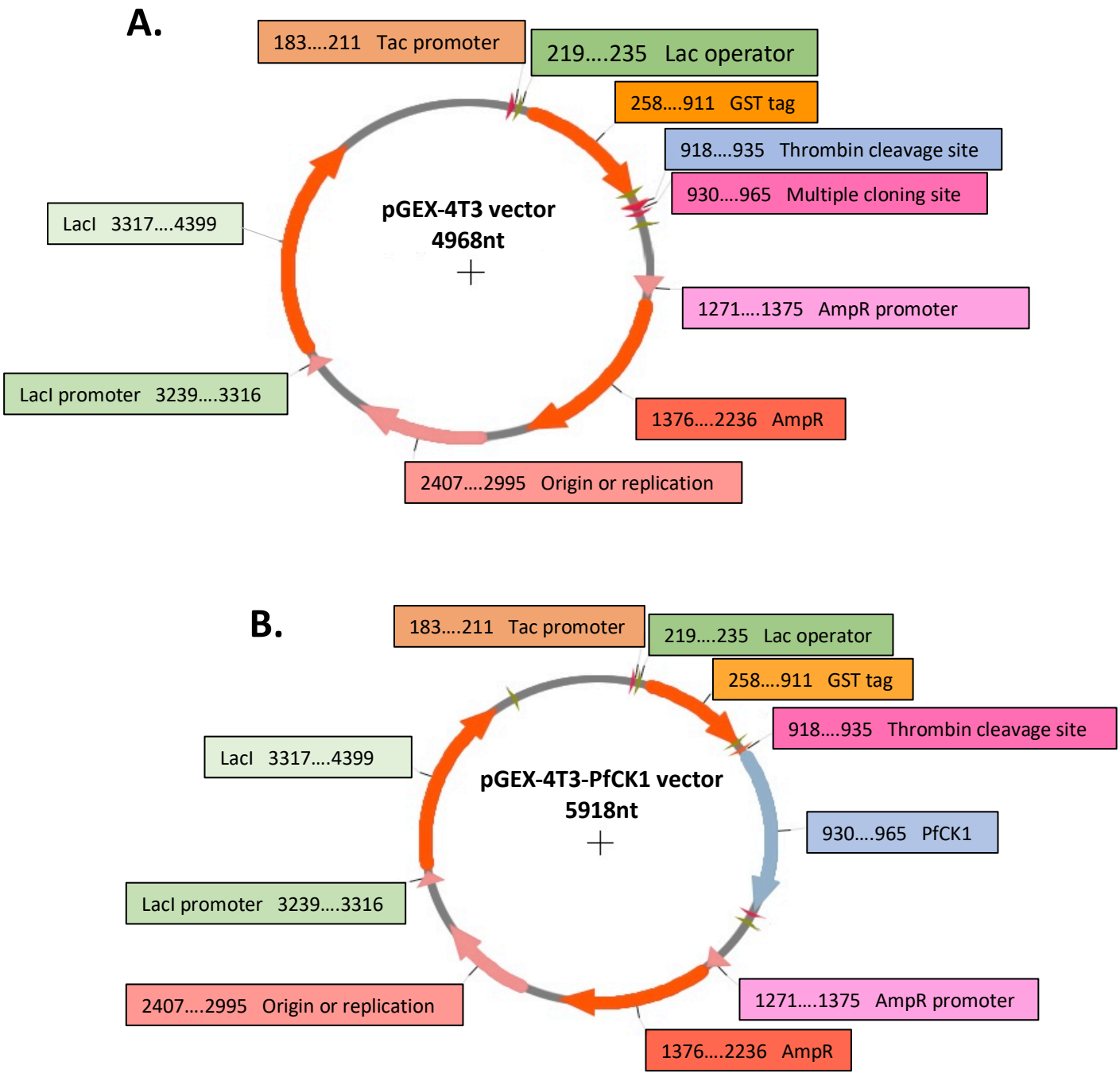

Figure 5.7. The pGEX-4T3 constructs generated in this study. The coding sequence of PfCK1 (omitting the stop codon) was cloned into the bacterial expression vector pGEX-4T3 (A) using the sites BamH1 and NotI to yield pGEX-4T3-PfCK1 (B). The resulting construct enables bacterial expression of recombinant PfCK1 tagged with GST at the C-terminus. This figure was produced using Serial Cloner version 2-6-1.

5.2.5. Expression and activity of recombinant PfCK1 protein

To test the sensitivity of each mutant PfCK1 to Purvalanol B, expression conditions of active protein were optimised using wild-type PfCK1. Following expression in *E. coli*, purification and analysis by polyacrylamide gel electrophoresis (PAGE) with Coomassie Blue staining (Figure 5.8A), a band of ~63kDa was observed in all fractions except in the non-induced bacterial lysates, corresponding to the approximate size of the PfCK1-GST chimera. The same band of ~63kDa was observed in the elution fractions which correspond to purified PfCK1 obtained by affinity purification (see section 2.5.4). Expression and purification of PfCK1 was verified by Western blot analysis using an immunopurified anti-PfCK1 antibody raised against a PfCK1 peptide (see materials and methods), which confirmed that the ~63kDa band observed in all fractions (except non-induced) was indeed PfCK1. The same purification conditions were used to purify the K38M kinase-dead mutant (data not shown) (Dorin-Semblat et al., 2015).

Wild-type PfCK1 activity in each elution fraction (purified enzyme) was verified by radiochemical methods as described previously (Dorin-Semblat et al., 2011), incubating 4ug protein aliquots with α-casein and [ɣ-^{32}P] ATP as the phosphate donor. PfCK2α and PfCK1 K38M kinase dead mutant were included as positive and negative controls, respectively. Incubation mixtures were resolved by SDS-PAGE and subsequently dry gels underwent autoradiography. A strong signal at ~30kDa was detected in the PfCK2α sample (lane 5, Figure 5.8) corresponding to phosphorylated α-casein as expected, with a secondary signal also observed at ~60kDa, consistent with kinase autophosphorylation. Both the 30kDa and 60kDa radioactive bands were absent in fractions from the K38M kinase dead mutant, but also from those generated with the wild-type PfCK1 extract, indicating that the protein expressed in

E. coli lacks kinase activity (lanes 1-4). To try to solve this issue, a parasite-based expression system was established.

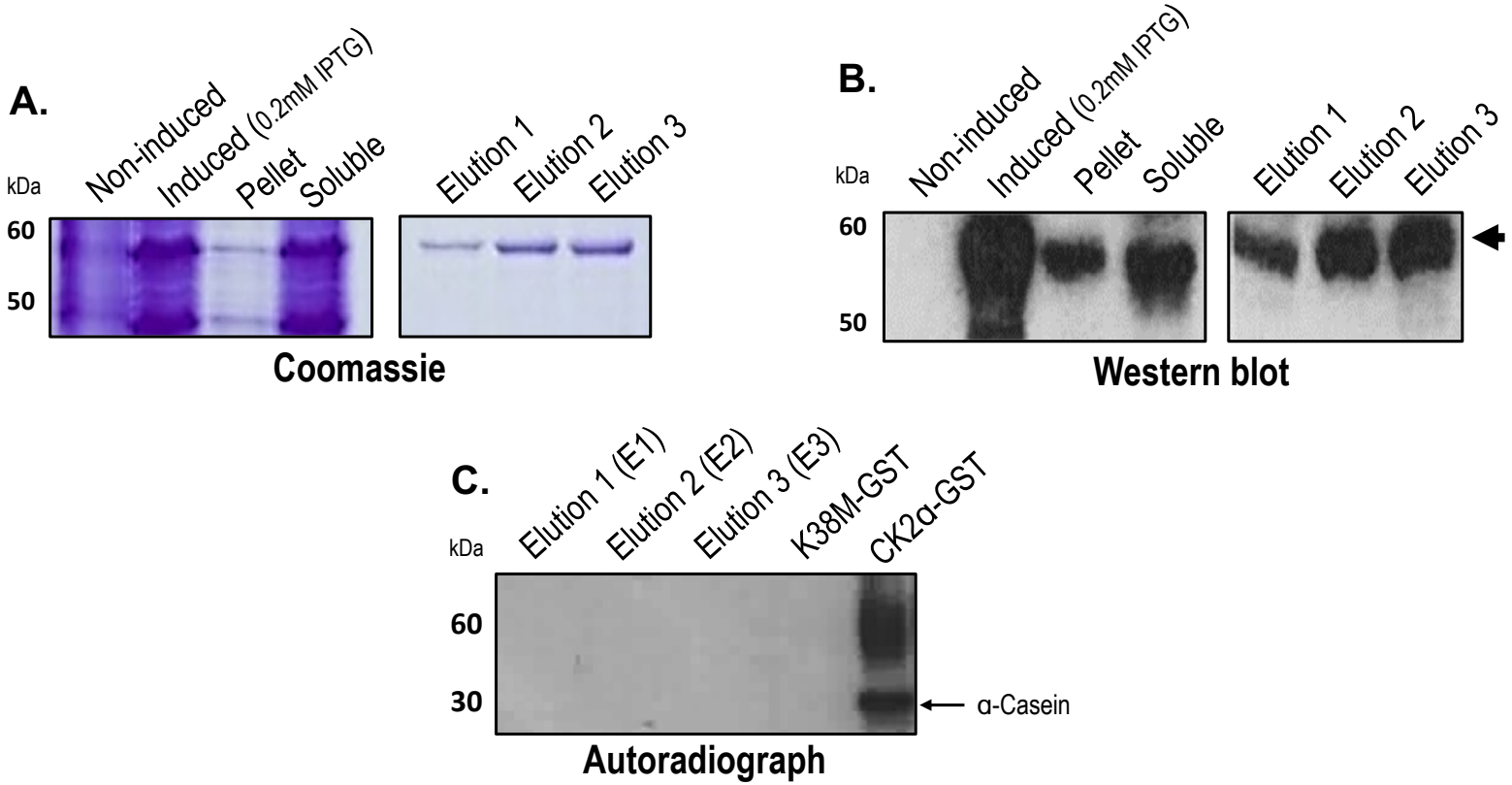

Figure 5.8. Expression and purification of recombinant *P. falciparum* CK1. A) PfCK1 was cloned and expressed in pGEX-4T3 plasmids. BL21 Gold cells containing this construct were induced for 18hrs at 20°C with 0.2M isopropyl-1-thio-β-D-galactopyranoside as described under materials and methods (uninduced lane 1 & induced lane 2). Soluble protein was extracted (lane 4) and incubated with Glutathione S-Transferase (GST) sepharose beads to purify recombinant CK1. Lane 4 corresponds to insoluble protein material and lanes 5-7 are fractions obtained from subsequent elution's followed by staining with Coomassie Blue. B) Polyclonal immunopurified anti-PfCK1 antibody was used to detect recombinant protein in each fraction. Arrow indicates full-length PfCK1-GST. C) Equal volumes of each elution fraction were assayed for activity against alpha-casein using [γ-^{32}P] ATP as the phosphate donor and analysed by SDS PAGE and autoradiography. Recombinant PfCK2α-GST and PfCK1-GST (K38M) kinase dead mutant were used as positive and negative controls respectively (lanes 4 & 5).

5.2.6. Parasite expression of recombinant PfCK1

We used the *P. falciparum* expression plasmid pGLUX (Figure 5.9A) as the vector to introduce mutant PfCK1 into wild type 3D7 parasites for episomal protein expression. This plasmid contains the human *dhfr* expression cassette which encodes resistance to the inhibitor WR99210, thus enabling positive selection of parasites that have incorporated the plasmid and allows fusion of the cloned ORFs with GFP to assist with purification and detection of cloned proteins. PfCK1 genes were cloned into the pGLUX plasmid under the control of the *P. falciparum* chloroquine resistance transporter (*Pf*crt) promoter, which drives constitutive gene expression of PfCK1 C-terminally tagged with GFP.

The 969bp fragment from each PfCK1 mutant prepared above was amplified by PCR using primers flanked by *XhoI* and *KpnI* restriction sites (see Table 2.2, Chapter 2), enabling each fragment to be inserted into pGLUX between the Pfcrt promoter and GFP (Figure 5.9B). Wild-type 3D7 parasites were transfected by electroporation (section 2.1.12) with 100-150ug of high-quality DNA ($A_{260}/A_{280} \geq 1.85$) with each of the nine pGlux-PfCK1 mutant constructs plus one wild type pGlux-PfCK1 construct. Two days post-transfection parasite cultures were incubated with 5nM of the selecting drug WR99210, which caused a loss of visually detectable parasitaemia. Twenty-one days post-transfection drug resistant parasites were observed in the transfected cultures.

To check that every transfected parasite line was expressing a GFP-tagged protein, mixed stage parasite cultures were harvested by centrifugation, lysed and immunoprecipitated with GFP Trap® agarose beads to precipitate PfCK1-GFP (see section 2.5.6.1). Protein fractions eluted from the beads were run on a 4-12% w/v SDS-polyacrylamide gel and transferred to a

nitrocellulose membrane for analysis by Western blot (see section 2.5.3). Lysates from wild-type 3D7 parasites were used as a negative control and parasites expressing PfCK1-GFP from the endogenous locus (prepared in [15]) were used as a positive control. Blots probed with anti-GFP antibody revealed a faint 63kDa signal in samples expressing PfCK1-GFP from the episome, indicating a low level of expression relative to PfCK1-GFP expressed from the endogenous locus. Wild-type lysates showed no GFP signal as expected.

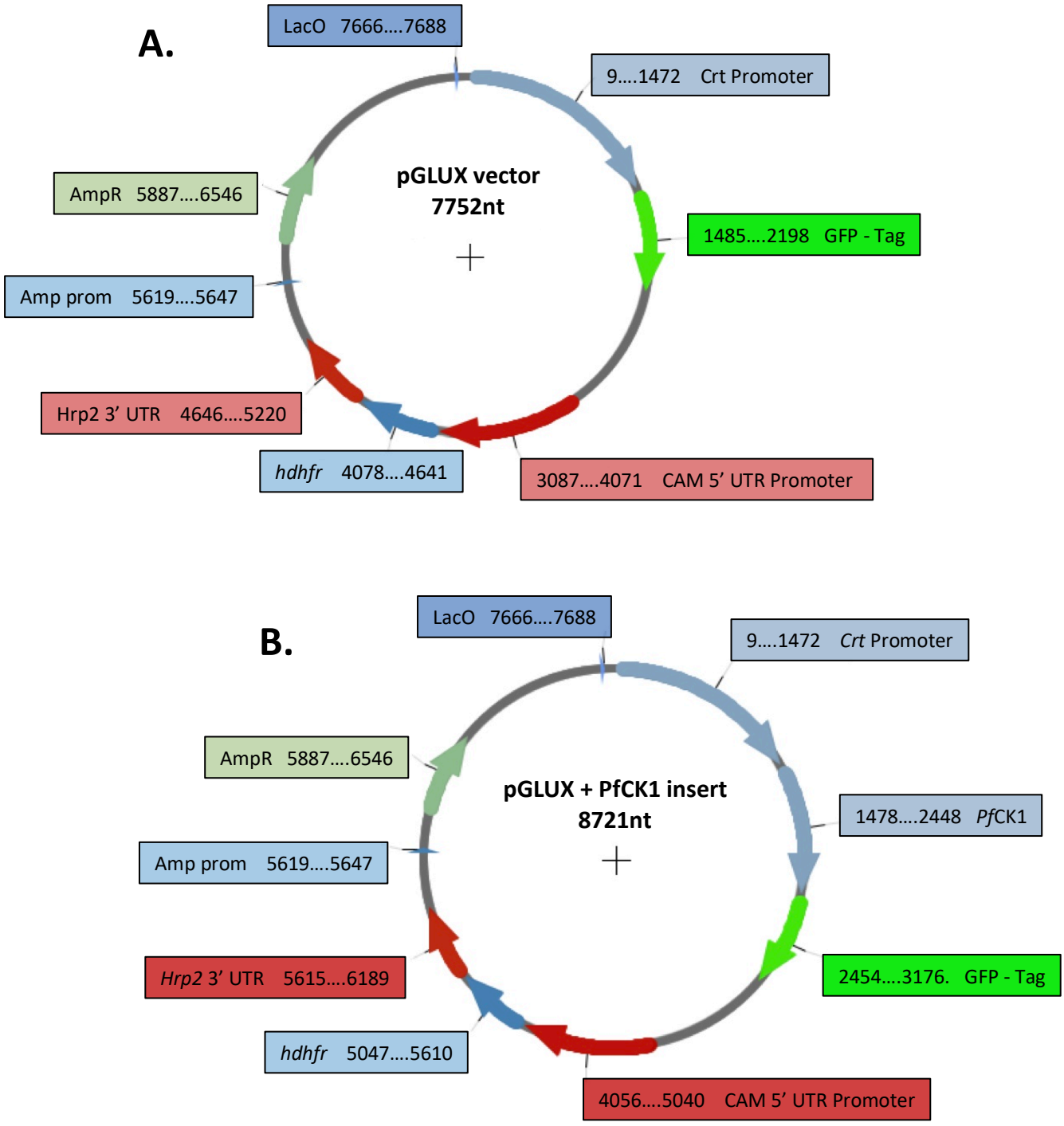

Figure 5.9. pGLUX plasmids used for parasite-based expression. The pGLUX parasite expression vector (A) was cloned with the 969bp coding fragment of PfCK1 (stop codon omitted) between the XhoI and KpnI restriction sites. Wild-type 3D7 parasites were transfected with resulting pGLUX-PfCK1 plasmids (B) containing either one of nine mutants or non-mutated PfCK1, fused to green fluorescent protein (GFP) at the C-terminus. Expression of the enzyme is driven by the P. falciparum crt (chloroquine resistance transporter) promotor. This plasmid contains the human dihydrofolate reductase (hdhfr) cassette enabling positive selection of transfected parasites with WR99210. This figure was produced using Serial Cloner version 2-6-1.

5.2.7. PfCK1 mutations do not confer resistance in growth inhibition assays

As a direct measure of sensitivity to Purvalanol B, dose-response inhibition curves were generated for each of the PfCK1 mutant parasite lines generated in this study. Parasites were incubated for 72hrs in the presence of 2-fold dilutions of MIPS-0008408 (50 – 0.008uM) as described in section 5. 2, freeze-thawed and total DNA quantity present was measured by the SYBR Gold method as a proxy for parasite numbers. Parasites expressing wild-type PfCK1-GFP from the episome showed no significant change in sensitivity to MIPS-0008408 (IC_{50}: 24.3uM) (Figure 5.10), with IC_{50} values similar to those obtained with wild type 3D7 parasites (IC_{50}: 18.3uM). Showing that the small increase in kinase expression levels afforded by the episome does not affect drug sensitivity. Unfortunately, parasite lines expressing mutant PfCK1-GFP episomically did not show increased MIPS-0008408 IC_{50} either, indicating that the mutated proteins do not confer resistance under these conditions, and therefore they cannot be used as tools to inform about a possible role of PfCK1 in Purvalanol's mode of action.

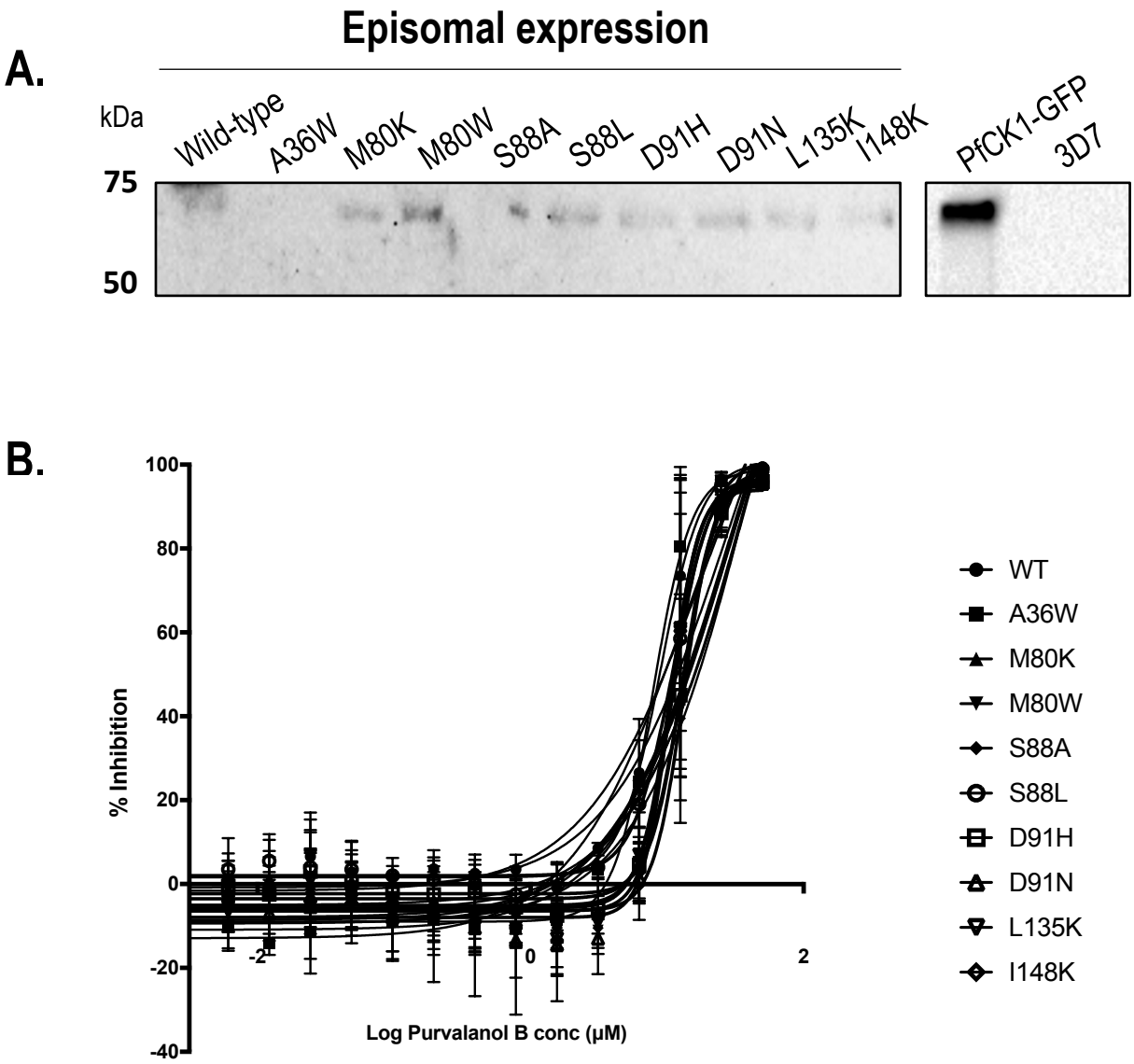

Figure 5.10. Dose-response inhibition of mutant PfCK1. Site-directed mutants of PfCK1 were sub-cloned into the P. falciparum expression vector pGLUX and transfected into wild-type 3D7 parasites. (A) PfCK1-GFP mutants expressed from the pGLUX episome immunoprecipitated with GFP Trap®. Blots are probed with anti-GFP antibody (1:2000). (B) Asynchronous parasites (200ul) were plated in 96 well format at a parasitaemia of 0.25% and haematocrit of 2% and incubated for a 72hr period in the presence of two-fold serial dilutions of MIPS-0008408. Each point represents a single drug dilution and denotes the % inhibition of parasite growth relative to a DMSO control, displaying the mean ± SD of triplicate samples. Dose-response curves and IC50 values were obtained with Graphpad Prism 7 using non-linear regression.

5.3. Discussion

5.3.1. Purvalanol B accumulates within infected red blood cells

Despite being a potent inhibitor of cyclin-dependent kinases and unlike Purvalanol A, Purvalanol B does not inhibit mammalian cells, presumably due to the presence of a carboxyl moiety on the 6-anilino substitution of the B derivative, expected to drastically reduce passive diffusion across cell membranes (Yenugonda et al., 2011). It was therefore unexpected that low micromolar concentrations of Purvalanol B were able to kill *P. falciparum in vitro* [9], suggesting that inhibition of parasite proliferation might not require cell entry.

We used live cellular imaging of ring stage parasite cultures, treated with fluorescent dansyl analogues of Purvalanol B, to determine whether these compounds localise to the exterior of the RBC membrane, as this would provide evidence for an extracellular mechanism of action. Our observations showed that dansylated Purvalanol B (MIPS-0010419) rapidly accumulates inside the parasite and not at the RBC membrane (top panel, Figure 5.2). This was also observed in parasites treated with MIPS-0010324 (bottom panel, Figure 5.2), the dansylated form of the kinase-inactive, methylated analogue of Purvalanol B (Knockaert et al., 2000). Our results also show that fluorescence is excluded from surrounding uRBCs, indicating that MIPS-0010419 and MIPS-0010325 specifically accumulate in cells infected with *P. falciparum* parasites. We hypothesise that Purvalanol B may be internalised by a mechanism inserted in the RBC membrane by *Plasmodium*, thereby giving the compounds access to intracellular targets whose inhibition contributes to parasite death. One possible transport process is internalisation via the *Plasmodium* Surface Anion Channel (PSAC) (Lisk and Desai, 2005, Gupta et al., 2018). Studies have shown that members of the *clag* multigene family, which are

considered to be responsible for the activity of PSAC, have been implicated in drug resistance (Sharma et al., 2013, Sharma et al., 2015). It could be that perhaps PSAC or another channel could mediate the import of Purvalanol B and it would be interesting to test this hypothesis by treating parasites simultaneously with fluorescent Purvalanol B analogues and PSAC inhibitors (Pain et al., 2016) and assessing whether fluorescence is excluded from iRBCs.

Alternatively, compound internalisation may have been helped by the fluorescent derivatisation of the compound, used to visualise its localisation. Other studies have shown that dansylation of Purvalanol B improves compound potency by increasing its membrane permeability (Ringer et al., 2010, Sirajuddin et al., 2012, Ringer et al., 2011). Similarly, we observed increased potency for the dansylated Purvalanol B analogues used in this study (MIPS-0010419 and MIPS-0010325, Figures 5.1) and for an additional dansylated Purvalanol B derivative not used in this study (B. Morahan, unpublished). Thus, we cannot rule out a possible influence that dansylation of Purvalanol B may have had on compound permeability. It is worth noting however, the compounds used in the published studies lacked the 6-anilino carboxyl group characteristic of Purvalanol B that we preserved in MIPS-0010419, and passive diffusion would be expected to also affect uRBC, which were never observed to fluoresce; if fluorescence can only be detected when concentrated at a specific location (in this instance within the parasite) then we would not detect fluorescence in the surrounding RBCs with the microscope used in this study. As such, more powerful microscopic methods may be required to this further.

5.3.2. Purvalanol B does not select for resistance

In a biochemical pull-down assay aimed at identifying the intracellular targets of Purvalanol B (Knockaert et al., 2000), PfCK1 was found to be the most over represented parasite kinase that interacts with the immobilised inhibitor, not the cyclin dependent kinases (CDKs) observed with mammalian cell extracts. Furthermore, it is thought that these interactions could be quite specific (Knockaert et al., 2000) thereby implicating PfCK1 as a likely physiological target of Purvalanol B in *P. falciparum*. In order to determine whether PfCK1 is the most sensitive target for this drug in the parasite, we attempted to select for cell lines resistant to Purvalanol B by performing single-step *in vitro* drug selection at 10X IC_{50} levels of the compound. *In vitro* selection is a method successfully used by our group (B. Morahan, unpublished) and by several others (reviewed in (Nzila and Mwai, 2010)) to investigate the intracellular targets of small molecular weight inhibitors.

The lack of emergence of drug resistant parasites in either 3D7 or multidrug resistant Dd2 strains, would be in better agreement with a hypothesis in which Purvalanol B targets several essential proteins with moderate potency, in agreement with the micromolar inhibition values obtained from parasite growth inhibition assays (Figure 5.1). However, a negative result in a single mutant selection experiment does not allow drawing biologically relevant conclusions. Genetic events that result in the acquisition of drug resistance *de novo* are spontaneous and are influenced by several factors including the number of circulating parasites and the number of mitotic events (Nzila and Mwai, 2010). The per-parasite resistance frequency (PRF), that is, the number of parasites in a given population of circulating parasites that will acquire a spontaneous mutation resulting in reduced sensitivity to a therapeutic is also known to vary depending on the inhibitor (White and Pongtavornpinyo,

2003, Preechapornkul et al., 2009, Rathod et al., 1997). For instance, the PFR for pyrimethamine is somewhere around 10^{11} whereas artemisinin is in the order of $10^{18} – 10^{19}$ (White and Pongtavornpinyo, 2003).

Given our findings that indicate Purvalanol B likely inhibits multiple targets, the PFR for this inhibitor will probably be quite high so it unlikely that parasite numbers used in this study were sufficient to select for resistance within the imposed timeframe. Despite using these parameters by our group to successfully obtain resistance mutations to another kinase inhibitor (Morahan, unpublished), a more appropriate experimental design for Purvalanol B resistance selection would thus need to include a larger starting parasite population. However, it should also be noted that increasing the number of parasites by orders of magnitude (for example to 10^{10} parasites) are technically challenging for an *in vitro* system. Thus, extending the duration of continuous selective pressure will also have an impact on the likelihood of selecting a spontaneous resistance mutation, particularly if sub-therapeutic or increasing levels of inhibitor are used (Korsinczky et al., 2000, Oduola et al., 1988). It would also be desirable to include a control inhibitor that is known to select for resistance mutations within a given period (Rathod et al., 1997).

We have shown in this study that parasites treated with the methylated Purvalanol B analogue (MIPS-0010345) display growth inhibition levels equivalent to those observed with the parental compound, indicating that the mechanism of action may not be entirely due to PK inhibition. After our failed attempt at selecting Purvalanol B resistant parasites, a study was published by Bullard *et al* (2015) in which they investigated the proteome of *P. falciparum* parasites treated with Purvalanol B (Bullard et al., 2015). The major findings of this study showed that components of the proteasome degradation pathway and enzymes involved in

redox homeostasis were overrepresented in Purvalanol B-treated cells, suggesting that Purvalanol B may kill parasites predominantly as a result of oxidative stress. It is well known that pharmacological inhibition of kinases results in upregulation of the proteasome degradation response (Lobbestael et al., 2016, McNaughton et al., 2016, Parr et al., 2012) and there is an established interplay between oxidative stress and protein degradation (de Paula et al., 2014, Maharjan et al., 2014, Ngo et al., 2013, Jung et al., 2014). Response to external stimuli, including those of oxidative stress, result in the triggering of various signalling cascades which recruit and activate kinases. This is well documented in humans (Burgoyne et al., 2007, Ray et al., 2012, Song et al., 2014, Paulsen et al., 2011) and in yeast (Li et al., 1998, Caterina et al., 2008) supporting a similar role for kinases in modulating redox homeostasis in *P. falciparum* and by extension an involvement of PKs in the mechanism of anti-parasitic action of Purvalanol B. It would be interesting to examine the proteome of *P. falciparum* parasites treated with the methyl Purvalanol B analogue, to see whether redox homeostasis is still affected. Since PfCK1 is described to represent the major kinase interacting with Purvalanol B, it is tempting to ascribe a role for this kinase in redox homeostasis, a hypothesis which could be experimentally tested.

5.3.3. Modelling and mutagenesis of PfCK1, and *in vitro* assessment of sensitivity to Purvalanol B

In silico modelling is a tool frequently deployed in so-called rational drug design (RDD), due its low cost and high-throughput capabilities (reviewed in (Wang et al., 2015)). While still in its infancy in malaria research, this method has gained a lot of momentum for drug R&D in various areas of cancer biology (Geetha et al., 2016, Mishra et al., 2015, Jha et al., 2017). *In silico* modelling generates a vast amount of information mined from the X-ray structures of

homologous proteins, providing ways of studying protein folding and investigating amino acid interactions and domain architecture in proteins without a solved 3D structure.

No information is available concerning the structure and features of PfCK1, and no crystal structure has been published to date. We present here the first modelled 3D structure of PfCK1 (Figure 5.5), the only member of the large eukaryotic CK1 family in *P. falciparum*. At the primary amino acid sequence level, PfCK1 shows a high degree of homology to all human CK1 isoforms (Figure 5.3A). However, the parasite kinase seems most closely related to CK1δ (70% homology in the kinase domain and 69% for whole kinase). Our superimposed PfCK1 structure illustrates very high homology (69%) and an excellent degree of fold similarity (zDOPE of -0.58/GA341 of 1.00) (Figure 5.5). Importantly, a high degree of conservation of key domain architecture obtained in our model. The C-terminal domain of CK1δ contains an insertion of 79 amino acids between position 316-342 which is heavily phosphorylated (Rivers et al., 1998, Graves and Roach, 1995, Knippschild et al., 2014). Many phospho-sites within this region are widely thought to be substrates for autophosphorylation, which generally results in kinase autoinhibition, with a complex regulation stemming from the actions of multiple protein phosphatases (PPs) and additional PKs (Eng et al., 2017, Knippschild et al., 2005, Rivers et al., 1998). Phosphatase action is thought to relieve kinase inhibition, underscoring the highly dynamic regulatory mechanisms of kinase activity. Nothing is known to date about the regulation of PfCK1 activity. The C-terminal autoinhibitory domain of human CK1 is absent in the PfCK1 structure, but modulation of activity by phosphorylation and dephosphorylation in other protein domains may still occur and could explain why PfCK1 is not expressed as an active kinase in an *E. coli* system (Figure 5.8).

CK1 enzymes are known to function as monomers. (reviewed in (Cheong and Virshup, 2011)) However an early crystallographic study suggests that CK1δ may form homodimers

(Longenecker et al., 1998). Amino acids implicated in homodimer formation are within the N-terminal catalytic domain and include Leu3, Leu11, Arg13, Lys14, Leu25, Leu39 and Tyr77 from one monomer, and Ile15, Leu25, Leu84, Asp91, Leu92, Phe95 and Leu135 from the other. Dimerization of CK1δ would likely result in a conformational change that blocks the ATP binding site, providing an additional mechanism for regulating kinase activity. Inspection of our model revealed that 86% of the amino acids involved in dimerization are either identical or conserved in PfCK1 and may hint to a similar regulatory mechanism, a hypothesis that clearly requires experimental testing. It may also be interesting to examine whether these enzymes can form heterodimers with other CK1 isoforms, as this would enable PfCK1 to redirect host CK1 activity during infection.

We utilised the PfCK1 model to identify amino acid residues that we predicted may interact with Purvalanol B, so that we could perturb these interactions through site-directed mutagenesis. In a similar approach, three-dimensional structures have been derived for a small number of other *P. falciparum* proteins using different modelling approaches, all of them producing highly conserved molecular architectures when compared to their higher eukaryotic homologues (Kumar et al., 2007, Droucheau et al., 2004, A. et al., 2003). In some instances, homology modelling has been useful in studying drug resistance in *P. falciparum* and in identifying candidate drugs for therapeutic use (Santos-Filho et al., 2001, Kumar et al., 2007), thus highlighting the potential of this method in RDD.

In this work we identified seven candidate residues potentially involved in interactions with ATP and inhibitory analogues, given the predicted 3D pose of their side chains in facing an inhibitor. These residues were mutated, and the altered proteins cloned in parasite

expression vectors for drug resistance studies. We successfully obtained transfectant parasite lines expressing these mutant variants of PfCK1-GFP. Had we observed a reproducible increase in IC_{50}, it would have been an indication that PfCK1 is the most sensitive target for Purvalanol B in *Plasmodium*, warranting a more detailed analysis of the mutated enzyme. This would have also enabled using the drug as a tool to investigate the role of PfCK1 in parasite biology and the investigation of other targets. For example, *in vitro* parasite growth inhibition assays have demonstrated that *P. falciparum* field isolates with chloroquine (CQ) IC_{50} values greater than 100nM were significantly less sensitive to piperiquine, implicating the *Pfmdr1* transporter in resistance to this artemisinin partner drug (Mungthin et al., 2017, Dhingra et al., 2017).

As it was, we found that no mutant variant of PfCK1 displayed any significant decrease in sensitivity to Purvalanol B compared to parasites expressing wild-type PfCK1-GFP from the episome (Fig 5.10B). This may have been due to the low levels of episomal expression observed for the cloned genes (Figure 5.10A). One explanation for this could be that the endogenous levels of wild type PfCK1 are greater than the levels of mutant PfCK1 expressed from the episome, as evidenced by low intensity signals detected by Western blot analysis of PfCK1-GFP mutants immunoprecipitated from parasite lysates (Figure 5.10A). A much lower abundance of mutant PfCK1 enzyme means that a significant rightward shift in Purvalanol B IC_{50} would not be observed. In follow-up work we will try to increase episome copy number by gradually increasing the concentration of the positive plasmid selection compound WR99210 and assess whether this results in a shift in the IC_{50} curve. If a rightward shift is observed, we will begin to investigate the sensitivity of each purified PfCK1-GFP enzyme to Purvalanol B.

We strongly suspect that Purvalanol B may be inhibiting multiple enzymes in *P. falciparum* and independent work in our group has recently demonstrated Purvalanol B inhibition of PfNek1 (B. Morahan, unpublished). Although PfCK1 is the most abundant interacting protein of immobilised Purvalanol B in *P. falciparum*, the protein is highly expressed throughout all stages of asexual development (Bozdech et al., 2003, Llinás et al., 2006, Dorin-Semblat et al., 2015) which means that other, perhaps more sensitive targets may have been underrepresented in the original pull-down experiments. For example, low abundancy or stage-specific proteins. This hypothesis is further strengthened by the recent use of immobilised Purvalanol B as a chemical probe for the enrichment of kinases in proteomic studies (Daub et al., Arend et al., 2017, Duncan et al., 2012), capable of capturing a large fraction of the kinome and evidencing a broad-spectrum of possible lethal targets. Although our original hypotheses of an extracellularly-exposed lethal target for Purvalanol B could not be tested, due to the unexpected intracellular accumulation of the available derivatives, the molecular tools developed for PfCK1 study will be used to investigate the function of this intriguing essential protein kinase, whose cellular location seems to change during parasite development (Dorin-Semblat et al., 2015). Purvalanol's anti-plasmodial activity also retains its translational interest, given the reduced number of new molecular entities being pursued as antimalarials. Future experiments may include using comparative proteomics to investigate PfCK1 immunoprecipitations from Purvalanol B treated and untreated parasites, to distinguish over or underrepresented pathways and interactors. Such results may come full circle and finally provide evidence for contributions by PfCK1 to the mechanism of antimalarial action of Purvalanol B.

In conclusion, we have demonstrated that fluorescent analogues of Purvalanol B accumulate within the parasite of iRBCs, showing the compound likely access multiple intracellular targets to effect parasite death. We have also generated the first known modelled structure of PfCK1, from which we constructed nine PfCK1 mutants and obtained transgenic parasite lines for each, thus providing useful tools to study the biology of PfCK1 in future experiments.

Chapter 6

General discussion

Plasmodium falciparum infection is still a significant burden on the public health systems of many developing countries, with hundreds of thousands of deaths occurring each year and high morbidity (Alonso and Tanner, 2013). Made worse by the emergence of drug resistance to the last front-line antimalarial (Cerqueira et al., 2017), mortality rates will climb if resistance spreads to other endemic regions like sub-Saharan Africa and therefore new drugs are greatly needed. Future drugs should have distinct chemical structures and act through previously unused targets, so as to circumvent efflux pumps and target-based resistance mechanisms. PKs are not currently targeted by any antimicrobial agents in use. Thus, the exploitation of PKs as potential therapeutic targets for the treatment of parasitic disease is a promising avenue of drug discovery that can piggy back on the success of targeting PKs in other human diseases, most notably cancer (Thrane et al., 2014, Friese-Hamim et al., 2017, Janjigian et al., 2014). Crucial to the establishment of PKs as useful drug targets in *P. falciparum* is understanding the mechanisms that underpin kinase-controlled cellular processes, like sexual commitment, metabolism, protein trafficking, lifecycle propagation and transmission, such that we can understand the therapeutic potential of hindering these processes in the parasite (Sinden et al., 2012, Alonso et al., 2011). Successful malaria eradication requires current gaps in our understanding of parasite biology to be addressed, as they are limiting the successful design of effective therapies such as drugs or vaccines for treatment and disease prevention.

In this thesis, we have focussed on increasing our understanding of the cellular functions of the essential *P. falciparum* PK PfCK1, primed by its description as the probable target of the kinase inhibitor Purvalanol B (Knockaert et al., 2000, Dorin-Semblat et al., 2015). It is well understood that in higher eukaryotes and other model organisms, CK1 proteins perform a plethora of biological tasks and

have been implicated in pathogenesis (Foldynová-Trantírková et al., 2010, Xu et al., 2005b), making CK1 an important therapeutic target. We have formulated several hypotheses concerning the function of PfCK1 during infection of RBCs, based on the known functions of CK1 in model eukaryotes - a concept referred to as functional homology.

Manipulation of the host response by *P. falciparum* is paramount to its survival. Results obtained in chapter 3 strongly suggest that PfCK1 functions in RBCs as a complex with host proteins GAPVD1 and SNX22 (Figures 3.1 and 3.5), two key players in protein trafficking pathways that may link PfCK1 to cellular trafficking and secretion. GAPVD1 is a key player in the regulation of the GLUT4 glucose receptor translocation to the plasma membrane in response to insulin stimulation in adipocytes (Lodhi et al., 2007) and it is required for the ubiquitination and degradation of EGFR in other human cell types (Su et al., 2007). SNX proteins are involved in endosomal trafficking pathways, largely by modulating retrograde protein transport from endosomes to the TGN (Teasdale and Collins, 2012). All SNX proteins contain a Phox-homology (PX) domain that regulates binding to PtdIns3P. SNX3, probably one of the best understood SNX proteins, is also involved in protein secretion (Feng et al., 2017, Zhang et al., 2011). The functions of the family member we have detected in complex with PfCK1, SNX22, remain elusive and it is unknown whether its expression is specific to RBC progenitors. Nevertheless, it is possible that SNX22 may coordinate endosomal trafficking pathways and possibly membrane protein recycling and secretion. Members of the SNX family link protein complexes with lipid regions enriched in PtdIns3P, thus connecting signalling pathways and making them candidates to facilitate PfCK1 signalling as well. Membrane recruitment of GAPVD1 by the effector molecule TC10 enables the activation of the small Ras-GTPase Rab5, a well-established marker of early-endosomes that functions by recruiting PtdIns3-kinase (PI3K) (Lodhi et al., 2008). Our data suggest that a similar process may be happening in RBCs, connecting GAPVD1 with SNX22 and PtdIns3P in signalling pathways hitherto unexpected in a cell without known active endocytosis.

Several models could be built to analyse the signalling events influencing association of PfCK1 with the SNX22/GAPVD1 complex and its possible role in the secretion of the parasite kinase. Firstly,

GAPVD1 could be recruited to the plasma membrane in response to a yet unknown upstream signal. Once at the membrane, GAPVD1 can recruit and activate PtdIns3P through typical effector molecules (for instance Rab5), thus providing a PtdIns3P-rich environment to recruit SNX22/PfCK1 complexes, pre-formed in the RBC cytoplasm. Indeed, published pull-down studies have demonstrated that CK1 isoforms enter into protein-protein interactions with both GAPVD1 and SNX family members (Huttlin et al., 2017, Hein et al., 2015), suggesting that these interactions may also be common in other cell types. Additionally, studies have demonstrated that inhibition of PI3K with the inhibitor wortmannin disrupts membrane translocation of GLUT1 and GLUT4 glucose transporters, the hallmark function of GAPVD1 (Clarke et al., 1994). The *P. falciparum* genome encodes a wortmannin-sensitive PfPI3K (Vaid et al., 2010) and thus, PI3K inhibitors could be used to study whether inhibition of PI3K results in a block in PfCK1 secretion, presumably by disrupting the formation of the GAPVD1/SNX22/PfCK1 membrane translocation mechanism.

Interactions between SNX proteins and pathogen effector molecules have been observed in infections with several intracellular bacteria. For instance, *Chlamydia trachomatis* inclusion membrane protein E (IncE) disrupts the formation of the SNX5/6 heterodimer and perturbs retromer-mediated endocytosis (Sun et al., 2017). Similarly, *Listeria monocytogenes* Lmo1656 protein is a secreted virulence factor that interacts with SNX6 (David et al., 2018), likely disrupting endosomal trafficking by a similar mechanism to *C. trachomatis*. These examples provide evidence of interactions between intracellular pathogens and endosomal trafficking machinery and we suspect that a similar mechanism also involving membrane recycling may be occurring in *P. falciparum*.

Recycling of membrane proteins has been identified in other cells and requires the involvement of sorting nexins to redirect these proteins back to the membrane by formation of a recycling endosome complex (Zhang et al., 2011, Harterink et al., 2011, Temkin et al., 2011). For instance, following endocytosis the β2-adrenergic receptor (βAR2) enters recycling endosomes that are tethered to retromer tubules (a microtubule network involved in endosome to membrane recycling) by SNX27 and other proteins including the retromer complex and is directed to the plasma membrane by Rab4

(Temkin et al., 2011). It has also been shown that EARP, an endosome-associated recycling protein complex consisting of the vacuolar protein sorting subunits Ang2, Vps52 and Vps53, plays a major role in the recycling endosome process (Schindler et al., 2015).

An alternative model to explain our data would therefore include the secretion of PfCK1 to the RBC membrane, followed by internalisation into endocytic vesicles and redirection to an endocytic recycling pathway for secretion to the extracellular medium. Once PfCK1 enters recycling endosomes, SNX22 binds to PtdIns3P enriched regions anchoring the complex to a tubule network through interactions with Vps52 (table 3.X) in an EARP-like structure, a mechanism hitherto unexplained in *P. falciparum* and RBCs. Subsequently, GAPVD1 binds to the endosome which recruitments a Rab effector and directs the complex to the RBC membrane for secretion. The identification of GAPVD1 phosphopeptides in our PfCK1-GFP precipitates (Table 3.3) bearing predicted PfCK1 phosphorylation motifs also provides some support for this hypothesis.

As outlined in chapter 4 of this study, PfCK1 trafficking also involves the parasite nucleus (Figure 4.1), exhibiting a bi-compartmental distribution in the parasite, consistent with the subcellular distribution of CK1 in other eukaryotes (Fu et al., 2001, Milne et al., 2001). Two basic amino acid clusters we identified in PfCK1 and suspect are solvent-facing (Figures 4.2 and 4.3) are comparable to monopartite classical NLS (cNLS) sequences found in many nuclear localised proteins that utilise the canonical NLS/importin pathway (Bennett et al., 2015, Chaston et al., 2017). We suspect that PfCK1 nuclear import may also be directed through the importin pathway and preliminary experiments from this study suggest that PfCK1 import is sensitive to Ivermectin (Figure 4.5), an inhibitor postulated to disrupt the formation of the importin/cargo complex (Panchal et al., 2014).

The frequency of basic amino acid clusters in proteins that look like a monopartite cNLS sequence means that rigorous testing is required to determine if they truly function as import signals (reviewed in (Lange et al., 2007)). Mutagenesis of the first two basic amino acids to Ala is usually the first approach to determine whether a suspected cNLS sequence is functional, by analysing if nuclear

import is disrupted. This method identified a functional cNLS sequence in the long-variant CK1□□isoform and it was successfully demonstrated that mutation of the first basic residues results in cytoplasmic accumulation (Fu et al., 2001). To test if either cNLS sequence identified in PfCK1 is functional, we have obtained two separate codon-optimised PfCK1 constructs containing mutations for both candidate cNLS sequences (154KKYR157→AAYR and 221KKDK224→AADK), and a third construct with both mutations in the same sequence, in case one cNLS can substitute for the activity of the other. We have begun transfecting parasites with plasmids expressing GFP-tagged PfCK1, bearing mutant cNLS sequences to investigate their functionality. If successful, this will provide the first evidence of a functional nuclear import sequence in this parasite kinase.

Next, if a functional cNLS is identified in PfCK1, its sequence will be attached to a reporter protein (this is usually GFP), without the rest of the protein sequence, to determine whether the cNLS sequence alone enables nuclear import. In parallel, we will further optimise our proteomics methods to precipitate PfCK1 from purified nuclei in an attempt to observe direct interactions between PfCK1 and the importin receptor, karyopherin. Finally, it would be desirable to utilise importin knock out parasites thus disabling the import pathway to induce cytoplasmic accumulation of PfCK1. However, knocking out the importin receptor will likely result in a lethal phenotype, an observation made in other studies examining gene knock out (Solyakov et al., 2011). To circumvent this issue, we will disrupt nuclear import with inhibitors.

The aim of chapter 4 was to explore the currently unknown functions of PfCK1 in the nucleus of asexual parasites. ChIP-Seq experiments performed in this study demonstrated that PfCK1 interacts with DNA-containing structures. These interactions could be similar to those established by mammalian CK1 homologs with chromatin remodelling enzymes and transcription factors (Sugiyama et al., 2010, Meng et al., 2010, Yang and Stockwell, 2008). This suggests that PfCK1 could act as a transcriptional regulator, or function in chromatin remodelling processes. We favour the latter possibility because in chapter 4 we identified PfCK2α as a probable interacting protein in PfCK1 complexes, and PfCK2 has

been described to be involved in the chromatin assembly pathway. Several studies have confirmed the interactions between PfCK1 and PfCK2 in pull-down experiments using recombinant proteins (Dorin-Semblat et al., 2015) and reciprocal immunoprecipitations from whole parasite lysates, using PfCK2 regulatory subunits (PfCK2β1 and β2) (Dastidar et al., 2012). Nevertheless, results obtained from ChIP-Seq experiments and subsequent mass spectrometry will provide more details about the functions of PfCK1 in the parasite nucleus.

Deaths associated with *P. falciparum* infection will be exacerbated by the continuous emergence of drug resistance to frontline antimalarials and such an upward trend has been noted in the latest WHO report (Organization, 2018). Therefore, new therapeutics are urgently needed. The final chapter of this thesis aimed at exploring PfCK1 as a possible therapeutic target, using the inhibitor Purvalanol B as a probe. In this study, we deployed bioinformatic approaches and modelling software to produce a predicted three-dimensional structure of PfCK1, aiming to identify and select amino acid residues for mutagenic studies, in order to explore the role of PfCK1 in the killing of *P. falciparum* by Purvalanol B. Results obtained in this chapter disproved our initial hypothesis of a singular involvement of PfCK1 in the Purvalanol B mechanism of action. Rather, we concluded that this compound likely targets multiple proteins. It is widely accepted that Purvalanol B is a potent and selective inhibitor of CDKs in mammalian cells, yet several studies have utilised Purvalanol B as a pan-kinase inhibitor for global kinase pull-down experiments (Daub et al., Duncan et al., 2012, Becker et al., 2004), adding support to our hypothesis that Purvalanol B is not as selective as first described (Knockaert et al., 2000).

The model we generated in this study (Figure 5.5) is, to the best of our knowledge, the first predicted three-dimensional structure of this parasite kinase, and it could be a useful tool for rational drug design. Modelling-based approaches with *P. falciparum* proteins have demonstrated that selective inhibition of parasite proteins over their human homologs can be possible (Kumar et al., 2007, Droucheau et al., 2004), and several inhibitors are available that show preferential inhibition of certain CK1 isoforms (Behrend et al., 2000, Walton et al., 2009, Mashhoon et al., 2000), despite those proteins

sharing a high degree of homology. Taken as a whole, our PfCK1 structure could be useful to design new compounds or modify existing compounds to preferentially inhibit PfCK1 over human homologs. This could provide new tools to study parasite biology and may also provide a therapeutic avenue for pharmacological targeting of PfCK1.

Our work to elucidate the biology of PfCK1 has rejected the hypothesis that this kinase might be the primary target of the anti-plasmodial activity of Purvalanol B; it has established that PfCK1 extracellular secretion is not mediated by microvesicles, unlike other macromolecules (Mantel et al., 2013) and it has resulted in the identification of a previously undescribed, functional endosomal transport pathway in RBCs that appears to be recruited by *P. falciparum*. This is a recycling mechanism used in nucleated cells from higher eukaryotes to maintain levels of specific membrane proteins (Belenkaya et al., 2008, Temkin et al., 2011, Leto and Saltiel, 2012). We hypothesise that this pathway contributes to the secretion of PfCK1 into the extracellular medium, opening up future research venues into the specific molecular mechanism.

We have also identified a role for PfCK1 in the parasite nucleus, generating molecular tools to study its nuclear transport and still ongoing experiments showing physical interactions between the kinase and chromatin components. Identification of the proteins that interact directly with PfCK1, in conjunction with sequencing of the associated DNA, will provide novel information about protein kinase-mediated epigenetic regulation in *P. falciparum*.

Taken as a whole, this work adds to the limited existing knowledge about the essential role of PfCK1 during the malaria intraerythrocytic cycle and enables new lines of enquiry into the cellular process that depend on this kinase in the parasite, providing new targets and ideas for pharmacological intervention. In this regard, the structural PfCK1 model we have built in the course of this study will be a resource for rational drug design until experimental X-ray structures can be generated for this protein.

Supplementary figures and tables

Table S3.1. List of quantified human and parasite proteins obtained from PfCK1-GFP and 3D7 immunoprecipitates.

Protein description	-Log p-value (t-test)	Log_2 difference (GFP/WT)	UniProt ID
GTPase-activating protein and VPS9 domain-containing protein 1	4.13	11.78	Q14C86
Sorting nexin-22	4.13	7.41	Q96L94
14-3-3 protein epsilon	2.93	2.29	P62258
Casein kinase I isoform alpha	2.66	4.98	P48729
Probable ubiquitin carboxyl-terminal hydrolase FAF-X	2.57	1.98	Q93008
T-complex protein 1 subunit eta	2.28	1.21	Q99832
T-complex protein 1 subunit epsilon	2.28	1.88	E7ENZ3
Polyubiquitin-B	2.26	0.57	J3QS39
Heat shock 70 kDa protein 1B	2.16	1.72	P0DMV9
Multifunctional protein ADE2	2.06	0.91	E9PBS1
T-complex protein 1 subunit zeta	2.05	1.58	P40227
Glucose-6-phosphate 1-dehydrogenase	2.04	1.02	P11413
Gamma-glutamylcyclotransferase	2.00	-0.48	O75223
Protein S100-A9	1.98	-3.05	P06702
Desmocollin-1	1.98	-2.65	Q08554
14-3-3 protein zeta/delta	1.92	1.69	P63104
Fructosamine-3-kinase	1.83	1.02	Q9H479
Aldehyde dehydrogenase family 16 member A1	1.78	0.72	Q8IZ83
Proteasome activator complex subunit 2	1.63	0.76	Q9UL46
Adenosylhomocysteinase	1.53	0.77	P23526
Glutathione reductase, mitochondrial	1.40	1.04	P00390
Fumarylacetoacetase	1.39	0.92	P16930
T-complex protein 1 subunit theta	1.38	1.62	P50990
Calpain-1 catalytic subunit	1.38	0.98	P07384
6-phosphogluconolactonase	1.37	0.69	O95336
T-complex protein 1 subunit alpha	1.35	1.12	P17987
Annexin A2	1.29	-2.07	P07355
Heat shock cognate 71 kDa protein	1.28	1.11	P11142
Casein kinase I	3.91	13.46	Q8IHZ9
40S ribosomal protein SA	3.07	1.86	Q8IJD4
Heat shock protein 70	2.50	2.63	Q8IB24
Heat shock protein 71	2.42	1.39	Q8I2X4
Tubulin beta chain	1.80	1.32	Q7KQL5
Pyridoxal 5-phosphate synthase subunit Pdx1	1.70	0.53	C6KT50

Proteins obtained are ranked by -Log p-value from lowest to highest, with a cut-off value of 1.3 (equivalent p-value ≤0.05). Highlighted in orange are parasite proteins obtained in precipitates and blue represent human proteins consistently identified in precipitations.

Table S3.2. List of parasite proteins obtained from a preliminary GAPVD1 immunoprecipitation and identified by spectral counting.

Protein description	Unique peptides		UniProt ID
	iRBC	uRBC	
GTPase-activating protein and VPS9 domain-containing	339	225	Q14C86
Sorting nexin-22 (H. sapiens)	40	46	Q96L94
Casein kinase 1, subunit alpha	8	60	P48729
Casein kinase 1	42		Q8IHZ9
Protein dopey homolog PFC0245c	153		O97239
Vacuolar protein sorting-associated protein 51 (putative)	64		Q8I2A9
Vacuolar protein sorting-associated protein 53 (putative)	36		Q8IBI7
Vacuolar protein sorting-associated protein 52 (putative)	30		Q8IE79
14-3-3 protein (putative)	21		C0H4V6
GTP-binding nuclear protein ran/tc4	19		Q7KQK6
Elongation factor 1-alpha	38		Q8I0P6
NLI interacting factor-like phosphatase (putative)	200		Q8IJR8
Heat shock 70 kDa protein	165		Q8IB24
Heat shock protein 70 (HSP70) homologue	79	2	Q8I2X4
Dynamin-like protein	78		Q8IHR4
Heat shock protein 86	24		Q8IC05
Polyadenylate-binding protein	33		Q8I5H4
RNA binding protein musashi (putative)	27		Q8I2Y5
DNA/RNA-binding protein Alba3	26		Q8IJX8
DNA/RNA-binding protein Alba4	16		Q8IDM3
Actin-1	26		Q8I4X0
Uga suppressor tRNA-associated antigenic protein (putative)	20		Q8I5Z4
Tubulin beta chain	17		Q7KQL5

Parasite proteins obtained are from a single immunoprecipitation experiment using lysates of magnet purified wild-type parasites. Highlighted in orange is PfCK1 and proteins shown in green represent parasite proteins which are predicted to be involved in vesicle trafficking. Shown in blue are the human proteins identified in PfCK1-GFP precipitates as high probability interactors to highlight the same proteins precipitate using GAPVD1 antibody.

Table S3.3. List of quantified human proteins recovered from GAPVD1 immunoprecipitations.

Protein description	-Log p-value (t-test)	Log_2 difference (GFP/WT)	UniProt ID
Spectrin beta chain, erythrocytic	2.54	-4.35	P11277
Protein-L-isoaspartate(D-aspartate) O-methyltransferase	2.47	2.02	P22061
Casein kinase I isoform alpha	2.46	-4.32	P48729
Protein 4.1	2.39	-3.47	P11171
Spectrin alpha chain, erythrocytic 1	2.12	-3.24	P02549
Heat shock 70 kDa protein 6	1.93	5.5	P17066
Erythrocyte band 7 integral membrane protein	1.56	0.81	P27105
Heat shock cognate 71 kDa protein	1.53	-0.94	P11142
Flavin reductase (NADPH)	1.52	1.21	P30043
Tropomodulin-1	1.46	-2.8	P28289
Ankyrin-1	1.42	-2.27	P16157
Dematin	1.37	-2.88	Q08495
Tropomyosin alpha-3 chain	1.32	-2.89	P06753
Catalase	1.3	1.2	P04040
Beta-adducin	1.3	-2.61	P35612
ATP synthase subunit alpha, mitochondrial	1.29	4.32	P25705
Sorting nexin-22	0.94	0.73	Q96L94
GTPase-activating protein and VPS9 domain-containing protein 1	0.82	0.58	Q14C86

Human proteins identified as high-probability interactors by the Label Free Quantification (LFQ) of triplicate experiments obtained from wild-type 3D7 lysates and ranked from highest to lowest by -log p-value (cut-off value of 1.3).

Table S3.4. List of quantified parasite proteins recovered from GAPVD1 immunoprecipitations.

Protein description	-Log p-value (t-test)	Log_2 difference (GFP/WT)	UniProt ID
DNA/RNA-binding protein Alba3	5.26	5.16	Q8IJX8
Polyadenylate-binding protein	4.98	6.27	Q8I5H4
Heat shock protein 70	4.95	4.74	Q8II24
Heat shock protein 70	4.22	6.15	Q8I2X4
GTP binding nuclear protein	4.22	5.36	Q7KQK6
Eukaryotic initiation factor 4A	3.96	5.93	Q8IKF0
Heat shock protein 70	3.95	7.39	Q8IB24
Actin-1	3.74	6.08	Q8I4X0
Heat shock protein 90	3.74	9.55	Q8IC05
60S acidic ribosomal protein P2	3.68	5.63	O00806
S-adenosylmethionine synthase	3.59	4.22	Q7K6A4
60S ribosomal protein L28	3.48	3.92	Q8IHU0
Heat shock protein 110	3.30	8.14	Q8IC01
60S acidic ribosomal protein P0	3.25	6.57	Q8II61
14-3-3 protein	3.25	6.02	C0H4V6
Karyopherin beta	3.21	4.37	Q8I3M5
Uncharacterised protein	3.01	6.98	Q8IKG9
Glyceraldehyde-3-phosphate dehydrogenase	3.00	5.81	Q8IKK7
Proline--tRNA ligase	2.95	4.99	Q8I5R7
Glycophorin-binding protein	2.93	6.25	Q8I6U8
40S ribosomal protein S12	2.88	5.13	O97249
NLI interacting factor-like phosphatase, putative	2.77	8.11	Q8IJR8
Vacuolar protein sorting-associated protein 51, putative	2.73	3.92	Q8I2A9
Casein kinase I	2.56	4.42	Q8IHZ9
Plasmepsin II	2.32	3.49	Q8I6V3
60S ribosomal protein L5	2.28	3.55	Q8ILL3
Ornithine aminotransferase	2.24	3.83	Q6LFH8
40S ribosomal protein S25	2.23	2.19	Q8ILN8
V-type H(+)-translocating pyrophosphatase, putative	2.17	3.50	Q8IKR1
Elongation factor 1-alpha	2.11	7.66	Q8I0P6
HAP protein	2.01	3.99	Q8IM15
40S ribosomal protein S19	1.92	2.29	Q8IFP2
Small exported membrane protein 1	1.57	3.82	Q8IC43

Parasite proteins identified as high-probability interactors by the Label Free Quantification (LFQ) of triplicate experiments obtained from wild-type 3D7 lysates and ranked from highest to lowest by -log p-value (cut-off value of 1.3). Blue highlights the parasite proteins PfCK1 and Vps-51, predicted to be involved in endosomal trafficking.

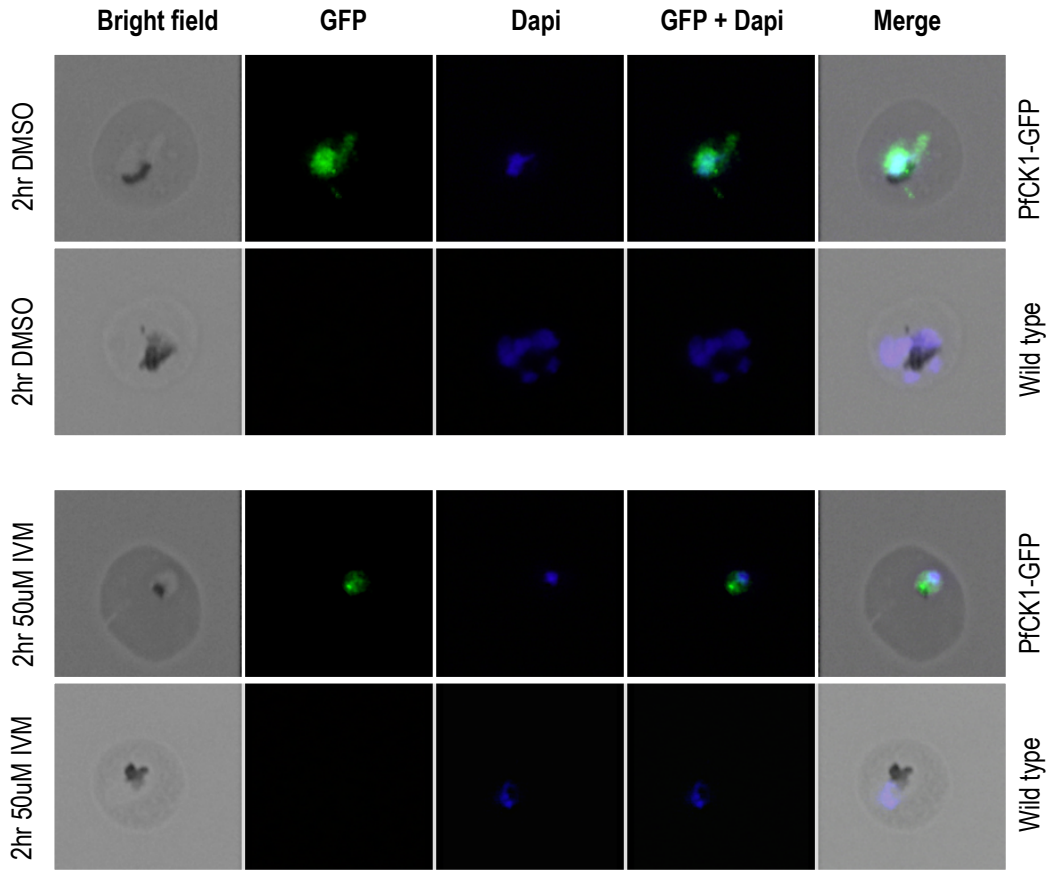

Figure S4.1. Effect of Ivermectin treatment on the nucleocytoplasmic shuttling of PfCK1-GFP. Magnet purified late stage parasites were recovered at 37°C for 1hr prior to incubation with drug for 2hr. Upper panel in each block are cells expressing PfCK1-GFP from the cognate locus and bottom panel in each are wild-type control cells. **(a)** DMSO treated control parasites after 2hr incubation and **(b)** parasites following 2hr incubation with 50μM Ivermectin (IVM) showing a small, circular parasite consistent with a death phenotype.

References

ADMYRE, C., BOHLE, B., JOHANSSON, S. M., FOCKE-TEJKL, M., VALENTA, R., SCHEYNIUS, A. & GABRIELSSON, S. 2007. B cell–derived exosomes can present allergen peptides and activate allergen-specific T cells to proliferate and produce TH2-like cytokines. *Journal of Allergy and Clinical Immunology,* 120**,** 1418-1424.

AGOP-NERSESIAN, C., EGARTER, S., LANGSLEY, G., FOTH, B. J., FERGUSON, D. J. P. & MEISSNER, M. 2010. Biogenesis of the Inner Membrane Complex Is Dependent on Vesicular Transport by the Alveolate Specific GTPase Rab11B. *PLOS Pathogens,* 6**,** e1001029.

AGOP-NERSESIAN, C., NAISSANT, B., BEN RACHED, F., RAUCH, M., KRETZSCHMAR, A. & THIBERGE, S. 2009. Rab11A-controlled assembly of the inner membrane complex is required for completion of apicomplexan cytokinesis. *PLOS Pathogens,* 5.

AGUILAR-GURRIERI, C., LARABI, A., VINAYACHANDRAN, V., PATEL, N. A., YEN, K., REJA, R., EBONG, I. O., SCHOEHN, G., ROBINSON, C. V., PUGH, B. F. & PANNE, D. 2016. Structural evidence for Nap1-dependent H2A–H2B deposition and nucleosome assembly. *The EMBO Journal,* 35**,** 1465-1482.

AICART-RAMOS, C., VALERO, R. A. & RODRIGUEZ-CRESPO, I. 2011. Protein palmitoylation and subcellular trafficking. *Biochimica et Biophysica Acta (BBA) - Biomembranes,* 1808**,** 2981-2994.

ALLAHVERDI, A., YANG, R., KOROLEV, N., FAN, Y., DAVEY, C. A., LIU, C.-F. & NORDENSKIÖLD, L. 2011. The effects of histone H4 tail acetylations on cation-induced chromatin folding and self-association. *Nucleic Acids Research,* 39**,** 1680-1691.

ALLOCCO, J. J., DONALD, R., ZHONG, T., LEE, A., TANG, Y. S., HENDRICKSON, R. C., LIBERATOR, P. & NARE, B. 2006. Inhibitors of casein kinase 1 block the growth of *Leishmania major* promastigotes in vitro. *International Journal for Parasitology,* 36**,** 1249-1259.

ALONSO, P. L., BROWN, G., AREVALO-HERRERA, M., BINKA, F., CHITNIS, C., COLLINS, F., DOUMBO, O. K., GREENWOOD, B., HALL, B. F., LEVINE, M. M., MENDIS, K., NEWMAN, R. D., PLOWE, C. V., RODRÍGUEZ, M. H., SINDEN, R., SLUTSKER, L. & TANNER, M. 2011. A Research Agenda to Underpin Malaria Eradication. *PLOS Medicine,* 8**,** e1000406.

ALONSO, P. L. & TANNER, M. 2013. Public health challenges and prospects for malaria control and elimination. *Nature Medicine,* 19**,** 150-155.

ALSTON, C. L., DAVISON, J. E., MELONI, F., VAN DER WESTHUIZEN, F. H., HE, L., HORNIG-DO, H.-T., PEET, A. C., GISSEN, P., GOFFRINI, P., FERRERO, I., WASSMER, E., MCFARLAND, R. & TAYLOR, R. W. 2012. Recessive germline SDHA and SDHB mutations causing leukodystrophy and isolated mitochondrial complex II deficiency. *Journal of Medical Genetics,* 49**,** 569-577.

AMIT, S., HATZUBAI, A., BIRMAN, Y., ANDERSEN, J. S., BEN-SHUSHAN, E., MANN, M., BEN-NERIAH, Y. & ALKALAY, I. 2002. Axin-mediated CKI phosphorylation of β-catenin at Ser 45: a molecular switch for the Wnt pathway. *Genes & Development,* 16**,** 1066-1076.

ANAMIKA, N., S. & A., K. 2005. A genomic perspective of protein kinases in *Plasmodium falciparum*. *Proteins: Structure, Function, and Bioinformatics,* 58**,** 180-189.

AREND, K. C., LENARCIC, E. M., VINCENT, H. A., RASHID, N., LAZEAR, E., MACDONALD, I. M., GILBERT, T. S. K., EAST, M. P., HERRING, L. E., JOHNSON, G. L., GRAVES, L. & MOORMAN, N. J. 2017. Kinome Profiling Identifies Druggable Targets For Novel HCMV Antivirals. *Molecular & Cellular Proteomics*.

AVRIL, M., TRIPATHI, A. K., BRAZIER, A. J., ANDISI, C., JANES, J. H., SOMA, V. L., SULLIVAN, D. J., BULL, P. C., STINS, M. F. & SMITH, J. D. 2012. A restricted subset of var genes mediates adherence of *Plasmodium falciparum*-infected erythrocytes to brain endothelial cells. *Proceedings of the National Academy of Sciences,* 109**,** E1782–E1790.

AYONG, L., DASILVA, T., MAUSER, J., ALLEN, C. M. & CHAKRABARTI, D. 2011. Evidence for prenylation-dependent targeting of a Ykt6 SNARE in *Plasmodium falciparum*. *Molecular and Biochemical Parasitology,* 175**,** 162-168.

BARBER, C. M., TURNER, F. B., WANG, Y., HAGSTROM, K., TAVERNA, S. D., MOLLAH, S., UEBERHEIDE, B., MEYER, B. J., HUNT, D. F., CHEUNG, P. & ALLIS, C. D. 2004. The enhancement of histone H4 and H2A serine 1 phosphorylation during mitosis and S-phase is evolutionarily conserved. *Chromosoma,* 112**,** 360-371.

BASNET, H., SU, X. B., TAN, Y., MEISENHELDER, J., MERKURJEV, D., OHGI, K. A., HUNTER, T., PILLUS, L. & ROSENFELD, M. G. 2014. Tyrosine phosphorylation of histone H2A by CK2 regulates transcriptional elongation. *Nature,* 516**,** 267.

BECKER, F., MURTHI, K., SMITH, C., COME, J., COSTA-ROLDÁN, N., KAUFMANN, C., HANKE, U., DEGENHART, C., BAUMANN, S., WALLNER, W., HUBER, A., DEDIER, S., DILL, S., KINSMAN, D., HEDIGER, M., BOCKOVICH, N., MEIER-EWERT, S., KLUGE, A. F. & KLEY, N. 2004. A Three-Hybrid Approach to Scanning the Proteome for Targets of Small Molecule Kinase Inhibitors. *Chemistry & Biology,* 11**,** 211-223.

BEENSTOCK, J., MELAMED, D., MOOSHAYEF, N., MORDECHAY, D., GARFINKEL, B. P., AHN, N. G., ADMON, A. & ENGELBERG, D. 2016. p38β Mitogen-Activated Protein Kinase Modulates Its Own Basal Activity by Autophosphorylation of the Activating Residue Thr180 and the Inhibitory Residues Thr241 and Ser261. *Molecular and Cellular Biology,* 36**,** 1540-1554.

BÉGUIN, A., HALES, S., ROCKLÖV, J., ÅSTRÖM, C., LOUIS, V. R. & SAUERBORN, R. 2011. The opposing effects of climate change and socio-economic development on the global distribution of malaria. *Global Environmental Change,* 21**,** 1209-1214.

BEHREND, L., MILNE, D. M., STÖTER, M., DEPPERT, W., CAMPBELL, L. E., MEEK, D. W. & KNIPPSCHILD, U. 2000. IC261, a specific inhibitor of the protein kinases casein kinase 1-delta and -epsilon, triggers the mitotic checkpoint and induces p53-dependent postmitotic effects. *Oncogene,* 19**,** 5303.

BELENKAYA, T. Y., WU, Y., TANG, X., ZHOU, B., CHENG, L., SHARMA, Y. V., YAN, D., SELVA, E. M. & LIN, X. 2008. The Retromer Complex Influences Wnt Secretion by Recycling Wntless from Endosomes to the Trans-Golgi Network. *Developmental Cell,* 14**,** 120-131.

BELTRAO, P., BORK, P., KROGAN, N. J. & VAN NOORT, V. 2013. Evolution and functional cross-talk of protein post-translational modifications. *Molecular Systems Biology,* 9.

BENNETT, S. M., ZHAO, L., BOSARD, C. & IMPERIALE, M. J. 2015. Role of a nuclear localization signal on the minor capsid Proteins VP2 and VP3 in BKPyV nuclear entry. *Virology,* 474**,** 110-116.

BENSON, D. A., KARSCH-MIZRACHI, I., LIPMAN, D. J., OSTELL, J. & WHEELER, D. L. 2005. GenBank. *Nucleic acids research,* 33**,** D34-D38.

BERI, D., BALAN, B., CHAUBEY, S., SUBRAMANIAM, S., SURENDRA, B. & TATU, U. 2017. A disrupted transsulphuration pathway results in accumulation of redox metabolites and induction of gametocytogenesis in malaria. *Scientific Reports,* 7**,** 40213.

BESHIR, K. B., SUTHERLAND, C. J., SAWA, P., DRAKELEY, C. J., OKELL, L., MWERESA, C. K., OMAR, S. A., SHEKALAGHE, S. A., KAUR, H., NDARO, A., CHILONGOLA, J., SCHALLIG, H. D. F. H., SAUERWEIN, R. W., HALLETT, R. L. & BOUSEMA, T. 2013. Residual *Plasmodium falciparum* Parasitemia in Kenyan Children After Artemisinin-Combination Therapy Is Associated With Increased Transmission to Mosquitoes and Parasite Recurrence. *Journal of Infectious Diseases,* 208**,** 2017-2024.

BESTEIRO, S., DUBREMETZ, J.-F. & LEBRUN, M. 2011. The moving junction of apicomplexan parasites: a key structure for invasion. *Cellular Microbiology,* 13**,** 797-805.

BEYZA ÖZTÜRK SARIKAYA, S., GÜLÇIN, İ. & SUPURAN, C. T. 2010. Carbonic Anhydrase Inhibitors: Inhibition of Human Erythrocyte Isozymes I and II with a Series of Phenolic Acids. *Chemical Biology & Drug Design,* 75**,** 515-520.

BODDY. J. A., MORITZ. R. L., SIMPSON. R. J., & COWMAN. A. F., 2009. Role of the *Plasmodium* Export Element in Trafficking Parasite Proteins to the Infected Erythrocyte. *Traffic,* 10**,** 285-299.

BOS, J. L., REHMANN, H. & WITTINGHOFER, A. 2007. GEFs and GAPs: Critical Elements in the Control of Small G Proteins. *Cell,* 129**,** 865-877.

BOWMAN, J. D., MERINO, E. F., BROOKS, C. F., STRIEPEN, B., CARLIER, P. R. & CASSERA, M. B. 2014. Antiapicoplast and Gametocytocidal Screening To Identify the Mechanisms of Action of Compounds within the Malaria Box. *Antimicrobial Agents and Chemotherapy,* 58**,** 811-819.

BOZDECH, Z., LLINÁS, M., PULLIAM, B. L., WONG, E. D., ZHU, J. & DERISI, J. L. 2003. The Transcriptome of the Intraerythrocytic Developmental Cycle of *Plasmodium falciparum*. *PLOS Biology,* 1**,** e5.

BOZDECH, Z., MOK, S., HU, G., IMWONG, M., JAIDEE, A., RUSSELL, B., GINSBURG, H., NOSTEN, F., DAY, N. P. J., WHITE, N. J., CARLTON, J. M. & PREISER, P. R. 2008. The transcriptome of *Plasmodium vivax* reveals divergence and diversity of transcriptional regulation in malaria parasites. *Proceedings of the National Academy of Sciences,* 105**,** 16290-16295.

BRANDT, G. S. & BAILEY, S. 2013. Dematin, a human erythrocyte cytoskeletal protein, is a substrate for a recombinant FIKK kinase from *Plasmodium falciparum*. *Molecular and Biochemical Parasitology,* 191**,** 20-23.

BUCK, A. H., COAKLEY, G., SIMBARI, F., MCSORLEY, H. J., QUINTANA, J. F., LE BIHAN, T., KUMAR, S., ABREU-GOODGER, C., LEAR, M., HARCUS, Y., CERONI, A., BABAYAN, S. A., BLAXTER, M., IVENS, A. & MAIZELS, R. M. 2014. Exosomes secreted by nematode parasites transfer small RNAs to mammalian cells and modulate innate immunity. *Nature Communications,* 5**,** 5488.

BUJNY, M. V., POPOFF, V., JOHANNES, L. & CULLEN, P. J. 2007. The retromer component sorting nexin-1 is required for efficient retrograde transport of Shiga toxin from early endosome to the trans Golgi network. *Journal of Cell Science,* 120**,** 2010-2021.

BULLARD, K. M., BROCCARDO, C. & KEENAN, S. M. 2015. Effects of cyclin-dependent kinase inhibitor Purvalanol B application on protein expression and developmental progression in intra-erythrocytic *Plasmodium falciparum* parasites. *Malaria Journal,* 14**,** 147.

BULLEN, H. E., CHARNAUD, S. C., KALANON, M., RIGLAR, D. T., DEKIWADIA, C., KANGWANRANGSAN, N., TORII, M., TSUBOI, T., BAUM, J., RALPH, S. A., COWMAN, A. F., DE KONING-WARD, T. F., CRABB, B. S. & GILSON, P. R. 2012. Biosynthesis, Localization, and Macromolecular Arrangement of the *Plasmodium falciparum* Translocon of Exported Proteins (PTEX). *Journal of Biological Chemistry,* 287**,** 7871-7884.

BURDA, P., PADILLA, S. M., SARKAR, S. & EMR, S. D. 2002. Retromer function in endosome-to-Golgi retrograde transport is regulated by the yeast Vps34 PtdIns 3-kinase. *Journal of Cell Science,* 115**,** 3889-3900.

BURGESS, R. J. & ZHANG, Z. 2013. Histone chaperones in nucleosome assembly and human disease. *Nature Structural & Molecular Biology,* 20**,** 14.

BURGOYNE, J. R., MADHANI, M., CUELLO, F., CHARLES, R. L., BRENNAN, J. P., SCHRÖDER, E., BROWNING, D. D. & EATON, P. 2007. Cysteine Redox Sensor in PKGIa Enables Oxidant-Induced Activation. *Science,* 317**,** 1393-1397.

CANTON, J. & KIMA, P. E. 2012. Targeting Host Syntaxin-5 Preferentially Blocks *Leishmania* Parasitophorous Vacuole Development in Infected Cells and Limits Experimental *Leishmania* Infections. *The American Journal of Pathology,* 181**,** 1348-1355.

CASADIO, F., LU, X., POLLOCK, S. B., LEROY, G., GARCIA, B. A., MUIR, T. W., ROEDER, R. G. & ALLIS, C. D. 2013. H3R42me2a is a histone modification with positive transcriptional effects. *Proceedings of the National Academy of Sciences,* 110**,** 14894-14899.

CATERINA, P., RAFFAELE, L., ELENA, C., MARIA, R., SONIA, F., A., P. L., GIOVANNA, C. & GEPPO, S. 2008. Phosphorylation of the *Saccharomyces cerevisiae* Grx4p glutaredoxin by the Bud32p kinase unveils a novel signaling pathway involving Sch9p, a yeast member of the Akt / PKB subfamily. *The FEBS Journal,* 275**,** 5919-5933.

CERQUEIRA, G. C., CHEESEMAN, I. H., SCHAFFNER, S. F., NAIR, S., MCDEW-WHITE, M., PHYO, A. P., ASHLEY, E. A., MELNIKOV, A., ROGOV, P., BIRREN, B. W., NOSTEN, F., ANDERSON, T. J. C. & NEAFSEY, D. E. 2017. Longitudinal genomic surveillance of *Plasmodium falciparum* malaria parasites reveals complex genomic architecture of emerging artemisinin resistance. *Genome Biology,* 18**,** 78.

CHARNAUD. S. C., JONSDOTTIR. T. K., SANDERS. P. R., BULLEN. H. E., DICKERMAN. B. K., KOUSKOUSIS. B., PALMER. C. S., PIETRZAK. H. M., LAUMAEA. A. E., ERAZO. A., MCHUGE. E., TILLEY. L., CRABB. B S., & GILSON. P. R. 2018. Spatial organization of protein export in malaria parasite blood stages. *Traffic,* 1-19.

CHARRIER, J.-D., DURRANT, S. J., GOLEC, J. M. C., KAY, D. P., KNEGTEL, R. M. A., MACCORMICK, S., MORTIMORE, M., O'DONNELL, M. E., PINDER, J. L., REAPER, P. M., RUTHERFORD, A. P., WANG, P. S. H., YOUNG, S. C. & POLLARD, J. R. 2011. Discovery of Potent and Selective Inhibitors of Ataxia Telangiectasia Mutated and Rad3 Related (ATR) Protein Kinase as Potential Anticancer Agents. *Journal of Medicinal Chemistry,* 54**,** 2320-2330.

CHASTON, J. J., STEWART, A. G. & CHRISTIE, M. 2017. Structural characterisation of TNRC6A nuclear localisation signal in complex with importin-alpha. *PLOS ONE,* 12**,** e0183587.

CHAUBEY, S., GROVER, M. & TATU, U. 2014. Endoplasmic Reticulum Stress Triggers Gametocytogenesis in the Malaria Parasite. *Journal of Biological Chemistry,* 289**,** 16662-16674.

CHEN, X., D'ARCY, S., RADEBAUGH, C. A., KRZIZIKE, D. D., GIEBLER, H. A., HUANG, L., NYBORG, J. K., LUGER, K. & STARGELL, L. A. 2016. Histone Chaperone Nap1 Is a Major Regulator of Histone H2A-H2B Dynamics at the Inducible GAL Locus. *Molecular and Cellular Biology,* 36**,** 1287-1296.

CHEN, Z., ZHAO, T.-J., LI, J., GAO, Y.-S., MENG, F.-G., YAN, Y.-B. & ZHOU, H.-M. 2011. Slow skeletal muscle myosin-binding protein-C (MyBPC1) mediates recruitment of muscle-type creatine kinase (CK) to myosin. *Biochemical Journal,* 436**,** 437-445.

CHEONG, J. K. & VIRSHUP, D. M. 2011. Casein kinase 1: complexity in the family. *The international journal of biochemistry & cell biology,* 43**,** 465-469.

CHEUNG, W. L., TURNER, F. B., KRISHNAMOORTHY, T., WOLNER, B., AHN, S.-H., FOLEY, M., DORSEY, J. A., PETERSON, C. L., BERGER, S. L. & ALLIS, C. D. 2005. Phosphorylation of Histone H4 Serine 1 during DNA Damage Requires Casein Kinase II in *S. cerevisiae*. *Current Biology,* 15**,** 656-660.

CHO, H.-S., SHIMAZU, T., TOYOKAWA, G., DAIGO, Y., MAEHARA, Y., HAYAMI, S., ITO, A., MASUDA, K., IKAWA, N., FIELD, H. I., TSUCHIYA, E., OHNUMA, S.-I., PONDER, B. A. J., YOSHIDA, M., NAKAMURA, Y. & HAMAMOTO, R. 2012. Enhanced HSP70 lysine methylation promotes proliferation of cancer cells through activation of Aurora kinase B. *Nature Communications,* 3**,** 1072.

CHOU, K.-C. & SHEN, H.-B. 2008. Cell-PLoc: a package of Web servers for predicting subcellular localization of proteins in various organisms. *Nature Protocols,* 3**,** 153-162.

CHU, C.-Y. & RANA, T. M. 2006. Translation Repression in Human Cells by MicroRNA-Induced Gene Silencing Requires RCK/p54. *PLOS Biology,* 4**,** e210.

CLARKE, J. F., YOUNG, P. W., YONEZAWA, K., KASUGA, M. & HOLMAN, G. D. 1994. Inhibition of the translocation of GLUT1 and GLUT4 in 3T3-L1 cells by the phosphatidylinositol 3-kinase inhibitor, wortmannin. *Biochemical Journal,* 300**,** 631-635.

COLLER, J. & PARKER, R. 2005. General Translational Repression by Activators of mRNA Decapping. *Cell,* 122**,** 875-886.

COLOMBO, M., RAPOSO, G., & THÉRY, C. 2014. Biogenesis, Secretion, and Intercellular Interactions of Exosomes and Other Extracellular Vesicles. *Annual Review of Cell and Developmental Biology,* 30**,** 255-289.

CONTI, E. & KURIYAN, J. 2000. Crystallographic analysis of the specific yet versatile recognition of distinct nuclear localization signals by karyopherin α. *Structure,* 8**,** 329-338.

CORNELIA, S., MELANIE, R., ESTHER, P., ERIC, H., DAVID, F., F., C. A., LEANN, T. & HANS-PETER, B. 2008. The Maurer's cleft protein MAHRP1 is essential for trafficking of PfEMP1 to the surface of *Plasmodium falciparum*-infected erythrocytes. *Molecular Microbiology,* 68**,** 1300-1314.

COX-SINGH, J., DAVIS, T. M. E., LEE, K.-S., SHAMSUL, S. S. G., MATUSOP, A., RATNAM, S., RAHMAN, H. A., CONWAY, D. J. & SINGH, B. 2008. *Plasmodium knowlesi* Malaria in Humans Is Widely Distributed and Potentially Life Threatening. *Clinical Infectious Diseases,* 46**,** 165-171.

CRABB, B. S. & GILSON, P. R. 2007. A new system for rapid plasmid integration in *Plasmodium* parasites. *Trends in Microbiology,* 15**,** 3-6.

CRUCIAT, C.-M. 2014. Casein kinase 1 and Wnt/β-catenin signaling. *Current Opinion in Cell Biology,* 31**,** 46-55.

DASTIDAR, E. G., DAYER, G., HOLLAND, Z. M., DORIN-SEMBLAT, D., CLAES, A., CHÊNE, A., SHARMA, A., HAMELIN, R., MONIATTE, M. & LOPEZ-RUBIO, J.-J. 2012. Involvement of *Plasmodium falciparum* protein kinase CK2 in the chromatin assembly pathway. *BMC biology,* 10**,** 5.

DASTIDAR, E. G., DZEYK, K., KRIJGSVELD, J., MALMQUIST, N. A., DOERIG, C., SCHERF, A. & LOPEZ-RUBIO, J.-J. 2013. Comprehensive Histone Phosphorylation Analysis and Identification of Pf14-3-3 Protein as a Histone H3 Phosphorylation Reader in Malaria Parasites. *PLOS ONE,* 8**,** e53179.

DAUB, H., OLSEN, J. V., BAIRLEIN, M., GNAD, F., OPPERMANN, F. S., KÖRNER, R., GREFF, Z., KÉRI, G., STEMMANN, O. & MANN, M. Kinase-Selective Enrichment Enables Quantitative Phosphoproteomics of the Kinome across the Cell Cycle. *Molecular Cell,* 31**,** 438-448.

DAUCH, D., RUDALSKA, R., COSSA, G., NAULT, J.-C., KANG, T.-W., WUESTEFELD, T., HOHMEYER, A., IMBEAUD, S., YEVSA, T., HOENICKE, L., PANTSAR, T., BOZKO, P., MALEK, N. P., LONGERICH, T., LAUFER, S., POSO, A., ZUCMAN-ROSSI, J., EILERS, M. & ZENDER, L. 2016. A MYC-aurora kinase A protein complex represents an actionable drug target in p53-altered liver cancer. *Nature Medicine,* 22**,** 744-753.

DAVID, D. J., PAGLIUSO, A., RADOSHEVICH, L., NAHORI, M.-A. & COSSART, P. 2018. -Lmo1656 is a secreted virulence factor of Listeria monocytogenes that interacts with the sortin nexin 6-BAR complex. *Journal of Biological Chemistry*.

DAVIDSON, G., WU, W., SHEN, J., BILIC, J., FENGER, U., STANNEK, P., GLINKA, A. & NIEHRS, C. 2005. Casein kinase 1 [gamma] couples Wnt receptor activation to cytoplasmic signal transduction. *Nature,* 438**,** 867-872.

DAVIDSON, L., MUNIZ, L. & WEST, S. 2014. 3′ end formation of pre-mRNA and phosphorylation of Ser2 on the RNA polymerase II CTD are reciprocally coupled in human cells. *Genes & Development*.

DE PAULA, R. G., DE MAGALHÃES ORNELAS, A. M., MORAIS, E. R., DE CASTRO BORGES, W., NATALE, M., MAGALHÃES, L. G. & RODRIGUES, V. 2014. Biochemical characterization and role of the proteasome in the oxidative stress response of adult *Schistosoma mansoni* worms. *Parasitology Research,* 113**,** 2887-2897.

DELVES, M. J., RUECKER, A., STRASCHIL, U., LELIÈVRE, J., MARQUES, S., LÓPEZ-BARRAGÁN, M. J., HERREROS, E. & SINDEN, R. E. 2013. Male and Female *Plasmodium falciparum* Mature Gametocytes Show Different Responses to Antimalarial Drugs. *Antimicrobial Agents and Chemotherapy,* 57**,** 3268-3274.

DEPPING, R., STEINHOFF, A., SCHINDLER, S. G., FRIEDRICH, B., FAGERLUND, R., METZEN, E., HARTMANN, E. & KÖHLER, M. 2008. Nuclear translocation of hypoxia-inducible factors (HIFs): Involvement of the classical importin α/β pathway. *Biochimica et Biophysica Acta (BBA) - Molecular Cell Research,* 1783**,** 394-404.

DERY, V., DUAH, N. O., AYANFUL-TORGBY, R., MATREVI, S. A., ANTO, F. & QUASHIE, N. B. 2015. An improved SYBR Green-1-based fluorescence method for the routine monitoring of *Plasmodium falciparum* resistance to anti-malarial drugs. *Malaria journal,* 14**,** 481.

DHAYALAN, A., RAJAVELU, A., RATHERT, P., TAMAS, R., JURKOWSKA, R. Z., RAGOZIN, S. & JELTSCH, A. 2010. THE DNMT3A PWWP domain reads histone 3 lysine 36 trimethylation and guides DNA methylation. *Journal of Biological Chemistry*.

DHINGRA, S. K., REDHI, D., COMBRINCK, J. M., YEO, T., OKOMBO, J., HENRICH, P. P., COWELL, A. N., GUPTA, P., STEGMAN, M. L., HOKE, J. M., COOPER, R. A., WINZELER, E., MOK, S., EGAN, T. J. & FIDOCK, D. A. 2017. A Variant PfCRT Isoform Can Contribute to *Plasmodium falciparum* Resistance to the First-Line Partner Drug Piperaquine. *mBio,* 8.

DI VIZIO, D., KIM, J., HAGER, M. H., MORELLO, M., YANG, W., LAFARGUE, C. J., TRUE, L. D., RUBIN, M. A., ADAM, R. M., BEROUKHIM, R., DEMICHELIS, F. & FREEMAN, M. R. 2009. Oncosome Formation in Prostate Cancer: Association with a Region of Frequent Chromosomal Deletion in Metastatic Disease. *Cancer Research,* 69**,** 5601-5609.

DIAZ, R. J., GOLBOURN, B., SHEKARFOROUSH, M., SMITH, C. A. & RUTKA, J. T. 2012. Aurora kinase B/C inhibition impairs malignant glioma growth in vivo. *Journal of Neuro-Oncology,* 108**,** 349-360.

DIXON. M. W. A., HAWTHORNE. P. L., TOBIAS, S., ANDERSON. K. L., TRENHOLME. K R., & GARDINER. D. L., 2008. Targeting of the Ring Exported Protein 1 to the Maurer's Clefts is Mediated by a Two-Phase Process. *Traffic,* 9**,** 1316-1326.

DOERIG, C., BILLKER, O., HAYSTEAD, T., SHARMA, P., TOBIN, A. B. & WATERS, N. C. 2008. Protein kinases of malaria parasites: an update. *Trends in Parasitology,* 24**,** 570-577.

DONALD, R. G. K., ZHONG, T., MEIJER, L. & LIBERATOR, P. A. 2005. Characterization of two *T. gondii* CK1 isoforms. *Molecular and Biochemical Parasitology,* 141**,** 15-27.

DORIN-SEMBLAT, D., DEMARTA-GATSI, C., HAMELIN, R., ARMAND, F., CARVALHO, T. G., MONIATTE, M., DOERIG, C. 2015. Malaria Parasite-Infected Erythrocytes Secrete PfCK1, the *Plasmodium* Homologue of the Pleiotropic Protein Kinase Casein Kinase 1. *PLOS ONE***,** 22.

DORIN-SEMBLAT, D., SCHMITT, S., SEMBLAT, J. P., SICARD, A., REININGER, L., GOLDRING, D., PATTERSON, S., QUASHIE, N., CHAKRABARTI, D., MEIJER, L. & DOERIG, C. 2011. *Plasmodium falciparum* NIMA-related kinase Pfnek-1: sex-specificity and assessment of essentiality for the erythrocytic asexual cycle. *Microbiology,* 157.

DROUCHEAU, E., PRIMOT, A., THOMAS, V., MATTEI, D., KNOCKAERT, M., RICHARDSON, C., SALLICANDRO, P., ALANO, P., JAFARSHAD, A., BARATTE, B., KUNICK, C., PARZY, D., PEARL, L., DOERIG, C. & MEIJER, L. 2004. *Plasmodium falciparum* glycogen synthase kinase-3: molecular model, expression, intracellular localisation and selective inhibitors. *Biochimica et Biophysica Acta (BBA) - Proteins and Proteomics,* 1697**,** 181-196.

DUCE, I. & SCOTT, R. 1985. Actions of dihydroavermectin B1α on insect muscle. *British journal of pharmacology,* 85**,** 395-401.

DUFFY, S., LOGANATHAN, S., HOLLERAN, J. P. & AVERY, V. M. 2016. Large-scale production of *Plasmodium falciparum* gametocytes for malaria drug discovery. *Nature Protocols,* 11**,** 976.

DUNCAN, J. S., WHITTLE, M. C., NAKAMURA, K., ABELL, A. N., MIDLAND, A. A., ZAWISTOWSKI, J. S., JOHNSON, N. L., GRANGER, D. A., JORDAN, N. V., DARR, D. B., USARY, J., KUAN, P.-F., SMALLEY, D. M., MAJOR, B., HE, X., HOADLEY, K. A., ZHOU, B., SHARPLESS, N. E., PEROU, C. M., KIM, W. Y., GOMEZ, S. M., CHEN, X., JIN, J., FRYE, S. V., EARP, H. S., GRAVES, L. M. & JOHNSON, G. L. 2012. Dynamic Reprogramming of the Kinome In Response to Targeted MEK Inhibition In Triple Negative Breast Cancer. *Cell,* 149**,** 307-321.

WEIR, M. E,. MANN, J. E., CORWIN, T., FULTON, Z. W., HAO, J. M., MANISCALO, J. F., KENNEY, M. C., ROQUE, K. M. R., CHAPDELAINE, E. F., STELZL, U., DEMING, P. B., BALLIF, B. A. & HINKLE, K. L. 2016. Novel autophosphorylation sites of Src family kinases regulate kinase activity and SH2 domain-binding capacity. *FEBS Letters,* 590**,** 1042-1052.

EBINE, K., HIRAI, M., SAKAGUCHI, M., YAHATA, K., KANEKO, O. & SAITO-NAKANO, Y. 2016. *Plasmodium* Rab5b is secreted to the cytoplasmic face of the tubovesicular network in infected red blood cells together with N-acylated adenylate kinase 2. *Malaria Journal,* 15**,** 323.

EKSI, S., MORAHAN, B. J., HAILE, Y., FURUYA, T., JIANG, H., ALI, O., XU, H., KIATTIBUTR, K., SURI, A., CZESNY, B., ADEYEMO, A., MYERS, T. G., SATTABONGKOT, J., SU, X.-Z. & WILLIAMSON, K. C. 2012. *Plasmodium falciparum* Gametocyte Development 1 (*Pfgdv1*) and Gametocytogenesis Early Gene Identification and Commitment to Sexual Development. *PLOS Pathogens,* 8**,** e1002964.

ELLIOTT, D. A., MCINTOSH, M. T., HOSGOOD, H. D., CHEN, S., ZHANG, G., BAEVOVA, P. & JOINER, K. A. 2008. Four distinct pathways of hemoglobin uptake in the malaria parasite *Plasmodium falciparum*. *Proceedings of the National Academy of Sciences,* 105**,** 2463-2468.

ELSWORTH, B., SANDERS, P. R., NEBL, T., BATINOVIC, S., KALANON, M., NIE, C. Q., CHARNAUD, S. C., BULLEN, H. E., DE KONING WARD, T. F., TILLEY, L., CRABB, B. S. & GILSON, P. R. 2016. Proteomic analysis reveals novel proteins associated with the *Plasmodium* protein exporter PTEX and a loss of complex stability upon truncation of the core PTEX component, PTEX150. *Cellular Microbiology,* 18**,** 1551-1569.

ENG, G. W. L., EDISON & VIRSHUP, D. M. 2017. Site-specific phosphorylation of casein kinase 1 δ (CK1δ) regulates its activity towards the circadian regulator PER2. *PLOS ONE,* 12**,** e0177834.

ENGELBRECHT, D. & COETZER, T. L. 2016. *Plasmodium falciparum* exhibits markers of regulated cell death at high population density in vitro. *Parasitology International,* 65**,** 715-727.

ESTHER, P., SEBASTIAN, R., ANOUK, M., ANDREW, H., LEANN, T., ERIC, H. & HANS-PETER, B. 2010. MAHRP2, an exported protein of *Plasmodium falciparum*, is an essential component of Maurer's cleft tethers. *Molecular Microbiology,* 77**,** 1136-1152.

EUSTERMANN, S., SCHALL, K., KOSTREWA, D., LAKOMEK, K., STRAUSS, M., MOLDT, M. & HOPFNER, K.-P. 2018. Structural basis for ATP-dependent chromatin remodelling by the INO80 complex. *Nature,* 556**,** 386-390.

EYASE, F. L., AKALA, H. M., INGASIA, L., CHERUIYOT, A., OMONDI, A., OKUDO, C., JUMA, D., YEDA, R., ANDAGALU, B., WANJA, E., KAMAU, E., SCHNABEL, D., BULIMO, W., WATERS, N. C., WALSH, D. S. & JOHNSON, J. D. 2013. The Role of *Pfmdr1* and *Pfcrt* in Changing Chloroquine, Amodiaquine, Mefloquine and Lumefantrine Susceptibility in Western-Kenya *P. falciparum* Samples during 2008–2011. *PLOS ONE,* 8**,** e64299.

EZOUGOU, C. N., BEN-RACHED, F., MOSS, D. K., LIN, J.-W., BLACK, S., KNUEPFER, E., GREEN, J. L., KHAN, S. M., MUKHOPADHYAY, A., JANSE, C. J., COPPENS, I., YERA, H., HOLDER, A. A. & LANGSLEY, G. 2014. *Plasmodium falciparum* Rab5B Is an N-Terminally Myristoylated Rab GTPase That Is Targeted to the Parasite's Plasma and Food Vacuole Membranes. *PLOS ONE,* 9**,** e87695.

FABBRO, D., COWAN-JACOB, S. W., MÖBITZ, H. & MARTINY-BARON, G. 2012. Targeting cancer with small-molecular-weight kinase inhibitors. *Kinase Inhibitors.* Springer.

FENG, S., STREETS, A. J., NESIN, V., TRAN, U., NIE, H., ONOPIUK, M., WESSELY, O., TSIOKAS, L. & ONG, A. C. M. 2017. The Sorting Nexin 3 Retromer Pathway Regulates the Cell Surface Localization and Activity of a Wnt-Activated Polycystin Channel Complex. *Journal of the American Society of Nephrology,* 28**,** 2973-2984.

FERNANDEZ-GARCIA, P., PELAEZ, R., HERRERO, P. & MORENO, F. 2012. Phosphorylation of yeast hexokinase 2 regulates its nucleocytoplasmic shuttling. *Journal of Biological Chemistry*.

FISCHER, P, M., 2017. Approved and Experimental Small-Molecule Oncology Kinase Inhibitor Drugs: A Mid-2016 Overview. *Medicinal Research Reviews,* 37**,** 314-367.

FLETCHER, G. C., ELBEDIWY, A., KHANAL, I., RIBEIRO, P. S., TAPON, N. & THOMPSON, B. J. 2015. The Spectrin cytoskeleton regulates the Hippo signalling pathway. *The EMBO Journal*, p.e201489642

FLOTOW, H., GRAVES, P. R., WANG, A. Q., FIOL, C. J., ROESKE, R. W. & ROACH, P. J. 1990. Phosphate groups as substrate determinants for casein kinase I action. *Journal of Biological Chemistry,* 265**,** 14264-14269.

FLOTOW, H. & ROACH, P. J. 1991. Role of acidic residues as substrate determinants for casein kinase I. *Journal of Biological Chemistry,* 266**,** 3724-7.

FOLDYNOVÁ-TRANTÍRKOVÁ, S., SEKYROVÁ, P., TMEJOVÁ, K., BRUMOVSKÁ, E., BERNATÍK, O., BLANKENFELDT, W., KREJČÍ, P., KOZUBÍK, A., DOLEŽAL, T., TRANTÍREK, L. & BRYJA, V. 2010. Breast cancer-specific mutations in CK1ε inhibit Wnt/β-catenin and activate the Wnt/Rac1/JNK and NFAT pathways to decrease cell adhesion and promote cell migration. *Breast Cancer Research,* 12**,** R30.

FONTES, M. R., TRAZEL, T., GABOR, T., ANNA, J., IMRE, P. & BOSTJAN, K. 2003. Role of flanking sequences and phosphorylation in the recognition of the simian-virus-40 large T-antigen nuclear localization sequences by importin-α. *Biochemical Journal,* 375**,** 339-349.

FRIESE-HAMIM, M., BLADT, F., LOCATELLI, G., STAMMBERGER, U. & BLAUKAT, A. 2017. The selective c-Met inhibitor tepotinib can overcome epidermal growth factor receptor inhibitor resistance mediated by aberrant c-Met activation in NSCLC models. *American Journal of Cancer Research,* 7**,** 962-972.

FU, Z., CHAKRABORTI, T., MORSE, S., BENNETT, G. S. & SHAW, G. 2001. Four Casein Kinase I Isoforms Are Differentially Partitioned between Nucleus and Cytoplasm. *Experimental Cell Research,* 269**,** 275-286.

FUCHS, S. M., KIZER, K. O., BRABERG, H., KROGAN, N. J. & STRAHL, B. D. 2012. RNA Polymerase II Carboxyl-terminal Domain Phosphorylation Regulates Protein Stability of the Set2 Methyltransferase and Histone H3 Di- and Trimethylation at Lysine 36. *Journal of Biological Chemistry,* 287**,** 3249-3256.

FUGEL, W., OBERHOLZER, A. E., GSCHLOESSL, B., DZIKOWSKI, R., PRESSBURGER, N., PREU, L., PEARL, L. H., BARATTE, B., RATIN, M., OKUN, I., DOERIG, C., KRUGGEL, S., LEMCKE, T., MEIJER, L. & KUNICK, C. 2013. 3,6-Diamino-4-(2-halophenyl)-2-benzoylthieno[2,3-b]pyridine-5-carbonitriles Are Selective Inhibitors of *Plasmodium falciparum* Glycogen Synthase Kinase-3. *Journal of Medicinal Chemistry,* 56**,** 264-275.

FUJITA, M. & KINOSHITA, T. 2012. GPI-anchor remodeling: Potential functions of GPI-anchors in intracellular trafficking and membrane dynamics. *Biochimica et Biophysica Acta (BBA) - Molecular and Cell Biology of Lipids,* 1821**,** 1050-1058.

GAJER, J. M., FURDAS, S. D., GRÜNDER, A., GOTHWAL, M., HEINICKE, U., KELLER, K., COLLAND, F., FULDA, S., PAHL, H. L., FICHTNER, I., SIPPL, W. & JUNG, M. 2015. Histone acetyltransferase inhibitors block neuroblastoma cell growth in vivo. *Oncogenesis,* 4**,** e137.

GAMO, F.-J., SANZ, L. M., VIDAL, J., DE COZAR, C., ALVAREZ, E., LAVANDERA, J.-L., VANDERWALL, D. E., GREEN, D. V., KUMAR, V. & HASAN, S. 2010. Thousands of chemical starting points for antimalarial lead identification. *Nature,* 465**,** 305-310.

GARNER, P. 2013. Artemisinin Combination Therapy: A Good Antimalarial, but Is the Dose Right? *PLOS Med,* 10**,** e1001565.

GAVRILJUK, K., ITZEN, A., GOODY, R. S., GERWERT, K. & KÖTTING, C. 2013. Membrane extraction of Rab proteins by GDP dissociation inhibitor characterized using attenuated total reflection infrared spectroscopy. *Proceedings of the National Academy of Sciences,* 110**,** 13380-13385.

GEETHA, P., SIVARAM, A. J., JAYAKUMAR, R. & GOPI MOHAN, C. 2016. Integration of in silico modeling, prediction by binding energy and experimental approach to study the amorphous chitin nanocarriers for cancer drug delivery. *Carbohydrate Polymers,* 142**,** 240-249.

GHANSAH, A., AMENGA-ETEGO, L., AMAMBUA-NGWA, A., ANDAGALU, B., APINJOH, T., BOUYOU-AKOTET, M., CORNELIUS, V., GOLASSA, L., ANDRIANARANJAKA, V. H., ISHENGOMA, D., JOHNSON, K., KAMAU, E., MAÏGA-ASCOFARÉ, O., MUMBA, D., TINDANA, P., TSHEFU-KITOTO, A., RANDRIANARIVELOJOSIA, M., WILLIAM, Y., KWIATKOWSKI, D. P. & DJIMDE, A. A. 2014. Monitoring parasite diversity for malaria elimination in sub-Saharan Africa. *Science,* 345**,** 1297-1298.

GHERARDI, E., BIRCHMEIER, W., BIRCHMEIER, C. & WOUDE, G. V. 2012. Targeting MET in cancer: rationale and progress. *Nature Reviews Cancer,* 12**,** 89-103.

GILL, A. J. 2012. Succinate dehydrogenase (SDH) and mitochondrial driven neoplasia. *Pathology,* 44**,** 285-292.

GILL, A. J., BENN, D. E., CHOU, A., CLARKSON, A., MULJONO, A., MEYER-ROCHOW, G. Y., RICHARDSON, A. L., SIDHU, S. B., ROBINSON, B. G. & CLIFTON-BLIGH, R. J. 2010. Immunohistochemistry for SDHB triages genetic testing of SDHB, SDHC, and SDHD in paraganglioma-pheochromocytoma syndromes. *Human Pathology,* 41**,** 805-814.

GOODMAN, C. D. & MCFADDEN, G. I. 2014. Ycf93 (Orf105), a Small Apicoplast-Encoded Membrane Protein in the Relict Plastid of the Malaria Parasite *Plasmodium falciparum* That Is Conserved in Apicomplexa. *PLOS ONE,* 9**,** e91178.

GOVINDASAMY, K., JEBIWOTT, S., JAIJYAN, D. K., DAVIDOW, A., OJO, K. K., VAN VOORHIS, W. C., BROCHET, M., BILLKER, O. & BHANOT, P. 2016. Invasion of hepatocytes by *Plasmodium* sporozoites requires cGMP-dependent protein kinase and calcium dependent protein kinase 4. *Molecular Microbiology,* 102**,** 349-363.

GRAVES, P. R. & ROACH, P. J. 1995. Role of COOH-terminal Phosphorylation in the Regulation of Casein Kinase Iδ. *Journal of Biological Chemistry,* 270**,** 21689-21694.

GRAY, N. S., WOKICKA, L., THUNNISSEN, A.-M. W. H., NORMAN, T. C., SOOJIN, K., ESPINOZA, F. H., MORGAN, D. O., BARNES, G., LECLERC, S., MEIJER, L., SUNG-HOU, K., LOCKHART, D. J. & SCHULTZ, P. G. 1998. Exploiting chemical libraries, structure, and genomics in the search for kinase inhibitors. *Science,* 281**,** 533-538.

GREER, Y. E., GAO, B., YANG, Y., NUSSENZWEIG, A. & RUBIN, J. S. 2017. Lack of Casein Kinase 1 Delta Promotes Genomic Instability - The Accumulation of DNA Damage and Down-Regulation of Checkpoint Kinase 1. *PLOS ONE,* 12**,** e0170903.

GRINDHEIM, A. K., HOLLÅS, H., RAMIREZ, J., SARASTE, J., TRAVÉ, G. & VEDELER, A. 2014. Effect of Serine Phosphorylation and Ser25 Phospho-Mimicking Mutations on Nuclear Localisation and Ligand Interactions of Annexin A2. *Journal of Molecular Biology,* 426**,** 2486-2499.

GROZINGER, C. M. & SCHREIBER, S. L. 2000. Regulation of histone deacetylase 4 and 5 and transcriptional activity by 14-3- 3-dependent cellular localization. *Proceedings of the National Academy of Sciences,* 97**,** 7835-7840.

GRÜRING, C., HEIBER, A., KRUSE, F., UNGEFEHR, J., GILBERGER, T.-W. & SPIELMANN, T. 2011. Development and host cell modifications of *Plasmodium falciparum* blood stages in four dimensions. *Nature Communications,* 2**,** 165.

GRÜRING, C., MOON, R. W., LIM, C., HOLDER, A. A., BLACKMAN, M. J. & DURAISINGH, M. T. 2014. Human red blood cell-adapted *Plasmodium knowlesi* parasites: a new model system for malaria research. *Cellular microbiology,* 16**,** 612-620.

GUERREIRO, A., DELIGIANNI, E., SANTOS, J. M., SILVA, P. A., LOUIS, C., PAIN, A., JANSE, C. J., FRANKE-FAYARD, B., CARRET, C. K., SIDEN-KIAMOS, I. & MAIR, G. R. 2014. Genome-wide RIP-Chip analysis of translational repressor-bound mRNAs in the *Plasmodium* gametocyte. *Genome Biology,* 15**,** 493.

GUPTA, A., BALABASKARAN-NINA, P., NGUITRAGOOL, W., SAGGU, G. S., SCHURECK, M. A. & DESAI, S. A. 2018. CLAG3 Self-Associates in Malaria Parasites and Quantitatively Determines Nutrient Uptake Channels at the Host Membrane. *mBio,* 9.

GURNETT, A. M., LIBERATOR, P. A., DULSKI, P. M., SALOWE, S. P., DONALD, R. G. K., ANDERSON, J. W., WILTSIE, J., DIAZ, C. A., HARRIS, G., CHANG, B., DARKIN-RATTRAY, S. J., NARE, B., CRUMLEY, T., BLUM, P. S., MISURA, A. S., TAMAS, T., SARDANA, M. K., YUAN, J., BIFTU, T. & SCHMATZ, D. M. 2002. Purification and Molecular Characterization of cGMP-dependent Protein Kinase from Apicomplexan Parasites: A novel chemotherapeutic target. *Journal of Biological Chemistry,* 277**,** 15913-15922.

GUTTERY, D. S., ROQUES, M., HOLDER, A. A. & TEWARI, R. 2015. Commit and Transmit: Molecular Players in *Plasmodium* Sexual Development and Zygote Differentiation. *Trends in Parasitology,* 31**,** 676-685.

HALL, N., KARRAS, M., RAINE, J. D., CARLTON, J. M., KOOIJ, T. W. A., BERRIMAN, M., FLORENS, L., JANSSEN, C. S., PAIN, A., CHRISTOPHIDES, G. K., JAMES, K., RUTHERFORD, K., HARRIS, B., HARRIS, D., CHURCHER, C., QUAIL, M. A., ORMOND, D., DOGGETT, J., TRUEMAN, H. E., MENDOZA, J., BIDWELL, S. L., RAJANDREAM, M.-A., CARUCCI, D. J., YATES, J. R., KAFATOS, F. C., JANSE, C. J., BARRELL, B., TURNER, C. M. R., WATERS, A. P. & SINDEN, R. E. 2005. A Comprehensive Survey of the *Plasmodium* Life Cycle by Genomic, Transcriptomic, and Proteomic Analyses. *Science,* 307**,** 82-86.

HALLÉE, S. & RICHARD, D. 2015. Evidence that the Malaria Parasite *Plasmodium falciparum* Putative Rhoptry Protein 2 Localizes to the Golgi Apparatus throughout the Erythrocytic Cycle. *PLOS ONE,* 10**,** e0138626.

HARMSE, L., VAN ZYL, R., GRAY, N., SCHULTZ, P., LECLERC, S., MEIJER, L., DOERIG, C. & HAVLIK, I. 2001. Structure-activity relationships and inhibitory effects of various purine derivatives on the in vitro growth of *Plasmodium falciparum*. *Biochemical Pharmacology,* 62**,** 341-348.

HARTERINK, M., PORT, F., LORENOWICZ, M. J., MCGOUGH, I. J., SILHANKOVA, M., BETIST, M. C., VAN WEERING, J. R. T., VAN HEESBEEN, R. G. H. P., MIDDELKOOP, T. C., BASLER, K., CULLEN, P. J. & KORSWAGEN, H. C. 2011. A SNX3-dependent retromer pathway mediates retrograde transport of the Wnt sorting receptor Wntless and is required for Wnt secretion. *Nature Cell Biology,* 13**,** 914.

HAUSMANN, M., WAGNER, E., LEE, J.-H., SCHROCK, G., SCHAUFLER, W., KRUFCZIK, M., PAPENFU, PORT, M., BESTVATER, F. & SCHERTHAN, H. 2018. Super-resolution localization microscopy of radiation-induced histone H2AX-phosphorylation in relation to H3K9-trimethylation in HeLa cells. *Nanoscale,* 10**,** 4320-4331.

HEBIGUCHI, M., HIROKAWA, M., GUO, Y.-M., SAITO, K., WAKUI, H., KOMATSUDA, A., FUJISHIMA, N., TAKAHASHI, N., TAKAHASHI, T. & SASAKI, T. 2008. Dynamics of human erythroblast enucleation. *International journal of hematology,* 88**,** 498-507.

HEIBER, A., KRUSE, F., PICK, C., GRÜRING, C., FLEMMING, S., OBERLI, A., SCHOELER, H., RETZLAFF, S., MESÉN-RAMÍREZ, P., HISS, J. A., KADEKOPPALA, M., HECHT, L., HOLDER, A. A., GILBERGER, T.-W. & SPIELMANN, T. 2013. Identification of New PNEPs Indicates a Substantial Non-PEXEL Exportome and Underpins Common Features in *Plasmodium falciparum* Protein Export. *PLOS Pathogens,* 9**,** e1003546.

HEIN, MARCO Y., HUBNER, NINA C., POSER, I., COX, J., NAGARAJ, N., TOYODA, Y., GAK, IGOR A., WEISSWANGE, I., MANSFELD, J., BUCHHOLZ, F., HYMAN, ANTHONY A. & MANN, M. 2015. A Human Interactome in Three Quantitative Dimensions Organized by Stoichiometries and Abundances. *Cell,* 163**,** 712-723.

HENKELS, K, M., FRONDORF, K., GONZALEZ-MEJIA, M, E., DOSEFF, A, L., & GOMEZ-CAMBRONERO, J. 2011. IL-8-induced neutrophil chemotaxis is mediated by Janus kinase 3 (JAK3). *FEBS Letters,* 585**,** 159-166.

HERMAN, E, K., ALI, M., FIELD, M, C,. M & DACKS, J, B. 2018. Regulation of early endosomes across eukaryotes: Evolution and functional homology of Vps9 proteins. *Traffic,* 1-18.

HINTERSTEINER, M., AMBRUS, G., BEDNENKO, J., SCHMIED, M., KNOX, A. J. S., GSTACH, H., SEIFERT, J.-M., SINGER, E. L., GERACE, L. & AUER, M. 2010. Identification of a small molecule inhibitor of importin beta mediated nuclear import by confocal on-bead screening of tagged one-bead one-compound libraries. *ACS chemical biology,* 5**,** 967-979.

HIRATA, T., FUJITA, M., NAKAMURA, S., GOTOH, K., MOTOOKA, D., MURAKAMI, Y., MAEDA, Y., KINOSHITA, T. & PARTON, R. G. 2015. Post-Golgi anterograde transport requires GARP-dependent endosome-to-TGN retrograde transport. *Molecular Biology of the Cell,* 26**,** 3071-3084.

HISS, J. A., PRZYBORSKI, J. M., SCHWARTE, F., LINGELBACH, K. & SCHNEIDER, G. 2008. The *Plasmodium* Export Element Revisited. *PLOS ONE,* 3**,** e1560.

HO, Y., MASON, S., KOBAYASHI, R., HOEKSTRA, M. & ANDREWS, B. 1997. Role of the casein kinase I isoform, Hrr25, and the cell cycle-regulatory transcription factor, SBF, in the transcriptional response to DNA damage in *Saccharomyces cerevisiae*. *Proceedings of the National Academy of Sciences,* 94**,** 581-586.

HOLTON, S., MERCKX, A., BURGESS, D., DOERIG, C., NOBLE, M. & ENDICOTT, J. 2003. Structures of P. falciparum PfPK5 Test the CDK Regulation Paradigm and Suggest Mechanisms of Small Molecule Inhibition. *Structure,* 11**,** 1329-1337.

HUH, W.-K., FALVO, J. V., GERKE, L. C., CARROLL, A. S., HOWSON, R. W., WEISSMAN, J. S. & O'SHEA, E. K. 2003. Global analysis of protein localization in budding yeast. *Nature,* 425**,** 686.

HUMPHREY, SEAN J., YANG, G., YANG, P., FAZAKERLEY, DANIEL J., STÖCKLI, J., YANG, JEAN Y. & JAMES, DAVID E. 2013. Dynamic Adipocyte Phosphoproteome Reveals that Akt Directly Regulates mTORC2. *Cell Metabolism,* 17**,** 1009-1020.

HUNJA, C. W., UNGER, H., FERREIRA, P. E., LUMSDEN, R., MORRIS, S., AMAN, R., ALEXANDER, C., MITA, T. & CULLETON, R. 2013. Travellers as sentinels: Assaying the worldwide distribution of polymorphisms associated with artemisinin combination therapy resistance in *Plasmodium falciparum* using malaria cases imported into Scotland. *International Journal for Parasitology,* 43**,** 885-889.

HUTTLIN, E. L., BRUCKNER, R. J., PAULO, J. A., CANNON, J. R., TING, L., BALTIER, K., COLBY, G., GEBREAB, F., GYGI, M. P., PARZEN, H., SZPYT, J., TAM, S., ZARRAGA, G., PONTANO-VAITES, L., SWARUP, S., WHITE, A. E., SCHWEPPE, D. K., RAD, R., ERICKSON, B. K., OBAR, R. A., GURUHARSHA, K. G., LI, K., ARTAVANIS-TSAKONAS, S., GYGI, S. P. & HARPER, J. W. 2017. Architecture of the human interactome defines protein communities and disease networks. *Nature,* 545**,** 505.

HYLAND, E. M., COSGROVE, M. S., MOLINA, H., WANG, D., PANDEY, A., COTTEE, R. J. & BOEKE, J. D. 2005. Insights into the Role of Histone H3 and Histone H4 Core Modifiable Residues in *Saccharomyces cerevisiae*. *Molecular and Cellular Biology,* 25**,** 10060-10070.

IKADAI, H., SHAW SALIBA, K., KANZOK, S. M., MCLEAN, K. J., TANAKA, T. Q., CAO, J., WILLIAMSON, K. C. & JACOBS-LORENA, M. 2013. Transposon mutagenesis identifies genes essential for *Plasmodium falciparum* gametocytogenesis. *Proceedings of the National Academy of Sciences,* 110**,** E1676–E1684.

ITO, T., BULGER, M., KOBAYASHI, R. & KADONAGA, J. T. 1996. Drosophila NAP-1 is a core histone chaperone that functions in ATP-facilitated assembly of regularly spaced nucleosomal arrays. *Molecular and Cellular Biology,* 16**,** 3112-3124.

JACKSON, A, J., CLUCAS, C., MAMCZUR, N, J., FERGUSON. D, J., & MEISSNER, M. 2013. *Toxoplasma gondii* Syntaxin 6 Is Required for Vesicular Transport Between Endosomal-Like Compartments and the Golgi Complex. *Traffic,* 14**,** 1166-1181.

JAMBOU, R., ZAHRAOUI, A., OLOFSSON, B., TAVITIAN, A. & JAUREGUIBERRY, G. 1996. Small GTP-binding proteins in *Plasmodium falciparum*. *Biology of the Cell,* 88**,** 113-121.

JANG, B.-C., MUÑOZ-NAJAR, U., PAIK, J.-H., CLAFFEY, K., YOSHIDA, M. & HLA, T. 2003. Leptomycin B, an Inhibitor of the Nuclear Export Receptor CRM1, Inhibits COX-2 Expression. *Journal of Biological Chemistry,* 278**,** 2773-2776.

JANJIGIAN, Y. Y., SMIT, E. F., GROEN, H. J. M., HORN, L., GETTINGER, S., CAMIDGE, D. R., RIELY, G. J., WANG, B., FU, Y., CHAND, V. K., MILLER, V. A. & PAO, W. 2014. Dual Inhibition of EGFR with Afatinib and Cetuximab in Kinase Inhibitor-Resistant *EGFR*-Mutant Lung Cancer with and without T790M Mutations. *Cancer Discovery*.

JANOUŠKOVEC, J., HORÁK, A., OBORNÍK, M., LUKEŠ, J. & KEELING, P. J. 2010. A common red algal origin of the apicomplexan, dinoflagellate, and heterokont plastids. *Proceedings of the National Academy of Sciences,* 107**,** 10949-10954.

JANSSEN, A., BREUER, G. A., BRINKMAN, E. K., VAN DER MEULEN, A. I., BORDEN, S. V., VAN STEENSEL, B., BINDRA, R. S., LAROCQUE, J. R. & KARPEN, G. H. 2016. A single double-strand break system reveals repair dynamics and mechanisms in heterochromatin and euchromatin. *Genes & Development,* 30**,** 1645-1657.

JHA, S. K., SINGH, H. R., SINHA, R. K. & PRAKASH, P. 2017. In Silico Modelling of Hepatocellular Carcinoma Linked PARP-1 Protein and Screening of Potential Inhibitors. *Applications of Biotechnology for Sustainable Development*, 157-168.

JIANG, L., MU, J., ZHANG, Q., NI, T., SRINIVASAN, P., RAYAVARA, K., YANG, W., TURNER, L., LAVSTSEN, T., THEANDER, T. G., PENG, W., WEI, G., JING, Q., WAKABAYASHI, Y., BANSAL, A., LUO, Y., RIBEIRO, J. M. C., SCHERF, A., ARAVIND, L., ZHU, J., ZHAO, K. & MILLER, L. H. 2013. PfSETvs methylation of histone H3K36 represses virulence genes in *Plasmodium falciparum*. *Nature,* 499**,** 223.

JONES, MATTHEW L., COLLINS, MARK O., GOULDING, D., CHOUDHARY, JYOTI S. & RAYNER, JULIAN C. 2012. Analysis of Protein Palmitoylation Reveals a Pervasive Role in *Plasmodium* Development and Pathogenesis. *Cell Host & Microbe,* 12**,** 246-258.

JONES, P. A. 2012. Functions of DNA methylation: islands, start sites, gene bodies and beyond. *Nature Reviews Genetics,* 13**,** 484.

JUNG, T., HÖHN, A. & GRUNE, T. 2014. The proteasome and the degradation of oxidized proteins: Part III—Redox regulation of the proteasomal system. *Redox Biology,* 2**,** 388-394.

KAISER, G., DE NIZ, M., ZUBER, B., BURDA, P.-C., KORNMANN, B., HEUSSLER, V. T. & STANWAY, R. R. 2016. High resolution microscopy reveals an unusual architecture of the *Plasmodium berghei* endoplasmic reticulum. *Molecular Microbiology,* 102**,** 775-791.

KATAYAMA, H. & SEN, S. 2010. Aurora kinase inhibitors as anticancer molecules. *Biochimica et Biophysica Acta (BBA) - Gene Regulatory Mechanisms,* 1799**,** 829-839.

KATRIS, N. J., VAN DOOREN, G. G., MCMILLAN, P. J., HANSSEN, E., TILLEY, L. & WALLER, R. F. 2014. The Apical Complex Provides a Regulated Gateway for Secretion of Invasion Factors in *Toxoplasma*. *PLOS Pathogens,* 10**,** e1004074.

KEERTHIVASAN, G., SMALL, S., LIU, H., WICKREMA, A. & CRISPINO, J. D. 2010. Vesicle trafficking plays a novel role in erythroblast enucleation. *Blood,* 116**,** 3331-3340.

KENSCHE, PHILIP R., HOEIJMAKERS, WIETEKE ANNA M., TOENHAKE, CHRISTA G., BRAS, M., CHAPPELL, L., BERRIMAN, M. & BÁRTFAI, R. 2016. The nucleosome landscape of *Plasmodium falciparum* reveals chromatin architecture and dynamics of regulatory sequences. *Nucleic Acids Research,* 44**,** 2110-2124.

KISHORE, S. P., PERKINS, S. L., TEMPLETON, T. J. & DEITSCH, K. W. 2009. An unusual recent expansion of the C-terminal domain of RNA polymerase II in primate malaria parasites features a motif otherwise found only in mammalian polymerases. *Journal of molecular evolution,* 68**,** 706-714.

KIZER, K. O., PHATNANI, H. P., SHIBATA, Y., HALL, H., GREENLEAF, A. L. & STRAHL, B. D. 2005. A Novel Domain in Set2 Mediates RNA Polymerase II Interaction and Couples Histone H3 K36 Methylation with Transcript Elongation. *Molecular and Cellular Biology,* 25**,** 3305-3316.

KNIPPSCHILD, U., GOCHT, A., WOLFF, S., HUBER, N., LÖHLER, J. & STÖTER, M. 2005. The casein kinase 1 family: participation in multiple cellular processes in eukaryotes. *Cellular signalling,* 17**,** 675-689.

KNIPPSCHILD, U., KRÜGER, M., RICHTER, J., XU, P., GARCÍA-REYES, B., PEIFER, C., HALEKOTTE, J., BAKULEV, V. & BISCHOF, J. 2014. The CK1 family: contribution to cellular stress response and its role in carcinogenesis. *Frontiers in oncology,* 4.

KNOCKAERT, M., GRAY, N., DAMIENS, E., CHANG, Y., GRELLIER, P., GRANT, K., FERGUSSON, D., MOTTRAM, J., SOETE, M. & DUBREMETZ, J. 2000. Intracellular targets of cyclin-dependent kinase inhibitors: identification by affinity chromatography using immobilised inhibitors. *Chemistry & biology,* 7**,** 411-422.

KORNILOV, R., PUHKA, M., MANNERSTRÖM, B., HIIDENMAA, H., PELTONIEMI, H., SILJANDER, P., SEPPÄNEN-KAIJANSINKKO, R. & KAUR, S. 2018. Efficient ultrafiltration-based protocol to deplete extracellular vesicles from fetal bovine serum. *Journal of Extracellular Vesicles,* 7**,** 1422674.

KORSINCZKY, M., CHEN, N., KOTECKA, B., SAUL, A., RIECKMANN, K. & CHENG, Q. 2000. Mutations in *Plasmodium falciparum*Cytochrome b That Are Associated with Atovaquone Resistance Are Located at a Putative Drug-Binding Site. *Antimicrobial agents and chemotherapy,* 44**,** 2100-2108.

KRAI, P., DALAL, S. & KLEMBA, M. 2014. Evidence for a Golgi-to-Endosome Protein Sorting Pathway in *Plasmodium falciparum*. *PLOS ONE,* 9**,** e89771.

KRAPIVINSKY, G., KRAPIVINSKY, L., RENTHAL, N. E., SANTA-CRUZ, A., MANASIAN, Y. & CLAPHAM, D. E. 2017. Histone phosphorylation by TRPM6's cleaved kinase attenuates adjacent arginine methylation to regulate gene expression. *Proceedings of the National Academy of Sciences,* 114**,** E7092-E7100.

KRIEK, N., TILLEY, L., HORROCKS, P., PINCHES, R., ELFORD, B. C., FERGUSON, D. J. P., LINGELBACH, K. & NEWBOLD, C. I. 2003. Characterization of the pathway for transport of the cytoadherence-mediating protein, PfEMP1, to the host cell surface in malaria parasite-infected erythrocytes. *Molecular Microbiology,* 50**,** 1215-1227.

KUMAR, R., PAVITHRA, S. R. & TATU, U. 2007. Three-dimensional structure of heat shock protein 90 from *Plasmodium falciparum*: molecular modelling approach to rational drug design against malaria. *Journal of biosciences,* 32**,** 531-536.

LAIA, S.-R. & MANEL, E. 2015. Targeting the histone orthography of cancer: drugs for writers, erasers and readers. *British Journal of Pharmacology,* 172**,** 2716-2732.

LAKSHMANAN, V., BRAY, P. G., VERDIER-PINARD, D., JOHNSON, D. J., HORROCKS, P., MUHLE, R. A., ALAKPA, G. E., HUGHES, R. H., WARD, S. A., KROGSTAD, D. J., SIDHU, A. B. S. & FIDOCK, D. A. 2005. A critical role for PfCRT K76T in *Plasmodium falciparum* verapamil-reversible chloroquine resistance. *The EMBO Journal,* 24**,** 2294-2305.

LAM, V., YING LI, M., MURPHY, K., KWOK, R. & CHIU, J. 2015. Casein Kinase 1 Alpha (CK1a) Promotes Nuclear Entry of PERIOD and Represses CLOCK transcriptional activity in the *Drosophila melanogaster* Circadian Clock. *The FASEB Journal,* 29**,** 724.26.

LAMOUR, S. D., STRASCHIL, U., SARIC, J. & DELVES, M. J. 2014. Changes in metabolic phenotypes of *Plasmodium falciparum* in vitro cultures during gametocyte development. *Malaria Journal,* 13**,** 468.

LAN, J., LEPIKHOV, K., GIEHR, P. & WALTER, J. 2017. Histone and DNA methylation control by H3 serine 10/threonine 11 phosphorylation in the mouse zygote. *Epigenetics & Chromatin,* 10**,** 5.

LANGE, A., MILLS, R. E., LANGE, C. J., STEWART, M., DEVINE, S. E. & CORBETT, A. H. 2007. Classical Nuclear Localization Signals: Definition, Function, and Interaction with Importin α. *Journal of Biological Chemistry,* 282**,** 5101-5105.

LASONDER, E., GREEN, J. L., CAMARDA, G., TALABANI, H., HOLDER, A. A., LANGSLEY, G. & ALANO, P. 2012a. The *Plasmodium falciparum* Schizont Phosphoproteome Reveals Extensive Phosphatidylinositol and cAMP-Protein Kinase A Signaling. *Journal of Proteome Research,* 11**,** 5323-5337.

LASONDER, E., RIJPMA, S. R., VAN SCHAIJK, B. C., HOEIJMAKERS, W. A., KENSCHE, P. R., GRESNIGT, M. S., ITALIAANDER, A., VOS, M. W., WOESTENENK, R. & BOUSEMA, T. 2016. Integrated transcriptomic and proteomic analyses of P. falciparum gametocytes: molecular insight into sex-specific processes and translational repression. *Nucleic acids research,* 44**,** 6087-6101.

LASONDER, E., TREECK, M., ALAM, M. & TOBIN, A. B. 2012b. Insights into the *Plasmodium falciparum* schizont phospho-proteome. *Microbes and Infection,* 14**,** 811-819.

LAWRENCE, R. T., SEARLE, B. C., LLOVET, A. & VILLEN, J. 2016. Plug-and-play analysis of the human phosphoproteome by targeted high-resolution mass spectrometry. *Nature Methods,* 13**,** 431-434.

LE ROCH, K. G., JOHNSON, J. R., FLORENS, L., ZHOU, Y., SANTROSYAN, A., GRAINGER, M., YAN, S. F., WILLIAMSON, K. C., HOLDER, A. A., CARUCCI, D. J., YATES, J. R. & WINZELER, E. A. 2004. Global analysis of transcript and protein levels across the *Plasmodium falciparum* life cycle. *Genome Research,* 14**,** 2308-2318.

LEBA, L.-J., MUSSET, L., PELLEAU, S., ESTEVEZ, Y., BIRER, C., BRIOLANT, S., WITKOWSKI, B., MÉNARD, D., DELVES, M. J. & LEGRAND, E. 2015. Use of *Plasmodium falciparum* culture-adapted field isolates for in vitro exflagellation-blocking assay. *Malaria journal,* 14**,** 1-4.

LEE, M. G., VILLA, R., TROJER, P., NORMAN, J., YAN, K.-P., REINBERG, D., DI CROCE, L. & SHIEKHATTAR, R. 2007. Demethylation of H3K27 Regulates Polycomb Recruitment and H2A Ubiquitination. *Science,* 318**,** 447-450.

LEKE, R. G. F. & TAYLOR, D. W. 2011. The use of intermittent preventive treatment with sulfadoxine-pyrimethamine for preventing malaria in pregnant women. *Clinical Infectious Diseases, 53, 231-233*.

LENOIR, M., USTUNEL, C., RAJESH, S., KAUR, J., MOREAU, D., GRUENBERG, J. & OVERDUIN, M. 2018. Phosphorylation of conserved phosphoinositide binding pocket regulates sorting nexin membrane targeting. *Nature Communications,* 9**,** 993.

LESTER, D. S., HERMOSO, T. & JAFFE, C. L. 1990. Extracellular phosphorylation in the parasite, *Leishmania major*. *Biochimica et Biophysica Acta (BBA) - Molecular Cell Research,* 1052**,** 293-298.

LETO, D. & SALTIEL, A. R. 2012. Regulation of glucose transport by insulin: traffic control of GLUT4. *Nature Reviews Molecular Cell Biology,* 13**,** 383.

LEYKAUF, K., TREECK, M., GILSON, P. R., NEBL, T., BRAULKE, T., COWMAN, A. F., GILBERGER, T. W. & CRABB, B. S. 2010. Protein Kinase A Dependent Phosphorylation of Apical Membrane Antigen 1 Plays an Important Role in Erythrocyte Invasion by the Malaria Parasite. *PLOS Pathogens,* 6**,** e1000941.

LI, F., YI, L., ZHAO, L., ITZEN, A., GOODY, R. S. & WU, Y.-W. 2014. The role of the hypervariable C-terminal domain in Rab GTPases membrane targeting. *Proceedings of the National Academy of Sciences,* 111**,** 2572-2577.

LI, S., AULT, A., MALONE, C. L., RAITT, D., DEAN, S., JOHNSTON, L. H., DESCHENES, R. J. & FASSLER, J. S. 1998. The yeast histidine protein kinase, Sln1p, mediates phosphotransfer to two response regulators, Ssk1p and Skn7p. *The EMBO Journal,* 17**,** 6952-6962.

LI, Y., LIN, J., LI, L., PENG, Y., WANG, W., ZHOU, Y., TANG, D., ZHAO, X., YU, F. & LIU, X. 2016. DHHC-cysteine-rich domain S-acyltransferase protein family in rice: organization, phylogenetic relationship and expression pattern during development and stress. *Plant Systematics and Evolution,* 302**,** 1405-1417.

LIEWEN, H., MEINHOLD-HEERLEIN, I., OLIVEIRA, V., SCHWARZENBACHER, R., LUO, G., WADLE, A., JUNG, M., PFREUNDSCHUH, M. & STENNER-LIEWEN, F. 2005. Characterization of the human GARP (Golgi associated retrograde protein) complex. *Experimental Cell Research,* 306**,** 24-34.

LIN, B. C., HARRIS, D. R., KIRKMAN, L. M. D., PEREZ, A. M., QIAN, Y., SCHERMERHORN, J. T., HONG, M. Y., WINSTON, D. S., XU, L., LIEBER, A. M., HAMILTON, M. & BRANDT, G. S. 2017. The anthraquinone emodin inhibits the non-exported FIKK kinase from *Plasmodium falciparum*. *Bioorganic Chemistry,* 75**,** 217-223.

LISK, G. & DESAI, S. A. 2005. The Plasmodial Surface Anion Channel Is Functionally Conserved in Divergent Malaria Parasites. *Eukaryotic Cell,* 4**,** 2153-2159.

LIU, J., CARVALHO, L. P., BHATTACHARYA, S., CARBONE, C. J., KUMAR, K. G. S., LEU, N. A., YAU, P. M., DONALD, R. G. K., WEISS, M. J., BAKER, D. P., MCLAUGHLIN, K. J., SCOTT, P. & FUCHS, S. Y. 2009. Mammalian Casein Kinase 1α and Its *Leishmanial* Ortholog Regulate Stability of IFNAR1 and Type I Interferon Signaling. *Molecular and Cellular Biology,* 29**,** 6401-6412.

LLINÁS, M., BOZDECH, Z., WONG, E. D., ADAI, A. T. & DERISI, J. L. 2006. Comparative whole genome transcriptome analysis of three *Plasmodium falciparum* strains. *Nucleic Acids Research,* 34**,** 1166-1173.

LO, W.-S., DUGGAN, L., TOLGA , N. C., EMRE, BELOTSERKOVSKYA, R., LANE, W. S., SHIEKHATTAR, R. & BERGER, S. L. 2001. Snf1--a Histone Kinase That Works in Concert with the Histone Acetyltransferase Gcn5 to Regulate Transcription. *Science,* 293**,** 1142-1146.

LOBBESTAEL, E., CIVIERO, L., DE WIT, T., TAYMANS, J. M., GREGGIO, E. & BAEKELANDT, V. 2016. Pharmacological LRRK2 kinase inhibition induces LRRK2 protein destabilization and proteasomal degradation. *Scientific Reports,* 6**,** 33897.

LODHI, I. J., BRIDGES, D., CHIANG, S.-H., ZHANG, Y., CHENG, A., GELETKA, L. M., WEISMAN, L. S. & SALTIEL, A. R. 2008. Insulin Stimulates Phosphatidylinositol 3-Phosphate Production via the Activation of Rab5. *Molecular Biology of the Cell,* 19**,** 2718-2728.

LODHI, I. J., CHIANG, S.-H., CHANG, L., VOLLENWEIDER, D., WATSON, R. T., INOUE, M., PESSIN, J. E. & SALTIEL, A. R. 2007. Gapex-5, a Rab31 Guanine Nucleotide Exchange Factor that Regulates Glut4 Trafficking in Adipocytes. *Cell Metabolism,* 5**,** 59-72.

LONGENECKER, K. L., ROACH, P. J. & HURLEY, T. D. 1998. Crystallographic studies of casein kinase I delta toward a structural understanding of auto-inhibition. *Acta Crystallographica Section D: Biological Crystallography,* 54, 473-475.

LOW, H., CHUA, C. S. & SIM, T.-S. 2012. *Plasmodium falciparum* possesses a unique dual-specificity serine/threonine and tyrosine kinase, Pfnek3. *Cellular and Molecular Life Sciences,* 69**,** 1523-1535.

LUCET, I., TOBIN, A., DREWRY, D., WILKS, A. F. & DOERIG, C. 2012. Plasmodium kinases as targets for new-generation antimalarials. *Future Medicinal Chemistry,* 4**,** 2295-2310.

LUGER, K., MÄDER, A. W., RICHMOND, R. K., SARGENT, D. F. & RICHMOND, T. J. 1997. Crystal structure of the nucleosome core particle at 2.8 Å resolution. *Nature,* 389**,** 251.

LUO, L., HANNEMANN, M., KOENIG, S., HEGERMANN, J., AILION, M., CHO, M.-K., SASIDHARAN, N., ZWECKSTETTER, M., RENSING, S. A., EIMER, S. & LINSTEDT, A. D. 2011. The *Caenorhabditis elegans* GARP complex contains the conserved Vps51 subunit and is required to maintain lysosomal morphology. *Molecular Biology of the Cell,* 22**,** 2564-2578.

MACDONALD, N., WELBURN, J. P. I., NOBLE, M. E. M., NGUYEN, A., YAFFE, M. B., CLYNES, D., MOGGS, J. G., ORPHANIDES, G., THOMSON, S., EDMUNDS, J. W., CLAYTON, A. L., ENDICOTT, J. A. & MAHADEVAN, L. C. 2005. Molecular Basis for the Recognition of Phosphorylated and Phosphoacetylated Histone H3 by 14-3-3. *Molecular Cell,* 20**,** 199-211.

MACHNICKA, B., GROCHOWALSKA, R., BOGUSŁAWSKA, D. M., SIKORSKI, A. F. & LECOMTE, M. C. 2012. Spectrin-based skeleton as an actor in cell signaling. *Cellular and Molecular Life Sciences,* 69**,** 191-201.

MAHARJAN, S., OKU, M., TSUDA, M., HOSEKI, J. & SAKAI, Y. 2014. Mitochondrial impairment triggers cytosolic oxidative stress and cell death following proteasome inhibition. *Scientific Reports,* 4**,** 5896.

MAIR, G. R., BRAKS, J. A. M., GARVER, L. S., WIEGANT, J. C. A. G., HALL, N., DIRKS, R. W., KHAN, S. M., DIMOPOULOS, G., JANSE, C. J. & WATERS, A. P. 2006a. Regulation of Sexual Development of *Plasmodium* by Translational Repression. *Science,* 313**,** 667-669.

MAIR, G. R., BRAKS, J. A. M., GARVER, L. S., WIEGANT, J. C. A. G., HALL, N., DIRKS, R. W., KHAN, S. M., DIMOPOULOS, G., JANSE, C. J. & WATERS, A. P. 2006b. Regulation of Sexual Development of *Plasmodium* by Translational Repression. *Science,* 313**,** 667-669.

MAIR, G. R., LASONDER, E., GARVER, L. S., FRANKE-FAYARD, B. M. D., CARRET, C. K., WIEGANT, J. C. A. G., DIRKS, R. W., DIMOPOULOS, G., JANSE, C. J. & WATERS, A. P. 2010. Universal Features of Post-Transcriptional Gene Regulation Are Critical for *Plasmodium* Zygote Development. *PLOS Pathogens,* 6**,** e1000767.

MANNING, G., WHYTE, D. B., MARTINEZ, R., HUNTER, T. & SUDARSANAM, S. 2002. The protein kinase complement of the human genome. *Science,* 298**,** 1912+.

MANTEL, P.-Y., HOANG, ANH N., GOLDOWITZ, I., POTASHNIKOVA, D., HAMZA, B., VOROBJEV, I., GHIRAN, I., TONER, M., IRIMIA, D., IVANOV, ALEXANDER R., BARTENEVA, N. & MARTI, M. 2013. Malaria-Infected Erythrocyte-Derived Microvesicles Mediate Cellular Communication within the Parasite Population and with the Host Immune System. *Cell Host & Microbe,* 13**,** 521-534.

MARTIN, B. R., WANG, C., ADIBEKIAN, A., TULLY, S. E. & CRAVATT, B. F. 2012. Global profiling of dynamic protein palmitoylation. *Nature Methods,* 9**,** 84-89.

MARTINEZ-RUCOBO, FUENSANTA W., KOHLER, R., VAN DE WATERBEEMD, M., HECK, ALBERT J. R., HEMANN, M., HERZOG, F., STARK, H. & CRAMER, P. 2015. Molecular Basis of Transcription-Coupled Pre-mRNA Capping. *Molecular Cell,* 58**,** 1079-1089.

MASHHOON, N., DEMAGGIO, A. J., TERESHKO, V., BERGMEIER, S. C., EGLI, M., HOEKSTRA, M. F. & KURET, J. 2000. Crystal Structure of a Conformation-selective Casein Kinase-1 Inhibitor. *Journal of Biological Chemistry,* 275**,** 20052-20060.

MAVROU, A., BRAKSPEAR, K., HAMDOLLAH-ZADEH, M., DAMODARAN, G., BABAEI-JADIDI, R., OXLEY, J., GILLATT, D. A., LADOMERY, M. R., HARPER, S. J., BATES, D. O. & OLTEAN, S. 2014. Serine–arginine protein kinase 1 (SRPK1) inhibition as a potential novel targeted therapeutic strategy in prostate cancer. *Oncogene,* 34**,** 4311.

MAYOR, A. G., GÓMEZ-OLIVÉ, X., APONTE, J. J., CASIMIRO, S., MABUNDA, S., DGEDGE, M., BARRETO, A. & ALONSO, P. L. 2001. Prevalence of the K76T Mutation in the Putative *Plasmodium falciparum* Chloroquine Resistance Transporter (pfcrt) Gene and Its Relation to Chloroquine Resistance in Mozambique. *The Journal of Infectious Diseases,* 183**,** 1413-1416.

MCCOLLUM, A. M., MUELLER, K., VILLEGAS, L., UDHAYAKUMAR, V. & ESCALANTE, A. A. 2007. Common origin and fixation of *Plasmodium falciparum* dhfr and dhps mutations associated with sulfadoxine-pyrimethamine resistance in a low-transmission area in South America. *Antimicrobial agents and chemotherapy,* 51**,** 2085-2091.

MCCOLLUM, A. M., POE, A. C., HAMEL, M., HUBER, C., ZHOU, Z., SHI, Y. P., OUMA, P., VULULE, J., BLOLAND, P. & SLUTSKER, L. 2006. Antifolate resistance in *Plasmodium falciparum*: multiple origins and identification of novel dhfr alleles. *The Journal of infectious diseases,* 194**,** 189-197.

MCNAUGHTON, M., PITMAN, M., PITSON, S. M., PYNE, N. J. & PYNE, S. 2016. Proteasomal degradation of sphingosine kinase 1 and inhibition of dihydroceramide desaturase by the sphingosine kinase inhibitors, SKi or ABC294640, induces growth arrest in androgen-independent LNCaP-AI prostate cancer cells. *Oncotarget,* 7**,** 16663-16675.

MEGGIO, F., PERICH, J. W., MARIN, O. & PINNA, L. A. 1992. The comparative efficiencies of the Ser(P)-, Thr(P)- and Tyr(P)-residues as specificity determinants for casein kinase-1. *Biochemical and Biophysical Research Communications,* 182**,** 1460-1465.

MENG, Q.-J., MAYWOOD, E. S., BECHTOLD, D. A., LU, W.-Q., LI, J., GIBBS, J. E., DUPRÉ, S. M., CHESHAM, J. E., RAJAMOHAN, F., KNAFELS, J., SNEED, B., ZAWADZKE, L. E., OHREN, J. F., WALTON, K. M., WAGER, T. T., HASTINGS, M. H. & LOUDON, A. S. I. 2010. Entrainment of disrupted circadian behavior through inhibition of casein kinase 1 (CK1) enzymes. *Proceedings of the National Academy of Sciences,* 107**,** 15240-15245.

MERINO, M. C., ZAMPONI, N., VRANYCH, C. V., TOUZ, M. C. & RÓPOLO, A. S. 2014. Identification of Giardia lamblia DHHC Proteins and the Role of Protein S-palmitoylation in the Encystation Process. *PLOS Neglected Tropical Diseases,* 8**,** e2997.

MIAO, J., CHEN, Z., WANG, Z., SHRESTHA, S., LI, X., LI, R. & CUI, L. 2017. Sex-Specific Biology of the Human Malaria Parasite Revealed from the Proteomes of Mature Male and Female Gametocytes. *Molecular & Cellular Proteomics,* 16**,** 537-551.

MILNE, D. M., LOOBY, P. & MEEK, D. W. 2001. Catalytic Activity of Protein Kinase CK1δ (Casein Kinase 1δ) Is Essential for Its Normal Subcellular Localization. *Experimental Cell Research,* 263**,** 43-54.

MIOTTO, O., ALMAGRO-GARCIA, J., MANSKE, M., MACINNIS, B., CAMPINO, S., ROCKETT, K. A., AMARATUNGA, C., LIM, P., SUON, S., SRENG, S., ANDERSON, J. M., DUONG, S., NGUON, C., CHUOR, C. M., SAUNDERS, D., SE, Y., LON, C., FUKUDA, M. M., AMENGA-ETEGO, L., HODGSON, A. V. O., ASOALA, V., IMWONG, M., TAKALA-HARRISON, S., NOSTEN, F., SU, X.-Z., RINGWALD, P., ARIEY, F., DOLECEK, C., HIEN, T. T., BONI, M. F., THAI, C. Q., AMAMBUA-NGWA, A., CONWAY, D. J., DJIMDÉ, A. A., DOUMBO, O. K., ZONGO, I., OUEDRAOGO, J.-B., ALCOCK, D., DRURY, E., AUBURN, S., KOCH, O., SANDERS, M., HUBBART, C., MASLEN, G., RUANO-RUBIO, V., JYOTHI, D., MILES, A., O'BRIEN, J., GAMBLE, C., OYOLA, S. O., RAYNER, J. C., NEWBOLD, C. I., BERRIMAN, M., SPENCER, C. C. A., MCVEAN, G., DAY, N. P., WHITE, N. J., BETHELL, D., DONDORP, A. M., PLOWE, C. V., FAIRHURST, R. M. & KWIATKOWSKI, D. P. 2013. Multiple populations of artemisinin-resistant *Plasmodium falciparum* in Cambodia. *Nature Genetics,* 45**,** 648-55.

MISHRA, R. K., WEI, C., HRESKO, R. C., BAJPAI, R., HEITMEIER, M., MATULIS, S. M., NOOKA, A. K., ROSEN, S. T., HRUZ, P. W., SCHILTZ, G. E. & SHANMUGAM, M. 2015. In Silico Modeling-based Identification of Glucose Transporter 4 (GLUT4)-selective Inhibitors for Cancer Therapy. *Journal of Biological Chemistry,* 290**,** 14441-14453.

MITCHELL, D. A., HAMEL, L. D., ISHIZUKA, K., MITCHELL, G., SCHAEFER, L. M. & DESCHENES, R. J. 2012. The Erf4 Subunit of the Yeast Ras Palmitoyl Acyltransferase Is Required for Stability of the Acyl-Erf2 Intermediate and Palmitoyl Transfer to a Ras2 Substrate. *Journal of Biological Chemistry,* 287**,** 34337-34348.

MITCHELL, D. A., MITCHELL, G., LING, Y., BUDDE, C. & DESCHENES, R. J. 2010. Mutational Analysis of *Saccharomyces cerevisiae* Erf2 Reveals a Two-step Reaction Mechanism for Protein Palmitoylation by DHHC Enzymes. *Journal of Biological Chemistry,* 285**,** 38104-38114.

MORSE, D., WEBSTER, W., KALANON, M., LANGSLEY, G. & MCFADDEN, G. I. 2016. *Plasmodium falciparum* Rab1A Localizes to Rhoptries in Schizonts. *PLOS ONE,* 11**,** e0158174.

MOSAMMAPARAST, N., EWART, C. S. & PEMBERTON, L. F. 2002. A role for nucleosome assembly protein 1 in the nuclear transport of histones H2A and H2B. *The EMBO Journal,* 21**,** 6527-6538.

MUNGTHIN, M., WATANATANASUP, E., SITTHICHOT, N., SUWANDITTAKUL, N., KHOSITNITHIKUL, R. & WARD, S. A. 2017. Influence of the pfmdr1 Gene on In Vitro Sensitivities of Piperaquine in Thai Isolates of *Plasmodium falciparum*. *The American Journal of Tropical Medicine and Hygiene,* 96**,** 624-629.

MVUMBI, D. M., BOREUX, R., SACHELI, R., LELO, M., LENGU, B., NANI-TUMA, S., MELIN, P., NTUMBA, K., LUNGANZA, K. & DEMOL, P. 2013. Assessment of pfcrt 72-76 haplotypes eight years after chloroquine withdrawal in Kinshasa, Democratic Republic of Congo. *Malaria journal,* 12**,** 459.

NGO, J. K., POMATTO, L. C. D. & DAVIES, K. J. A. 2013. Upregulation of the mitochondrial Lon Protease allows adaptation to acute oxidative stress but dysregulation is associated with chronic stress, disease, and aging. *Redox Biology,* 1**,** 258-264.

NOJIMA, T., GOMES, T., GROSSO, ANA RITA F., KIMURA, H., DYE, MICHAEL J., DHIR, S., CARMO-FONSECA, M. & PROUDFOOT, NICHOLAS J. 2015. Mammalian NET-Seq Reveals Genome-wide Nascent Transcription Coupled to RNA Processing. *Cell,* 161**,** 526-540.

NZILA, A. & MWAI, L. 2010. In vitro selection of *Plasmodium falciparum* drug-resistant parasite lines. *Journal of Antimicrobial Chemotherapy,* 65**,** 390-398.

OCHOLA, L. B., SIDDONDO, B. R., OCHOLLA, H., NKYA, S., KIMANI, E. N., WILLIAMS, T. N., MAKALE, J. O., LILJANDER, A., URBAN, B. C., BULL, P. C., SZESTAK, T., MARSH, K. & CRAIG, A. G. 2011. Specific Receptor Usage in *Plasmodium falciparum* Cytoadherence Is Associated with Disease Outcome. *PLOS ONE,* 6**,** e14741.

ODUOLA, A. M. J., MILHOUS, W. K., WEATHERLY, N. F., BOWDRE, J. H. & DESJARDINS, R. E. 1988. *Plasmodium falciparum*: Induction of resistance to mefloquine in cloned strains by continuous drug exposure in vitro. *Experimental Parasitology,* 67**,** 354-360.

OHNO, Y., KIHARA, A., SANO, T. & IGARASHI, Y. 2006. Intracellular localization and tissue-specific distribution of human and yeast DHHC cysteine-rich domain-containing proteins. *Biochimica et Biophysica Acta (BBA) - Molecular and Cell Biology of Lipids,* 1761**,** 474-483.

OKAMURA, H., ARAMBURU, J., GARCÍA-RODRÍGUEZ, C., VIOLA, J. P. B., RAGHAVAN, A., TAHILIANI, M., ZHANG, X., QIN, J., HOGAN, P. G. & RAO, A. 2000. Concerted Dephosphorylation of the Transcription Factor NFAT1 Induces a Conformational Switch that Regulates Transcriptional Activity. *Molecular Cell,* 6**,** 539-550.

OKAMURA, H., GARCIA-RODRIGUEZ, C., MARTINSON, H., QIN, J., VIRSHUP, D. M. & RAO, A. 2004. A Conserved Docking Motif for CK1 Binding Controls the Nuclear Localization of NFAT1. *Molecular and Cellular Biology,* 24**,** 4184-4195.

OKUWAKI, M., KATO, K. & NAGATA, K. 2010. Functional characterization of human nucleosome assembly protein 1-like proteins as histone chaperones. *Genes to Cells,* 15**,** 13-27.

OLADIPO, O. O., WELLINGTON, O. A. & SUTHERLAND, C. J. 2015. Persistence of chloroquine-resistant haplotypes of *Plasmodium falciparum* in children with uncomplicated Malaria in Lagos, Nigeria, four years after change of chloroquine as first-line antimalarial medicine. *Diagnostic Pathology,* 10**,** 41.

OLIGSCHLAEGER, Y., MIGLIANICO, M., CHANDA, D., SCHOLZ, R., THALI, R. F., TUERK, R., STAPLETON, D. I., GOOLEY, P. R. & NEUMANN, D. 2015. The Recruitment of AMP-activated Protein Kinase to Glycogen Is Regulated by Autophosphorylation. *Journal of Biological Chemistry,* 290**,** 11715-11728.

PABLO, S., ANA, J., H., B. V., C., A. C. & E., A. J. 2005. Basic region of residues 228–231 of protein kinase CK1α is involved in its interaction with axin: Binding to axin does not affect the kinase activity. *Journal of Cellular Biochemistry,* 94**,** 217-224.

PAHARI, S., CORMARK, R. D., BLACKSHAW, M. T., LIU, C., ERICKSON, J. L. & SCHULTZ, E. A. 2014. *Arabidopsis* UNHINGED encodes a VPS51 homolog and reveals a role for the GARP complex in leaf shape and vein patterning. *Development,* 141**,** 1894-1905.

PAIN, M., FULLER, A. W., BASORE, K., PILLAI, A. D., SOLOMON, T., BOKHARI, A. A. B. & DESAI, S. A. 2016. Synergistic Malaria Parasite Killing by Two Types of Plasmodial Surface Anion Channel Inhibitors. *PLOS ONE,* 11**,** e0149214.

PALMEIRIM, M. S., HÜRLIMANN, E., KNOPP, S., SPEICH, B., BELIZARIO, V., JR., JOSEPH, S. A., VAILLANT, M., OLLIARO, P. & KEISER, J. 2018. Efficacy and safety of co-administered ivermectin plus albendazole for treating soil-transmitted helminths: A systematic review, meta-analysis and individual patient data analysis. *PLOS Neglected Tropical Diseases,* 12**,** e0006458.

PANCHAL, M., RAWAT, K., KUMAR, G., KIBRIA, K. M., SINGH, S., KALAMUDDIN, M., MOHMMED, A., MALHOTRA, P. & TUTEJA, R. 2014. *Plasmodium falciparum* signal recognition particle components and anti-parasitic effect of ivermectin in blocking nucleo-cytoplasmic shuttling of SRP. *Cell Death & Disease,* 5**,** e994.

PARK, Y.-J. & LUGER, K. 2006. The structure of nucleosome assembly protein 1. *Proceedings of the National Academy of Sciences,* 103**,** 1248-1253.

PARR, C., CARZANIGA, R., GENTLEMAN, S. M., VAN LEUVEN, F., WALTER, J. & SASTRE, M. 2012. Glycogen Synthase Kinase 3 Inhibition Promotes Lysosomal Biogenesis and Autophagic Degradation of the Amyloid-β Precursor Protein. *Molecular and Cellular Biology,* 32**,** 4410-4418.

PATEL-HETT, S., WANG, H., BEGONJA, A. J., THON, J. N., ALDEN, E. C., WANDERSEE, N. J., AN, X., MOHANDAS, N., HARTWIG, J. H. & ITALIANO, J. E. 2011. The spectrin-based membrane skeleton stabilizes mouse megakaryocyte membrane systems and is essential for proplatelet and platelet formation. *Blood,* 118**,** 1641-1652.

PATRICK, M., TOMAS, L., ZUZANA, H. & LIBOR, M. 2018. Nuclear localisation of 53BP1 is regulated by phosphorylation of the nuclear localisation signal. *Biology of the Cell,* 110**,** 137-146.

PAULSEN, C. E., TRUONG, T. H., GARCIA, F. J., HOMANN, A., GUPTA, V., LEONARD, S. E. & CARROLL, K. S. 2011. Peroxide-dependent sulfenylation of the EGFR catalytic site enhances kinase activity. *Nature chemical biology,* 8**,** 57-64.

PEASE, B. N., HUTTLIN, E. L., JEDRYCHOWSKI, M. P., TALEVICH, E., HARMON, J., DILLMAN, T., KANNAN, N., DOERIG, C., CHAKRABARTI, R., GYGI, S. P. & CHAKRABARTI, D. 2013. Global Analysis of Protein Expression and Phosphorylation of Three Stages of *Plasmodium falciparum* Intraerythrocytic Development. *Journal of Proteome Research,* 12**,** 4028-4045.

PENG, Y., GRASSART, A., LU, R., WONG, CATHERINE C. L., YATES, J., III, BARNES, G. & DRUBIN, DAVID G. 2015. Casein Kinase 1 Promotes Initiation of Clathrin-Mediated Endocytosis. *Developmental Cell,* 32**,** 231-240.

PETER, L., SANG-MIN, P., CHUN-SHIK, S., WON-KI, H. & JI-SOOK, H. 2011. Regulation of yeast Yak1 kinase by PKA and autophosphorylation-dependent 14-3-3 binding. *Molecular Microbiology,* 79**,** 633-646.

PETRONCZKI, M., MATOS, J., MORI, S., GREGAN, J., BOGDANOVA, A., SCHWICKART, M., MECHTLER, K., SHIRAHIGE, K., ZACHARIAE, W. & NASMYTH, K. 2006. Monopolar Attachment of Sister Kinetochores at Meiosis I Requires Casein Kinase 1. *Cell,* 126**,** 1049-1064.

PHYO, A. P., NKHOMA, S., STEPNIEWSKA, K., ASHLEY, E. A., NAIR, S., MCGREADY, R., LER MOO, C., AL-SAAI, S., DONDORP, A. M., LWIN, K. M., SINGHASIVANON, P., DAY, N. P. J., WHITE, N. J., ANDERSON, T. J. C. & NOSTEN, F. 2012. Emergence of artemisinin-resistant malaria on the western border of Thailand: a longitudinal study. *The Lancet,* 379**,** 1960-1966.

POLITIS, E. G., ROTH, A. F. & DAVIS, N. G. 2005. Transmembrane Topology of the Protein Palmitoyl Transferase Akr1. *Journal of Biological Chemistry,* 280**,** 10156-10163.

PREECHAPORNKUL, P., IMWONG, M., CHOTIVANICH, K., PONGTAVORNPINYO, W., DONDORP, A. M., DAY, N. P. J., WHITE, N. J. & PUKRITTAYAKAMEE, S. 2009. *Plasmodium falciparum* pfmdr1 Amplification, Mefloquine Resistance, and Parasite Fitness. *Antimicrobial Agents and Chemotherapy,* 53**,** 1509-1515.

PROMMANA, P., UTHAIPIBULL, C., WONGSOMBAT, C., KAMCHONWONGPAISAN, S., YUTHAVONG, Y., KNUEPFER, E., HOLDER, A. A. & SHAW, P. J. 2013. Inducible Knockdown of *Plasmodium* Gene Expression Using the *glmS* Ribozyme. *PLOS ONE,* 8**,** e73783.

QAZI, K. R., GEHRMANN, U., DOMANGE JORDÖ, E., KARLSSON, M. C. I. & GABRIELSSON, S. 2009. Antigen-loaded exosomes alone induce Th1-type memory through a B cell–dependent mechanism. *Blood,* 113**,** 2673-2683.

QUEVILLON, E., SPIELMANN, T., BRAHIMI, K., CHATTOPADHYAY, D., YERAMIAN, E. & LANGSLEY, G. 2003. The *Plasmodium falciparum* family of Rab GTPases. *Gene,* 306**,** 13-25.

RACHED, F. B., NDJEMBO-EZOUGOU, C., CHANDRAN, S., TALABANI, H., YERA, H., DANDAVATE, V., BOURDONCLE, P., MEISSNER, M., TATU, U. & LANGSLEY, G. 2012. Construction of a *Plasmodium falciparum* Rab-interactome identifies CK1 and PKA as Rab-effector kinases in malaria parasites. *Biology of the Cell,* 104**,** 34-47.

RASTOGI, R., VERMA, J. K., KAPOOR, A., LANGSLEY, G. & MUKHOPADHYAY, A. 2016. Rab5 Isoforms Specifically Regulate Different Modes of Endocytosis in *Leishmania*. *Journal of Biological Chemistry,* 291**,** 14732-14746.

RATHOD, P. K., MCERLEAN, T. & LEE, P.-C. 1997. Variations in frequencies of drug resistance in *Plasmodium falciparum*. *Proceedings of the National Academy of Sciences,* 94**,** 9389-9393.

RAY, P. D., HUANG, B.-W. & TSUJI, Y. 2012. Reactive oxygen species (ROS) homeostasis and redox regulation in cellular signaling. *Cellular Signalling,* 24**,** 981-990.

REDDY, K. D., MALIPEDDI, J., DEFORTE, S., PEJAVER, V., RADIVOJAC, P., UVERSKY, V. N. & DESCHENES, R. J. 2017. Physicochemical sequence characteristics that influence S-palmitoylation propensity. *Journal of Biomolecular Structure and Dynamics,* 35**,** 2337-2350.

REGEV-RUDZKI, N., WILSON, DANNY W., CARVALHO, TERESA G., SISQUELLA, X., COLEMAN, BRADLEY M., RUG, M., BURSAC, D., ANGRISANO, F., GEE, M., HILL, ANDREW F., BAUM, J. & COWMAN, ALAN F. 2013. Cell-Cell Communication between Malaria-Infected Red Blood Cells via Exosome-like Vesicles. *Cell,* 153**,** 1120-1133.

REININGER, L., BILLKER, O., TEWARI, R., MUKHOPADHYAY, A., FENNELL, C., DORIN-SEMBLAT, D., DOERIG, C., GOLDRING, D., HARMSE, L., RANFORD-CARTWRIGHT, L., PACKER, J. & DOERIG, C. 2005. A NIMA-related Protein Kinase Is Essential for Completion of the Sexual Cycle of Malaria Parasites. *Journal of Biological Chemistry,* 280**,** 31957-31964.

REININGER, L., TEWARI, R., FENNELL, C., HOLLAND, Z., GOLDRING, D., RANFORD-CARTWRIGHT, L., BILLKER, O. & DOERIG, C. 2009. An Essential Role for the *Plasmodium* Nek-2 Nima-related Protein Kinase in the Sexual Development of Malaria Parasites. *Journal of Biological Chemistry,* 284**,** 20858-20868.

RIBAUT, C., BERRY, A., CHEVALLEY, S., REYBIER, K., MORLAIS, I., PARZY, D., NEPVEU, F., BENOIT-VICAL, F. & VALENTIN, A. 2008. Concentration and purification by magnetic separation of the erythrocytic stages of all human *Plasmodium* species. *Malaria Journal,* 7**,** 45.

RICHTER, J., BISCHOF, J., ZAJA, M., KOHLHOF, H., OTHERSEN, O., VITT, D., ALSCHER, V., POSPIECH, I., GARCÍA-REYES, B., BERG, S., LEBAN, J. & KNIPPSCHILD, U. 2014. Difluoro-dioxolo-benzoimidazol-benzamides As Potent Inhibitors of CK1δ and ε with Nanomolar Inhibitory Activity on Cancer Cell Proliferation. *Journal of Medicinal Chemistry,* 57**,** 7933-7946.

RINGER, L., SIRAJUDDIN, P., HECKLER, M., GHOSH, A., SUPRYNOWICZ, F., YENUGONDA, V. M., BROWN, M. L., TORETSKY, J. A., ÜREN, A., LEE, Y., MACDONALD, T. J., RODRIGUEZ, O., GLAZER, R. I., SCHLEGEL, R. & ALBANESE, C. 2011. VMY-1-103 is a novel CDK inhibitor that disrupts chromosome organization and delays metaphase progression in medulloblastoma cells. *Cancer Biology & Therapy,* 12**,** 818-826.

RINGER, L., SIRAJUDDIN, P., MAHIDHAR YENUGONDA, V., GHOSH, A., DIVITO, K., TRABOSH, V., PATEL, Y., BROPHY, A., GRINDROD, S. & LISANTI, M. P. 2010. VMY-1-103, a dansylated analog of purvalanol B, induces caspase-3-dependent apoptosis in LNCaP prostate cancer cells. *Cancer biology & therapy,* 10**,** 320-325.

RIVERS, A., GIETZEN, K. F., VIELHABER, E. & VIRSHUP, D. M. 1998. Regulation of Casein Kinase I ε and Casein Kinase I δ by an in Vivo Futile Phosphorylation Cycle. *Journal of Biological Chemistry,* 273**,** 15980-15984.

ROMANI, L., WHITFELD, M. J., KOROIVUETA, J., KAMA, M., WAND, H., TIKODUADUA, L., TUICAKAU, M., KOROI, A., ANDREWS, R., KALDOR, J. M. & STEER, A. C. 2015. Mass Drug Administration for Scabies Control in a Population with Endemic Disease. *New England Journal of Medicine,* 373**,** 2305-2313.

ROSKOSKI JR, R. 2003. STI-571: an anticancer protein-tyrosine kinase inhibitor. *Biochemical and Biophysical Research Communications,* 309**,** 709-717.

ROSSETTO, D., AVVAKUMOV, N. & CÔTÉ, J. 2012. Histone phosphorylation. *Epigenetics,* 7**,** 1098-1108.

ROTH, A. F., FENG, Y., CHEN, L. & DAVIS, N. G. 2002. The yeast DHHC cysteine-rich domain protein Akr1p is a palmitoyl transferase. *The Journal of Cell Biology,* 159**,** 23-28.

ROTH, A. F., PAPANAYOTOU, I., DAVIS, N. G. & GUTKIND, J. S. 2011. The yeast kinase Yck2 has a tripartite palmitoylation signal. *Molecular Biology of the Cell,* 22**,** 2702-2715.

ROTH, A. F., WAN, J., BAILEY, A. O., SUN, B., KUCHAR, J. A., GREEN, W. N., PHINNEY, B. S., YATES III, J. R. & DAVIS, N. G. 2006. Global Analysis of Protein Palmitoylation in Yeast. *Cell,* 125**,** 1003-1013.

RUBINFELD, B., TICE, D. A. & POLAKIS, P. 2001. Axin-dependent Phosphorylation of the Adenomatous Polyposis Coli Protein Mediated by Casein Kinase 1ε. *Journal of Biological Chemistry,* 276**,** 39037-39045.

RUIZ-CARRILLO, D., LIN, J., EL SAHILI, A., WEI, M., SZE, S. K., CHEUNG, P. C. F., DOERIG, C. & LESCAR, J. 2018. The protein kinase CK2 catalytic domain from *Plasmodium falciparum*: crystal structure, tyrosine kinase activity and inhibition. *Scientific Reports,* 8**,** 7365.

RUIZENDAAL, E., TAHITA, M. C., TRAORÉ-COULIBALY, M., TINTO, H., SCHALLIG, H. D. F. H. & MENS, P. F. 2017. Presence of quintuple dhfr N51, C59, S108 – dhps A437, K540 mutations in *Plasmodium falciparum* isolates from pregnant women and the general population in Nanoro, Burkina Faso. *Molecular and Biochemical Parasitology,* 217**,** 13-15.

RUSSO, I., BABBITT, S., MURALIDHARAN, V., BUTLER, T., OKSMAN, A. & GOLDBERG, D. E. 2010. Plasmepsin V licenses *Plasmodium* proteins for export into the host erythrocyte. *Nature,* 463**,** 632.

SABNIS. Y. A., DESHAI. P. V., ROSENTHAL. P. J., & AVERY. M. A., 2003. Probing the structure of falcipain-3, a cysteine protease from *Plasmodium falciparum*: Comparative protein modeling and docking studies. *Protein Science,* 12**,** 501-509.

SACCO, F., PERFETTO, L., CASTAGNOLI, L. & CESARENI, G. 2012. The human phosphatase interactome: An intricate family portrait. *Febs Letters,* 586**,** 2732-2739.

SAFEUKUI, I., CORREAS, J.-M., BROUSSE, V., HIRT, D., DEPLAINE, G., MULÉ, S., LESURTEL, M., GOASGUEN, N., SAUVANET, A. & COUVELARD, A. 2008. Retention of *Plasmodium falciparum* ring-infected erythrocytes in the slow, open microcirculation of the human spleen. *Blood,* 112**,** 2520-2528.

SAKUNO, T. & WATANABE, Y. 2015. Phosphorylation of Cohesin Rec11/SA3 by Casein Kinase 1 Promotes Homologous Recombination by Assembling the Meiotic Chromosome Axis. *Developmental Cell,* 32**,** 220-230.

SALDI, T., CORTAZAR, M. A., SHERIDAN, R. M. & BENTLEY, D. L. 2016. Coupling of RNA Polymerase II Transcription Elongation with Pre-mRNA Splicing. *Journal of Molecular Biology,* 428**,** 2623-2635.

SÁNCHEZ-MARTÍNEZ, C., GELBERT, L. M., LALLENA, M. J. & DE DIOS, A. 2015. Cyclin dependent kinase (CDK) inhibitors as anticancer drugs. *Bioorganic & Medicinal Chemistry Letters,* 25**,** 3420-3435.

SANTOS, J. A., LOGARINHO, E., TAPIA, C., ALLENDE, C. C., ALLENDE, J. E. & SUNKEL, C. E. 1996. The casein kinase 1 alpha gene of *Drosophila melanogaster* is developmentally regulated and the kinase activity of the protein induced by DNA damage. *Journal of Cell Science,* 109**,** 1847-1856.

SANTOS, R., URSU, O., GAULTON, A., BENTO, A. P., DONADI, R. S., BOLOGA, C. G., KARLSSON, A., AL-LAZIKANI, B., HERSEY, A., OPREA, T. I. & OVERINGTON, J. P. 2016. A comprehensive map of molecular drug targets. *Nature Reviews Drug Discovery,* 16**,** 19.

SANTOS-FILHO, O. A., DE ALENCASTRO, R. B. & FIGUEROA-VILLAR, J. D. 2001. Homology modeling of wild type and pyrimethamine/cycloguanil-cross resistant mutant type *Plasmodium falciparum* dihydrofolate reductase. A model for antimalarial chemotherapy resistance. *Biophysical Chemistry,* 91**,** 305-317.

SARGEANT, T. J., MARTI, M., CALER, E., CARLTON, J. M., SIMPSON, K., SPEED, T. P. & COWMAN, A. F. 2006. Lineage-specific expansion of proteins exported to erythrocytes in malaria parasites. *Genome Biology,* 7**,** R12.

SCHIBLER, A., KOUTELOU, E., TOMIDA, J., WILSON-PHAM, M., WANG, L., LU, Y., CABRERA, A. P., CHOSED, R. J., LI, W., LI, B., SHI, X., WOOD, R. D. & DENT, S. Y. R. 2016. Histone H3K4 methylation regulates deactivation of the spindle assembly checkpoint through direct binding of Mad2. *Genes & Development,* 30**,** 1187-1197.

SCHINDLER, C., CHEN, Y., PU, J., GUO, X. & BONIFACINO, J. S. 2015. EARP is a multisubunit tethering complex involved in endocytic recycling. *Nature Cell Biology,* 17**,** 639.

SCHITTEK, B. & SINNBERG, T. 2014. Biological functions of casein kinase 1 isoforms and putative roles in tumorigenesis. *Molecular Cancer,* 13**,** 231.

SCHLATTNER, U., GEHRING, F., VERNOUX, N., TOKARSKA-SCHLATTNER, M., NEUMANN, D., MARCILLAT, O., VIAL, C. & WALLIMANN, T. 2004. C-terminal Lysines Determine Phospholipid Interaction of Sarcomeric Mitochondrial Creatine Kinase. *Journal of Biological Chemistry,* 279**,** 24334-24342.

SCHULZE, J., KWIATKOWSKI, M., BORNER, J., SCHLÜTER, H., BRUCHHAUS, I., BURMESTER, T., SPIELMANN, T. & PICK, C. 2015. The *Plasmodium falciparum* exportome contains non-canonical PEXEL/HT proteins. *Molecular Microbiology,* 97**,** 301-314.

SEBASTIAN, S., BROCHET, M., COLLINS, MARK O., SCHWACH, F., JONES, MATTHEW L., GOULDING, D., RAYNER, JULIAN C., CHOUDHARY, JYOTI S. & BILLKER, O. 2012. A *Plasmodium* Calcium-Dependent Protein Kinase Controls Zygote Development and Transmission by Translationally Activating Repressed mRNAs. *Cell Host & Microbe,* 12**,** 9-19.

SGOURDOU, P., MISHRA-GORUR, K., SAOTOME, I., HENAGARIU, O., TUYSUZ, B., CAMPOS, C., ISHIGAME, K., GIANNIKOU, K., QUON, J. L., SESTAN, N., CAGLAYAN, A. O., GUNEL, M. & LOUVI, A. 2017. Disruptions in asymmetric centrosome inheritance and WDR62-Aurora kinase B interactions in primary microcephaly. *Scientific Reports,* 7**,** 43708.

SHARMA, C., WANG, H.-X., LI, Q., KNOBLICH, K., REISENBICHLER, E. S., RICHARDSON, A. L. & HEMLER, M. E. 2017. Protein Acyltransferase DHHC3 Regulates Breast Tumor Growth, Oxidative Stress, and Senescence. *Cancer Research,* 77**,** 6880-6890.

SHARMA, G. G., SO, S., GUPTA, A., KUMAR, R., CAYROU, C., AVVAKUMOV, N., BHADRA, U., PANDITA, R. K., PORTEUS, M. H., CHEN, D. J., COTE, J. & PANDITA, T. K. 2010. MOF and Histone H4 Acetylation at Lysine 16 Are Critical for DNA Damage Response and Double-Strand Break Repair. *Molecular and Cellular Biology,* 30**,** 3582-3595.

SHARMA, K., D'SOUZA, ROCHELLE C. J., TYANOVA, S., SCHAAB, C., WIŚNIEWSKI, JACEK R., COX, J. & MANN, M. 2014. Ultradeep Human Phosphoproteome Reveals a Distinct Regulatory Nature of Tyr and Ser/Thr-Based Signaling. *Cell Reports,* 8**,** 1583-1594.

SHARMA, P., RAYAVARA, K., ITO, D., BASORE, K. & DESAI, S. A. 2015. A CLAG3 Mutation in an Amphipathic Transmembrane Domain Alters Malaria Parasite Nutrient Channels and Confers Leupeptin Resistance. *Infection and Immunity,* 83**,** 2566-2574.

SHARMA, P., WOLLENBERG, K., SELLERS, M., ZAINABADI, K., GALINSKY, K., MOSS, E., NGUITRAGOOL, W., NEAFSEY, D. & DESAI, S. A. 2013. An Epigenetic Antimalarial Resistance Mechanism Involving Parasite Genes Linked to Nutrient Uptake. *Journal of Biological Chemistry,* 288**,** 19429-19440.

SHRIVASTAVA, S. K., GUPTA, R. K., MAHANTA, J. & DUBEY, M. L. 2014. Correlation of Molecular Markers, Pfmdr1-N86Y and Pfcrt-K76T, with In Vitro Chloroquine Resistant *Plasmodium falciparum*, Isolated in the Malaria Endemic States of Assam and Arunachal Pradesh, Northeast India. *PLOS ONE,* 9**,** e103848.

SILVERMAN, J. M., CLOS, J., DE'OLIVEIRA, C. C., SHIRVANI, O., FANG, Y., WANG, C., FOSTER, L. J. & REINER, N. E. 2010a. An exosome-based secretion pathway is responsible for protein export from *Leishmania* and communication with macrophages. *Journal of Cell Science,* 123**,** 842-852.

SILVERMAN, J. M., CLOS, J., HORAKOVA, E., WANG, A. Y., WIESGIGL, M., KELLY, I., LYNN, M. A., MCMASTER, W. R., FOSTER, L. J., LEVINGS, M. K. & REINER, N. E. 2010b. *Leishmania* Exosomes Modulate Innate and Adaptive Immune Responses through Effects on Monocytes and Dendritic Cells. *The Journal of Immunology,* 185**,** 5011-5022.

SINDEN, R. E., CARTER, R., DRAKELEY, C. & LEROY, D. 2012. The biology of sexual development of *Plasmodium*: the design and implementation of transmission-blocking strategies. *Malaria Journal,* 11**,** 70.

SIRAJUDDIN, P., DAS, S., RINGER, L., RODRIGUEZ, O. C., SIVAKUMAR, A., LEE, Y.-C., UREN, A., FRICKE, S. T., ROOD, B., OZCAN, A., WANG, S. S., KARAM, S., YENUGONDA, V., SALINAS, P., PETRICOIN III, E., PISHVAIAN, M., LISANTI, M. P., WANG, Y., SCHLEGEL, R., MOASSER, B. & ALBANESE, C. 2012. Quantifying the CDK inhibitor VMY-1-103's activity and tissue levels in an in vivo tumor model by LC-MS/MS and by MRI. *Cell Cycle,* 11**,** 3801-3809.

SKUTELSKY, E. & DANON, D. 1970. Comparative study of nuclear expulsion from the late erythroblast and cytokinesis. *Experimental Cell Research,* 60**,** 427-436.

SLEEBS, B. E., LOPATICKI, S., MARAPANA, D. S., O'NEILL, M. T., RAJASEKARAN, P., GAZDIK, M., GÜNTHER, S., WHITEHEAD, L. W., LOWES, K. N., BARFOD, L., HVIID, L., SHAW, P. J., HODDER, A. N., SMITH, B. J., COWMAN, A. F. & BODDEY, J. A. 2014. Inhibition of Plasmepsin V Activity Demonstrates Its Essential Role in Protein Export, PfEMP1 Display, and Survival of Malaria Parasites. *PLOS Biology,* 12**,** e1001897.

SOLYAKOV, L., HALBERT, J., ALAM, M. M., SEMBLAT, J.-P., DORIN-SEMBLAT, D., REININGER, L., BOTTRILL, A. R., MISTRY, S., ABDI, A. & FENNELL, C. 2011. Global kinomic and phospho-proteomic analyses of the human malaria parasite *Plasmodium falciparum*. *Nature communications,* 2**,** 565.

SON, O., KIM, S., SHIN, Y.-J., KIM, W.-Y., KOH, H.-J. & CHEON, C.-I. 2015. Identification of nucleosome assembly protein 1 (NAP1) as an interacting partner of plant ribosomal protein S6 (RPS6) and a positive regulator of rDNA transcription. *Biochemical and Biophysical Research Communications,* 465**,** 200-205.

SONG, J. H., AN, N., CHATTERJEE, S., KISTNER-GRIFFIN, E., MAHAJAN, S., MEHROTRA, S. & KRAFT, A. S. 2014. Deletion of Pim kinases elevates the cellular levels of reactive oxygen species and sensitizes to K-Ras-induced cell killing. *Oncogene,* 34**,** 3728.

SOUNG, Y. H., KASHYAP, T., NGUYEN, T., YADAV, G., CHANG, H., LANDESMAN, Y. & CHUNG, J. 2017. Selective Inhibitors of Nuclear Export (SINE) compounds block proliferation and migration of triple negative breast cancer cells by restoring expression of ARRDC3. *Oncotarget,* 8**,** 52935-52947.

SPIELMANN, T. & BECK, H. P. 2000. Analysis of stage-specific transcription in *Plasmodium falciparum* reveals a set of genes exclusively transcribed in ring stage parasites. *Molecular and Biochemical Parasitology,* 111**,** 453-458.

SPYCHER, C., RUG, M., KLONIS, N., FERGUSON, D. J. P., COWMAN, A. F., BECK, H.-P. & TILLEY, L. 2006. Genesis of and Trafficking to the Maurer's Clefts of *Plasmodium falciparum*-Infected Erythrocytes. *Molecular and Cellular Biology,* 26**,** 4074-4085.

STARK, C., BREITKREUTZ, B.-J., REGULY, T., BOUCHER, L., BREITKREUTZ, A. & TYERS, M. 2006. BioGRID: a general repository for interaction datasets. *Nucleic acids research,* 34**,** D535-D539.

STROCHLIC, T. I., SETTY, T. G., SITARAM, A. & BURD, C. G. 2007. Grd19/Snx3p functions as a cargo-specific adapter for retromer-dependent endocytic recycling. *The Journal of Cell Biology,* 177**,** 115-125.

SU, X., KONG, C. & STAHL, P. D. 2007. GAPex-5 Mediates Ubiquitination, Trafficking, and Degradation of Epidermal Growth Factor Receptor. *Journal of Biological Chemistry,* 282**,** 21278-21284.

SUAZO, K. F., SCHABER, C., PALSULEDESAI, C. C., JOHN, A. R. O. & DISTEFANO, M. D. 2016. Global proteomic analysis of prenylated proteins in Plasmodium falciparum using an alkyne-modified isoprenoid analogue. *Scientific Reports,* 6.

SUGIYAMA, Y., HATANO, N., SUEYOSHI, N., SUETAKE, I., TAJIMA, S., KINOSHITA, E., KINOSHITA-KIKUTA, E., KOIKE, T. & KAMESHITA, I. 2010. The DNA-binding activity of mouse DNA methyltransferase 1 is regulated by phosphorylation with casein kinase 1δ/ε. *Biochemical Journal,* 427**,** 489-497.

SUN, Q., YONG, X., SUN, X., YANG, F., DAI, Z., GONG, Y., ZHOU, L., ZHANG, X., NIU, D., DAI, L., LIU, J.-J. & JIA, D. 2017. Structural and functional insights into sorting nexin 5/6 interaction with bacterial effector IncE. *Signal Transduction And Targeted Therapy,* 2**,** 17030.

SWEARINGEN, K. E., LINDNER, S. E., FLANNERY, E. L., VAUGHAN, A. M., MORRISON, R. D., PATRAPUVICH, R., KOEPFLI, C., MULLER, I., JEX, A., MORITZ, R. L., KAPPE, S. H. I., SATTABONGKOT, J. & MIKOLAJCZAK, S. A. 2017. Proteogenomic analysis of the total and surface-exposed proteomes of *Plasmodium vivax* salivary gland sporozoites. *PLOS Neglected Tropical Diseases,* 11**,** e0005791.

TALEVICH, E., TOBIN, A. B., KANNAN, N. & DOERIG, C. 2012. An evolutionary perspective on the kinome of malaria parasites. *Philosophical Transactions of the Royal Society B: Biological Sciences,* 367**,** 2607-2618.

TAN, S.-T., DAI, C., LIU, H.-T. & XUE, H.-W. 2013. Arabidopsis Casein Kinase1 Proteins CK1.3 and CK1.4 Phosphorylate Cryptochrome2 to Regulate Blue Light Signaling. *The Plant Cell,* 25**,** 2618-2632.

TAO, D., KING, J. G., TWEEDELL, R. E., JOST, P. J., BODDEY, J. A. & DINGLASAN, R. R. 2014. The Acute Transcriptomic and Proteomic Response of HC-04 Hepatoma Cells to Hepatocyte Growth Factor and its Implications for *Plasmodium falciparum* Sporozoite Invasion. *Molecular & Cellular Proteomics,* 13**,** 1153-1164.

TARDAT, M., BRUSTEL, J., KIRSH, O., LEFEVBRE, C., CALLANAN, M., SARDET, C. & JULIEN, E. 2010. The histone H4 Lys 20 methyltransferase PR-Set7 regulates replication origins in mammalian cells. *Nature Cell Biology,* 12**,** 1086-1093.

TAY, C, L., JONES, M, L., HODSON, N., THERON, M., CHOUDHARY, J, S., & RAYNER, J, C,. 2016. Study of *Plasmodium falciparum* DHHC palmitoyl transferases identifies a role for PfDHHC9 in gametocytogenesis. *Cellular Microbiology,* 18**,** 1596-1610.

TEASDALE, ROHAN D. & COLLINS, BRETT M. 2012. Insights into the PX (phox-homology) domain and SNX (sorting nexin) protein families: structures, functions and roles in disease. *Biochemical Journal,* 441**,** 39-59.

TEMKIN, P., LAUFFER, B., JÄGER, S., CIMERMANCIC, P., KROGAN, N. J. & VON ZASTROW, M. 2011. SNX27 mediates retromer tubule entry and endosome-to-plasma membrane trafficking of signalling receptors. *Nature Cell Biology,* 13**,** 715.

TEMPERINI, C., INNOCENTI, A., SCOZZAFAVA, A., MASTROLORENZO, A. & SUPURAN, C. T. 2007. Carbonic anhydrase activators: l-Adrenaline plugs the active site entrance of isozyme II, activating better isoforms I, IV, VA, VII, and XIV. *Bioorganic & Medicinal Chemistry Letters,* 17**,** 628-635.

TEWARI, R., STRASCHIL, U., BATEMAN, A., BÖHME, U., CHEREVACH, I., GONG, P., PAIN, A. & BILLKER, O. 2010. The Systematic Functional Analysis of *Plasmodium* Protein Kinases Identifies Essential Regulators of Mosquito Transmission. *Cell Host & Microbe,* 8**,** 377-387.

THE RTS,S CLINICAL TRIALS PARTNERSHIP. 2012. A Phase 3 Trial of RTS,S/AS01 Malaria Vaccine in African Infants. *New England Journal of Medicine,* 367**,** 2284-2295.

THEODORA, S., S, F. K., CATHERINE, B. B. & MICHAEL, L. 2009. Export of PfSBP1 to the *Plasmodium falciparum* Maurer's Clefts. *Traffic,* 10**,** 137-152.

THRANE, S., PEDERSEN, A. M., THOMSEN, M. B. H., KIRKEGAARD, T., RASMUSSEN, B. B., DUUN-HENRIKSEN, A. K., LÆNKHOLM, A. V., BAK, M., LYKKESFELDT, A. E. & YDE, C. W. 2014. A kinase inhibitor screen identifies Mcl-1 and Aurora kinase A as novel treatment targets in antiestrogen-resistant breast cancer cells. *Oncogene,* 34**,** 4199.

THUY-NHIEN, N., TUYEN, N. K., TONG, N. T., VY, N. T., THANH, N. V., VAN, H. T., HUONG-THU, P., QUANG, H. H., BONI, M. F., DOLECEK, C., FARRAR, J., THWAITES, G. E., MIOTTO, O., WHITE, N. J. & HIEN, T. T. 2017. K13 Propeller Mutations in *Plasmodium falciparum* Populations in Regions of Malaria Endemicity in Vietnam from 2009 to 2016. *Antimicrobial Agents and Chemotherapy,* 61.

TIBÚRCIO, M., DIXON, M. W., LOOKER, O., YOUNIS, S. Y., TILLEY, L. & ALANO, P. 2015. Specific expression and export of the *Plasmodium falciparum* Gametocyte EXported Protein-5 marks the gametocyte ring stage. *Malaria journal,* 14**,** 334.

TIGNO-ARANJUEZ, J. T., BENDERITTER, P., ROMBOUTS, F., DEROOSE, F., BAI, X., MATTIOLI, B., COMINELLI, F., PIZARRO, T. T., HOFLACK, J. & ABBOTT, D. W. 2014. In Vivo Inhibition of RIPK2 Kinase Alleviates Inflammatory Disease. *Journal of Biological Chemistry,* 289**,** 29651-29664.

TILLO, S. E., XIONG, W.-H., TAKAHASHI, M., MIAO, S., ANDRADE, A. L., FORTIN, D. A., YANG, G., QIN, M., SMOODY, B. F., STORK, P. J. S. & ZHONG, H. 2017. Liberated PKA Catalytic Subunits Associate with the Membrane via Myristoylation to Preferentially Phosphorylate Membrane Substrates. *Cell Reports,* 19**,** 617-629.

TOMAS, A. M., MARGOS, G., DIMOPOULOS, G., VAN LIN, L. H. M., DE KONING-WARD, T. F., SINHA, R., LUPETTI, P., BEETSMA, A. L., RODRIGUEZ, M. C., KARRAS, M., HAGER, A., MENDOZA, J., BUTCHER, G. A., KAFATOS, F., JANSE, C. J., WATERS, A. P. & SINDEN, R. E. 2001. P25 and P28 proteins of the malaria ookinete surface have multiple and partially redundant functions. *The EMBO Journal,* 20**,** 3975-3983.

TONKIN, M. L., ROQUES, M., LAMARQUE, M. H., PUGNIÈRE, M., DOUGUET, D., CRAWFORD, J., LEBRUN, M. & BOULANGER, M. J. 2011. Host Cell Invasion by Apicomplexan Parasites: Insights from the Co-Structure of AMA1 with a RON2 Peptide. *Science,* 333**,** 463-467.

TRAN, P. N., BROWN, S. H. J., MITCHELL, T. W., MATUSCHEWSKI, K., MCMILLAN, P. J., KIRK, K., DIXON, M. W. A. & MAIER, A. G. 2014. A female gametocyte-specific ABC transporter plays a role in lipid metabolism in the malaria parasite. *Nature Communications,* 5.

TROJER, P., LI, G., SIMS, R. J., VAQUERO, A., KALAKONDA, N., BOCCUNI, P., LEE, D., ERDJUMENT-BROMAGE, H., TEMPST, P., NIMER, S. D., WANG, Y.-H. & REINBERG, D. 2007. L3MBTL1, a Histone-Methylation-Dependent Chromatin Lock. *Cell,* 129**,** 915-928.

TSAI, C.-F., WANG, Y.-T., YEN, H.-Y., TSOU, C.-C., KU, W.-C., LIN, P.-Y., CHEN, H.-Y., NESVIZHSKII, A. I., ISHIHAMA, Y. & CHEN, Y.-J. 2015. Large-scale determination of absolute phosphorylation stoichiometries in human cells by motif-targeting quantitative proteomics. *Nature Communications,* 6**,** 6622.

TSAI, C.-J. & NUSSINOV, R. 2013. The molecular basis of targeting protein kinases in cancer therapeutics. *Seminars in Cancer Biology,* 23**,** 235-242.

TUN, K. M., IMWONG, M., LWIN, K. M., WIN, A. A., HLAING, T. M., HLAING, T., LIN, K., KYAW, M. P., PLEWES, K., FAIZ, M. A., DHORDA, M., CHEAH, P. Y., PUKRITTAYAKAMEE, S., ASHLEY, E. A., ANDERSON, T. J. C., NAIR, S., MCDEW-WHITE, M., FLEGG, J. A., GRIST, E. P. M., GUERIN, P., MAUDE, R. J., SMITHUIS, F., DONDORP, A. M., DAY, N. P. J., NOSTEN, F., WHITE, N. J. & WOODROW, C. J. 2015. Spread of artemisinin-resistant *Plasmodium falciparum* in Myanmar: a cross-sectional survey of the K13 molecular marker. *The Lancet Infectious Diseases,* 15**,** 415-421.

TWU, O., DE MIGUEL, N., LUSTIG, G., STEVENS, G. C., VASHISHT, A. A., WOHLSCHLEGEL, J. A. & JOHNSON, P. J. 2013. Trichomonas vaginalis Exosomes Deliver Cargo to Host Cells and Mediate Host∶Parasite Interactions. *PLOS Pathogens,* 9**,** e1003482.

UKAEGBU, U. E. & DEITSCH, K. W. 2015. The Emerging Role for RNA Polymerase II in Regulating Virulence Gene Expression in Malaria Parasites. *PLOS Pathogens,* 11**,** e1004926.

UKAEGBU, U. E., KISHORE, S. P., KWIATKOWSKI, D. L., PANDARINATH, C., DAHAN-PASTERNAK, N., DZIKOWSKI, R. & DEITSCH, K. W. 2014. Recruitment of PfSET2 by RNA Polymerase II to Variant Antigen Encoding Loci Contributes to Antigenic Variation in *P. falciparum*. *PLOS Pathogens,* 10**,** e1003854.

VAID, A., RANJAN, R., SMYTHE, W. A., HOPPE, H. C. & SHARMA, P. 2010. PfPI3K, a Phosphatidylinositol-3 kinase from *Plasmodium falciparum*, is exported to the host erythrocyte and is involved in hemoglobin trafficking. *Blood*.

VALADI, H., EKSTROM, K., BOSSIOS, A., SJOSTRAND, M., LEE, J. J. & LOTVALL, J. O. 2007. Exosome-mediated transfer of mRNAs and microRNAs is a novel mechanism of genetic exchange between cells. *Nature Cell Biology,* 9**,** 654-659.

VAUGHAN, A. M., MIKOLAJCZAK, S. A., WILSON, E. M., GROMPE, M., KAUSHANSKY, A., CAMARGO, N., BIAL, J., PLOSS, A. & KAPPE, S. H. I. 2012. Complete *Plasmodium falciparum* liver-stage development in liver-chimeric mice. *The Journal of Clinical Investigation,* 122**,** 3618-3628.

VEIGA, M. I., DHINGRA, S. K., HENRICH, P. P., STRAIMER, J., GNÄDIG, N., UHLEMANN, A.-C., MARTIN, R. E., LEHANE, A. M. & FIDOCK, D. A. 2016. Globally prevalent PfMDR1 mutations modulate *Plasmodium falciparum* susceptibility to artemisinin-based combination therapies. *Nature Communications,* 7**,** 11553.

VICTOR, P., ORIANO, M., FLAVIO, M., C., A. C., E., A. J. & A., P. L. 1999. Optimal sequences for non-phosphate-directed phoshorylation by protein kinase CK1 (casein kinase-1) – a re-evaluation. *European Journal of Biochemistry,* 260**,** 520-526.

VILLERBU, N., GABEN, A.-M., REDEUILH, G. & MESTER, J. 2002. Cellular effects of purvalanol A: A specific inhibitor of cyclin-dependent kinase activities. *International Journal of Cancer,* 97**,** 761-769.

VINCENSINI, L., RICHERT, S., BLISNICK, T., VAN DORSSELAER, A., LEIZE-WAGNER, E., RABILLOUD, T. & BRAUN BRETON, C. 2005. Proteomic Analysis Identifies Novel Proteins of the Maurer's Clefts, a Secretory Compartment Delivering *Plasmodium falciparum* Proteins to the Surface of Its Host Cell. *Molecular & Cellular Proteomics,* 4**,** 582-593.

VOGT, M., DOMOSZLAI, T., KLESHCHANOK, D., LEHMANN, S., SCHMITT, A., POLI, V., RICHTERING, W. & MÜLLER-NEWEN, G. 2011. The role of the N-terminal domain in dimerization and nucleocytoplasmic shuttling of latent STAT3. *Journal of Cell Science*.

WALLIMANN, T., TOKARSKA-SCHLATTNER, M. & SCHLATTNER, U. 2011. The creatine kinase system and pleiotropic effects of creatine. *Amino Acids,* 40**,** 1271-1296.

WALTON, K. M., FISHER, K., RUBITSKI, D., MARCONI, M., MENG, Q.-J., SLÁDEK, M., ADAMS, J., BASS, M., CHANDRASEKARAN, R., BUTLER, T., GRIFFOR, M., RAJAMOHAN, F., SERPA, M., CHEN, Y., CLAFFEY, M., HASTINGS, M., LOUDON, A., MAYWOOD, E., OHREN, J., DORAN, A. & WAGER, T. T. 2009. Selective Inhibition of Casein Kinase 1ϵ Minimally Alters Circadian Clock Period. *Journal of Pharmacology and Experimental Therapeutics,* 330**,** 430-439.

WANDINGER-NESS, A. & ZERIAL, M. 2014. Rab Proteins and the Compartmentalization of the Endosomal System. *Cold Spring Harbor Perspectives in Biology,* 6.

WANG, L., LU, A., ZHOU, H.-X., SUN, R., ZHAO, J., ZHOU, C.-J., SHEN, J.-P., WU, S.-N. & LIANG, C.-G. 2013. Casein Kinase 1 Alpha Regulates Chromosome Congression and Separation during Mouse Oocyte Meiotic Maturation and Early Embryo Development. *PLOS ONE,* 8**,** e63173.

WANG, Y., XING, J., XU, Y., ZHOU, N., PENG, J., XIONG, Z., LIU, X., LUO, X., LUO, C., CHEN, K., ZHENG, M. & JIANG, H. 2015. In silico ADME/T modelling for rational drug design. *Quarterly Reviews of Biophysics,* 48**,** 488-515.

WHITE, C. L., SUTO, R. K. & LUGER, K. 2001. Structure of the yeast nucleosome core particle reveals fundamental changes in internucleosome interactions. *The EMBO Journal,* 20**,** 5207-5218.

WHITE, N. J. & PONGTAVORNPINYO, W. 2003. The *de novo* selection of drug–resistant malaria parasites. *Proceedings of the Royal Society of London. Series B: Biological Sciences,* 270**,** 545-554.

WIESNER, C., EL AZZOUZI, K. & LINDER, S. 2013. A specific subset of RabGTPases controls cell surface exposure of MT1-MMP, extracellular matrix degradation and three-dimensional invasion of macrophages. *Journal of Cell Science,* 126**,** 2820-2833.

WILKES, J. M. & DOERIG, C. 2008. The protein-phosphatome of the human malaria parasite *Plasmodium falciparum*. *BMC Genomics,* 9**,** 412.

WILSON, R. J. M., DENNY, P. W., PREISER, P. R., RANGACHARI, K., ROBERTS, K., ROY, A., WHYTE, A., STRATH, M., MOORE, D. J., MOORE, P. W. & WILLIAMSON, D. H. 1996. Complete Gene Map of the Plastid-like DNA of the Malaria Parasite *Plasmodium falciparum*. *Journal of Molecular Biology,* 261**,** 155-172.

WINTER, S., SIMBOECK, E., FISCHLE, W., ZUPKOVITZ, G., DOHNAL, I., MECHTLER, K., AMMERER, G. & SEISER, C. 2008. 14-3-3 Proteins recognize a histone code at histone H3 and are required for transcriptional activation. *The EMBO Journal,* 27**,** 88-99.

WORBY, C. A. & DIXON, J. E. 2002. Sorting out the cellular functions of sorting nexins. *Nature Reviews Molecular Cell Biology,* 3**,** 919.

WORLD HEALTH ORGANISATION. 2015. World Malaria report 2016. Geneva: WHO; 2014.

WORLD HEALTH ORGANISATION. 2016. World Malaria Report 2015. Geneva: WHO; 2015.

WORLD HEALTH ORGANISATION. 2018. World Malaria Report 2017. Geneva: WHO; 2017.

WU, X., BRADLEY, M. J., CAI, Y., KÜMMEL, D., DE LA CRUZ, E. M., BARR, F. A. & REINISCH, K. M. 2011. Insights regarding guanine nucleotide exchange from the structure of a DENN-domain protein complexed with its Rab GTPase substrate. *Proceedings of the National Academy of Sciences,* 108**,** 18672-18677.

WU, Y.-W., OESTERLIN, L. K., TAN, K.-T., WALDMANN, H., ALEXANDROV, K. & GOODY, R. S. 2010. Membrane targeting mechanism of Rab GTPases elucidated by semisynthetic protein probes. *Nature Chemical Biology,* 6**,** 534-540.

WURTZ, N., FALL, B., PASCUAL, A., FALL, M., BARET, E., CAMARA, C., NAKOULIMA, A., DIATTA, B., FALL, K. B., MBAYE, P. S., DIÉMÉ, Y., BERCION, R., WADE, B. & PRADINES, B. 2014. Role of Pfmdr1 in In Vitro *Plasmodium falciparum* Susceptibility to Chloroquine, Quinine, Monodesethylamodiaquine, Mefloquine, Lumefantrine, and Dihydroartemisinin. *Antimicrobial Agents and Chemotherapy,* 58**,** 7032-7040.

XHEMALCE, B. & KOUZARIDES, T. 2010. A chromodomain switch mediated by histone H3 Lys 4 acetylation regulates heterochromatin assembly. *Genes & Development,* 24**,** 647-652.

XU, F., ZHANG, K. & GRUNSTEIN, M. 2005a. Acetylation in Histone H3 Globular Domain Regulates Gene Expression in Yeast. *Cell,* 121**,** 375-385.

XU, Y., PADIATH, Q. S., SHAPIRO, R. E., JONES, C. R., WU, S. C., SAIGOH, N., SAIGOH, K., PTÁČEK, L. J. & FU, Y.-H. 2005b. Functional consequences of a CKIδ mutation causing familial advanced sleep phase syndrome. *Nature,* 434**,** 640.

YADAV, M. K. & SWATI, D. 2012. Comparative genome analysis of six malarial parasites using codon usage bias based tools. *Bioinformation,* 8**,** 1230-1239.

YAMAUCHI, L. M., COPPI, A., SNOUNOU, G. & SINNIS, P. 2007. *Plasmodium* sporozoites trickle out of the injection site. *Cellular Microbiology,* 9**,** 1215-1222.

YAN, G., LUO, W., LU, Z., LUO, X., LI, L., LIU, S., LIU, Y., TANG, M., DONG, Z. & CAO, Y. 2007. Epstein–Barr virus latent membrane protein 1 mediates phosphorylation and nuclear translocation of annexin A2 by activating PKC pathway. *Cellular Signalling,* 19**,** 341-348.

YAN, M. S., TURGEON, P. J., MAN, H.-S. J., DUBINSKY, M. K., HO, J. J. D., EL-RASS, S., WANG, Y.-D., WEN, X.-Y. & MARSDEN, P. A. 2018. Histone acetyltransferase 7 (KAT7)-dependent intragenic histone acetylation regulates endothelial cell gene regulation. *Journal of Biological Chemistry,* 293**,** 4381-4402.

YANG, W. S. & STOCKWELL, B. R. 2008. Inhibition of casein kinase 1-epsilon induces cancer-cell-selective, PERIOD2-dependent growth arrest. *Genome Biology,* 9**,** R92.

YENUGONDA, V. M., DEB, T. B., GRINDROD, S. C., DAKSHANAMURTHY, S., YANG, Y., PAIGE, M. & BROWN, M. L. 2011. Fluorescent cyclin-dependent kinase inhibitors block the proliferation of human breast cancer cells. *Bioorganic & Medicinal Chemistry,* 19**,** 2714-2725.

YOUNG, J. A., FIVELMAN, Q. L., BLAIR, P. L., DE LA VEGA, P., LE ROCH, K. G., ZHOU, Y., CARUCCI, D. J., BAKER, D. A. & WINZELER, E. A. 2005. The *Plasmodium falciparum* sexual development transcriptome: A microarray analysis using ontology-based pattern identification. *Molecular and Biochemical Parasitology,* 143**,** 67-79.

ZELENAK, C., EBERHARD, M., JILANI, K., QADRI, S. M., MACEK, B. & LANG, F. 2012. Protein Kinase CK1α Regulates Erythrocyte Survival. *Cellular Physiology and Biochemistry,* 29**,** 171-180.

ZEMP, I., WANDREY, F., RAO, S., ASHIONO, C., WYLER, E., MONTELLESE, C. & KUTAY, U. 2014. CK1δ and CK1ε are components of human 40S subunit precursors required for cytoplasmic 40S maturation. *Journal of Cell Science,* 127**,** 1242-1253.

ZHANG, M., JOYCE, B. R., SULLIVAN, W. J. & NUSSENZWEIG, V. 2013. Translational Control in *Plasmodium* and *Toxoplasma* Parasites. *Eukaryotic Cell,* 12**,** 161-167.

ZHANG, P., WU, Y., BELENKAYA, T. Y. & LIN, X. 2011. SNX3 controls Wingless/Wnt secretion through regulating retromer-dependent recycling of Wntless. *Cell Research,* 21**,** 1677.

ZHAO, Q., RANK, G., TAN, Y. T., LI, H., MORITZ, R. L., SIMPSON, R. J., CERRUTI, L., CURTIS, D. J., PATEL, D. J., ALLIS, C. D., CUNNINGHAM, J. M. & JANE, S. M. 2009. PRMT5-mediated methylation of histone H4R3 recruits DNMT3A, coupling histone and DNA methylation in gene silencing. *Nature Structural & Molecular Biology,* 16**,** 304.

ZHENG, B., MA, Y.-C., OSTROM, R. S., LAVOIE, C., GILL, G. N., INSEL, P. A., HUANG, X.-Y. & FARQUHAR, M. G. 2001. RGS-PX1, a GAP for $G\alpha_s$ and Sorting Nexin in Vesicular Trafficking. *Science,* 294**,** 1939-1942.

ZHONG, S., GOTO, H., INAGAKI, M. & DONG, Z. 2003. Phosphorylation at serine 28 and acetylation at lysine 9 of histone H3 induced by trichostatin A. *Oncogene,* 22**,** 5291.

ZHOU, H., DI PALMA, S., PREISINGER, C., PENG, M., POLAT, A. N., HECK, A. J. R. & MOHAMMED, S. 2013. Toward a Comprehensive Characterization of a Human Cancer Cell Phosphoproteome. *Journal of Proteome Research,* 12**,** 260-271.

ZINECKER, C. F., STRIEPEN, B., GEYER, H., GEYER, R., DUBREMETZ, J.-F. & SCHWARZ, R. T. 2001. Two glycoforms are present in the GPI-membrane anchor of the surface antigen 1 (P30) of *Toxoplasma gondii*. *Molecular and Biochemical Parasitology,* 116**,** 127-135.

ZOU, S., WANG, C., CUI, Z., GUO, P., MENG, Q., SHI, X., GAO, Y., YANG, G. & HAN, Z. 2016. β-Elemene induces apoptosis of human rheumatoid arthritis fibroblast-like synoviocytes via reactive oxygen species-dependent activation of p38 mitogen-activated protein kinase. *Pharmacological Reports,* 68**,** 7-11.

ZUFALL, F., FRANKE, C. & HATT, H. 1989. The insecticide avermectin Bla activates a chloride channel in crayfish muscle membrane. *Journal of Experimental Biology,* 142**,** 191-205.